Thermal History of the Middle and Late Miocene Southern Ocean - Diatom Evidence

Die thermale Entwicklung des Südozeans im mittleren und oberen Miozän – eine Rekonstruktion anhand von Diatomeen

---

Bernd M. Censarek

Ber. Polarforsch. Meeresforsch. 430 (2002)
ISSN 1618 - 3193

Bernd M. Censarek

Alfred-Wegener-Institut für Polar- und Meeresforschung
PF120161, D-27515 Bremerhaven

Die vorliegende Arbeit ist die inhaltlich unveränderte Fassung einer Dissertation, die 2002 im Fachbereich Geowissenschaften der Universität Bremen vorgelegt wurde.

Contents

Abstract

In order to augment our understanding of paleoclimate and paleoceanographic changes during the Middle and Late Miocene in the Southern Ocean and Antarctica the diatom record obtained from a latitudinal transect across the Atlantic sector of the Southern Ocean was studied. Geographical distribution patterns, stratigraphical occurrences and abundance fluctuations of diatom species were investigated in six Miocene sedimentary sequences recovered by the Ocean Drilling Program (Sites 689, 690, 701, 704, 1088 and 1092). The results provide evidence for the thermal development of the Southern Ocean surface waters.

Biostratigraphic investigations were carried out to establish or revise age models for these sedimentary sections. Additionally, these investigations reveal latitudinal differences in stratigraphic ranges of species, which are related to latitudinal differences in surface water masses reflecting the climatic development in Antarctica. Two stratigraphic diatom zonations are erected that are applicable to the areas south and north of the Polar Front.

Thermal demands of extinct Miocene diatom taxa are deduced to calculate the ratio between warm-water diatoms and those indicating cold-water masses. The resulting relative paleotemperatures are used to estimate the development of the latitudinal thermal gradient.

The thermal gradient reveals a short-term thermal decoupling of the Southern Ocean from the adjacent oceans at ca. 10.5 Ma after the Middle Miocene climate optimum (ca. 17-15 Ma). An increase of the thermal gradient is observed between 9.3 and 8.6 Ma. This increase led to a strong thermal decoupling of the Southern Ocean from the adjacent oceans, which continued up to the Miocene-Pliocene boundary (5.3 Ma). This is interpreted as a consequence of strong cooling on the Antarctic continent, which might be linked to the build up of the West Antarctic Ice Sheet. The temporary closure of the Panama Isthmus during the Late Miocene might have favoured ice accumulation in Antarctica by the establishment of an ocean circulation pattern, which was possibly similar to the recent one. During the Late Miocene several warm and cold periods superimposed by a long-term cooling trend could be discovered between ca. 7 and 5.3 Ma (Messinian). Latitudinal frontal displacements are delineated for this time period.

The thermal history of the Southern Ocean generally has an impact on global climate development by volume changes of the Antarctic ice sheet causing sea level fluctuations. Beside tectonic movements, these cyclic sea level fluctuations are proposed to have caused the isolation, desiccation, cyclic sedimentation and reflooding of the Mediterranean basin. The revealed Southern Ocean and Antarctic thermal development provides evidence for the influence of glacio-eustatic processes during the isolation of the Mediterranean basin.

Kurzfassung

Um die paläoklimatische und paläozeanographische Entwicklung im Südozean und der Antarktis zu rekonstruieren, wurden die geographischen Verteilungsmuster, stratigraphischen Vorkommen und Häufigkeitsfluktuationen von Diatomeen-Arten an sechs mittel- und obermiozänen Sediment-Abschnitten untersucht. Anhand der Sedimente, welche im Rahmen des Ozean-Tiefbohr-Programmes (Sites 689, 690, 701, 704, 1088, 1092) entlang eines latitudinalen Schnittes durch den atlantischen Sektor des Südozeans erbohrt wurden, konnten Hinweise auf die thermale Entwicklung der Wassermassen des Südozeans abgeleitet werden.

Mittels biostratigraphischer Untersuchungen wurden Altersmodelle für die Kern-Abschnitte erstellt bzw. revidiert. Es zeigten sich latitudinale Unterschiede im stratigraphischen Auftreten einzelner Arten, welche auf unterschiedliche thermale Entwicklungen im Oberflächenwasser verweisen. Hieraus resultierten zwei Diatomeen-Zonierungen, jeweils eine für den nördlichen und südlichen Bereich des Südozeans.

Die thermalen Ansprüche ausgestorbener Diatomeen-Arten wurden abgeschätzt. Über das Verhältnis von Warmwasser- zu Kaltwasserarten wurden relative Paläotemperaturen bestimmt. Aus diesen konnte die Entwicklung des latitudinalen thermalen Gradienten abgeleitet werden.

Der thermale Gradient zeigt um 10.8 Ma eine kurzzeitige verstärkte thermale Abkopplung des Südozeans von den angrenzenden Ozeanwassermassen. Ein Anstieg des thermalen Gradienten zwischen 9.3 und 8.6 Ma dokumentiert die zunehmende thermale Isolation des Südpolarmeeres. Hieraus können Hinweise auf die Entwicklung des westantarktischen Eisschildes abgeleitet werden. Eine zeitweilige Schließung des Isthmus von Panama im späten Miozän ermöglichte die Ausbildung eines dem heutigen ähnlichen Ozean-Zirkulationsmusters, was wiederum Hinweise auf die antarktische Vereisungsgeschichte gibt. Während einer lang andauernden Abkühlung im späten Miozän (Messinian) konnten zwischen ca. 7 und 5.3 Ma mehrere kältere und wärmere Zeitabschnitte ermittelt werden. Hieraus wurden die relativen latitudinalen Verschiebungen der hydrographischen Fronten abgeleitet.

Die thermale Entwicklung des Südozeans beeinflusst die globale Klimaentwicklung u.a. durch Meeresspiegelschwankungen, welche auf Änderungen des antarktischen Eisvolumens zurückgeführt werden. Neben tektonischen Bewegungen werden jene Meeresspiegelschwankungen als Steuermechanismen für die Isolation, Austrocknung und erneute Flutung des Mittelmeer-Beckens (Messinische Salzkrise) im Bereich des obersten Miozäns postuliert. Die abgeleitete thermale Entwicklung des Südozeans lässt den Schluss zu, dass Meeresspiegelschwankungen zumindest auf die Isolation des Mittelmeeres vom Atlantik einen Einfluss gehabt haben.

1. Introduction

The climate on Earth cooled considerably along the Cenozoic period from the Early Eocene warm greenhouse condition to the Late Quaternary ice house, which is characterised by large polar ice-sheets and distinct glacial-interglacial cyclicity (Hays et al., 1976; Zachos et al., 2001). The evolution of ice sheets in Antarctica and the plate tectonic development in the southern hemisphere strongly influence this climate deterioration. The initial glaciation of Antarctica started at the Eocene/Oligocene boundary and was associated with the opening of the Tasmanian Gateway, which provided the water exchange between the Indian and the Pacific Ocean. The subsequent opening of the Drake Passage during the Oligocene was the final step to the establishment of a circum-Antarctic current (Kennett, 1977; Hambrey et al., 1991; Ehrmann, 1994; Barrett, 1999). However, the exact timing of this event is yet not well constrained (Barker and Burrell, 1977; Lawver et al., 1992; Shipboard Scientific Party, 2001; Zachos et al., 2001; Latimer and Fillipelli, 2002). An unrestricted vigorous Antarctic Circumpolar Current (ACC) was established during the Early Miocene and caused the thermal isolation of Antarctica (Kennett, 1977; Lawver et al., 1992). The Early and Middle Miocene represent a period of relative warmth with an East Antarctic Ice Sheet (EAIS) that was distinctly smaller than during the colder Oligocene, as indicated by the deep-sea stable isotope record and relatively high sea level stands (Haq et al., 1987; Abreu and Anderson, 1998; Zachos et al., 2001). After the Middle Miocene climatic optimum centered around 17-15 Ma, isotope and sea level data indicate a gradual cooling and the waxing of the major ice sheets on the Antarctic continent (Kennett, 1977).

The build-up of the West Antarctic Ice Sheet (WAIS), which started in the early Late Miocene according to sedimentological and clay mineralogical data obtained from ODP Leg 113, was the most important event in the Late Miocene (Kennett and Barker, 1990). Concomitant environmental changes are documented by a northward shift of biosiliceous sedimentation within the Southern Ocean and a significant evolutionary turnover in diatom species combined with increasing species diversity (Baldauf and Barron, 1990; Barron and Baldauf, 1995). It is believed that the EAIS, which is largely grounded above the sea level, is less dynamic and less sensitive to climate and sea level variations than the smaller WAIS grounded largely below sea level (De Santis et al., 1999).

Sea level fluctuations, which are caused by volume changes of the Antarctic ice sheets, are postulated beside regional tectonic movements to be initiated and controlled by the events known as Messinian Salinity Crisis (MSC). During the latest Miocene (Messinian) the Mediterranean Basin was temporarily isolated from the Atlantic Ocean, desiccated and flooded again at the Miocene-Pliocene boundary (Benson et al., 1991; Kastens, 1992; Hodell et al., 2001; Krijgsman et al., 2001; Vidal et al., 2001). However, the impact of sea level fluctuation caused by ice volume changes in Antarctica on the evolution of the MSC is still under discussion due to the lack of continuous Southern Ocean sediment records documenting the cryospheric evolution during the Messinian.

The Early Pliocene is generally regarded as a relatively warm period, interrupted by a few short-term cold events (Burckle et al., 1992). The possible instability of the Antarctic ice sheets during the Early Pliocene and their effects on global climate are still under debate (Warnke et al., 1996; Harwood and Webb, 1998). Reconstructions of Late Neogene climatic evolution are mainly based on the eustatic sea level curve and stable oxygen isotope composition of benthic foraminifera (Haq et al., 1987; Abreu and Anderson, 1998; Zachos et al., 2001). However, a carefully composition reveals distinct discrepancies between the sea level curve and the benthic oxygen isotope curve (Zachos et al., 2001; Fig. 3.9). In order to improve our knowledge of the climate variability in the Middle and Late Miocene Southern Ocean we use the diatom record as an independent proxy for thermal evolution.

1.1 Diatoms - proxies for Late Neogene environment

Diatoms - *Bacillariophyceae* - are microscopic unicellular algae. Their fossilised remains (species composition and abundance fluctuations) can be used for paleoenvironmental reconstructions in the southern high latitudes (e.g. Pichon et al., 1987; Barron, 1992b; Zielinski et al., 1998; Gersonde and Zielinski, 2000; Kunz-Pirrung et al., 2002). Temporal and spatial occurrence of distinct diatom assemblages can be paleoecologically studied by:

- Mathematical-statistical methods (e.g. transfer-function based methods). Transfer-functions, established by a dataset of the spatial distribution of diatom species in surface sediments connected with direct observations of surface water temperatures, are used to calculate absolute paleotemperatures (Pichon et al., 1987; Kunz-Pirrung et al., 2002; Bianchi and Gersonde, subm.).

- Interpretations of occurrences and abundance fluctuations considering specific ecological requirements, e.g. reconstruction of sea-ice distribution (Crosta et al., 1998; Gersonde and Zielinski, 2000) or calculations of ratios between selected diatom species, which reveal relative paleoecological information (e.g. Kanaya and Koizumi, 1966; Barron, 1992b).

However, while most studies are based on modern analogs provide quantitative values of surface water parameters, paleotemperature reconstructions of pre-Pleistocene diatom records must rely on the distribution of extinct taxa. Studies based on abundance fluctuations and distribution patterns of extinct diatoms have been done successfully for the estimation of Late Neogene climate variability at Northern and Equatorial Pacific and Southern Ocean diatom records (Donahue, 1970; Koizumi, 1985, 1990; Barron, 1986, 1992b and 1996).

1.2 Objectives and outline of this study

A similar approach is chosen here to reconstruct the thermal history of the Southern Ocean during the Middle and Late Miocene in order to improve our understanding of progressive thermal isolation of Antarctica and coupled climate events. Objectives of this study are:

- to improve diatom biostratigraphic zonation and establish a chronostratigraphy for middle and upper Miocene sedimentary sections at Southern Ocean deep-sea drill sites.
- to define temperature demands of extinct Miocene diatom species.
- to unravel the thermal development of the Middle and Late Miocene Southern Ocean based on selected diatom abundance fluctuations and distribution patterns.
- to provide evidences for the Antarctic cryospheric evolution.
- to compare Antarctic ice volume variability, derived from Southern Ocean thermal development, with the climate history of the Mediterranean Basin in order to study the impact of glacio-eustatic processes on the development of Messinian Salinity Crisis.

These objectives are addressed by three articles, which are outlined below (Chapter 2 to 4).

Chapter 2 "Miocene Diatom Biostratigraphy at ODP Sites 689, 690, 1088, 1092 (Atlantic Sector of the Southern Ocean)" (Censarek and Gersonde, 2002, Marine Micropaleontology, in press) presents detailed biostratigraphical investigations of four middle to upper Miocene sedimentary sequences. Locations of the sites are shown in Figure 1.1. Two age models from previous studies (Sites 689, 690) are revised and two age models are established (Sites 1088, 1092). Considering latitudinal differences in stratigraphic ranges and occurrence patterns of individual species two diatom zonations are proposed that are applicable to the northern and southern area of the Southern Ocean. First and last occurrence datums of diatom species are revised. This biostratigraphic study provides the basis for the further paleoecological and paleoceanographical studies on diatom occurrences and assemblages.

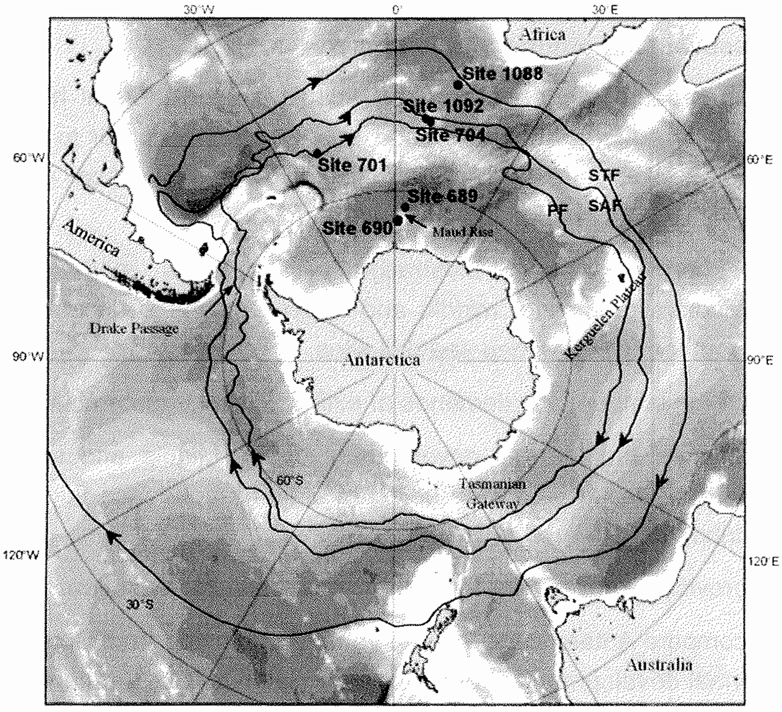

Fig. 1.1: Map of the study area. Relevant topographic features and locations of studied drill sites are presented. Oceanographic fronts are taken from Orsi et al. (1995); PF= Polarfront; SAF= Subantarctic Front; STF= Subtropical Front. Bathymetric data: Smith and Sandwell (1997).

Chapter 3 "Miocene Climate Evolution of the Southern Ocean - Sea Surface Development as Derived from the Diatom Record (ODP Sites 689, 690, 1088 and 1092" (Censarek and Gersonde, subm. b, Marine Micropaleontology) presents a diatom based paleoclimate reconstruction. Temperature demands of extinct diatom taxa are determined and ratios of cold- and warm-water indicating species are used to estimate relative paleotemperatures and the development of the latitudinal thermal gradient. Results are compared with the global climatic evolution as documented by the sea level and oxygen isotope curves. The latitudinal thermal gradient of the Southern Ocean, which is reconstructed for the time interval between ca. 17 and 4 Ma, illustrates the decoupling of the Southern Ocean from surrounding water masses and provides evidences for the Antarctic cryospheric history. The onset of a strong and stable thermal gradient within the Southern Ocean surface waters at ca. 9.5 Ma is associated with a build up of the WAIS. Furthermore, for a particular time period during the Late Miocene, the temporary establishment of an ocean circulation pattern, which might be close to the present one, is proposed.

The publication presented in Chapter 4 "Late Miocene Southern Ocean Thermal Development and its Connection to Mediterranean Climate History - Diatom Evidences from ODP Site 701 and 704" (Censarek and Gersonde, subm. c, Marine Geology) focuses the paleoclimate study on late Tortonian and Messinian stages. Sites 701 and 704 represent two of the few stratigraphically continuous Messinian sedimentary sections. Diatom biostratigraphies are established and age models are revised. The Late Miocene thermal development of the Southern Ocean is reconstructed by the occurrence patterns and abundance fluctuations of selected warm- and cold-water indicating diatom taxa. Relative paleotemperature curves are presented. Additionally, to delineate roughly the development of the hydrographic frontal system, the diatom records from ODP Sites 689, 1088 and 1092 are considered. The estimation of variation in Antarctic ice volume during the Late Miocene, which is derived from the thermal evolution of the Southern Ocean, gives important hints for the role of the glacio-eustatic sea level fluctuations for the development of the Messinian Salinity Crisis.

The included papers show that Miocene diatoms are useful tools for stratigraphic investigations (Chapter 2). Furthermore they provide the basis for paleoecologically based reconstructions of Southern Ocean thermal history (Chapter 3, 4) revealing climate coupled developments as the MSC (Chapter 4).

2. Miocene Diatom Biostratigraphy at ODP Sites 689, 690, 1088, 1092 (Atlantic Sector of the Southern Ocean)*

B. Censarek and R. Gersonde

Alfred Wegener Institute for Polar and Marine Research, Bremerhaven, Germany

(Marine Micropaleontology, 45 (3-4), pp. 309-356, 2002)

2.1 Abstract

Four ODP sites located between 64°S and 41°S in the eastern Atlantic sector of the Southern Ocean were investigated to refine the Miocene diatom biostratigraphic zonation tied to the geomagnetic chronology. The Miocene diatom stratigraphy from two sites located on Maud Rise (ODP Leg 113) is revised considering the progress in diatom biostratigraphic research, diatom taxonomy and magnetostratigraphic age assignment during the past 10 years. A new diatom zonation was erected for Site 1092 (ODP Leg 177) located on Meteor Rise integrating a magnetostratigraphic interpretation of the shipboard data. This zonation was also applied to Site 1088 (ODP Leg 177) located on Astrid Ridge. The study is focused to Middle and Upper Miocene sequences. It reveals latitudinal differentiations in stratigraphic species ranges and species occurrence pattern that are related to latitudinal differences in surface water masses reflecting the climatic development of the Antarctic cryosphere. Considering the latitudinal differences, two stratigraphic zonations are proposed that are applicable to the northern and southern zone of the Southern Ocean, respectively. The southern Southern Ocean Miocene diatom biostratigraphic zonation consists of 16 zones in which 11 represent new or modified zones. The northern biostratigraphic zonation contains 10 diatom zones allowing a stratigraphic resolution in a range of 0.2 to 2 m.y. This paper also includes the taxonomic transfer of seven Miocene diatom taxa from genus *Nitzschia* Hassall to *Fragilariopsis* Hustedt.

---

*Reprinted from Marine Micropalaeontology, 45 (3-4), Censarek and Gersonde, Miocene Diatom Biostratigraphy at ODP Sites 689, 690, 1088, 1092 (Atlantic Sector of the Southern Ocean), pp. 309-356, 2002, with permission from Elsevier Science.

2.2 Introduction

First diatom zonation of Miocene strata has been proposed by McCollum (1975), based on Deep Sea Drilling Project (DSDP) Leg 28 cores recovered in the Pacific sector of the Southern Ocean. In the following years, Schrader (1976), Weaver and Gombos (1981) and Ciesielski (1983, 1986) refined the biostratigraphic zonations. The invention of the advanced hydraulic piston coring (APC) at the end of the 1980th allowed the recovery of undisturbed Neogene sections and the establishment of geomagnetic polarity records. Gersonde and Burckle (1990) have proposed the first Southern Ocean Miocene diatom stratigraphic zonation tied directly to a geomagnetic record. This was developed based on ODP Leg 113 Holes 689B and 690B recovered on Maud Rise, located in the southeastern realm of the Weddell Sea. Diatom species ranges and zones were tied to the geomagnetic record established by Spieß (1990) and the Geomagnetic Polarity Time Scale (GPTS) of Berggren et al. (1985) was used for absolute age assignments. Further refinement of this zonation came from the studies of Baldauf and Barron (1991) and Harwood and Maruyama (1992) based on sediment sequences recovered during ODP Legs 119 and 120 in the Indian sector of the Southern Ocean (Fig. 2.1). The latter authors also presented a comprehensive historical overview of the progress of Southern Ocean diatom biostratigraphic research. The GPTS established by Cande and Kent (1992) was used by Barron and Baldauf (1995) to compile Cenozoic biostratigraphic diatom zonations from high and low latitudes. A revised compilation of Gersonde et al. (1998) which also considered the absolute age assignments presented in the GPTS of Cande and Kent (1995) was the baseline for shipboard diatom biostratigraphic studies during Leg 177. However, Leg 177 shipboard investigations resulted in the preliminary revision of the Late Miocene diatom zonation (Shipboard Scientific Party, 1999c). Ramsay and Baldauf (1999) presented a recent and very comprehensive compilation of diatom biostratigraphic data obtained from 17 DSDP and ODP Sites located in the Southern Ocean. All data were adjusted to the GPTS of Cande and Kent (1995). The objective of this study was the development of a biochronological framework in which primary stratigraphical datums were validated and applied consistently throughout the Southern Ocean. In the present paper we reinvestigate the Miocene sequences from ODP Leg 113 Holes 689B and 690B recovered on Maud Rise (Fig. 2.2, Tab. 2.1), originally studied by Gersonde and Burckle (1990).

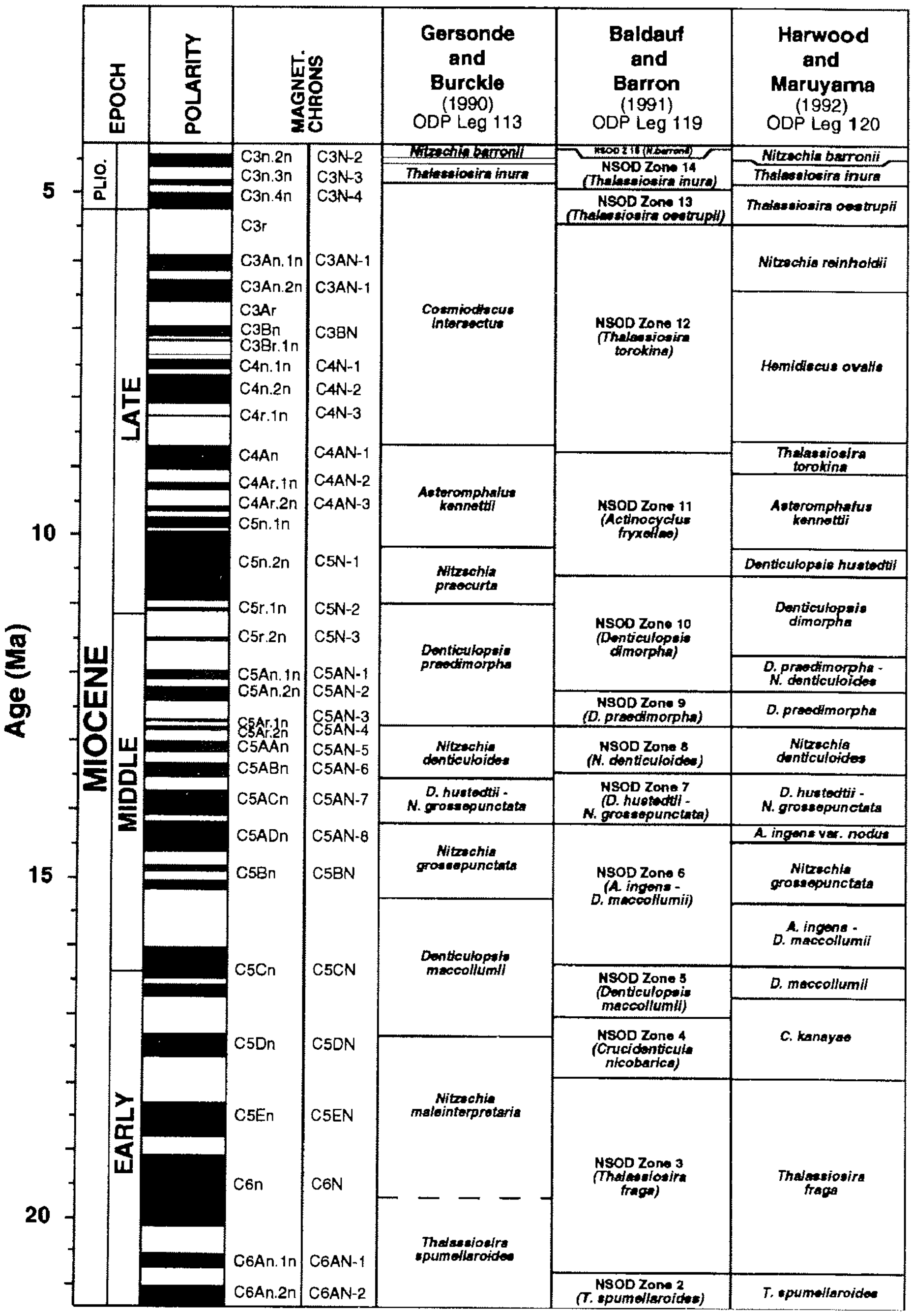

Figure 2.1 (both sides): Miocene diatom zonations from ODP Legs 113, 119 and 120 (Gersonde and Burckle, 1990; Baldauf and Barron, 1991; Harwood and Maruyama, 1992), which were tied to the Geomagnetic Polarity Time Scale of Cande and Kent (1995). Additionally the new southern and northern Southern Ocean diatom zonations are shown.

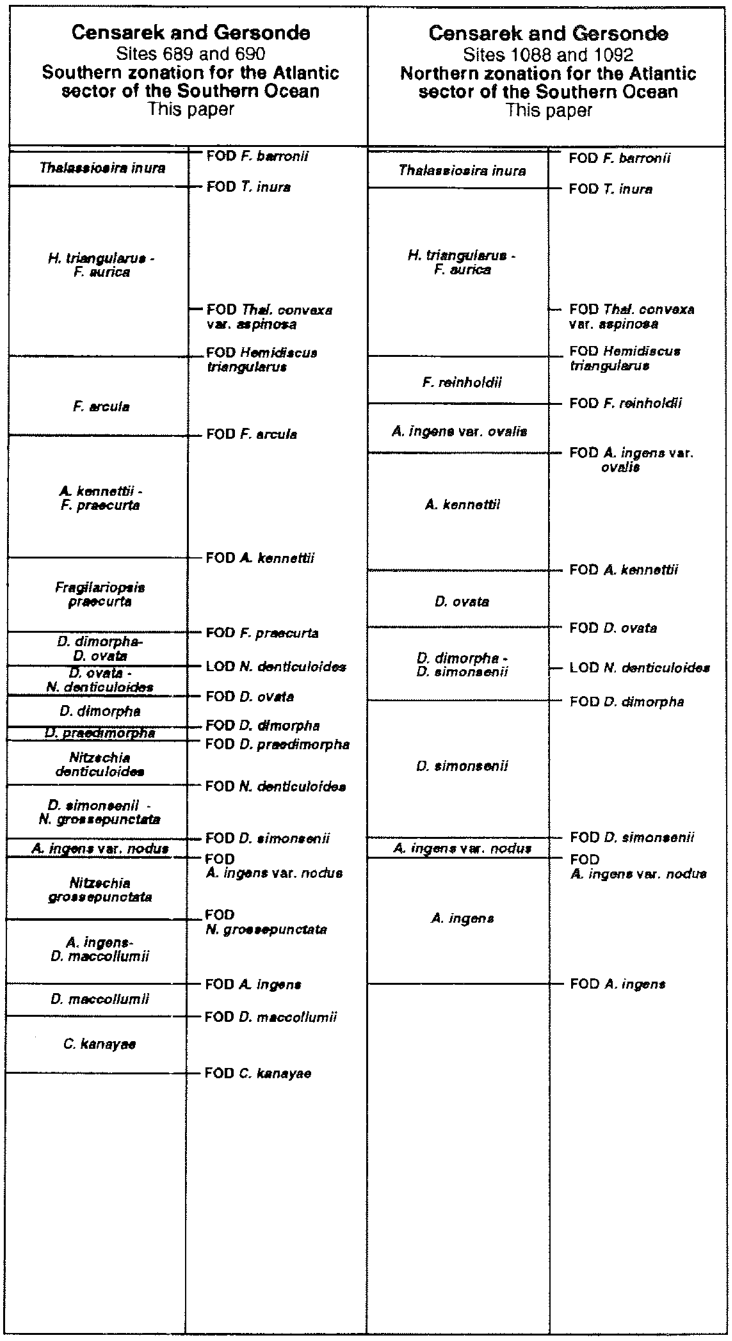

The designations of the geomagnetic polarity record is according to Cande and Kent (1992) (left column) and as proposed by Berggren et al. (1985) and Spieß (1990) (right column).

Considering the progress in diatom biostratigraphical research since 1990, revisions of age assignments of the geomagnetic record as well as revisions of the taxonomy of typical Miocene diatom species we propose an amended stratigraphic zonation for the late Early Miocene to the Late Miocene. We discuss the stratigraphic occurrence pattern of biostratigraphic marker species used as zonal definitions considering the results of previous studies of Leg 113, 114, 119 and 120. In contrast to Gersonde and Burckle (1990) and the following presentations of Ciesielski (1991), Baldauf and Barron (1991) and Harwood and Maruyama (1992), who based their study on abundance estimations of the taxa, we define the ranges of stratigraphic marker species upon the counting of up to 400 specimen per sample. We also considered the taxonomic refinements of taxa belonging to the genus *Denticulopsis*, proposed by Yanagisawa and Akiba (1990). This allowed the definition of ranges of three new *Denticulopsis* species in the Middle and Late Miocene. Out of these, two taxa were recognised as previously being included to *D. hustedtii*, and one is a new combination of different varieties close to *D. dimorpha*. The diatom zone and species ranges were dated based on the geomagnetic record established by Spieß (1990) according to the age assignments of the GPTS proposed by Berggren et al. (1995). As far as possible, the newly established zonation was also applied to the Leg 177 Sites 1092 and 1088, drilled in the area of the Antarctic Circumpolar Current (ACC) (Fig. 2.2, Tab. 2.1). Apparent latitudinal changes in species composition and abundance patterns, related to latitudinal differentiations of surface water masses, imposed the establishment of a modified zonation only applicable to the ACC realm. More comprehensive studies on the latitudinal variability of species abundance and occurrence patterns based on quantitative analyses of the diatom assemblages are presented in Censarek and Gersonde (subm. b). To improve and confirm the diatom biostratigraphic interpretation at Site 1092 a correlation to magnetostratigraphic datum points was needed. In the absence of shore-based magnetostratigraphic data sets for the Middle and Lower Miocene sections of Site 1092, we propose a preliminary interpretation based on the shipboard magnetic inclination data (Shipboard Scientific Party, 1999b). We also consider five available magnetostratigraphic datum points of the shipboard interpretation (Shipboard Scientific Party, 1999b), that have been approved by the shipboard paleomagnetists J. Channell and J. Stoner (Channell, pers. comm. 2000). At Site 1088 the complete lack of magnetostratigraphic data is due to magnetic inclinations that remained less than expected for this site location and declinations that were highly scattered (Shipboard Scientific Party, 1999a).

Unfortunately, the diatom biostratigraphy of Miocene sections recovered during Leg 114 in the realm of the ACC has never been published appropriately, except for a data report presented by Ciesielski (1991). We considered these data together with geomagnetic records presented by Clement and Hailwood (1991) and Hailwood and Clement (1991b). To refine our latest Miocene zonations we considered shipboard stratigraphical results obtained at Sites 701 and 704 (Ciesielski and Kristoffersen et al., 1988; Ciesielski, 1991), also using additional sample sets from these sites.

2.3 Material and methods

Samples for the biostratigraphic investigations were taken during Leg 113 (January to March 1987) and Leg 177 (December 1997 to February 1998) aboard JOIDES Resolution and postcruise in the Lamont and Bremen ODP core repositories. All sites considered in this study were drilled by the Advanced Hydraulic Piston Corer (APC) or the Extended Core Barrel (XCB) systems. The sample spacing in Holes 689B and 690B results in a maximum resolution up to 150 k.y. For the Leg 177 Sites 1088 and 1092, where two resp. four holes have been drilled, a resolution up to 50 k.y. is reached.

For quantitative and qualitative diatom study, microscope slides with randomly distributed microfossils were used. The cleaning of raw material and the preparation of permanent mounts for light microscopy follows the standard technique developed at the Alfred Wegener Institute (Gersonde and Zielinski, 2000). The resin for the slides was Mountex (nd = 1.67) except for samples from Site 1088 Meltmount (nd = 1.662) was used. Up to 400 diatom specimen were counted per sample using a Zeiss "Axioskop" microscope with apochromatic optics at a magnification of 1000×. Light photomicrographs were made with an AVT-Horn b/w camera coupled with a Mitsubishi video copy printer system.

The counting followed the concepts proposed by Schrader and Gersonde (1978). Detailed data sets of counting results are presented in a separate paper focusing to the paleoceanographic significance of diatom species distribution (Censarek and Gersonde, subm. b).

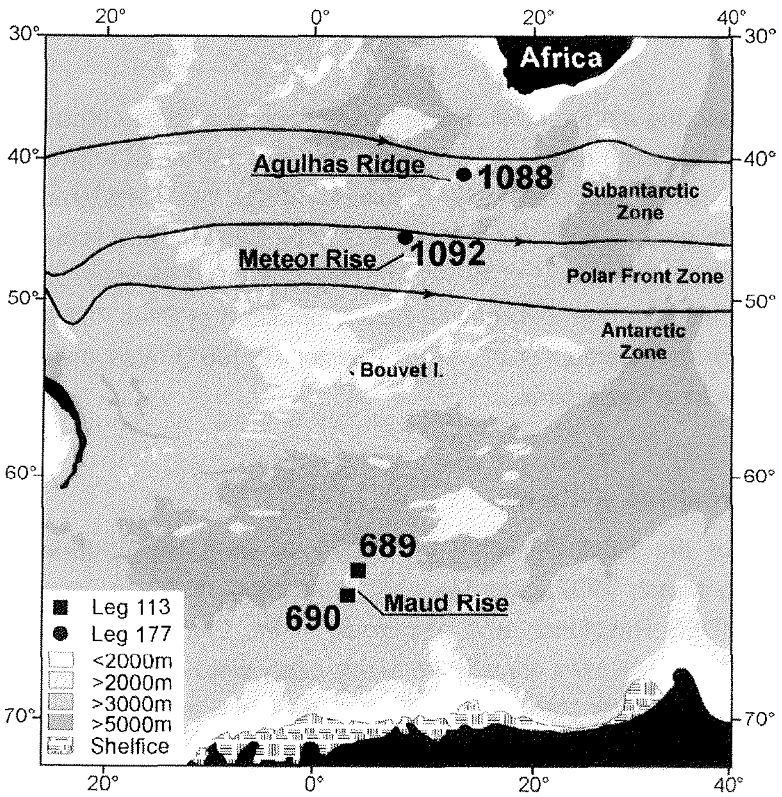

Figure 2.2: Location of Sites 689, 690, 1088 and 1092. Frontal zones according to Peterson and Stramma (1991).

Table 2.1: Location of investigated ODP sites and hydrographic settings.

Leg-Site/Holes	Latitude	Longitude	Water-depth	Location	Location/Hydrography	Investigated-section
113-689B	64°31.01´S	03°05.99´E	2080 m	Maud Rise	Weddell Sea/Antarctic Zone	11-62 mbsf
113-690B	65°09.63´S	01°12.30´E	2914 m	Maud Rise	Weddell Sea/Antarctic Zone	13-50 mbsf
177-1088B-C	41°08.16´S	13°33.77´E	2082 m	Agulhas Ridge	Southeast Atlantic Ocean/ Subantarctic Zone	34-224 mcd
177-1092A-D	46°24.70´S	07°04.79´E	1974 m	Meteor Rise	Southeast Atlantic Ocean/Polar Front Zone	60-211 mcd

For stratigraphic purposes absolute valve counts were converted to abundance classes following the ODP-style: D = dominant (>60% of total assemblage), A = abundant (30%-60%), C = common (15%-30%), F = few (3%-15%), R = rare (< 3%) and T = trace (species encountered only sporadically).

Spread sheets showing the site by site stratigraphic occurrences of selected diatom species are available from a data report (Censarek and Gersonde, subm. a), also accessible at *www-odp.tamu. edu/publications.* The diatom preservation was classified "good" when lightly silicified forms are present and no alteration of frustules could be observed, "moderate" when lightly-silicified diatoms are still present but with some alterations and "poor" if only some strongly silicified often fragmented diatoms could be observed.

The definition and nomination of zones is in accordance to the International Stratigraphic Guide (Steininger and Piller, 1999; Salvador, 1994). We tried to rely our zonal boundary definitions as much as possible on the First Occurrence Datum (FOD) of taxa that are well defined and easily to identify. The use of Last Occurrence Datum (LOD) may result in stratigraphic misinterpretation due to reworking of older species into younger sediment.

Depth assignments of zonal boundaries, species ranges and unconformities presented as mbsf (meters below sea floor) or mcd (meters composite depth) were calculated as the midpoint between the core depths of samples below and above these events or boundaries. Tiepoints for the establishment of mcd at the Leg 177 sites are presented in the individual site chapters in Gersonde et al. (1999). Zonal boundary ages, ages of species ranges and age ranges of disconformities were calculated assuming constant sedimentation rates between the various geomagnetic and biostratigraphic data points. The second digit of the calculated absolute age assignments of the stratigraphic was rounded up or down to a 0.05 m.y. step. Exceptions are such events that can directly be tied to a magnetostratigraphic event.

For paleomagnetic measurements at Site 1092 the shipboard pass-through magnetometer was used (Shipboard Scientific Party, 1999c). The measurements were made every 5 cm allowing a stratigraphic resolution of 3 k.y. Detailed shipboard paleomagnetic sampling and measurement methods of Leg 177 sites were documented in the Initial Reports (Shipboard Scientific Party, 1999c). The paleomagnetic polarity was determined directly from stable 25 mt demagnetised inclinations. Negative inclination values less than -45° were interpreted as normal polarity, positive values greater than 45° as reversed polarity. The bimodal grouping of polarity values results in a normal and reversed polarity pattern, illustrated as black/white pattern in Figure 2.10.

2.4 Definition of lower Pliocene/Miocene Diatom Zones

The latitudinal differentiation of the hydrographic parameters of Southern Ocean surface waters results in apparent latitudinal differentiations of the composition of diatom assemblages and the occurrence of stratigraphic markers. Considering this differentiation we propose two diatom biostratigraphic zonations that are applicable for the northern and the southern zone of the Southern Ocean, respectively (Fig. 2.1). The southern Southern Ocean diatom zonation (SSODZ) is based on the reinvestigation of Sites 689 and 690 (Maud Rise) and also considers previous stratigraphic results of Baldauf and Barron (1991) and Harwood and Maruyama (1992) from the Indian sector of the Southern Ocean. All sites from these studies bearing Miocene sequences are located south of the present Polar Front, except Site 737 located on the northern Kerguelen Plateau. At Site 737 diatoms have consistently been recovered in Middle Miocene through Lower Pliocene and Quaternary sediments (Baldauf and Barron, 1991). Unfortunately, the geomagnetic record obtained in the Miocene of Site 737 is rather incomplete, due to poor sediment recovery (Sakai and Keating, 1991). The northern Southern Ocean diatom zonation (NSODZ) is primarily based on the results obtained from Site 1092 located close to the Subantarctic Front (Fig. 2.2). Additional geomagnetic data from ODP Leg 114 Sites 699, 701 and 704 (Hailwood and Clement, 1991a, b; Clement and Hailwood, 1991), which have been combined with diatom occurrence data from the same sites (Ciesielski and Kristoffersen et al., 1988; Ciesielski, 1991) have also been considered. Ranges of selected Miocene diatom species and the SSODZ and NSODZ, are correlated to the geomagnetic time scale of Berggren at al. (1995) and presented in Figure 2.3.

2.4.1 Definition of southern Southern Ocean diatom biostratigraphic zonation (SSODZ)

Thalassiosira inura Partial Range Zone

Authors: Gersonde and Burckle (1990), revised by Baldauf and Barron (1991) as NSOD Zone 14 (*T. inura* Partial Range Zone), revised herein.

Definition of top: FOD of *Fragilariopsis barronii.*

Definition of base: FOD of *Thalassiosira inura.*

Age: Early Pliocene, ca. 4.9 - ca. 4.5 Ma.

Paleomagnetic correlation: This zone ranges from the uppermost portion of Subchron C3n.3r close to the base of Subchron C3n.3n to the interval between the top of C3n.2n and the lowermost portion of Subchron C3n.1r.

Discussion: Gersonde and Burckle (1990) placed the FOD of *F. barronii*, which defines the top of the zone, approximately into the middle of Subchron C3N-2 (Fig. 2.1). Baldauf and Barron (1991) report in their revision of the zonal description (NSOD Zone 14, *Thalassiosira inura* Zone) erroneously a correlation of the FOD of *F. barronii* to Chron C3AN-2 instead to Subchron C3R-1 (=C3n.1r). This can be deduced from the diatom occurrence pattern presented in their range chart for Site 745 and the magnetostratigraphic data presented by Sakai and Keating (1991) from the same site. Also the stratigraphic occurrence pattern of *F. barronii* at Site 745, presented by Baldauf and Barron (1991) in their figure 6, does not coincide with the range chart data. We propose to place the FOD of *F. barronii* within the interval between the top of C3n.2n and the lowermost portion of Subchron C3n.1r on the base oft Sites 689, 690 and 695 (Gersonde and Burckle, 1990) and Site 745 (Baldauf and Barron, 1991).

There are however indications, that the FOD of *F. barronii* may be diachronous, having an older FOD in the northern area of the Southern Ocean (see discussion in NSODZ section). Taxonomic problems relate to this taxon because earlier (Weaver and Gombos, 1981; Ciesielski, 1983; Barron, 1985a) it was erroneously identified as *Nitzschia angulata* (= the extant *Fragilariopsis rhombica*) are discussed in Gersonde (1991).

Gersonde and Burckle (1990) defined the base of this zone based on the FOD of *T. inura*, which was placed at the base of Subchron C3n.3n (Fig. 2.1), as recorded from Site 695. This is in accordance with the findings of Baldauf and Barron (1991) from Site 745. However, in their zonal description Baldauf and Barron (1991) erroneously indicated a wrong paleomagnetic assignment (C3AR-2) for the base of the *T. inura* Zone and a wrong species range is shown in figure 6. Based on a comparison of the range chart data of Baldauf and Barron (1991) and the geomagnetic polarity record, presented in the stratigraphic summary of Site 745 (Barron et al., 1991), the FOD of *T. inura* at Site 745 can be placed at or very close to the base of C3n.3n.

Considering the confusion about the FOD of *T. inura* and previous problematic species identification (see discussion in Gersonde, 1991), more stratigraphic investigations are needed to strengthen the stratigraphic range of this taxon and thus the base of the *Thalassiosira inura* Zone.

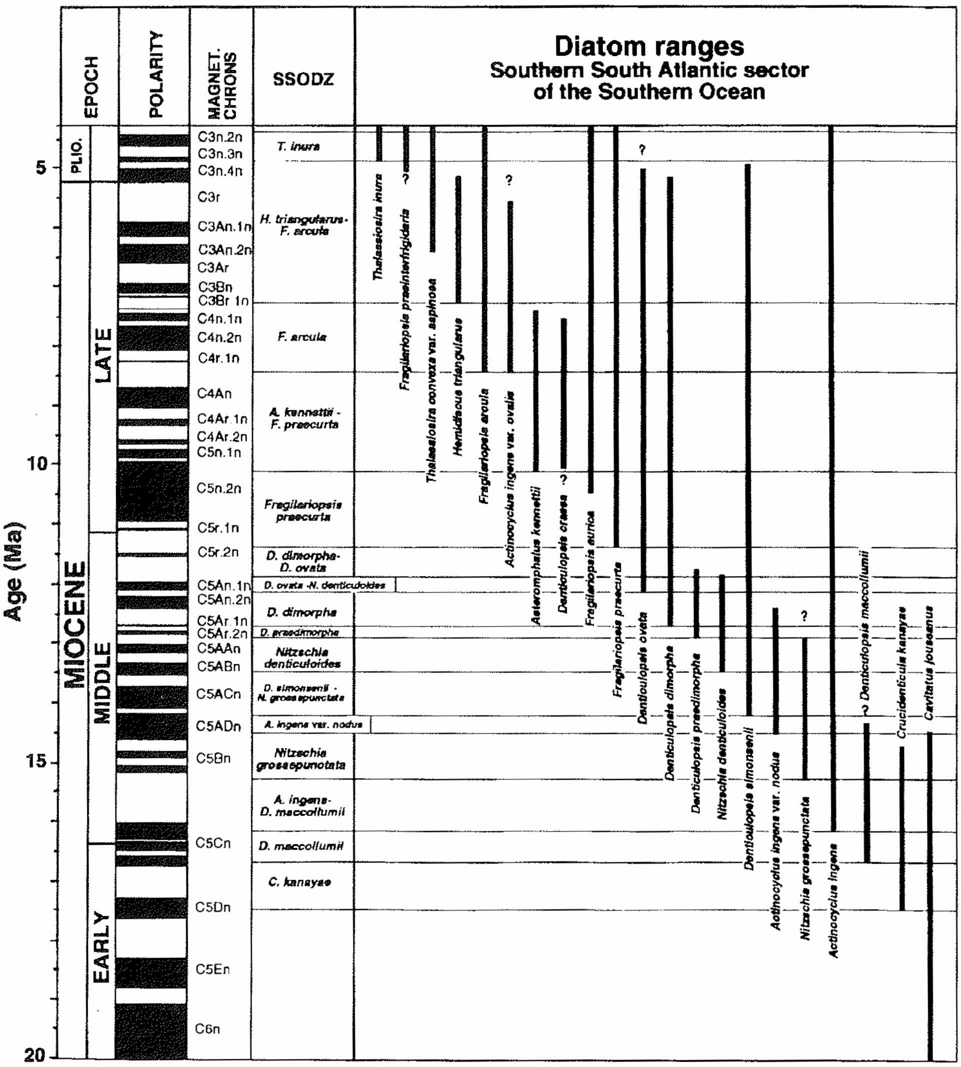

Figure 2.3 (both sites): Ranges of selected Miocene diatom species, diatom zonations as herein defined correlated to the GPTS of Berggren at al. (1995). SSODZ/NSODZ = Southern/Northern Southern Ocean diatom zonation.

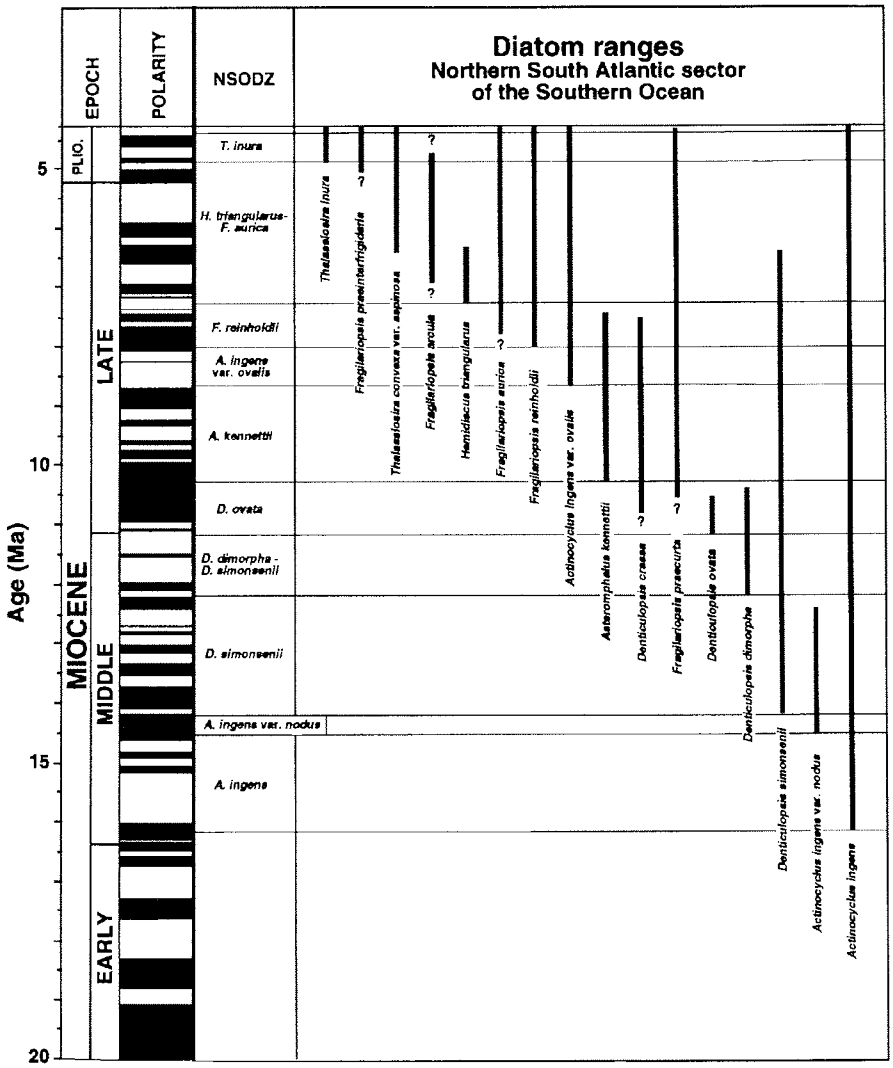
Age (Ma)
5
10
15
20
EPOCH
PLIO.
MIOCENE
LATE
MIDDLE
EARLY
POLARITY
NSODZ
T. inura
H. triangularus-
F. aurica
F. reinholdii
A. ingens
var. ovalis
A. kennettii
D. ovata
D. dimorpha -
D. simonsenii
D. simonsenii
A. ingens var. nodus
A. ingens
Diatom ranges
Northern South Atlantic sector
of the Southern Ocean
Thalassiosira inura
Fragilariopsis praeinterfrigidaria
Thalassiosira convexa var. aspinosa
Fragilariopsis arcula
Hemidiscus triangularus
Fragilariopsis aurica
Fragilariopsis reinholdii
Actinocyclus ingens var. ovalis
Asteromphalus kennettii
Denticulopsis crassa
Fragilariopsis praecurta
Denticulopsis ovata
Denticulopsis dimorpha
Denticulopsis simonsenii
Actinocyclus ingens var. nodus
Actinocyclus ingens
?

Hemidiscus triangularus-Fragilariopsis aurica **Partial Range Zone**

Authors: Censarek and Gersonde, herein.

Definition of top: FOD of *Thalassiosira inura.*

Definition of base: FOD of *Hemidiscus triangularus.*

Age: Late Miocene to Early Pliocene, 7.3 - ca. 4.9 Ma.

Paleomagnetic correlation: The zone ranges from the upper part of Subchron C3Br.2r up to the uppermost portion of Subchron C3n.3r close to the base of Subchron C3n.3n.

Discussion: In its upper part this zone is equivalent to the NSOD Zone 13 (*Thalassiosira oestrupii* Zone) and in its lower portion it covers the upper part of the NSOD 12 Zone (*Thalassiosira torokina* Zone), both proposed by Baldauf and Barron (1991). Harwood and Maruyama (1992) replaced the NSOD 12 Zone by the *Nitzschia reinholdii* and the *Hemidiscus ovalis* zones (Fig. 2.1). Within the *N. reinholdii* Zone, Harwood and Maruyama (1992) distinguished two subzones and defined the subzone boundary by the joint occurrence of the last occurrence (LO) of *Neobrunia mirabilis* and the LOD of *H. triangularus* near the top of Subchron C3AN-1 (Fig. 2.1).

In Southern Ocean sediments the FOD of *T. oestrupii* has only been documented from Holes 737A and 745B (Baldauf and Barron, 1991) and was cited to an age of 5.1 Ma. According to the chronology of Berggren et al. (1985), used by Baldauf and Barron (1991), this would fall within the lower reversed interval of Chron C3 at or close to the Miocene/Pliocene boundary. This is in conflict to the data presented in the Leg 119 range charts presented by Baldauf and Barron (1991), which indicate a younger age of the *T. oestrupii* FOD. Considering the paleomagnetic interpretations of Sakai and Keating (1991), the FOD falls close to the lower boundary of Subchron C3n.4n. According to Berggren et al. (1995) this datum is located in the lowermost Pliocene around 5.2 Ma. In our study we could not confirm the FOD of *T. oestrupii* because the first stratigraphic occurrence of this taxon is not documented at Sites 689 and 1092 due to the occurrence of a disconformity (Figs. 2.4, 2.10). At Site 690 the FO of *T. oestrupii* was found in the *T. inura* Zone (Fig. 2.6). Considering the generally rare occurrence pattern of *T. oestrupii* in our records and the unclear age determination of its FOD presented by Baldauf and Barron (1991), we decided not to consider the FOD of *T. oestrupii* as a stratigraphic marker until more reliable data are available.

In addition, we decided not to consider *Thalassiosira miocenica* and *Thalassiosira torokina,* whose FODs define the base of the *N. reinholdii* Zone of Harwood and Maruyama (1992) and the base of the NSOD Zone 12 (*T. torokina* Zone) of Baldauf and Barron (1991), respectively, because of their scattered occurrence pattern (Censarek and Gersonde, subm. a). The nominate taxa of our *H. triangularus-F. aurica* Zone can easily be identified and their range is documented by a continuous occurrence pattern.

The FOD of *H. triangularus* has been identified in Hole 689B (Fig. 2.4) and could be assigned to an age of 7.3 Ma (upper part of Subchron C3Br.2r). A similar age assignment was found by the study of Hole 704B, ODP Leg 114 considering the paleomagnetic data presented by Hailwood and Clement (1991b). However, the stratigraphic range of *H. triangularus* does not cover the total range of the *H. triangularus-F. aurica* Zone (Fig. 2.4). In Hole 689B the LO of this species correlates to the upper lower part of Subchron C3n.4n, while at Site 1092 the LO was found to correlate to the middle of C3An.2n. The middle and upper portion of the *H. triangularus-F. aurica* Zone is characterised by the presence of *F. aurica* in the absence of *T. inura*. The FOD of *F. aurica* can be placed around 10 Ma, in the upper portion of the *F. praecurta* Zone (Figs. 2.4, 2.6). Other useful marker species in the *H. triangularus-F. aurica* Zone are *Thalassiosira convexa* var. *aspinosa* and *Fragilariopsis praeinterfrigidaria.T. convexa* var. *aspinosa* has its FOD in the lowermost portion of Subchron C3An.2n at around 6.5 Ma (interpolated in Hole 689B), while in Hole 690B the first occurrence (FO) of this species is at a hiatus (18.7 mbsf) which covers Subchron C4n.1n to the lower part of Subchron C3n.4n (Fig. 2.6). This datum is corroborated by the study of Hole 746A (Leg 119), where it was correlated to the lower middle portion of Chron C3An.2n (Baldauf and Barron, 1991). At Site 704 (Leg 114) the FO of *T. convexa* var. *aspinosa* can be placed into the lower portion of Chron C3An (Ciesielski, 1991; Hailwood and Clement, 1991b). The FO of *Fragilariopsis praeinterfrigidaria* was recorded from Hole 745B (Leg 119) to correlate to the upper portion of Subchron C3n.3n (Baldauf and Barron, 1991). At Site 699 (Georgia Rise) the FO of this species falls into Chron C3An, whereas at Site 704 (Meteor Rise) the FO of a taxon labelled as *Fragilariopsis* aff. *praeinterfrigidaria* was placed somewhere in the lower portion of the Gilbert Chron (Ciesielski, 1991; Hailwood and Clement, 1991a, b). In Hole 695A the base of the stratigraphic range of the species was placed in the upper part of Chron C3n.3n (Gersonde and Burckle, 1990). This differs from the results of the investigation at Sites 689 and 690, where the FO is found in Chron C3n.4n and in the upper portion of C3n.3r, respectively (Figs. 2.4, 2.6). It thus can be summarised that the FOD of *F. praeinterfrigidaria* was found in the lower portion of the Gilbert Chron, except at Site 699, where an older age for this event was marked. More data are needed to constrain this age assignment and to check if the occurrence pattern of the taxon is diachronous in the Southern Ocean.

Fragilariopsis arcula Partial Range Zone

Authors: Censarek and Gersonde, herein.

Definition of top: FOD of *Hemidiscus triangularus*.

Definition of base: FOD of *Fragilariopsis arcula*.

Age: middle Late Miocene, 8.45 - 7.3 Ma.

Paleomagnetic correlation: This zone ranges from the lower part of Subchron C4r up to the Subchron C3Br.2r.

Remark: This zone replaces the lower portion of the *C. intersectus* Zone of Gersonde and Burckle (1990) as well as the lower part of NSOD Zone 12 (*T. torokina* Zone) of Baldauf and Barron (1991). The FO of *A. ingens* var. *ovalis,* a species that occurs only in rare abundances in the southern part of the Southern Ocean is close to the FOD of *F. arcula* (8.45 Ma). At Leg 120 Sites 747, 748 and 751 the stratigraphical range of *F. arcula* is disturbed by disconformities (Harwood and Maruyama, 1992).

Asteromphalus kennettii - *Fragilariopsis praecurta* Partial Range Zone

Authors: Censarek and Gersonde, herein.

Definition of top: FOD of *Fragilariopsis arcula*.

Definition of base: FOD of *Asteromphalus kennettii*.

Age: Late Miocene, ca.10.15 - 8.45 Ma.

Paleomagnetic correlation: The zone ranges from the middle portion of Subchron C5n.2n up to the lower part of Subchron C4r.

Discussion: This zone is close to the *A. kennettii* Zone of Gersonde and Burckle (1990) that was modified by Harwood and Maruyama (1992) and the northern Southern Ocean *A. kennettii* Zone (this paper). Gersonde and Burckle (1990) defined the top of their *A. kennettii* Zone by the FOD of *Cosmiodiscus intersectus*, a taxon that was included to *Thalassiosira oliverana* var. *sparsa* by

Harwood and Maruyama (1992). Baldauf and Barron (1991) proposed to replace the *A. kennettii* Zone of Gersonde and Burckle (1990) by the NSOD 11 (*Actinocyclus fryxellae)* Zone, arguing, that the nominate species of the *A. kennettii* Zone should not be used as a biostratigraphic marker because its occurrence might be easily biased by selective dissolution. However, Harwood and Maruyama (1992) reestablished the *A. kennettii* Zone of Gersonde and Burckle (1990) while modifying the definition of the top by the FOD of *Thalassiosira torokina*.

Consistently with our results, *A. kennettii* was reported from Leg 119 Holes 744A and 746A having its FO in the middle portion of Chron C5n.2n (Baldauf and Barron, 1991). In the northern area of the Southern Ocean the FOD of *A. kennettii* might occur somewhat earlier (see discussion of *A. kennettii* Zone in NSODZ section). We did not consider *A. fryxellae* and *T. torokina* as taxonomic markers for the SSODZ because of the rare and scattered occurrence of both taxa in the studied holes.

Fragilariopsis praecurta **Partial Range Zone**

Authors: Gersonde and Burckle (1990), revised herein.

Definition of top: FOD of *Asteromphalus kennettii.*

Definition of base: FOD of *Fragilariopsis praecurta.*

Age: Middle to Late Miocene, 11.4 - ca. 10.15 Ma.

Paleomagnetic correlation: The zone ranges from the Subchron C5r.2r up to the middle portion of Subchron C5n.2n.

Discussion: This zone was originally described as *Nitzschia praecurta* Zone (Gersonde and Burckle, 1990). The transfer of *Nitzschia praecurta* to the genus *Fragilariopsis* by Gersonde and Bárcena (1998) resulting in the new zonal name. Gersonde and Burckle (1990) correlated the base of the zone with the reversed interval between Subchrons C5N-2 and C5N-1. However, in the magnetostratigraphical interpretation of Spieß (1990) the normal polarised interval C5N-2 is documented as C5N-3, which was translated to the nomenclature of Cande and Kent (1992) in C5n.2n. Thus, we place the base of the *Fragilariopsis praecurta* Zone into Subchron C5r.2r (Figs. 2.4, 2.6).

Denticulopsis dimorpha - Denticulopsis ovata Partial Range Zone

Authors: Censarek and Gersonde, herein.

Definition of top: FOD of *Fragilariopsis praecurta.*

Definition of base: LOD of *Nitzschia denticuloides.*

Age: upper Middle Miocene, 11.8 - 11.4 Ma.

Paleomagnetic correlation: The zone ranges from the middle of Subchron C5r.3r up to Subchron C5r.2r.

Discussion: The *D. dimorpha-D. ovata* Zone correlates with the upper portion of *the D. praedimorpha* Zone of Gersonde and Burckle (1990), the middle portion of the NSOD Zone 10 (*D. dimorpha* Zone) of Baldauf and Barron (1991) and the lower portion of the *D. dimorpha* Zone of Harwood and Maruyama (1992). We propose to use the LOD of *N. denticuloides* as a stratigraphical event for redefinition of the zonal base of the *D. dimorpha* Zone, as proposed by Harwood and Maruyama (1992). The age assignment for the *N. denticuloides* LOD placed by Harwood and Maruyama (1992) near or slightly below the base of magnetostratigraphic Subchron C5N-3 (=C5r.2n) relies on an extrapolation because this subchron is present at none of the OPD Leg 120 sites. However, Harwood and Maruyama's estimate is only slightly younger than our absolute age assignment (11.8 Ma) that is based on a linear extrapolation of the sedimentation rate at Site 690 between Subchrons C5n.2n and C5An.1n. Further stratigraphic information on the range of *N. denticuloides* comes from Hole 737B (Baldauf and Barron, 1991), but unfortunately no magnetostratigraphic data are available from this site. At Site 1092 we found the LO of *N. denticuloides* also between C5n.2n and C5An.1n (Fig. 2.10).

Denticulopsis ovata-Nitzschia denticuloides Partial Range Zone

Authors: Censarek and Gersonde, herein.

Definition of top: LOD of *Nitzschia denticuloides.*

Definition of base: FOD of *Denticulopsis ovata.*

Age: Middle Miocene, 12.1 - 11.8 Ma.

Paleomagnetic correlation: The zone ranges from the Subchron C5An.1r up to the middle portion of Subchron C5r.3r.

Discussion: This zone is closely related to the *D. praedimorpha-N. denticuloides* Zone of Harwood and Maruyama (1992) and falls within the lower portion of the NSOD Zone 10 (*D. dimorpha* Zone) of Baldauf and Barron (1991). The base of both, the *D. praedimorpha-N. denticuloides* Zone and the *D. dimorpha* Zone was defined by the FOD of *D. dimorpha* which defines the base of the following *D. dimorpha* Zone in our SSODZ. The occurrence of *D. ovata*, a species originally described by Schrader (1976) as *Denticula hustedtii* var. *ovata* and emended by Yanagisawa and Akiba (1990), allows a zonal refinement in the lower portion of Chron C5. The FO of *D. ovata* is located in Hole 748B (Leg 120) between Subchrons C5n.2n and C5An.1n (Harwood and Maruyama, 1992).

Denticulopsis dimorpha Partial Range Zone

Authors: Baldauf and Barron (1991) as NSOD Zone 10 (*D. dimorpha* acme zone), modified herein.

Definition of top: FOD of *Denticulopsis ovata.*

Definition of base: FOD of *Denticulopsis dimorpha.*

Age: Middle Miocene, 12.75 - 12.1 Ma.

Paleomagnetic correlation: The zone ranges from the Subchron C5Ar.2r up to the middle portion of Chron C5r.3r.

Discussion: The original definition of the zonal top (LCO of *D. dimorpha*) was replaced by the FOD of *Denticulopsis ovata.* The species counting revealed that the FOD of *D. dimorpha* is older than previously reported (Gersonde and Burckle, 1990) and is correlated to Subchron C5Ar.2r (Figs. 2.4, 2.6).

Denticulopsis praedimorpha Partial Range Zone

Authors: Gersonde and Burckle (1990), modified by Baldauf and Barron (1991) as NSOD Zone 9 (*D. praedimorpha* Partial Range Zone), modified herein.

Definition of top: FOD of *Denticulopsis dimorpha.*

Definition of base: FOD of *Denticulopsis praedimorpha.*

Age: Middle Miocene, 12.85 - 12.75 Ma.

Paleomagnetic correlation: The zone ranges from the upper part of Subchron C5Ar.3r up to the Subchron C5Ar.2r.

Discussion: This zone is equivalent to the lower portion of the *D. praedimorpha* Zone described by Gersonde and Burckle (1990) and modified by Baldauf and

Barron (1991) (Fig. 2.1). In their zonal description, Baldauf and Barron (1991) presented an erroneous magnetostratigraphic age assignment for the base of this zone. The first stratigraphic occurrence of the nominate taxon is not documented at Site 744 due to the occurrence of a hiatus, which however is not indicated in figure 4 of Baldauf and Barron (1991). Also at Leg 120 Sites, the base of this zone is not documented (Harwood and Maruyama, 1992). Based on our species counting we found a slightly earlier FOD of *D. praedimorpha* than presented by Gersonde and Burckle (1990) from Sites 689 and 690 (Figs. 2.4, 2.6).

Nitzschia denticuloides **Partial Range Zone**

Authors: Weaver and Gombos (1981), redefined by Gersonde and Burckle (1990), revised herein.

Definition of top: FOD of *Denticulopsis praedimorpha.*

Definition of base: FOD of *Nitzschia denticuloides.*

Age: Middle Miocene, 13.5 - 12.85 Ma.

Paleomagnetic correlation: The zone ranges from the lower portion of Chron C5ABn up to the upper part of Subchron C5Ar.3r.

Discussion: Gersonde and Burckle (1990) defined the top of the zone by the FOD of *D. praedimorpha* to replace the last abundant appearance datum (LAAD) of *N. denticuloides* as proposed by Weaver and Gombos (1981). The FOD of *N. denticuloides* was correlated to lower portion of Chron C5ABn in Holes 747A and 751A (Harwood and Maruyama, 1992). In their zonal description, Gersonde and Burckle (1990) present a FOD of *N. denticuloides* that falls between Subchrons C5AN-7 (=C5ACn) and C5AN-6 (=C5ABn). This is inconsistent with the data presented in their Hole 689B range charts, where first *N. denticuloides* were reported from an interval that correlates with the upper portion of C5ABn. Our reinvestigation found that the FOD of *N. denticuloides* in Hole 689B coincides with the results from Harwood and Maruyama (1992) and can be correlated with the lower portion of Chron C5ABn (Fig. 2.4).

Our study also shows that a stratigraphic coincidence of the LOD of *N. grossepunctata* with the FOD of *N. denticuloides*, as reported by Weaver and Gombos (1981) and Gersonde and Burckle (1990), must be questioned. We found rare but continuous occurrences of *N. grossepunctata* ranging into the lower portion of the *N. denticuloides* Zone (Fig. 2.3). *N. denticuloides*, *Cruciden-*

ticula nicobarica, Actinocyclus ingens var. *nodus* and *Nitzschia grossepunctata* comprise the typical diatom assemblage of this zone (Figs. 2.4, 2.6).

Denticulopsis simonsenii - Nitzschia grossepunctata Partial Range Zone

Authors: Gersonde and Burckle (1990), renamed herein.

Definition of top: FOD of *Nitzschia denticuloides.*

Definition of base: FOD of *Denticulopsis simonsenii.*

Age: Middle Miocene, 14.2 - 13.5 Ma.

Paleomagnetic correlation: The zone ranges from the top of Chron C5ADn up to the lower portion of Chron C5ABn.

Discussion: Considering revision of the genus *Denticulopsis* (Yanagisawa and Akiba, 1990) the former *D. hustedtii - N. grossepunctata* Zone (Gersonde and Burckle, 1990) was renamed (Fig. 2.1). The stratigraphic ranges of *Denticulopsis* taxa at Holes 689B and 690B confirm that specimen previously related to *D. hustedtii* are conspecific with *D. simonsenii*, a taxon newly described by Yanagishawa and Akiba (1990). Baldauf and Barron (1991) reported at Site 744 a FOD of *D. simonsenii* (as *D. hustedtii*) correlated to Chron C5ADn, which agrees with our results.

Actinocyclus ingens var. *nodus* Partial Range Zone

Authors: Harwood and Maruyama (1992).

Definition of top: FOD of *Denticulopsis simonsenii.*

Definition of base: FOD of *Actinocyclus ingens* var. *nodus.*

Age: Middle Miocene, ca. 14.35 - 14.2 Ma.

Paleomagnetic correlation: This zone ranges from the middle portion to the top of Chron C5ADn.

Nitzschia grossepunctata Partial Range Zone

Authors: Weaver and Gombos (1981), redefined by Gersonde and Burckle (1990), modified by Harwood and Maruyama (1992).

Definition of top: FOD of *Actinocyclus ingens* var. *nodus.*

Definition of base: FOD of *Nitzschia grossepunctata.*

Age: early Middle Miocene, 15.2 - ca. 14.35 Ma.

Paleomagnetic correlation: The zone ranges from the upper portion of Chron C5Br up to the middle part of Chron C5ADn.

Discussion: Weaver and Gombos (1981) defined the top of the zone with the LOD of *C. lewisianus*. This was redefined by Gersonde and Burckle (1990) by the FOD of *D. hustedtii* (= FOD of *D. simonsenii*). Introducing the *A. ingens* var. *nodus* Zone, Harwood and Maruyama (1992) divided this zone into two zones. Thus, the present *N. grossepunctata* Zone is equivalent to the middle and lower portion of the *N. grossepunctata* Zone of Gersonde and Burckle (1990) (Fig. 2.1). Characteristic assemblages in the lower portion of this zone comprise nominate species, *Cavitatus jouseanus* and *F. maleinterpretaria* (Figs. 2.4, 2.6).

Actinocyclus ingens - Denticulopsis maccollumii Partial Range Zone

Authors: Baldauf and Barron (1991), modified by Harwood and Maruyama (1992).

Definition of top: FOD of *Nitzschia grossepunctata.*

Definition of base: FOD of *Actinocyclus ingens.*

Age: late Early Miocene, ca. 16.2 - 15.2 Ma.

Paleomagnetic correlation: The zone ranges from the middle portion of Chron C5Cn.1n up to upper portion of Chron C5Br.

Discussion: Baldauf and Barron (1991) established the NSOD Zone 6 (*A. ingens - D. maccollumii*) Zone using the FOD of *A. ingens* for the definition of the base. The upper portion of the NSOD Zone 6 is equivalent to the *A. ingens* var. *nodus* and the *Nitzschia grossepunctata* Zone, proposed, respectively revised by Harwood and Maruyama (1992). The lower portion of the NSOD Zone 6 is equivalent to the *A. ingens - D. maccollumii* Zone of Harwood and Maruyama (1992) who define its base by the FCOD (First common occurrence datum) of *A. ingens*. However, this definition is questionable because the base of this zone is not documented from any of the Leg 120 Sites. The evidence Harwood and Maruyama (1992) used for the FCOD is only based on a general statement that „*A. ingens* ... is known to occur ... in the lower lower Miocene". In addition, the sediments drilled during Leg 113 do not document the FOD of *A. ingens* due to the occurrence of disconformities. For definition and age assignment of the base of the *A. ingens-D. maccollumii* Zone we follow Baldauf and Barron (1991) using the FOD of *A. ingens*, which occurs in Hole 744B in the upper portion of

Chron C5n with an age of ca. 16.2 Ma according to the GPTS of Cande and Kent (1995).

Denticulopsis maccollumii Partial Range Zone

Authors: McCollum (1975), renamed and modified by Gersonde and Burckle (1990), redefined by Harwood and Maruyama (1992).

Definition of top: FOD of *Actinocyclus ingens.*

Definition of base: FOD of *Denticulopsis maccollumii.*

Age: late Early Miocene, ca. 16.7 - ca. 16.2 Ma.

Paleomagnetic correlation: This zone ranges from the uppermost part of Chron C5Cr up to the middle portion of Chron C5Cn.1n.

Discussion: Gersonde and Burckle (1990) renamed this zone from *Denticula antarctica* to *D. maccollumii* Zone and modified the top of the zone. Later on Harwood and Maruyama (1992) defined the top with the FCOD of *A. ingens*. In Hole 747A, as well as in Hole 751A, the FO of *D. maccollumii* falls with the upper portion of Chron C5Cr (Harwood and Maruyama, 1992). Baldauf and Barron (1991) reported the same for Site 744.

Crucidenticula kanayae Partial Range Zone

Authors: Harwood and Maruyama (1992).

Definition of top: FOD of *Denticulopsis maccollumii.*

Definition of base: FOD of *Crucidenticula kanayae.*

Age: late Early Miocene, ca. 17.4 - ca. 16.7 Ma.

Paleomagnetic correlation: This zone ranges from the middle of Chron C5D up to the uppermost part of Chron C5Cr.

Remark: This zone established by Harwood and Maruyama (1992) comprises portions of the *D. maccollumii* and *N. maleinterpretaria* Zone proposed by Gersonde and Burckle (1990). The FO of *C. kanayae* is documented in Hole 744B (Leg 119) and correlated to the lower portion of Chron C5Dn (Baldauf and Barron, 1991). Harwood and Maruyama (1992) report the same from Holes 747A, 748B and 751A.

2.4.2 Definition of northern Southern Ocean diatom biostratigraphic zonation (NSODZ)

***Thalassiosira inura* Partial Range Zone**

Authors: Gersonde and Burckle (1990), revised by Baldauf and Barron (1991) as NSOD Zone 14 (*T. inura* Partial Range Zone), revised herein.

Definition of top: FOD of *Fragilariopsis barronii.*

Definition of base: FOD of *Thalassiosira inura.*

Age: Early Pliocene, ca. 4.9 - ca. 4.5 Ma.

Paleomagnetic correlation: This zone ranges from the uppermost portion of Subchron C3n.3r close to the base of Subchron C3n.3n to interval between the top of C3n.2n and the lowermost portion of Subchron C3n.1r.

Remark: Sediments related to this zone are bounded by disconformities at Site 1092. For this reason we use the zonal definitions and age assignments applied to the southern zonation. Characteristic species within the *T. inura* Zone are *F. praeinterfrigidaria* and *F. lacrima* (Fig. 2.10).

Discussion: Ciesielski (1983) notes that the FOD of *N. angulata* (=*F. barronii*) is diachronous in most of his cores. From Site 704 a FO of the species in Subchron C3n.2n is reported (Ciesielski, 1991; Hailwood and Clement, 1991b). This differs from our results in the southern zonation (lowermost portion of C3n.1r). Due to the occurrence of disconformities in the Lower Pliocene of Leg 177 Sites 1090 and 1092 (Zielinski and Gersonde, 2002) that do not allow a definition of the FOD of *F. barronii*, the exact timing of this event in the northern portion of the Southern Ocean is not possible and awaits for further investigations.

***Hemidiscus triangularus-Fragilariopsis aurica* Partial Range Zone**

Authors: Censarek and Gersonde, herein.

Definition of top: FOD of *Thalassiosira inura.*

Definition of base: FOD of *Hemidiscus triangularus.*

Age: Late Miocene to Early Pliocene, 7.3 - ca. 4.9 Ma.

Paleomagnetic correlation: The zone ranges from the upper part of Subchron C3Br.2r up to the uppermost portion of Subchron C3n.3r close to the base of Subchron C3n.3n.

Remark: This zone is stratigraphically equivalent to the *H. triangularus-F. aurica* Zone proposed for the southern zonation of the Southern Ocean (Fig. 2.1). A disconformity bounds the upper portion of the *H. triangularus* Zone at Site 1092 (Fig. 2.10). For further discussion see zonal description in SSODZ section.

Fragilariopsis reinholdii Partial Range Zone

Authors: Censarek and Gersonde, herein.

Definition of top: FOD of *Hemidiscus triangularus*.

Definition of base: FOD of *Fragilariopsis reinholdii*.

Age: Late Miocene, ca. 7.95 - 7.3 Ma.

Paleomagnetic correlation: The zone ranges from the lower portion of Subchron C4n.2n up to the upper portion of Subchron C3Br.2r.

Remark: Nominate species has been transferred to the genus *Fragilariopsis* (Zielinski and Gersonde, 2002).

Discussion: Our zone is not identical with the *Nitzschia reinholdii* Zone proposed by Harwood and Maruyama (1992) and defined by the FOD of *Thalassiosira miocenica* (base) and the FOD of *T. oestrupii* (top). Reasons for not following the zonation proposed by Harwood and Maruyama (1992) are discussed in the description of the *H. triangularus-F. aurica* Zone presented in the SSODZ section. The *F. reinholdii* Zone is equivalent to the upper portion of the *F. arcula* Zone proposed for the SSODZ (see above), the middle portion of the *Hemidiscus ovalis* Zone of Harwood and Maruyama (1992) and lower parts of the long-ranging *Cosmiodiscus intersectus* and NSOD 12 (*T. torokina* Zone) Zones proposed by Gersonde and Burckle (1990) and Baldauf and Barron (1991) for the Late Miocene, respectively (Fig. 2.1). Together with the following *Actinocyclus ingens* var. *ovalis* Zone the *F. reinholdii* Zone helps to refine the Late Miocene diatom zonation in the northern area of the Southern Ocean. The FO of *F. reinholdii* was placed into the lower portion of Subchron C4n.2n. This is consistent with the data from Ciesielski (1991) who reports the FO of *F. reinholdii* in Hole 704B (Leg 114) from the upper portion of Chron C4An, according to the data of Hailwood and Clement (1991b). However, erroneously a wrong age assignment for this event was presented in table 3 of Hailwood and Clement (1991b). Further indication for the FO age assignment of *F. reinholdii* in southern latitudes comes from Baldauf and Barron (1991). They report the FO of a *Fragilariopsis* *marina/F. reinholdii*-group in Hole 746A to be correlated to the lower portion of an extended normal polarised interval (?C4n.2n) of Chron C4. Thus the FOD of *F. reinholdii* in the northern zone of the Southern Ocean is synchronous or nearly synchronous to its FOD in the Equatorial Pacific, where it was placed into Chron C4 (Barron, 1992a).

Actinocyclus ingens var. *ovalis* Partial Range Zone

Authors: Harwood and Maruyama (1992), modified herein.

Definition of top: FOD of *Fragilariopsis reinholdii.*

Definition of base: FOD of *Actinocyclus ingens* var. *ovalis.*

Age: Late Miocene, 8.7 - ca. 7.95 Ma.

Paleomagnetic correlation: The zone ranges from the base of Subchron C4r.2r up to the lower portion of Subchron C4n.2n.

Discussion: This zone is equivalent to the lower portion of the *Hemidiscus ovalis* Zone of Harwood and Maruyama (1992). Harwood and Maruyama (1992) transferred *Actinocyclus ingens* var. *ovalis* to *Hemidiscus ovalis.* We cannot follow this transfer because of the lack of distinct morphological characteristics that would require a transfer of the original taxon to the genus *Hemidiscus.* In Hole 747A (Leg 120) the FO of the species is in Chron C4An (Harwood and Maruyama, 1992). The FOD of *A. ingens* var. *ovalis* was found in Hole 746A (Leg 119) in the lower portion of a normal polarity interval in Chron C4 (Baldauf and Barron, 1991). In Hole 689B we found the base of the stratigraphical range of *A. ingens* var. *ovalis* in the lowermost part of Chron C4 (Fig. 2.4).

Asteromphalus kennettii Partial Range Zone

Authors: Gersonde and Burckle (1990), modified by Harwood and Maruyama (1992), modified herein.

Definition of top: FOD of *Actinocyclus ingens* var. *ovalis.*

Definition of base: FOD of *Asteromphalus kennettii.*

Age: early Late Miocene, ca. 10.3 - 8.7 Ma.

Paleomagnetic correlation: This zone ranges from Subchron C5n.2n up to the base of Subchron C4r.2r.

Discussion: This zone is close to the *Asteromphalus kennettii-Fragilariopsis praecurta* Zone of our SSODZ (for discussion see SSODZ section). However, the definition of the top of this zone differs. Another difference might concern the basal age of the zone. Linear extrapolation of sedimentation rates at Site 1092 as well as in Hole 704B (see data in Ciesielski, 1991 and Hailwood and Clement, 1991b) indicate a slightly older (0.1-0.2 m.y.) FOD of *A. kennettii* in the northern area of the Southern Ocean (Tab. 2.3).

Denticulopsis ovata Partial Range Zone

Authors: Censarek and Gersonde, herein.

Definition of top: FOD of *Asteromphalus kennettii.*

Definition of base: FOD of *Denticulopsis ovata.*

Age: early Late Miocene, 11.1 - ca. 10.3 Ma.

Paleomagnetic correlation: This zone ranges from the upper portion of Subchron C5r.2r up to the middle part of Subchron C5n.2n.

Denticulopsis dimorpha - D. simonsenii Partial Range Zone

Authors: Censarek and Gersonde, herein.

Definition of top: FOD of *Denticulopsis ovata.*

Definition of base: FOD of *Denticulopsis dimorpha.*

Age: upper Middle Miocene, 12.1 - 11.1 Ma.

Paleomagnetic correlation: This zone ranges from the upper portion of Subchron C5An.1r up to the upper part of Subchron C5r.2r.

Discussion: This zone is equivalent to the *D. praedimorpha-N. denticuloides* Zone and the lower part of the *D. dimorpha* Zone of Harwood and Maruyama (1992). In the lower portion of this zone the LO of *N. denticuloides* at 11.8 Ma provides a useful stratigraphic datum (Fig. 2.1). The reliability of this datum is discussed in description of the *Denticulopsis dimorpha-Denticulopsis praedimorpha* Partial Range Zone (see SSODZ section).

Denticulopsis simonsenii Partial Range Zone

Authors: Censarek and Gersonde, herein.

Definition of top: FOD of *Denticulopsis dimorpha*.

Definition of base: FOD of *Denticulopsis simonsenii*.

Age: Middle Miocene, 14.2 - 12.1 Ma.

Paleomagnetic correlation: This zone ranges from the top of Chron C5ADn up to the upper part of Subchron C5An.1r.

Remark: For discussion about the FOD of *D. simonsenii* see *Denticulopsis simonsenii-Nitzschia grossepunctata* Partial Range Zone in the SSODZ section.

Actinocyclus ingens var. *nodus* Partial Range Zone

Authors: Harwood and Maruyama (1992).

Definition of top: FOD of *Denticulopsis simonsenii*.

Definition of base: FOD of *Actinocyclus ingens* var. *nodus*.

Age: Middle Miocene, ca.14.35 -14.2 Ma.

Paleomagnetic correlation: This zone ranges from the middle portion to the top of Chron C5ADn.

Remark: This zone is equivalent to the *Actinocyclus ingens* var. *nodus* Partial Range Zone of the SSODZ.

Actinocyclus ingens Partial Range Zone

Authors: Baldauf and Barron (1991), modified by Harwood and Maruyama (1992), modified and renamed herein.

Definition of top: FOD of *Actinocyclus ingens* var. *nodus*.

Definition of base: FOD of *Actinocyclus ingens*.

Age: lower Middle Miocene, ca. 16.2 - ca. 14.35 Ma.

Paleomagnetic correlation: This zone ranges from the upper portion Chron C5Cn up to the middle portion of Chron C5ADn.

Discussion: We propose this zone only preliminarily because of the problematic age assignment and the occurrence of disconformities around the Early/Middle Miocene boundary at Site 1092. For age assignment of the FOD of

A. ingens we follow Baldauf and Barron (1991) who placed the FOD of *A. ingens* in Hole 744B in the upper portion of Chron C5n. For further discussion see *A. ingens-D. maccollumii* Zone in the SSODZ section.

2.5 Description of sites

2.5.1 Site 689

Site 689 (64°31.01'S, 3°5.99'E) is located near the northeastern crest of Maud Rise at a water depth of 2080 m. In this study we reinvestigated a sediment interval between 10 and 62 mbsf from Hole 689B, which represents the most continuously recovered hole out of four drilled at Site 689 (Shipboard Scientific Party, 1988a). The pelagic, mostly biogenic sediments contain common to abundant diatoms with good to moderate preservation. The obtained stratigraphic data are presented on Figures 2.4 and 2.5 and in Table 2.2.

Range charts of the stratigraphic occurrence of selected diatom species are available from a data report (Table 1 in Censarek and Gersonde, subm. a), also accessible under *www-odp.tamu.edu/publications*. The reinvestigation of the Early Miocene to Early Pliocene section identified four disconformities (Fig. 2.5). The lowermost hiatus was placed at 58.8 mbsf, separating the Early Miocene from the Middle Miocene and spanning ca. 16-17.3 Ma. Two disconformities occur in the Middle Miocene and have been located at 55.1 and 43.8 mbsf. In the latest Miocene (18.1 mbsf) we found a hiatus that covers a time interval from ca. 6.4 to 5.4 Ma. The calculated average sedimentation rates range between 1 and 15 m/m.y. and reach highest values in the Late Miocene and Early Pliocene. The occurrence of *T. inura* in the absence of *F. barronii* in Sample 113-689B-2H-5, 27-28 cm, places the interval above Sample 113-689B-2H-5, 55-56 cm (11.71 mbsf) into the *T. inura* Zone. There is no diatom bio- and magnetostratigraphic evidence for the short ranging hiatus at 11.7 mbsf assumed by Gersonde and Burckle (1990). The following zone is the *H. triangularus-F. aurica* Zone, which is interrupted by the uppermost Miocene hiatus at 18.1 mbsf for a time period of extrapolated 5.4 - 6.4 Ma. Gersonde and Burckle (1990) and Spieß (1990) also report this disconformity. Below this hiatus there is the lowermost portion of Subchron C3An.2n. The base of the *H. triangularus-F. aurica* Zone is placed between samples 113-689B-3H-3, 148-150 cm and 113-689B-3H-4, 56-58 cm, marked by the FOD of *H. triangularus*. Another datum point in this zone is the FOD of *T. convexa* var. *aspinosa* (6.55 Ma) at 18.68 mbsf. Other characteristic diatoms besides the nominate species are *Fragilariopsis* *donahuensis*, *F. praecurta* and *F. arcula*. The base of the subsequent *F. arcula* Zone is placed between samples 113-689B-3H-5, 114-115 cm and 113-689B-3H-6, 28-29 cm at 21.94 mbsf. This zone is characterised by the co-occurrence of *F. arcula* and *A. ingens* var. *ovalis*. Between samples 113-689B-4H-3, 114-115 cm and 113-689B-4H-4, 29-30 cm at 28.59 mbsf is the base of the *A. kennettii-F. praecurta* Zone, which is defined by the FOD of *A. kennettii* at 10.15 Ma. This zone spans a time interval of approx. 1.7 m.y. The diatom assemblages of this zone are characterised by high abundance of *A. ingens* (Censarek and Gersonde, subm. a). This taxon is accompanied by rarer occurrences of *F. claviceps*, *F. donahuensis* and *F. praecurta*. The long-ranging *Fragilariopsis praecurta* Zone has its base between samples 113-689B-5H-3, 114-115 cm and 113-689B-5H-3, 145-147 cm at 37.94 mbsf. Characteristic species found in the *F. praecurta* Zone are *Thalassiosira yabei*, *D. dimorpha*, *D. ovata*, *Actinocyclus karstenii* and, in the upper portion of the zone, *F. aurica*. The Middle to Late Miocene boundary is in the lower portion of the *F. praecurta* Zone. The base of the underlying *Denticulopsis dimorpha-Denticulopsis ovata* Zone is placed between samples 113-689B-5H-6, 28-29 cm and 113-689B-5H-6, 114-115 cm at 43.06 mbsf. The base is defined by the LOD of *Nitzschia denticuloides* (11.8 Ma). The occurrence of *D. dimorpha*, *D. praedimorpha* characterise the assemblages of this zone. The following *D. ovata-N. denticuloides* Zone is marked by a disconformity at 43.8 mbsf. This hiatus, which is also reported by Gersonde and Burckle (1990), spans from 11.9 to 12.4 Ma and omits the normal polarised Subchrons C5An.1n and C5An.2n and thus most of the *D. ovata-N. denticuloides* Zone and the upper portion of the underlying *D. dimorpha* Zone. The hiatus is very likely tied to major oceanographic changes associated with the Middle Miocene cooling event (Censarek and Gersonde, subm. a). The base of the *Denticulopsis dimorpha* Zone between samples 113-689B-6H-3, 28-29 cm and 113-689B-6H-3, 114-115 cm, is defined by the FOD of the nominate species. The FO of Denticulopsis praedimorpha between samples 113-689B-6H-4, 28-29 cm and 113-689B-6H-4, 114-115 cm at 48.51 mbsf places the interval above into the D. praedimorpha Zone.

Figure 2.4 (right): Stratigraphic ranges of selected diatom species in the reinvestigated Miocene section of Hole 689B and diatom zonal assignment tied to the geomagnetic data of Spieß (1990). The chron nomenclature is according to Cande and Kent (1992). Dotted lines indicate scattered and trace occurrences of diatom taxa

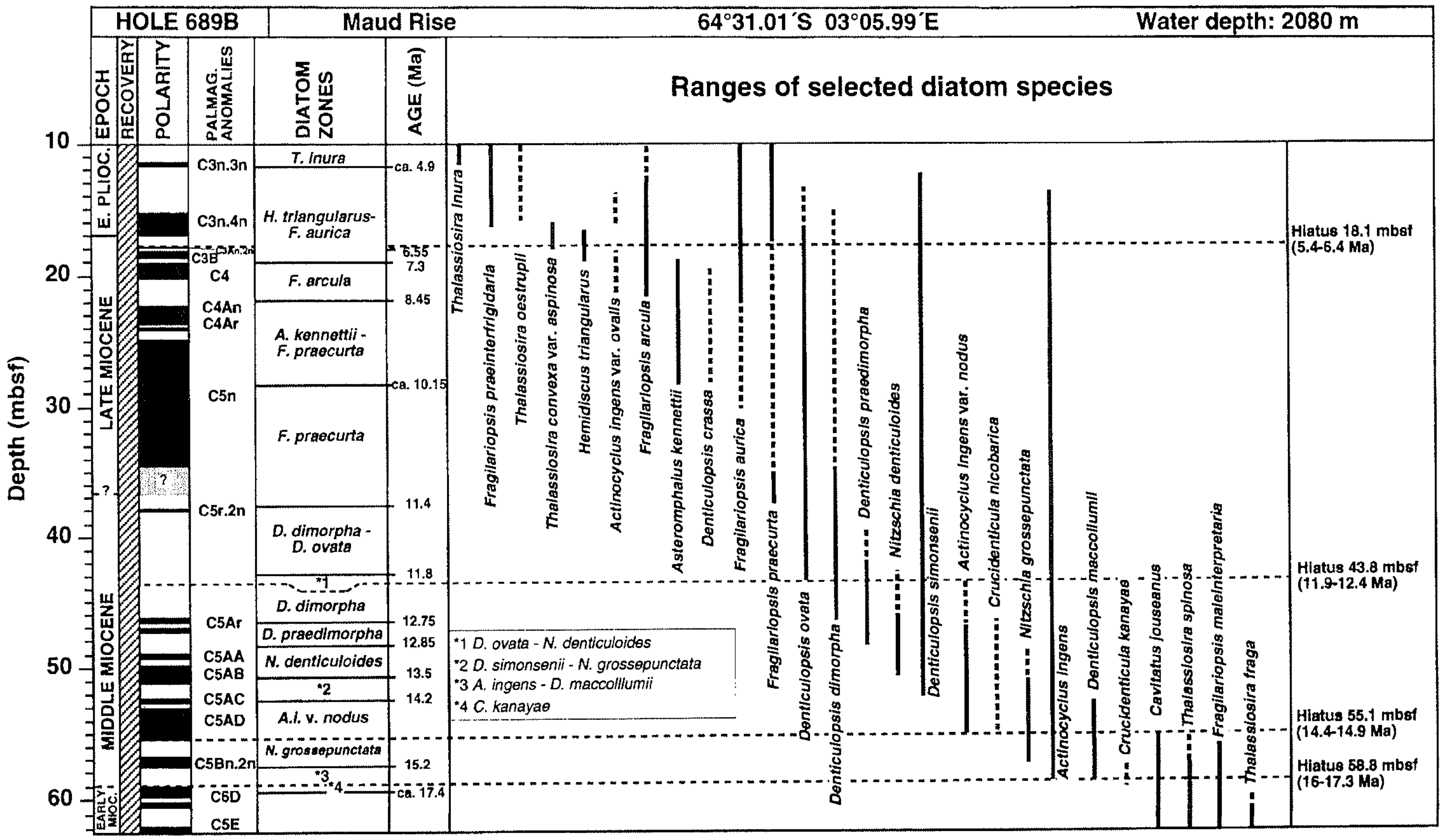
HOLE 689B
Maud Rise
64°31.01´S 03°05.99´E
Water depth: 2080 m
Ranges of selected diatom species
EPOCH
RECOVERY
POLARITY
PALMAG. ANOMALIES
DIATOM ZONES
AGE (Ma)
Depth (mbsf)
10
20
30
40
50
60
E. PLIOC.
LATE MIOCENE
MIDDLE MIOCENE
EARLY MIOC.
?
C3n.3n
C3n.4n
C3An.2n
C3B
C4
C4An
C4Ar
C5n
C5r.2n
C5Ar
C5AA
C5AB
C5AC
C5AD
C5Bn.2n
C6D
C5E
T. inura
H. triangularus- F. aurica
F. arcula
A. kennettii - F. praecurta
F. praecurta
D. dimorpha - D. ovata
*1
D. dimorpha
D. praedimorpha
N. denticuloides
*2
A.i. v. nodus
N. grossepunctata
*3
*4
ca. 4.9
6.55
7.3
8.45
ca. 10.15
11.4
11.8
12.75
12.85
13.5
14.2
15.2
ca. 17.4
Thalassiosira inura
Fragilariopsis praeinterfrigidaria
Thalassiosira oestrupii
Thalassiosira convexa var. aspinosa
Hemidiscus triangularus
Actinocyclus ingens var. ovalis
Fragilariopsis arcula
Asteromphalus kennettii
Denticulopsis crassa
Fragilariopsis aurica
Fragilariopsis praecurta
Denticulopsis ovata
Denticulopsis dimorpha
Denticulopsis praedimorpha
Nitzschia denticuloides
Denticulopsis simonsenii
Actinocyclus ingens var. nodus
Crucidenticula nicobarica
Nitzschia grossepunctata
Actinocyclus ingens
Denticulopsis maccollumii
Crucidenticula kanayae
Cavitatus jouseanus
Thalassiosira spinosa
Fragilariopsis maleinterpretaria
Thalassiosira fraga
*1 D. ovata - N. denticuloides
*2 D. simonsenii - N. grossepunctata
*3 A. ingens - D. maccollumii
*4 C. kanayae
Hiatus 18.1 mbsf (5.4-6.4 Ma)
Hiatus 43.8 mbsf (11.9-12.4 Ma)
Hiatus 55.1 mbsf (14.4-14.9 Ma)
Hiatus 58.8 mbsf (16-17.3 Ma)

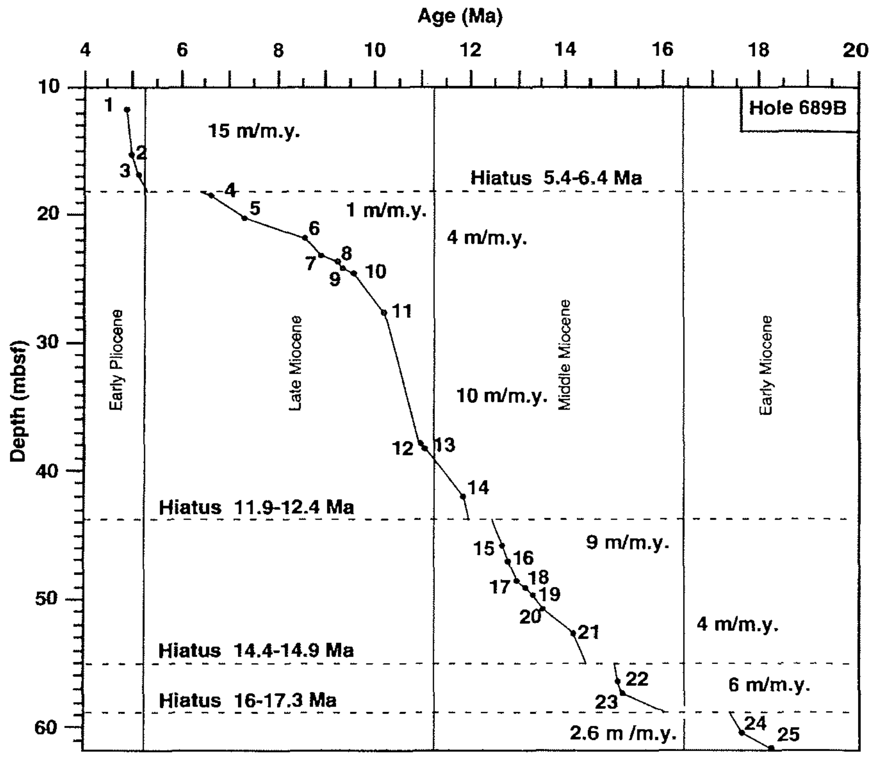

Figure 2.5: Age-depth diagram for the Miocene of Hole 689B and calculated average sedimentation rates. For definition of stratigraphic datum points compare Table 2.2.

In this zone few occurrences of D. praedimorpha, Actinocyclus ingens var. nodus, Denticulopsis simonsenii and N. denticuloides are noted. The next biostratigraphic unit is the N. denticuloides Zone found between samples 113-689B-6H-5, 114-115 cm and 113-689B-6H-6, 28-29 cm at 50.76 mbsf. Typical species within this zone are Crucidenticula nicobarica, Nitzschia grossepunctata, A. ingens var. nodus and D. simonsenii. The FO of D. simonsenii between samples 113-689B-6H-7, 28-29 cm and 113-689B-7H-1, 28-29 cm places the interval above into the D. simonsenii-N. grossepunctata Zone. Below this interval the quality of diatom preservation decreases. The lower portion of the following A. ingens var. nodus Zone is omitted by a hiatus found at 55.1 mbsf ranging from ca. 14.4 to 14.9 Ma.

Table 2.2: Definition of stratigraphic datum points in the Miocene section of Hole 689B used to construct the age-depth diagram in Figure 2.5.

Datum points	Depth (mbsf)	Age (Ma)	Definition
1	11.72	4.89	Base C3n.3n
2	15.17	4.98	Top C4n.3n
3	16.92	5.23	Base C4n.3n
Hiatus	18.1	5.4-6.4	
4	18.67	6.567	Base 3An.2n
5	20.05	7.3	FOD *H. triangularus*
6	22.15	8.699	Top C4An
7	23.65	9.025	Base C4An
8	23.81	9.230	Top C4Ar.1n
9	24.17	9.308	Base C4Ar.1n
10	24.67	9.58	Top C4Ar.2n
11	27.72	10.15	FOD *A. kennettii*
12	37.93	10.949	Base C5n
13	38.26	11.4	FOD *F. praecurta*
14	42.01	11.8	LOD *N. denticuloides*
Hiatus	43.8	11.9-12.4	
15	45.93	12.678	Top C5Ar.1n
16	47.18	12.819	Base C5Ar.2n
17	48.68	12.991	Top C5AA
18	49.18	13.139	Base C5AA
19	49.68	13.302	Top C5AB
20	50.91	13.51	Base C5AB
21	52.8	14.2	FOD *D. simonsenii*
Hiatus	55.1	14.4-14.9	
22	56.53	15.034	Top C5Bn.2n
23	57.4	15.155	Base C5Bn.2n
Hiatus	58.8	16-17.3	
24	60.4	17.615	Base C5Dn
25	61.76	18.281	Top C5En

This disconformity, also reported by Gersonde and Burckle (1990) and Spieß (1990), is indicated by the joint FOs of *A. ingens* var. *nodus*, *C. nicobarica* and the LOD of *Cavitatus jouseanus*. Besides the nominate species the assemblage of the *A. ingens* var. *nodus* Zone is characterised by *Denticulopsis maccollumii*, *C. nicobarica* and *N. grossepunctata*. Below the hiatus the *N. grossepunctata* Zone was recognised with its base between samples 113-689B-7H-3, 145-147 cm and 113-689B-7H-4, 28-29 cm at 57.51 mbsf. The sediments at the base of the zone correspond to the lower portion of Subchron C5Bn.2n. Typical species within this zone are *C. jouseanus*, *Thalassiosira spinosa* and *Fragilariopsis maleinterpretaria*. The sediments of the lower *A. ingens-D. maccollumii* Zone and of the *D. maccollumii* Zone are not present due to a hiatus located at 58.8 mbsf. This conspicuous hiatus separates the Early from the Middle Miocene and spans from approx. 16 to 17.3 Ma. Similar hiatuses at the Early to Middle Miocene boundary can also be observed at Sites 690 and 1092. Occurrences of

A. ingens, *C. kanayae*, *C. jouseanus* and *F. maleinterpretaria* characterise the *A. ingens-D. maccollumii* Zone. The lowermost zone in the studied interval is the *Crucidenticula kanayae* Zone, whose base was found between samples 113-689B-7H-5, 28-29 cm and 113-689B-7H-5, 55-57 cm at 59.62 mbsf. The assemblage consists of only few diatom species, dominated by *F. maleinterpretaria*, *C. jouseanus* and *Coscinodiscus lewisianus*. Below this zone the assemblage is characterised by occurrences of *C. jouseanus*, *T. spinosa*, *F. maleinterpretaria* and *Thalassiosira fraga*.

2.5.2 Site 690

Site 690 (65°09.63'S, 01°12.30'E) is located on the western flank of Maud Rise in 2914 m water depth. Hole 690B contains a total sediment section of 213.4 m, providing the most continuous recovery of three drilled holes (Shipboard Scientific Party, 1988b). The lower Miocene to lowermost Pliocene sediments (51 to 13 mbsf) were restudied. A recovery gap, spanning at least a period of 0.1 m.y. disturbs the sediment below the Middle/Late Miocene boundary. The stratigraphic data are presented on Figures 2.6 and 2.7 and on Table 2.3. Range charts of the stratigraphic occurrence of selected diatom species from the studied interval are available from a data report (Table 2 in Censarek and Gersonde, subm. a), also accessible under *www-odp.tamu.edu/publications*.The study of the Lower Miocene to Lower Pliocene section identified five disconformities. The lowermost hiatus was placed at 48 mbsf and spans from ca. 18.2 to 17.8 Ma. As it was observed at Site 689, the Lower Miocene is separated from the Middle Miocene by a hiatus, located at 44.1 mbsf. The third disconformity, at 39 mbsf, has a range of about 0.6 m.y. in the lower portion of the Middle Miocene. At 18.7 mbsf the Miocene is separated from the Pliocene by a hiatus that ranges from ca. 7.6 Ma into the lowermost Pliocene. The uppermost disconformity identified in the studied section is at around 15.4 mbsf. The calculated average sedimentation rates range between 2 and 10 m/m.y. (Fig. 2.7) and display a similar pattern to the sedimentation rate at Site 689 (Fig. 2.5).

Figure 2.6 (right): Stratigraphic ranges of selected diatom species in the reinvestigated Miocene section of Hole 690B and diatom zonal assignment tied to the geomagnetic data of Spieß (1990). The chron nomenclature is according to Cande and Kent (1992). Dotted lines indicate scattered and trace occurrences of diatom taxa.

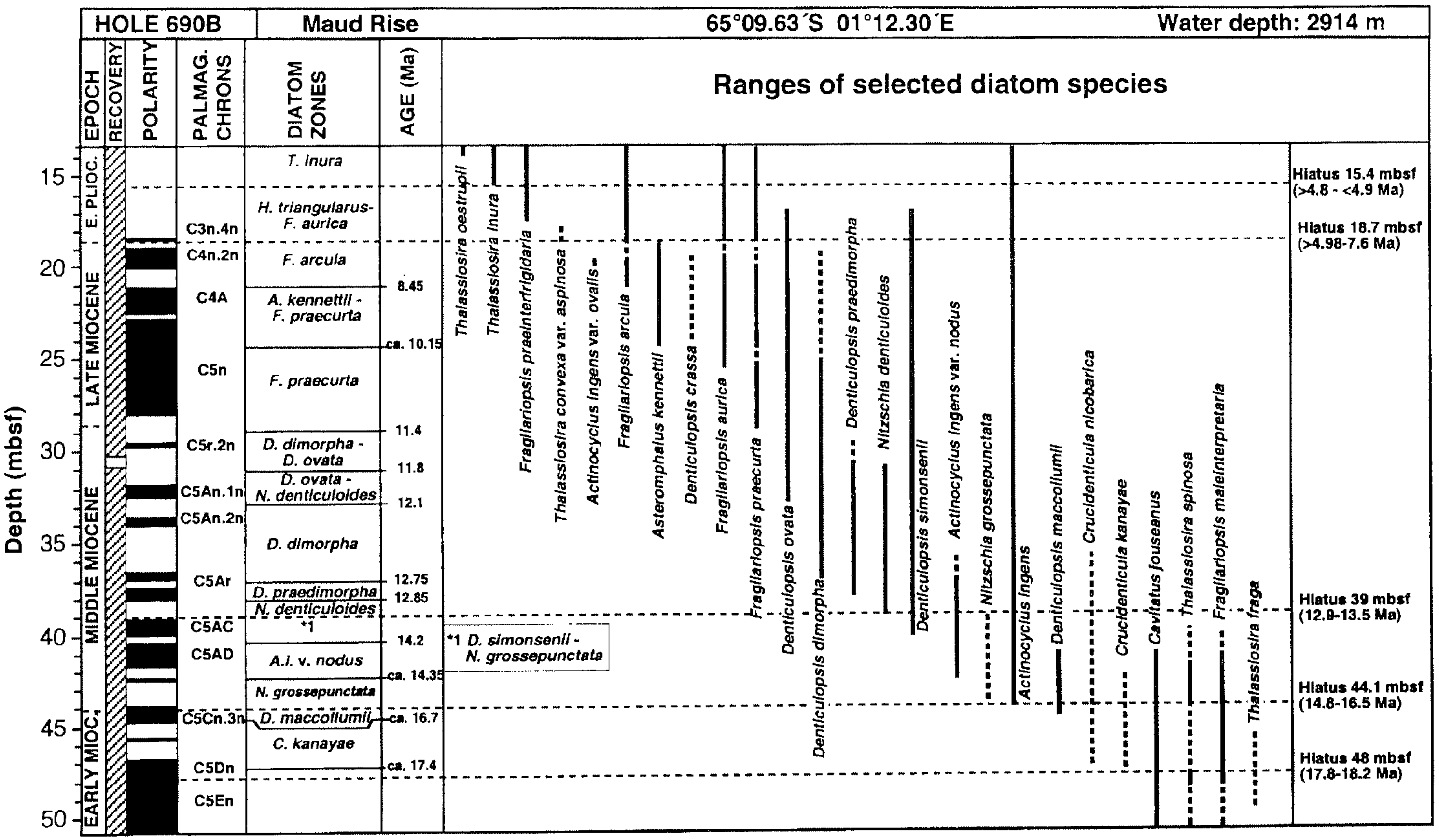
HOLE 690B
Maud Rise
65°09.63´S 01°12.30´E
Water depth: 2914 m
EPOCH
RECOVERY
POLARITY
PALMAG. CHRONS
DIATOM ZONES
AGE (Ma)
Ranges of selected diatom species
Depth (mbsf)
15
20
25
30
35
40
45
50
E. PLIOC.
LATE MIOCENE
MIDDLE MIOCENE
EARLY MIOC.
C3n.4n
C4n.2n
C4A
C5n
C5r.2n
C5An.1n
C5An.2n
C5Ar
C5AC
C5AD
C5Cn.3n
C5Dn
C5En
T. inura
H. triangularus-
F. aurica
F. arcula
A. kennettii -
F. praecurta
F. praecurta
D. dimorpha -
D. ovata
D. ovata -
N. denticuloides
D. dimorpha
D. praedimorpha
N. denticuloides
*1
A.i. v. nodus
N. grossepunctata
D. maccollumii
C. kanayae
8.45
ca. 10.15
11.4
11.8
12.1
12.75
12.85
14.2
ca. 14.35
ca. 16.7
ca. 17.4
*1 D. simonsenii -
N. grossepunctata
Thalassiosira oestrupii
Thalassiosira inura
Fragilariopsis praeinterfrigidaria
Thalassiosira convexa var. aspinosa
Actinocyclus ingens var. ovalis
Fragilariopsis arcula
Asteromphalus kennettii
Denticulopsis crassa
Fragilariopsis aurica
Fragilariopsis praecurta
Denticulopsis ovata
Denticulopsis dimorpha
Denticulopsis praedimorpha
Nitzschia denticuloides
Denticulopsis simonsenii
Actinocyclus ingens var. nodus
Nitzschia grossepunctata
Actinocyclus ingens
Denticulopsis maccollumii
Crucidenticula nicobarica
Crucidenticula kanayae
Cavitatus jouseanus
Thalassiosira spinosa
Fragilariopsis maleinterpretaria
Thalassiosira fraga
Hiatus 15.4 mbsf
(>4.8 - <4.9 Ma)
Hiatus 18.7 mbsf
(>4.98-7.6 Ma)
Hiatus 39 mbsf
(12.9-13.5 Ma)
Hiatus 44.1 mbsf
(14.8-16.5 Ma)
Hiatus 48 mbsf
(17.8-18.2 Ma)

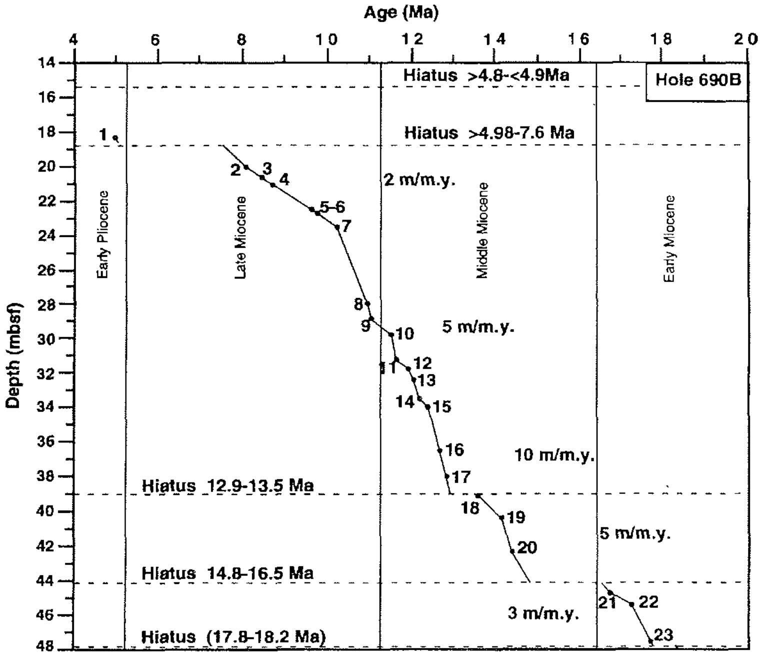

Figure 2.7: Age-depth diagram for the Miocene of Hole 690B and calculated average sedimentation rates. For definition of stratigraphic datum points compare Table 2.3.

The lack of Subchron C3n.3n (Spieß, 1990) and the report of a disconformity between 15.0 and 16.5 mbsf in the silicoflagellate biostratigraphy (McCartney and Wise, 1990) let us assume a short range hiatus (>4.8-<4.9 Ma) between samples 113-690B-3H-3, 27-28 cm and 113-690B-3H-3, 73-75 cm at 15.41 mbsf. The absence of *F. barronii* and the occurrence of *Thalassiosira inura* places the sediment interval above the hiatus into the *T. inura* Zone. It is underlain by the *H. triangularus-F. aurica* Zone that is disturbed by a hiatus at 18.7 mbsf, ranging from ca. 4.98 to 7.6 Ma. *F. praeinterfrigidaria* dominates the assemblage in the upper portion of the zone; accompanying species are *Eucampia antarctica* and *Fragilariopsis clementia*. The base of the following *F. arcula* Zone is recognised between samples 113-690B-3H-7, 27-28 cm and 113-690B-4H-1, 26-27 cm at 21.31 mbsf. *A. ingens* var. *ovalis* was rarely found in this zone. Other characteristic species are *Denticulopsis crassa* and *Actinocyclus karstenii*, both species having ther LO in the middle portion of the *F. arcula* Zone. The following *Asteromphalus kennettii-Fragilariopsis praecurta* Zone has its base between samples 113-690B-4H-2, 115-116 cm and 113-690B-4H-3, 26-27 cm, indicated by the FOD of *A. kennettii*. This interval is characterised by the continuous occurrence of *F. claviceps* and *F. donahuensis*. The base of the underlying *F. praecurta* Zone is located between samples 113-690B-4H-5, 115-116 cm and 113-690B-4H-6, 27-28 cm at 28.86 mbsf. The FO of *F. aurica* occurs in the upper middle portion of this zone, but has rare occurrences in this interval. The following *Denticulopsis dimorpha-Denticulopsis ovata* Zone is disturbed by a recovery gap, which is between 30.15 and 31.36 mbsf (Spieß, 1990). A hiatus proposed by Gersonde and Burckle (1990) to occur at 31.2 mbsf could not be confirmed.

The base of this zone is located at 31.82 mbsf between samples 113-690B-5H-1, 28-29 cm and 113-690B-5H-1, 116-117 cm. The LO of *D. praedimorpha* is identified in the upper portion of the *D. dimorpha- D. ovata* Zone near Subchron C5r.2n. The next biostratigraphical unit is the *D. ovata-N. denticuloides* Zone, which is defined by the FOD of *D. ovata* at 33.1 mbsf, between samples 113-690B-5H-2, 28-29 cm and 113-690B-5H-2, 115-116 cm. The base of the subsequent *D. dimorpha* Zone is defined by the FOD of the nominate species (36.95 mbsf), between samples 113-690B-5H-3, 115-116 cm and 113-690B-5H-4, 28-29 cm. The diatom assemblage within this zone consist mostly of the nominate species, *D. praedimorpha*, *N. denticuloides*, *A. ingens* and *D. simonsenii*. In the lower portion of the zone, the LO of *A. ingens* var. *nodus* is recognised. The base of the underlying *D. praedimorpha* Zone is located between samples 113-690B-5H-5, 28-29 cm and 113-690B-5H-5, 115-116 cm at 37.82 mbsf. High abundances of the nominate species characterise this short ranging zone. The subsequent *N. denticuloides* Zone is marked by a hiatus at 39 mbsf, which spans from about 12.9 to 13.5 Ma and includes a time interval that corresponds to Chrons C5AA and C5AB. Gersonde and Burckle (1990) also report this Middle Miocene hiatus. The base of the *Denticulopsis simonsenii-Nitzschia grossepunctata* Zone is recognised between samples 113-690B-5H-7, 28-29 cm and 113-690B-6H-1, 27-28 cm at 40.74 mbsf, which correlates to the upper portion of magnetostratigraphical Chron C5AD. Typical for this interval are high abundances of *A. ingens* and *Actinocyclus ingens* var. *nodus*. The lower boundary of the following *A. ingens* var. *nodus* Zone at 42.26 mbsf is between samples 113-690B-6H-1, 114-115 cm and 113-690B-6H-2, 27-28 cm. This base is defined by the FOD of the nominate species. Characteristic is the co-occurrence of *A. ingens* var. *nodus* with *D. maccollumii*. Due to a hiatus at 44.1 mbsf only the upper portion of the subsequent *Nitzschia grossepunctata* Zone is present. This hiatus spans a time interval of 14.8 to 16.5 Ma and is indicated by co-occurring FOs *of N. grossepunctata* and *A. ingens*. The hiatus includes a time interval that ranges from Chron C5B to the upper portion of Chron C5C, including the sediments of the lower *N. grossepunctata* and of the *A. ingens-D. maccollumii* zone. Below this hiatus the sediments of the lower *D. maccollumii* Zone are present, which has its base between samples 113-690B-6H-3, 27-28 cm and 113-690B-6H-3, 49-51 cm at 44.51 mbsf. The base of the following *Crucidenticula kanayae* Zone was encountered between samples 113-690B-6H-5, 114-115 cm and 113-690B-6H-5, 27-28 cm at 47.51 mbsf. The zone is characterised by the occurrences of species such as *Cavitatus jouseanus, Thalassiosira spinosa* and *Fragilariopsis maleinterpretaria,* as well as *Thalassiosira fraga* occurring trace abundances. A hiatus was identified below this zone at 48 mbsf, based on combined diatom, radiolarian (Abelmann, 1990) and magnetostratigraphic (Spieß, 1990) results.

Table 2.3: Definition of stratigraphic datum points in the Miocene section of Hole 690B used to construct the age-depth diagram in Figure 2.7.

Datum points	Depth (mbsf)	Age (Ma)	Definition
Hiatus	15.41	>4.8-<4.9	
1	18.32	4.98	Top C4n.3n
Hiatus	18.7	>4.98-7.6	
2	20.07	8.072	Base C4n.2n
3	20.66	8.45	FOD *F. arcula*
4	21.07	8.699	Top C4An
5	22.53	9.642	Base C4Ar.2n
6	22.76	9.74	Top C5n
7	23.62	10.15	FOD *A. kennettii*
8	28.03	10.949	Base C5n.2n
9	28.86	11.4	FOD *F. praecurta*
10	29.78	11.531	Base C5r.2n
11	31.28	11.8	FOD *N. denticuloides*
12	31.72	11.935	Top C5An.1n
13	32.45	12.078	Base C5An.1n
14	33.47	12.184	Top C5An.2n
15	33.95	12.401	Base C5An.2n
16	36.35	12.678	Top C5Ar.1n
17	37.97	12.819	Base C5Ar.2n
Hiatus	38.97	12.9-13.5	
18	39	13.703	Top C5AC
19	40.4	14.2	FOD *D. simonsenii*
20	42.26	14.35	FOD *A. ingens* var. *nodus*
Hiatus	44.1	14.8-16.5	
21	44.68	16.726	Base C5Cn.3n
22	45.41	17.277	Top C5Dn
23	47.51	17.4	FOD *C. kanayae*
Hiatus	48	17.8-18.2	

Another disconformity documented by Gersonde and Burckle (1990) at the top of Chron C5Dn could not be validated. The diatom preservation in the early Middle Miocene portion is poor to moderate, as reported for Hole 689B.

2.5.3 Site 1088

Site 1088 (41°08.16'S, 13°33.77'E) is located on the Agulhas Ridge in 2082 m water depth. This bathymetric setting places the site near the interface between North Atlantic Deep Water (NADW) and Circumpolar Deep Water (CDW). The drilling of three holes recovered predominantly calcareous ooze, Holocene to Middle Miocene in age. Diatoms are intermittent, mainly as a trace component, although some diatom-bearing nannofossil ooze is present. Our study is about sediment sequences recovered from Holes B and C. Stratigraphic data are presented in Figures 2.8 and 2.9 and in Table 2.4. Sediment barren of diatoms is marked grey in Figure 2.8. Range charts of the stratigraphic occurrence of selected diatom species from the studied interval are available from a data report (Table 3 in Censarek and Gersonde, subm. a), also accessible under *www-odp.tamu.edu/publications*.

No magnetostratigraphic data could be obtained at this site (Shipboard Scientific Party, 1999a). To support the scattered diatom biostratigraphic data for the Miocene section we include shipboard data based on the calcareous nannofossil record (Shipboard Scientific Party, 1999a). Calculated sedimentation rates are 14 m/m.y. in the middle Late Miocene, increasing up to 31 m/m.y. in the early Late Miocene and 11 m/m.y. during the Middle Miocene (Fig. 2.9). A probable Middle Miocene hiatus at 208.82 mcd was identified by shipboard calcareous nannofossil investigations (Shipboard Scientific Party, 1999a).

The uppermost zone is the *Thalassiosira inura* Zone. Its base was placed between samples 177-1088B-5H-3, 25-26 cm and 177-1088B-5H-2, 137-138 cm. *Neobrunia mirabilis* and *Fragilariopsis fossilis* dominate this zone, besides the nominate species and *Thalassiosira torokina*. An interval barren of diatoms is located from approx. 38 to 70 mcd. Within this interval the LOD of calcareous nannofossil *D. quinqueramus* at 46 mcd indicates an age of around 5.5 Ma (Shipboard Scientific Party, 1999a). Below this interval the *Fragilariopsis reinholdii* Zone has its base at 89.45 mcd between samples 177-1088B-10H-6, 0-1 cm and 177-1088B-10H-6, 90-91 cm.

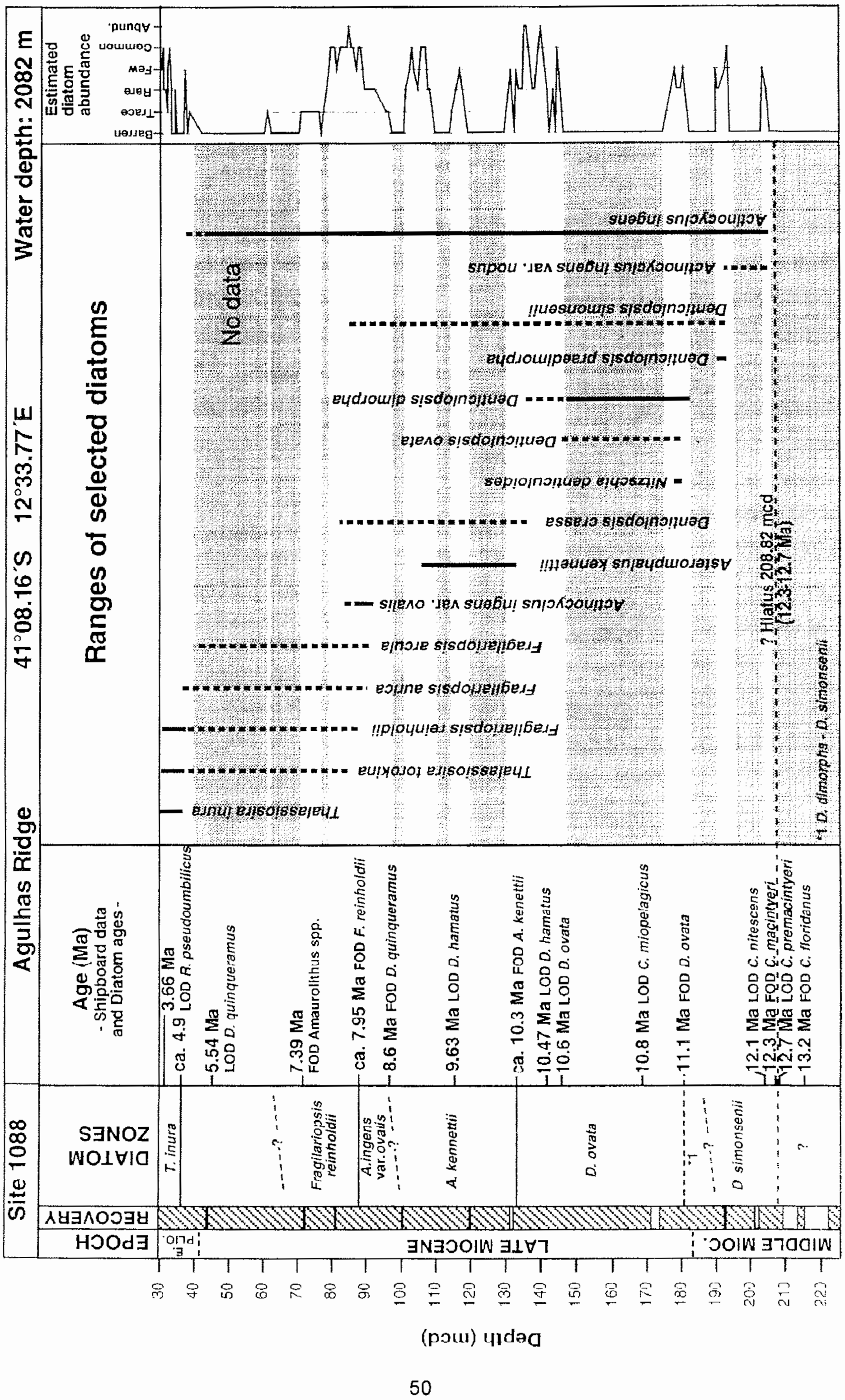
Site 1088
Agulhas Ridge
41°08.16'S 12°33.77'E
Water depth: 2082 m
EPOCH
RECOVERY
DIATOM ZONES
Age (Ma) - Shipboard data and Diatom ages -
Ranges of selected diatoms
Estimated diatom abundance
Barren
Trace
Rare
Few
Common
Abund.
PLIO. E
LATE MIOCENE
MIDDLE MIOC.
T. inura
Fragilariopsis reinholdii
A. ingens var. ovalis
A. kennettii
D. ovata
D simonsenii
?
3.66 Ma LOD R. pseudoumbilicus
ca. 4.9
5.54 Ma LOD D. quinqueramus
7.39 Ma FOD Amaurolithus spp.
ca. 7.95 Ma FOD F. reinholdii
8.6 Ma FOD D. quinqueramus
9.63 Ma LOD D. hamatus
ca. 10.3 Ma FOD A. kenettii
10.47 Ma LOD D. hamatus
10.6 Ma LOD D. ovata
10.8 Ma LOD C. miopelagicus
11.1 Ma FOD D. ovata
12.1 Ma LOD C. nitescens
12.3 Ma FOD C. macintyeri
12.7 Ma LOD C. premacintyeri
13.2 Ma FOD C. floridanus
No data
Thalassiosira inura
Thalassiosira torokina
Fragilariopsis reinholdii
Fragilariopsis aurica
Fragilariopsis arcula
Actinocyclus ingens var. ovalis
Asteromphalus kennettii
Denticulopsis crassa
Nitzschia denticuloides
Denticulopsis ovata
Denticulopsis dimorpha
Denticulopsis praedimorpha
Denticulopsis simonsenii
Actinocyclus ingens var. nodus
Actinocyclus ingens
? Hiatus 208.82 mcd (12.3-12.7 Ma)
↑1 D. dimorpha - D. simonsenii
30
40
50
60
70
80
90
100
110
120
130
140
150
160
170
180
190
200
210
220
Depth (mcd)

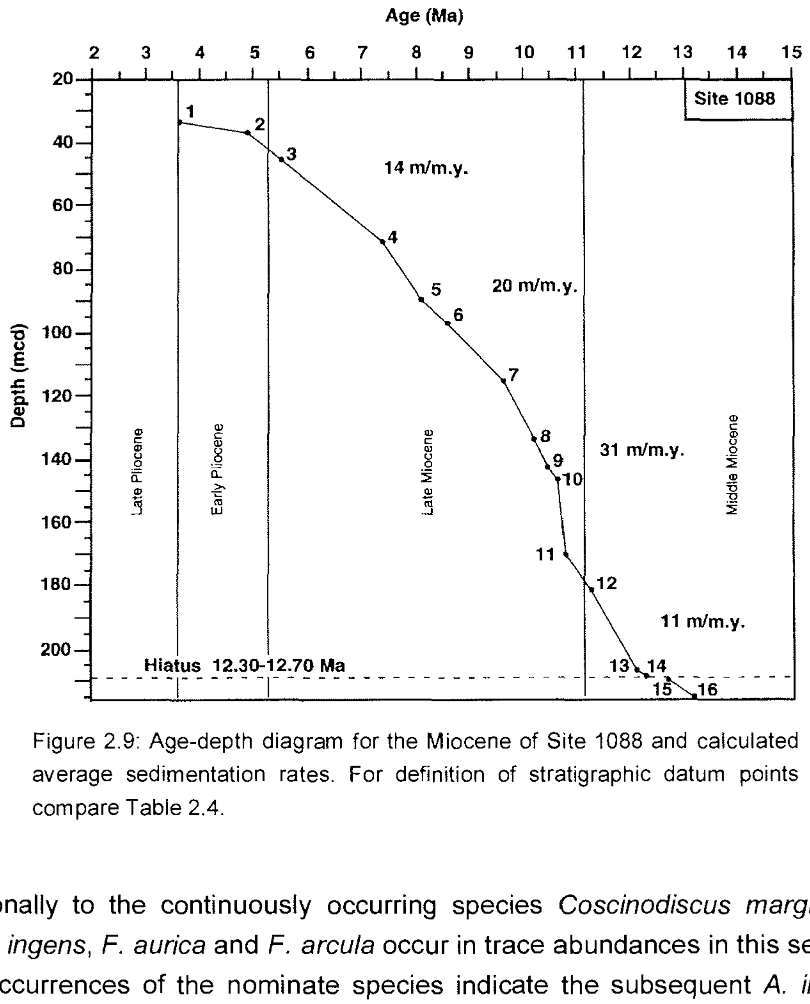

Figure 2.9: Age-depth diagram for the Miocene of Site 1088 and calculated average sedimentation rates. For definition of stratigraphic datum points compare Table 2.4.

Additionally to the continuously occurring species *Coscinodiscus marginatus* and *A. ingens*, *F. aurica* and *F. arcula* occur in trace abundances in this section. Few occurrences of the nominate species indicate the subsequent *A. ingens* var. *ovalis* Zone. The base of the zone could not be determined. Below a section barren of diatoms, from approx. 119 mcd to 130 mcd, we encountered the base of the *Asteromphalus kennettii* Zone between samples 177-1088C-2H-3, 20-21 cm and 177-1088C-3H-3, 20-21 cm. *Denticulopsis crassa* occurs sporadically in this interval. The sediment section is barren of diatoms between approx. 146 mcd and 179 mcd.

Figure 2.8 (left): Stratigraphical ranges of selected diatom species in the Miocene section of Site 1088 and diatom zonal assignment supported by nannofossil shipboard data (Shipboard Scientific Party, 1999a). Estimations of diatom abundances are also indicated. Dotted lines indicate scattered and trace occurrences.

The base of the subsequent *Denticulopsis ovata* Zone (11.1 Ma) is located above sample 177-1088C-9X-5, 95-96 cm at 181.42 mcd. This boundary is supported by the LOD of the calcareous nannofossil *C. miopelagicus*, which indicates an age of 10.8 Ma (Shipboard Scientific Party, 1999a). Below this, falls the *D. dimorpha - D. simonsenii-* and *D. simonsenii* Zone, recognised by the occurrence of assemblages which contain *N. denticuloides*, *D. praedimorpha* and *A. ingens* var. *nodus* and the nominate species. The disconformity at 208.82 mcd, spanning from 12.3 to 12.7 Ma could be estimated by nannofossil ages (Shipboard Scientific Party, 1999a). Below this hiatus diatoms are absent.

Table 2.4: Definition of stratigraphic datum points in the Miocene section of Site 1088 used to construct the age-depth diagram in Figure 2.9.

Datum points	Depth (mcd)	Age (Ma)	Definition
1	33.65	3.66	LOD *R. pseudoumilicus*
2	37.06	4.9	FOD *T. inura*
3	46.05	5.54	LOD *D. quinqueramus*
4	71.29	7.39	FOD *Amaurolithus* spp.
5	89.45	7.95	FOD *F. reinholdii*
6	97.3	8.6	FOD *D. quinqueramus*
7	115.2	9.63	LOD *D. hamatus*
8	134.02	10.3	FOD *A. kennettii*
9	142.49	10.47	FOD *D. hamatus*
10	146.14	10.6	LOD *D. ovata*
11	169.84	10.8	LOD *C. miopelagicus*
12	181.56	11.1	FOD *D. ovata*
13	206.15	12.1	LOD *C. nitescens*
14	208.27	12.3	FOD *C. macintyeri*
Hiatus	208.82	12.30-12.70	
15	209.37	12.7	LOD *C. premacintyeri*
16	214.84	13.2	LOD *C. floirdanus*

2.5.4 Site 1092

Site 1092 (46°24.70'S, 07°04.79'E) is located in 1974 m water depth on the northern Meteor Rise, one of the dominant topographic features in the southeast Atlantic that defines the westward limit of the Agulhas Basin. This site is located in the Polar Front Zone (PFZ). It is located above the regional carbonate lysocline and carbonate compensation depth (CCD) and within a mixing zone between NADW and the CDW water masses. Three holes were drilled by the APC at a high recovery rate. A composite section was constructed up to 210.54 mcd including a 150 m interval assigned to the Middle and the Late Miocene

(Shipboard Scientific Party, 1999b). The stratigraphic data are presented on Figures 2.10 and 2.11 and on Table 2.5. Range charts of the stratigraphic occurrence of selected diatom species from the studied interval are available from a data report (Table 4 in Censarek and Gersonde, subm. a), also accessible under *www-odp.tamu.edu/publications*. The pattern of sedimentation rates is similar to those obtained from the Maud Rise sites. Lower values are encountered during the Early Pliocene and Late Miocene (6-15 m/m.y.). Highest average sedimentation rates (32m/m.y.) were obtained around the Middle to Late Miocene boundary (Fig. 2.11). The preliminary magnetostratigraphic interpretation based on shipboard inclination data obtained from Shipboard Scientific Party (1999b) allows a correlation of diatom ranges with the magnetostratigraphic record.

The lower Lower Pliocene section is characterised by two disconformities at 64.3 mcd and 68.46 mcd. According to Zielinski and Gersonde (2002) the Lower Pliocene hiatus is located between samples 177-1092A-6H-6, 79-80 cm and 177-1092A-7H-1, 79-80 cm. The co-occurrence of *Fragilariopsis barronii* and *Fragilariopsis interfrigidaria* above this hiatus indicates that at least the *F. barronii* Zone (3.8-4.45 Ma) is absent. Findings of *Thalassiosira inura* (FOD of 4.9 Ma) and *F. praeinterfrigidaria* (3.8-?5.3 Ma) in the absence of *F. barronii* indicate that the section below the Lower Pliocene hiatus can be placed into the *T. inura* Zone. The lower part of this zone is removed by a hiatus, located between Samples 177-1092A-7H-3, 112-113 cm and 177-1092A-7H-3, 142-143. The FOD of *Fragilariopsis praeinterfrigidaria* was not recognised. This suggests that the hiatus at the Miocene/Pliocene boundary spans from 4.9 to 5.3 Ma. The normal polarised interval between the Upper Miocene-Lower Pliocene boundary hiatus and the Lower Pliocene hiatus is interpreted as Subchron C3n.2n, based upon the occurrence of the FOD of *Thalassiosira complicata* (ca. 4.45 Ma) at 67.23 mcd. The sediment below the Miocene/Pliocene disconformity can be correlated to the *Hemidiscus triangularus-Fragilariopsis aurica* Zone, revealing its base at 80.36 mcd, between samples 177-1092C-9H-3, 6-7 cm and 177-1092C-9H-2, 126-127 cm. The FOD of *H. triangularus* was interpreted to be at around 7.3 Ma. We encountered within the *H. triangularus-F. aurica* Zone the FO of *T. convexa* var. *aspinosa* between samples 177-1092A-8H-1, 79-80 cm and 177-1092B-8H-4, 66-67 cm at 6.55 Ma. Few to common occurrences of *Fragilariopsis reinholdii*, *Fragilariopsis praecurta* and *Fragilariopsis fossilis* have been encountered in this zone. Sediments below this interval represent the *F. reinholdii* Zone, which has its base at 87.67

mcd, between samples 177-1092A-9H-3, 79-80 cm and 177-1092A-9H-3, 88-89 cm. Based on the diatom record we interpret the geomagnetic record between 69 and 90 mcd to represent Subchrons C3An.1n to C4n.2n. Two short-ranging normal polarised events between 90.5 to 93 mcd could not be identified. The following *A. ingens* var. *ovalis* Zone has its base between samples 177-1092A-10H-2, 79-80 cm and 177-1092B-10H-4, 90-91 cm at 96.20 mcd. The base is defined by the FOD of the nominate species, showing only rare abundances in the lower portion of the zone. The FO of *A. kennettii* was encountered between samples 177-1092A-13H-6, 79-80 cm and 177-1092C-14H-2, 91-92 cm at 135.11 mcd. Also present are the nominate species, *Denticulopsis simonsenii*, *A. ingens,* and less abundances of *F. praecurta* and *D. crassa.* The underlying zone is the *Denticulopsis ovata* Zone, its base defined by the FO of *D. ovata* (160.39 mcd) between samples 177-1092B-16H-3, 117-118 cm and 177-1092B-16H-4, 67-68 cm. Characteristic species occurring in the *D. ovata* Zone are *Denticulopsis dimorpha,* which dominates in the lower portion; and *D. crassa*, with a FO in the lower part of this zone. The base of the subsequent *D. dimorpha-D. simonsenii* Zone is recognised between samples 177-1092A-17H-4, 79-80 cm and 177-1092A-17H-4, 79-80 cm. This zone is defined by the FO of *D. dimorpha* at 174.22 mcd. Within this zone the LO of *Nitzschia denticuloides* is found at a depth of 170.95 mcd and with an age of 11.8 Ma. The following *D. simonsenii* Zone is marked by a hiatus at 178.83 mcd, which spans from ca. 12.7 to 13.5 Ma. This is indicated by the joint FO of *D. praedimorpha* and *N. denticuloides* and the LO of *A. ingens* var. *nodus*. *Denticulopsis praedimorpha* occurs in only a few samples above this hiatus. The base of the *D. simonsenii* Zone (FO of the nominate species) is between samples 177-1092B-18H-3, 48-49 cm and 177-1092A-18H-2, 148-149 cm at 183.08 mcd. The FO of *A. ingens* between samples 177-1092A-19H-1, 79-80 cm and 177-1092A-19H-1, 104-105 cm (192.76 mcd) defines the *A. ingens* Zone. Considering the FODs of *D. simonsenii* and *Actinocyclus ingens* var. *nodus* at 183.08 mcd and 184.58 mcd, respectively, we propose to interpret the normal polarity interval between 187.52 and 182.48 mcd as Chron C5ADn. Between 188 and 192 mcd no shipboard geomagnetic polarity data are available. Based on the FOD of *A. ingens* at 192.76 mcd we tentatively assign the normal polarity interval around this depth to represent Chron C5Cn.

Figure 2.10 (right): Ranges of selected diatom species in the Miocene section of Site 1092. The geomagnetic polarity record is based on the shipboard inclination record (Shipboard Scientific Party, 1999b. The chron nomenclature is according to Cande and Kent (1992). Dotted lines indicate scattered and trace occurrences.

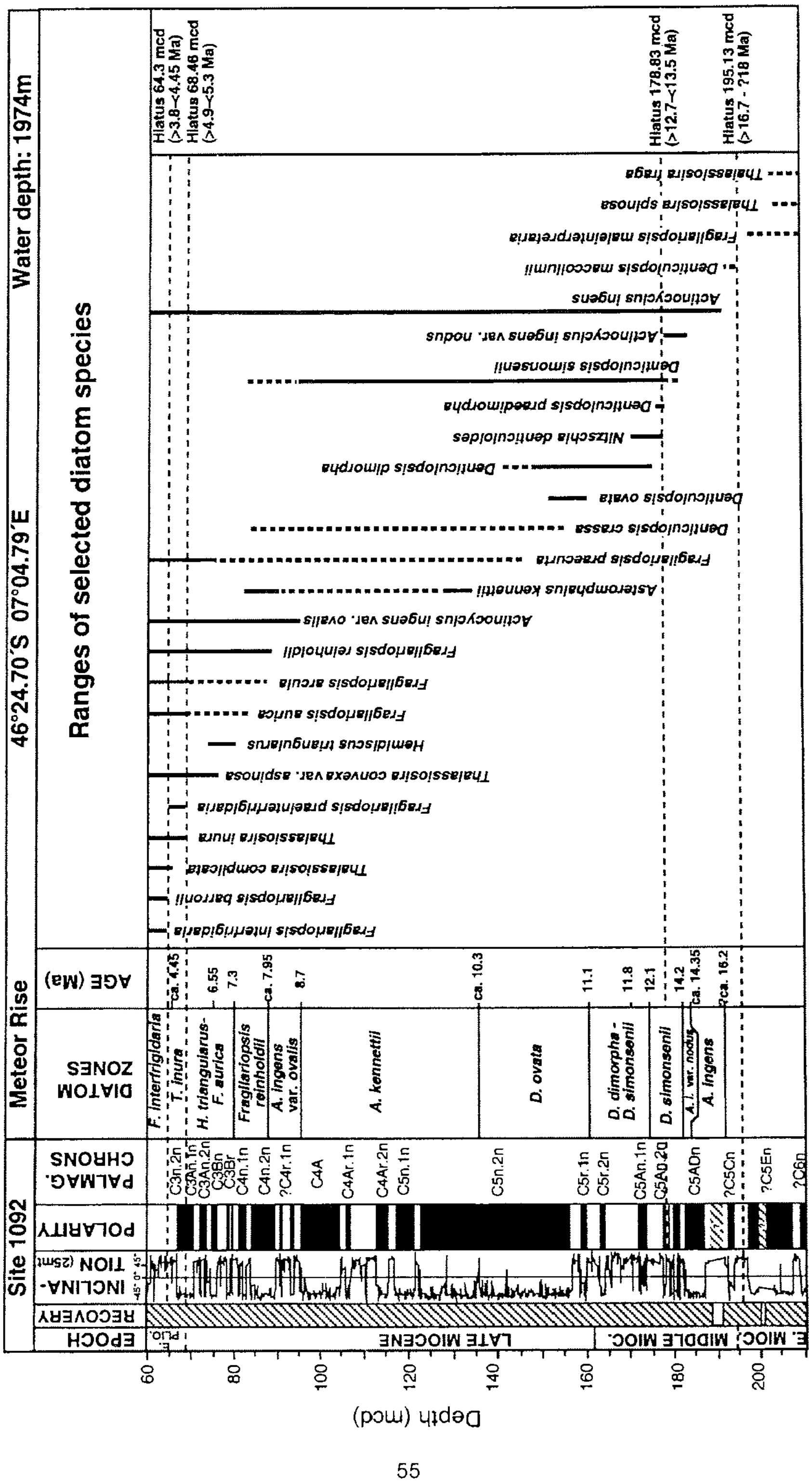
Site 1092
Meteor Rise
46°24.70'S 07°04.79'E
Water depth: 1974m
EPOCH
RECOVERY
INCLINATION (25mT)
-45° 0° 45°
POLARITY
PALMAG. CHRONS
DIATOM ZONES
AGE (Ma)
Ranges of selected diatom species
PLIO.
LATE MIOCENE
MIDDLE MIOC.
E. MIOC.
C3n.2n
C3An.1n
C3An.2n
C3Bn
C3Br
C4n.1n
C4n.2n
?C4r.1n
C4A
C4Ar.1n
C4Ar.2n
C5n.1n
C5n.2n
C5r.1n
C5r.2n
C5An.1n
C5AD.2n
C5ADn
?C5Cn
?C5En
?C6n
F. interfrigidaria
T. inura
H. triangularus - F. aurica
Fragilariopsis reinholdii
A. ingens var. ovalis
A. kennettii
D. ovata
D. dimorpha - D. simonsenii
D. simonsenii
A. i. var. nodus
A. ingens
ca. 4.45
6.55
7.3
ca. 7.95
8.7
ca. 10.3
11.1
11.8
12.1
14.2
ca. 14.35
?ca. 16.2
Fragilariopsis interfrigidaria
Fragilariopsis barronii
Thalassiosira complicata
Thalassiosira inura
Fragilariopsis praeinterfrigidaria
Thalassiosira convexa var. aspinosa
Hemidiscus triangularus
Fragilariopsis aurica
Fragilariopsis arcula
Fragilariopsis reinholdii
Actinocyclus ingens var. ovalis
Asteromphalus kennettii
Fragilariopsis praecurta
Denticulopsis crassa
Denticulopsis ovata
Denticulopsis dimorpha
Nitzschia denticuloides
Denticulopsis praedimorpha
Denticulopsis simonsenii
Actinocyclus ingens var. nodus
Actinocyclus ingens
Denticulopsis maccollumii
Fragilariopsis maleinterpretaria
Thalassiosira spinosa
Thalassiosira fraga
Hiatus 64.3 mcd (>3.8-<4.45 Ma)
Hiatus 68.46 mcd (>4.9-<5.3 Ma)
Hiatus 178.83 mcd (>12.7-<13.5 Ma)
Hiatus 195.13 mcd (>16.7 - ?18 Ma)
60
80
100
120
140
160
180
200
Depth (mcd)

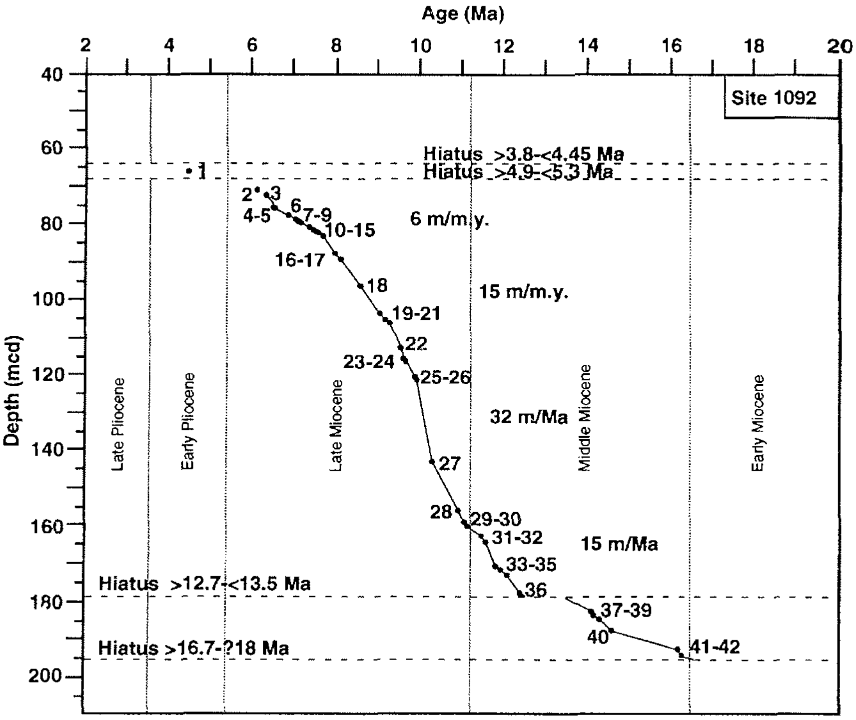

Figure 2.11: Age-depth diagram for the Miocene of Site 1092 and calculated average sedimentation rates. For definition of stratigraphic datum points compare Table 2.5.

For age assignment of the FOD of *A. ingens* we follow Baldauf and Barron (1991) who placed this FOD in the upper portion of Chron C5n (Hole 744 B). As a consequence of this interpretation, Chrons C5Bn and C5Br that span a time interval of more than 1 m.y. fall either in the magnetostratigraphic record gap and/or a hiatus should occur in this interval. Another explanation might be that the FOD of *A. ingens* in Southern Ocean sediments is diachronous and occurs in the northern zone of the Southern Ocean at a younger age compared to the southern zone. The incomplete stratigraphical range of *Denticuloides maccollumii* let us suggest a disconformity occurring at 195.13 mcd. The stratigraphic range of the missing sediments can be estimated considering the FO of *D. maccollumii* (ca. 16.7 Ma) and the age assignment of the assemblage recovered below 195 mcd consisting of *Fragilariopsis maleinterpretaria*, *Thalassiosira fraga* and *Thalassiosira spinosa*. An age of the lowermost portion of Site 1092 is suggested to be around 18-19 Ma, according to Baldauf and Barron (1991).

Table 2.5: Definition of stratigraphic datum points in the Miocene section of Site 1092 used used to construct the age-depth diagram in Figure 2.11. • - magnetostratigraphic datum points differs from the shipboard interpretation; ** - magnetostratigraphic datum point coincide with the shipbord interpretation (Shipboard Scientific Party, 1999b).

Datum points	Depth (mcd)	Age (Ma)	Definition
Hiatus	64.30	>3.8-<4.45	
1	66.12	4.480	Top C3n.2n
Hiatus	68.46	>4.9-<5.3	
2	71.58	6.137	Base C3An.1n
3	73.97	6.269	Top C3An.2n
4	75.38	6.55	FOD *T. convexa* var. *aspinosa*
5	75.45	6.567	Base C3An.2n
6	77.88	6.935	Top C3Bn
7	78.48	7.091	Base C3Bn
8	78.95	7.135	Top C3Br.1n
9	79.33	7.170	Base C3Br.1n
10	80.36	7.3	FOD *H. triangularus*
11	80.56	7.341	Top C3Br.2n
12	81.13	7.375	Base C3Br.2n
13	81.43	7.432	Top C4n.1n
14	82.68	7.562	Base C4n.1n
15	83.45	7.65	Top C4n.2n •
16	87.67	7.95	FOD *F. reinholdii*
17	89.16	8.072	Base C4n.2n
18	95.28	8.699	Top C4An *
19	104.31	9.025	Base C4An
20	105.32	9.230	Top C4Ar.1n
21	106.87	9.308	Base C4Ar.1n
22	112.73	9.580	Top C4Ar.2n
23	115.63	9.642	Base C4Ar.2n *
24	116.73	9.740	Top C5n.1n
25	121.58	9.880	Base C5n.1n
26	121.88	9.920	Top C5n.2n
27	143.82	10.3	FOD *A. kennettii*
28	156.69	10.949	Base C5n.2n **
29	159.90	11.052	Top C5r.1n
30	160.22	11.099	Base C5r.1n
31	163.00	11.476	Top C5r.2n
32	164.56	11.531	Base C5r.2n
33	170.95	11.8	LOD *N. denticuloides*
34	172.18	11.935	Top C5An.1n
35	173.03	12.078	Base C5An.1n
36	177.44	12.401	Top C5An.2n
Hiatus	178.83	>12.7-<13.5	
37	182.48	14.178	TopC5ADn
38	183.08	14.2	FOD *D. simonsenii*
39	184.58	14.35	FOD *A. ingens* v. *nodus*
40	187.52	14.612	Base C5ADn
41	192.76	16.2	FOD *A. ingens*
42	194.07	16.293	Base C5Cn.1n
Hiatus	195.13	>16.7-?18.0	

2.6 Discussion

The study of Miocene sections recovered at different latitudes in the Southern Ocean reveals apparent latitudinal differentiations of occurrence and stratigraphic range of biostratigraphic marker diatoms. Considering this pattern, we propose the use of two diatom zonations, applicable to the northern and southern area of the Southern Ocean, respectively. Further refinement comes from the application of new taxonomic concepts, proposed for the genus *Denticulopsis* by Yanagisawa and Akiba (1990).

The reinvestigation of Sites 689 and 690 results in a refinement of the diatom biostratigraphic zonation proposed by Gersonde and Burckle (1990), Baldauf and Barron (1991) and Harwood and Maruyama (1992) for Miocene marine deposits in southern-high latitudes. Based on these data we propose a southern Southern Ocean diatom biostratigraphic zonation (SSODZ). New or revised zones and stratigraphic ranges of diatom taxa can be defined for the middle Late Miocene (*F. arcula*- and *H. triangularus-F. aurica* Zone), the late Middle Miocene (*D. praedimorpha*-, *D. dimorpha*-, *D. ovata-N. denticuloides*- and *F. praecurta* Zone) and the late Early Miocene (*C. kanayae* Zone). However, the lack of stratigraphically useful first or last occurrences and the occurrence of disconformities in most Southern Ocean records prevents a further stratigraphic refinement of the latest Miocene in southern-high latitudes. The acquisition of species distribution data by counting instead of estimation of species abundance, as done by Gersonde and Burckle (1990), results in the revision of stratigraphic ranges of some taxa. The FODs of *D. dimorpha* and *D. praedimorpha* were found to be ca. 0.6 m.y. and ca. 0.1 m.y. older than reported by Gersonde and Burckle (1990). Revised diatom and geomagnetic polarity age assignments allows a recalculation of the stratigraphic range of disconformities at sites 689 and 690. The presence of the short ranging disconformities of Gersonde and Burckle (1990); in the middle Lower Pliocene of Hole 689B (11.7 mbsf), in the Upper Miocene of Hole 690B (21 mbsf) as well as the Middle Miocene of Hole 690B (31.2 mbsf) could not be confirmed. All other disconformities identified by Gersonde and Burckle (1990) from the Lower Miocene to Lower Pliocene sediment record at sites 689 and 690 could be verified and the age determinations were updated according to the GPTS of Berggren et al. (1995).

The study of Site 1092 reveals latitudinal differences in the occurrence and stratigraphic ranges of diatom species between the southern and northern zone of the Southern Ocean. The data obtained from this site were used for the establishment of a northern Southern Ocean diatom zonation (NSODZ), also considering paleomagnetic information and diatom distribution records from ODP Leg 114 sites (Hailwood and Clement, 1991a, b; Ciesielski, 1991). However, in the absence of shore-based stratigraphic refinement of the geomagnetic polarity record obtained from Site 1092 we needed to tie the diatom ranges to a magnetostratigraphic record that is based on the interpretation of shipboard inclination data (Shipboard Scientific Party, 1999b). Thus, further shore-based magnetostratigraphic investigations might lead to revisions of age assignments of our stratigraphic interpretation.

Latitudinal differentiations of the occurrence ranges of *D. dimorpha* and *D. ovata* are observed in the late Middle to early Late Miocene (Fig. 2.3). At the Maud Rise sites 689 and 690 both taxa display FOs occurring ca. 0.6 m.y. respectively 1 m.y. earlier than observed at 1092. While the ranges of both taxa are restricted to a period around the Middle/Late Miocene boundary at the northern site (1092), they reach into the latest Late Miocene at the sites close to the Antarctic continent (689, 690). These changes can be interpreted to mirror latitudinal differentiations of surface water in relation to the Antarctic cryosphere development. As a consequence of the major increase of the East Antarctic Ice Sheet (EAIS) and subsequent Antarctic cooling between 15 and 13 Ma, meridional temperature gradients increased (Flower and Kennett, 1993). A distinct sea level fall excursion between 10 and 11 Ma (Abreu and Anderson, 1998) might indicate a cooling event with a strong EAIS increase. This time interval has a close temporal relation to the occurrence pattern of *D. dimorpha* and *D. ovata* at Site 1092. It can be speculated that the occurrence of both taxa is indicative for a cold water excursion into the present central portion of the ACC related to a southern high latitude cooling event close to the Middle/Late Miocene boundary. Diachronous FODs were also observed in the Late Miocene, affecting the temporal and spatial distribution of species such as *F. arcula* and *F. aurica,* both occurring distinctly earlier at the Maud Rise sites. This might indicate latitudinal expansion of colder waters during the Late Miocene. A more detailed study reconstructing Southern Ocean surface water development based on Miocene diatom species ranges and abundance pattern is currently in progress (Censarek and Gersonde, subm. b).

The quantitative diatom reinvestigation at sites 689 and 690 allows a comparison with the stratigraphic interpretation of both sites recently proposed by Ramsay and Baldauf (1999). This is done exemplarily for Hole 689B, also considering the results obtained from the second site (690) drilled on Maud Rise (Fig. 2.12). Ramsay and Baldauf (1999) recalculated diatom occurrence datums and reassessed magnetostratigraphic interpretations obtained from 17 DSDP and ODP sites located in the Southern Ocean. This was accomplished by an iterative integrated process with the assumption that the sedimentary sequences were continuous. Due to this assumption some disconformities identified by Gersonde and Burckle (1990) and Gersonde et al. (1990) at sites 689 and 690 were not taken into account. The age model proposed by Ramsay and Baldauf (1999) for Hole 689B coincides with our results in the Early Pliocene, in the Late Middle to early Late Miocene and in the Early Miocene. Intervals bearing disagreements between the interpretation of Ramsay and Baldauf (1999), Gersonde and Burckle (1990) and this study are labelled 1 to 3 in Figure 2.12. Ramsay and Baldauf (1999) interpreted in Hole 689B the three normal polarised intervals between ca. 18 to 24 mbsf to represent chrons C4Ar to C4An (Fig. 2.12, Point 1). We interpreted this to represent C4An to C3An.2n. Our interpretation is based on the occurrence of the FOD of *T. convexa* at 18.58 mbsf, which has an age of 6.55 Ma and correlates to the lower portion of Subchron C3An.2n (see Hole 746A in Baldauf and Barron, 1991). Further we refer to the FOD of *Fragilariopsis arcula* to support our interpretation. This FOD is located in Hole 689 at 21.51 mbsf, in Hole 690B at 21.31 mbsf and correlates in both holes to the lower portion of Chron C4r (Figs. 2.4, 2.6). According to the interpretation of Ramsay and Baldauf (1999) the FOD of *F. arcula* would be diachronous between the two Maud Rise sites, occurring in the lower portion of C4Ar.2r, respectively in C4Ar.3r. Another reliable hint to support our interpretation comes from the FOD of *A. ingens* var. *ovalis*. Baldauf and Barron (1991) locate the FOD in Hole 746A close to the base of Subchron C4n.2n, an age assignment that was approved by Ramsay and Baldauf (1999). Applying the age model of Ramsay and Baldauf (1999) at Hole 689B, the FOD of *A. ingens* var. *ovalis* should fall into a hiatus at 18 mbsf. However, we found the FOD of *A. ingens* var. *ovalis* at 22.26 mbsf and interpreted this to correlate with the reversed portion of Chron C4r, thus close to the age assignment reported by Baldauf and Barron (1991). A similar age interpretation of the FOD of *A. ingens* var. *ovalis* results from the study of Hole 690B. The second discrepancy concerns the FOD of *Denticulopsis praedimorpha*, located at 47.77 mbsf in Hole 689B (Fig. 2.12, Point 2). Applying Ramsay and Baldauf's (1999) stratigraphic interpretation the FOD of *D. praedimorpha* would be diachronous between holes 689B and 690B, having an age of 12.51-12.76 Ma and 13.09-13.35 Ma, respectively.

Table 2.6: List of selected Miocene diatom events, ages from previous studies and new interpolated ages from the age-depth plots. Ages interpolated by linear relationship. Italic style: low reliability. References: 1 - Gersonde and Barcena (1998), 2 - Gersonde et al. (1998), 3 - Barron and Baldauf (1995), 4 - Barron (1992a).

Datum	**Estimated diatom ages (Ma)**				**Age (Ma)**	**Published age (Ma)**	**Ref.**
	SSODZ		NSODZ		SSODZ/NSODZ		
	689B	690B	1988	1092	rounded		
FOD *T. complicata*	-	-	-	-	? / ?	4.45	2
FOD *T. inura*	4.89	-	*4.17*	-	4.98 / *4.17*	4.92	1
FOD *F. praeinterfigidaria*	5.09	-	-	-	5.09 / n.p.	5.30	2
LOD *H. triangularus*	5.13	-	-	6.43	5.13 / 6.43		
FOD *Thal. convexa* var. *aspinosa*	6.58	-	-	6.54	6.58 / 6.54	6.70	4
FOD *H. triangularus*	7.3	-	-	7.3	7.3 / 7.3		
LOD *D. crassa*	*7.39*	*7.76*	-	7.51	*7.58* / 7.51		
FOD *F. reinholdii*	-	-	*8.23*	7.96	n.p. / 7.96	8.10	4
FOD *F. arcula*	8.49	8.41	-	*7.4*	8.45 / *7.4*	8.60	2
FOD *A.ingens* var. *ovalis*	*8.49*	-	-	8.7	*8.49* / 8.7	8.68	3
FOD *A. kennettii*	10.21	10.12	*10.3*	10.31	10.17 / 10.31	10.23	2
LOD *D. ovata*	*4.93*	-	*10.5*	10.6	*4.93* / 10.6		
FOD *F. aurica*	*9.5*	*10.3*	-	*6.94*	*9.9 / 6.94*		
FOD *D. crassa*	*10.12*	*9.7*	-	*10.95*	*9.91 / 10.95*		
FOD *F. praecurta*	11.43	11.40	-	*10.59*	11.42 / *10.59*	11.05	2
LOD *N. denticuloides*	*11.82*	11.78	-	11.86	11.78 / 11.86	11.70	2
FOD *D. ovata*	-	12.11	*11.1*	11.1	12.11 / 11.1		
FOD *D. dimorpha*	12.74	12.73	-	12.12	12.74 / 12.12	12.20	3
LOD *D. praedimorpha*	-	-	-	12.25	n.p. / 12.25		
FOD *D. praedimorpha*	12.92	12.81	-	-	12.87 / n.p.	12.84	3
FOD *N. denticuloides*	13.48	-	-	-	13.48 / n.p.	13.51	2
FOD *D. simonsenii*	14.18	14.3	-	*14.22*	14.24 / *14.22*	14.17	2
FOD *A. ingens* var. *nodus*	-	14.178-14.8	-	*14.35*	ca. 14.5 / *14.35*	14.38	2
FOD *N. grossepunctata*	15.2	-	-	-	15.2 / n.p.	15.38	2
FOD *A. ingens*	16-17.3	14.8-16.5	*16.2*	*12.3-12.7*	ca. 16.2 / *16.2*	16.20	2
FOD *D. maccollumii*	-	*16.7*	-	-	*16.7* / n.p.	16.75	2
FOD *C. kanayae*	17.28-17.61	17.27-17.61	-	-	ca. 16.7 / n.p.	17.72	3

Such a discrepancy between two sites that have been drilled nearby each other is rather unlikely. Harwood and Maruyama (1992) place the FOD of *D. praedimorpha* below C5Ar.2n (Hole 751A, Leg 120), an age assignment that was followed by Ramsay and Baldauf (1999). We considered the age assignment of Harwood and Maruyama (1992) and interpreted the normal polarity intervals at ca. 46 and 47 mbsf to represent C5Ar (Hole 689B). This age assignment is consistent with the stratigraphic interpretation in Hole 690B and shows that the age determination of Ramsay and Baldauf (1999) must be revised. The third disagreement occurs in the lower Middle Miocene (Fig. 2.12, Point 3). Ramsay and Baldauf (1999) proposed the normal polarity interval at ca. 57 mbsf to represent C5Cn.3n.

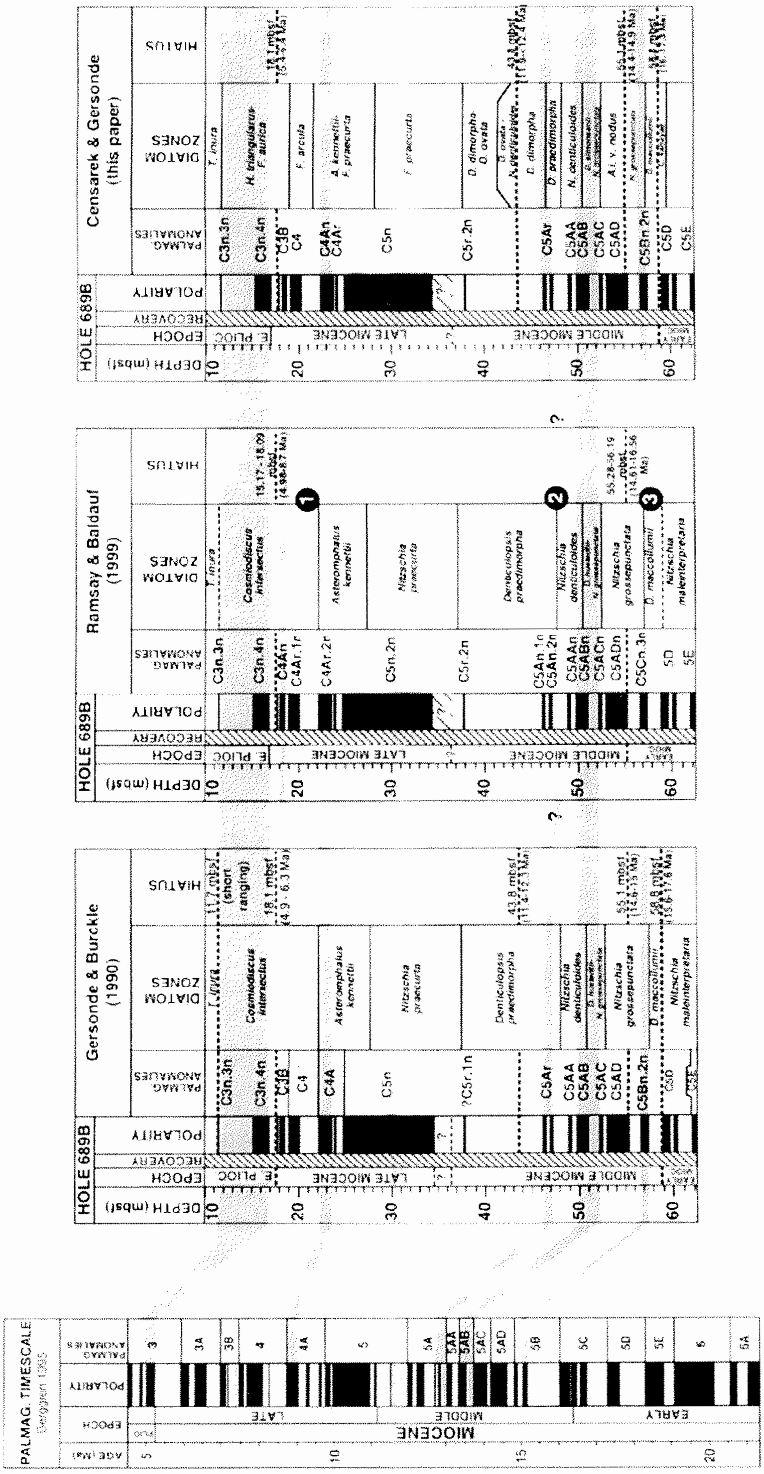
Censarek & Gersonde (this paper)
Ramsay & Baldauf (1999)
Gersonde & Burckle (1990)
HOLE 689B
DEPTH (mbsf)
EPOCH
RECOVERY
POLARITY
PALMAG. ANOMALIES
DIATOM ZONES
HIATUS
E. PLIOC
LATE MIOCENE
MIDDLE MIOCENE
EARLY MIOC.
PALMAG. TIMESCALE
Berggren 1995
AGE (Ma)
MIOCENE
LATE
MIDDLE
EARLY
PLIO
1
2
3

This is close to the FOD of *Nitzschia grossepunctata* at 57.99 mbsf. Applying the age interpretation of Ramsay and Baldauf (1999) the FOD of *N. grossepunctata* would be diachronous between holes 689B and 690B. The FO in Hole 689B having an age between 16.85 and 17.09 Ma (uppermost portion of Subchron C5Cr), whereas in Hole 690B the FO (43.77 mbsf) of this species would fall between 17.19 and 17.42 Ma (upper portion of Chron C5D). Harwood and Maruyama (1992) placed the FOD of *N. grossepunctata* into the uppermost portion of Chron C5Br (Hole 747A, Leg 120) an age assignment accepted by Ramsay and Baldauf (1999). This is consistent with our interpretation that the normal polarised chron at ca. 57 mbsf in Hole 689B represents C5Bn.2n. In Hole 690B the FO of *N. grossepunctata* is located at a hiatus (ca. 44 mbsf, 14.8-16.5 Ma) that omits C5Bn.2n. The hiatus is indicated by a sharp facies boundary between calcareous nannofossil-bearing sediments below and diatom ooze above. Thus the comparison of our stratigraphic interpretation of Miocene strata recovered at Maud Rise with the age model proposed by Ramsay and Baldauf (1999) shows that the method used by Ramsay and Baldauf (1999) for the establishment of stratigraphic age models may lead to misinterpretations of the geomagnetic record and to a diachronous occurrence pattern of species between the two Maud Rise holes. This can partly be ascribed to the fact that they did not examine additional new material and based their studies only on available data.

2.7 Summary

In this paper the reinvestigation of the Leg 113 Sites 689 and 690 and the study of Leg 177 Sites 1088 and 1092 leads to an improved dating of the stratigraphic species ranges considering the progress in diatom taxonomy and magnetostratigraphic age assignment as well as previous diatom biostratigraphic results of ODP Legs 113, 114, 119 and 120. Due to latitudinal changes in species composition and abundance pattern that can be related to latitudinal differentiations of surface water masses, two Miocene diatom zonations, a southern and a northern one, are established.

Figure 2.12 (left): Comparison of Hole 689B (Leg 113) age models with diatom zonations and magnetostratigraphical interpretations: Gersonde and Burckle (1990) based on the magnetostratigraphic interpretation of Spieß (1990), Ramsay and Baldauf (1999) and Censarek and Gersonde (this paper). All geomagentic polarity designations are in accordance to the nomenclature proposed by Cande and Kent (1992). Black marked numbers (1-3) mark stratigraphic discrepancies discussed in the text.

Despite the increased knowledge on the stratigraphic occurrence of southern high latitude Neogene diatoms, the biostratigraphic zonation of some time intervals is still not well elaborated. This is true especially for the late Late Miocene and the Miocene/Pliocene transition, as well as portions of the middle Miocene marked by the occurrence of disconformities at most sites drilled in the Southern Ocean. Also the delineation of the stratigraphic ranges of taxa such as *Thalassiosira inura*, *Asteromphalus kennettii*, *Fragilariopsis praeinterfrigidaria* and *F. aurica* needs further improvement.

2.8 Taxonomic notes and floral references

The first citation in the following list is the original description of the species, the other one are more recent references, where those with good illustrations were used. Plate and figure numbers given in parenthesis refer to illustrations of taxa in this paper.

2.8.1 New combinations

Considering the comments and descriptions of Round et al. (1990), Medlin and Sims (1993), Hasle et al. (1995) and Gersonde and Bárcena (1998) about the transfer of taxa belonging to the genus *Nitzschia* to the genus *Fragilariopsis* we follow the strategy proposed by Round et al. (1990) and transfer the following Miocene diatom taxa:

Fragilariopsis claviceps (Schrader) Censarek et Gersonde, comb. nov.

Basionym: Nitzschia claviceps Schrader, 1976, p. 633, pl. 2, figs. 2, 4.

Fragilariopsis cylindrica (Burckle) Censarek et Gersonde, comb. nov., (Plate 3, Fig. 24).

Basionym: *Nitzschia cylindrica* Burckle, 1972, p. 239, pl. 2, figs. 1-6.

Fragilariopsis donahuensis (Schrader) Censarek et Gersonde, comb. nov., (Plate 3, Figs. 13-14).

Basionym: *Nitzschia donahuensis* Schrader, 1976, p.633, pl. 2, fig. 30.

Fragilariopsis efferans (Schrader) Censarek et Gersonde, comb. nov.

Basionym: *Nitzschia efferans* Schrader, 1976, p. 633, pl. 2, figs. 1, 3, 5-7; Gersonde and Burckle, 1990, pl. 2, fig. 9.

Fragilariopsis miocenica (Burckle) Censarek et Gersonde, comb. nov.

Basionym: *Nitzschia miocenica* Burckle, 1972; Akiba and Yanagisawa, 1986, p. 469, pl. 39, figs. 7-15, pl. 41, figs. 1-2.

Fragilariopsis maleinterpretaria (Schrader) Censarek et Gersonde, comb. nov., (Plate 3, Fig. 26).

Basionym: *Nitzschia maleinterpretaria* Schrader, 1976, p.634, pl.2, figs. 9, 11-19, 21, 24; Gersonde and Burckle, 1990, pl. 2, figs. 13-16; Harwood and Maruyama, 1992, pl. 6, fig. 17-19.

Fragilariopsis pusilla (Schrader) Censarek et Gersonde, comb. nov. (Plate 3, Fig. 25).

Basionym: *Nitzschia pusilla* Schrader, 1976, p. 643, pl. 2, fig. 20; Gersonde and Bruckle, 1990, pl. 2, figs. 17-19.

2.8.2 Floral list

Actinocyclus curvatulus Janisch in Schmidt et al., 1878, pl. 57, fig. 31; Akiba, 1982, pp. 41-42, pl. 5, figs. 5a-6.

Actinocyclus fasciculatus Maruyama *in* Harwood and Maruyama, 1992, pl. 13, figs. 14-15.

Remarks: Harwood and Maruyama (1992) described *A. fasciculatus* from middle Pliocene sediments. We found it also in late Miocene sections. (Plate 1, Fig. 5).

Actinocyclus ingens Rattray, 1890, p.149, pl. 11, fig. 7; Whiting and Schrader, 1985; Gersonde 1990, pp. 791-792, pl. 1, fig 1, 3-5, pl. 4, fig. 1. Harwood and Maruyama, 1992, pl. 8, fig. 10, pl. 11, figs. 4 and 6, pl. 12, fig. 8. (Plate 1, Fig. 1).

Actinocyclus ingens var. *nodus* Baldauf, in Baldauf and Barron, 1980, p. 104, pl. 1, figs. 5-9; Gersonde 1990, p. 792, pl. 1, fig. 6, pl. 3. figs. 4-7. (Plate 1, Fig. 4.)

Actinocyclus ingens var. *ovalis* Gersonde, 1980, p. 792, pl. 1, fig. 7, pl. 3, figs. 1-3, pl. 5. figs. 4, 7, pl. 6, figs. 1, 4-5; Gersonde and Burckle, 1990, pl. 5, figs. 4-5; (Plate 1, Figs. 6, 8).

Actinocyclus karstenii Van Heurck, 1909, p. 44, pl. 12, fig. 158; Harwood and Maruyama, 1992, p. 700, pl. 13, figs. 1, 2, 6-8, 10, 11, 13.

Synonym: *Actinocyclus fryxellae* Barron, in Baldauf and Barron, 1991, pl. 1, figs. 1-2, 4.

Actinoptychus senarius Ehrenberg (Ehrenberg); Hendey, 1964, p. 95, pl. 23, figs. 1-2; Synonym: *A. undulatus* (Bailey) Ralfs in Pritchard, 1861; Hustedt, 1930, pp. 475-478, fig. 264. (Plate 5, Fig. 11).

Asteromphalus inaequabilis Gersonde, 1990, p. 792, pl. 2, fig. 4, and pl. 6, fig. 3.

Asteromphalus kennettii Gersonde, 1990, p. 793, pl. 2, fig. 1 and pl. 6, fig. 2. (Plate 1, Fig. 2.)

Azpeitia tabularis (Grunow) Fryxell and Sims, in Fryxell et al., 1986, p. 16 figs. XIV, XV, XXX-I. (Plate 1, Fig. 7).

Cavitatus jouseanus (Sheshukova-Poretzkaya), Williams, 1989, p. 260; Akiba et al., 1993, p. 20-22, figs. 6-20. Synonym:*Synedra jouseana* Schrader, 1973, p. 710, pl. 23, figs. 21-23, 25, 38. (Plate 5, Fig. 12).

Cavitatus miocenicus (Schrader) Akiba and Yanagishawa *in* Akiba et al., 1993, p. 28, figs.9-1 to 9-11. Synonym: *Synedra miocenica* Schrader, 1976, p. 636, pl. 1, figs. 1, 1a, 1b.

Chaetoceros spp. resting spores, not taxonomic differentiation made.

Corethron criophilum Castracane, 1886, p. 85, pl. 21, figs. 14, 15; Hargraves, 1968, p. 38, figs. 54-60; Harwood and Maruyama, 1992, pl. 19, figs. 12-15.

Coscinodiscus lewisianus Greville, 1866, p. 78, pl. 8, figs. 8-10; Schrader, 1973, pl. 8. figs. 1-6, 10, 15.

Coscinodiscus marginatus Ehrenberg. Hustedt, 1930, pp. 416-418, fig. 223.

Coscinodiscus rhombicus Castracane, 1886, p. 164, pl. 22, fig. 11; Schrader and Fenner, 1976, pl. 21, figs. 1-3, 5; Harwood and Maruyama, 1992, pl. 3, figs. 16-17, pl. 8, figs. 12-13, pl. 11, fig. 1. (Plate 1, Fig. 3).

Crucidenticula kanayae var. kanayae Akiba et Yanagisawa, 1986, p. 486, pl. 1, figs. 3-8; pl. 3, figs. 1-6, 9-10; Yanagisawa and Akiba, 1990, p. 229, pl. 1, figs. 33-35, 39, pl. 8, figs. 14-17. (Plate 2, Figs. 35-36).

Crucidenticula nicobarica (Grunow) Akiba and Yanagisawa, 1986, p. 486, pl. 1, fig. 9; pl. 2, fig. 1-7; pl. 5, figs. 1-9; Yanagisawa and Akiba, 1990, p. 232, pl. 1, figs. 23-29. (Plate 2, Figs. 25-26).

Denticulopsis crassa Yanagisawa et Akiba in Yanagisawa and Akiba, 1990, pp. 248-249, pl. 3, figs. 21-27, pl. 12, figs. 1-8. (Plate 2, Fig. 12).

Denticulopsis dimorpha (Schrader) Simonsen, 1979, p. 64; Yanagisawa and Akiba, 1990, p. 254, pl. 4, figs. 42-49, pl. 7, figs. 14-16. (Plate 2, Figs. 8-11).

Denticulopsis hustedtii (Simonsen et Kanaya) Simonsen emend., 1979; Yanagisawa and Akiba, 1990, pl. 3, figs. 14-19, pl. 11, figs. 11-13.

Denticulopsis maccollumii Simonsen, 1979, p.65; Gersonde, 1990, pl. 5, figs. 7-9; Schrader, 1976, p.631, pl.4, figs. 3, 22, 23, 25. (Plate 2, Figs. 32-34).

Denticulopsis ovata (Schrader) Yanagisawa and Akiba, 1990, pl. 6, figs. 6-14, 24-32.

Synonyms: *Denticula lauta* var. *ovata* Schrader, 1976, p. 632, pl. 4, fig. 7; *Denticula hustedtii* var. *ovata* Schrader, 1976, p. 632, pl.4, figs. 5, 6, 12, 14 and 15; *D. meridionalis* Maruyama in Harwood and Maruyama, 1992, p. 702, pl. 6, figs. 1-4; pl. 7, figs. 1-4, 6-9, 11-13; pl. 9, figs 1-4, 10-14; pl. 10, fig. 7 (Plate 2, Figs. 13-20).

Denticulopsis praedimorpha Barron ex Akiba 1982, pp. 46-48, pl. 11, figs. 9a-16, 18-27a; Yanagisawa and Akiba, 1990, p. 251, pl. 4, figs. 3-5, 10, 12-17, 39; pl. 5, figs. 4-12. (Plate 2, Figs. 1-6).

Denticulopsis simonsenii Yanagisawa and Akiba, 1990, pl. 3, figs. 1-3, pl. 11, figs. 1, 5. (Plate 2, Figs. 21-24).

Diploneis bombus Ehrenberg; Hustedt, 1933, Kieselalg., II, p. 704, figs. 1086a-c; Akiba, 1986, pl. 30, fig. 13. (Plate 5, Fig. 3).

Eucampia antarctica (Castracane) Mangin, 1914, p. 480, figs. 7-8; Mangin, 1915, pp. 58-66, figs. 41-44, pl. 1, fig. 1; Syvertsen and Hasle, 1983, pp. 181-187; Basionym: *Eucampia balaustium* Castracane, 1886, pp. 97-99, pl. 18, figs. 5-6.

Fragilariopsis arcula (Gersonde) Gersonde et Bárcena, 1998; Gersonde, 1991, pp. 143-144, pl. 2, fig. 4; pl. 4, fig. 4; pl. 5, figs. 1-6; Gersonde and Burckle, 1990, pl. 2, figs. 25-26. (Plate 3, Figs. 15-18).

Basionym: *Nitzschia arcula* Gersonde, 1991.

Fragilariopsis aurica (Gersonde) Gersonde et Bárcena, 1998; Gersonde, 1991, p. 144; pl. 1, figs. 18-25; pl. 3, figs. 5, 6; pl. 7, fig. 6; Gersonde and Burckle, 1990, pl. 1, figs. 11-13; Harwood and Maruyama, 1992, pl. 17, fig. 18. (Plate 3, Figs. 9-12).

Basionym: *Nitzschia aurica* Gersonde 1991.

Fragilariopsis barronii (Gersonde) Gersonde and Bárcena, 1998; Gersonde, 1991, p.146; pl. 3, fig. 6; pl. 4, figs. 1-3; pl. 5, figs. 7-17; Gersonde and Burckle, 1990, pl.1, figs. 11-13.

Basionym: *Nitzschia barronii* Gersonde, 1991.

Fragilariopsis claviceps (Schrader) Censarek and Gersonde, comb. nov.

Fragilariopsis clementia (Gombos) Zielinski et Gersonde, 2002;

Basionym: *Nitzschia clementia* Gombos 1977, p. 595, pl. 8, figs. 18-19; Gersonde and Burckle, 1990, pl. 2, figs. 22-23, Harwood and Maruyama, 1992, pl. 17, fig. 18. (Plate 3, Figs. 7-8).

Fragilariopsis cylindrica Censarek and Gersonde, comb. nov. (Plate 3, Fig. 24).

Fragilariopsis donahuensis (Schrader) Censarek et Gersonde, comb. nov. (Plate 3, Figs. 13-14).

Fragilariopsis efferans (Schrader) Censarek et Gersonde, comb. nov.

Fragilariopsis fossilis (Frenguelli) Medlin and Sims, 1993, pp. 332-333.

Basionym: *Pseudonitzschia fossilis* Frenguelli 1949

Synonym: *Nitzschia fossilis* (Frenguelli) Kanaya, in Kanaya and Koizumi, 1970; Schrader 1973, p. 707, pl. 4, figs. 9-11, 24, 25; Gersonde and Burckle, 1990, pl. 1 figs. 19-20. (Plate 3, Figs. 3-4).

Fragilariopsis lacrima (Gersonde) Gersonde and Bárcena, 1998; Gersonde, 1991, p. 148, pl. 1, figs. 1-6, 26, pl. 2. figs. 1-3; Gersonde and Burckle, 1990, pl.1, figs. 14-15. (Plate 3, Figs. 5-6).

Basionym: *Nitzschia lacrima* Gersonde, 1991.

Fragilariopsis maleinterpretaria (Schrader) Censarek and Gersonde, comb. nov. (Plate 3, Fig. 26).

Fragilariopsis miocenica (Burckle) Censarek and Gersonde, comb. nov.

Fragilariopsis praecurta (Gersonde) Gersonde and Bárcena, 1998; Gersonde, 1991, p. 148-149; pl. 1, fig. 7-17; pl. 2, figs. 5, 6; pl. 3, figs. 3, 4; pl. 10, fig. 7; Harwood and Maruyama, 1992, pl. 17, figs. 25-26. (Plate 3, Figs. 19-21).

Basionym: *Nitzschia praecurta* Gersonde, 1991.

Fragilariopsis praeinterfrigidaria (McCollum) Gersonde and Bárcena, 1998; McCollum, 1975, p. 535; pl. 10, fig. 1; Gersonde and Burckle, 1990, pl. 1, figs. 4-10. (Plate 3, Figs. 22-23).

Basionym: *Nitzschia praeinterfrigidaria* McCollum, 1975.

Fragilariopsis pusilla (Schrader) Censarek and Gersonde, comb. nov. (Plate 3, Fig. 25).

Fragilariopsis reinholdii (Kanaya ex Schrader) Zielinski et Gersonde, 2002; Akiba and Yanagisawa, 1986, p. 469, pl. 40, figs. 8-9; pl. 41, figs. 3-4. Gersonde and Burckle, 1990, pl. 1, fig. 1.

Basionym: *Nitzschia reinholdii* Kanaya et Koizumi, 1970 in Schrader 1973, pl. 4. figs. 12-16, pl. 5, figs. 1-9; (Plate 3, Figs.1-2).

Hemidiscus cuneiformis Wallich. Hustedt, 1930, pp. 904-907, fig. 542; Simonsen, 1972, pp. 267-272, figs. 7-11. (Plate 4, Fig. 5).

Hemidiscus karstenii Jousé in Jousé et al., 1963, pl. 1, Fig. 2. ; Jousé, 1965, pl. 1, figs. 6,7. Fenner, 1991, p. 98, pl. 1, fig. 2. (Plate 3, Fig. 27).

Hemidiscus triangularus (Jousé) Harwood and Maruyama, 1992

Basionym:*Cosmoidiscus insignis* f. *triangula*, Jousé, 1977, pl. 79, fig. 2; Ciesielski, 1983, p. 656, pl. 5, figs. 1-10; Ciesielski, 1986, pl. 4, figs. 5-6. (Plate 4, Figs. 1-4).

Katahiraia aspera Komara, 1976, p. 385, fig. 5; Gersonde, 1990, pl. 4, fig. 8.

Mediaria splendidia Sheshukova-Poretzkaya, Schrader, 1973, p. 706, pl. 3, figs. 14-15. Gersonde and Burckle, 1990, pl. 4, fig. 14. (Plate 5, Fig. 5).

Neobrunia mirabilis (Brun in Brun and Tempére) Kuntze, Hendey, 1981, p. 11, pl. 1, figs. 1-3, pl. 2, figs. 4-7, and pl. 3., figs. 10-13.

Nitzschia denticuloides Schrader, 1976, p. 633, pl. 3, figs. 7-8, 10, 12, 18-24; Gersonde and Burckle, 1990, pl. 2, figs, 7-8; Harwood and Maruyama, 1992, pl. 8, figs. 5-8, 17, pl. 9, figs. 24-26, pl. 10, fig. 1. (Plate 2, Figs. 27-31).

Nitzschia grossepunctata Schrader, 1976, p. 633, pl. 3, figs. 1-4; Gersonde and Burckle, 1990, pl. 2, figs. 3-6.(Plate 2, Figs. 37-38).

Nitzschia pseudokerguelensis Schrader, 1976, p. 634, pl.15, figs. 13-15; Gersonde and Burckle, 1990, pl. 2, fig. 2. (Plate 2, Fig. 39).

Paralia sulcata (Ehrenberg) Cleve. Hustedt, 1930, pp. 276-278, figs. 118-120.

Pleurosigma spp., only fragments of valves were found.

Proboscia barboi (Brun) Jordan and Priddle, 1991, p. 56, figs. 1-2; Fenner, 1991, pl. 3, figs. 1, 3.

Synonym: *Rhizosolenia barboi* (Brun) Temére and Peragallo.

Raphidodiscus marylandicus Christian. Schrader, 1976, p. 635, pl. 5, fig. 19; pl. 15, fig. 16.

Rhizosolenia antennata f. *semispina* Sundström, 1986, pp. 44-46, pl. 4, fig. 20, pl. 17, figs. 114, 116; Zielinski, 1993, p. 111, pl. 7, fig.1.

Rhizosolenia hebetata f. *semispina* (Hensen) Gran, 1904, p. 524, pl. 17, fig. 11; Hustedt, 1930, p. 590.

Rouxia antarctica (Heiden) Hanna 1930. Schrader, 1976, pl. 5, figs. 1-8.

Rouxia heteropolara Gombos, 1974, p. 275, fig. 1; Gersonde and Burckle, 1990, pl. 5, fig. 2.

Rouxia isopolica Schrader, 1976, pp. 635-336, pl. 5. figs. 9, 14, 15, 20.

Rouxia peragalli Brun and Heribaud in Heribaud. Abbott, 1974, p.318, pl. 9, figs. A-C; Hanna, 1930, p. 180-184, pl. 14, figs. 1, 5. McCollum, 1975, pl. 12, figs. 1, 2.

Rouxia naviculoides Schrader, 1973, p. 710, pl. 3, figs. 27-32.

Rouxia sp. 1 Gersonde in Gersonde and Burckle, 1990, pl. 4, fig. 15. (Plate 5, Fig. 8).

Rouxia sp. 2 Gersonde in Gersonde and Burckle, 1990, pl. 5, fig. 3.

Rouxia sp. 3 Gersonde in Gersonde and Burckle, 1990, pl. 5, fig. 1.

Stellarima microtrias (Ehrenberg) Hasle and Sims. Hustedt, 1958, pp. 113-114, pl. 3, figs. 18-19, pl. 5, fig. 39; Hasle et al., 1988, pp. 196-198, figs. 1-25.

Stephanopyxis turris (Greville and Arnott) Ralfs, in Pritchard, 1861; Hustedt, 1930, pp. 304-307, figs. 140-144.

Thalassionema nitzschioides Grunow. Hustedt, 1930, p. 244, fig. 725.

Thalassionema nitzschioides var. *capitulatum* (Castracane) Moreno-Ruiz and Licea, 1995, pp. 397-398, figs. 6-7, 42-43; Heiden and Kolbe, 1928, p. 565, pl. 5, fig. 119.

Thalassionema nitzschioides var. *inflatum* Heiden in Heiden and Kolbe 1928; Moreno-Ruiz and Licea, 1995, pp. 400-401, figs. 14-15, 20-22, 47-49.

Thalassionema nitzschioides var. *parvum* (Heiden) Moreno-Ruiz and Licea, 1995, p. 402, figs. 25-27, 57-58; Zielinski, 1993, pl. 6, figs. 7-8; Fenner et al., 1976, pl. 14, fig. 10; Gersonde, 1980, pp. 283-284, pl. 9, figs. 12-13.

Thalassiosira complicata Gersonde, 1991, pp. 150-151, pl. 3, figs. 1-2, pl. 5, figs. 18-20, pl. 6, figs. 1-6, pl. 7, figs. 1-5.

Thalassiosira convexa var. *aspinosa* Schrader, 1974, p. 916, pl. 2, figs. 8, 9, 13-21; Gersonde, 1990, pl. 3, figs. 2, 3. (Plate 4, Figs. 8-9).

Thalassiosira fraga Schrader in Schrader and Fenner, 1976; Akiba and Yanagisawa, 1986, p. 498, pl. 51, figs. 5-10; pl. 53, figs. 1-8. Gersonde, 1980, pl. 3, figs. 9, 10. (Plate 4, Fig. 6).

Thalassiosira inura Gersonde, 1991, p. 151, pl. 6, figs. 7-14; pl. 8, figs. 1-6; Harwood and Maruyama, 1992, pl. 14, figs. 12-16; pl. 5, fig. 14. (Plate 4, Figs. 11-12).

Thalassiosira leptopus (Grunow) Hasle and Fryxell, 1977, pp. 20-22, figs. 1-14; Hallegraeff, 1984, figs. 20a-b.

Thalassiosira miocenica Schrader, 1974, p. 916, pl. 22, figs. 1-5, 11-13; Barron, 1985a, pl. 11, fig. 11.

Thalassiosira oestrupii (Ostenfeld) Proschkina-Lavrenko. Schrader, 1973, p. 712, pl. 11, figs. 16-22, 26-33, 36, 39-45. (Plate 5, Figs. 9-10).

Thalassiosira oliverana (O'Meara) Makarova and Nikolaev. Fenner et al., 1976, p. 779, pl. 14, figs. 1-5.

*Thalassiosira oliverana*var. *sparsa* Harwood in Harwood and Maruyama, 1992, p. 708, pl.16, fig. 13. (Plate 5, Figs. 1-2).

Thalassiosira praelineata Jousé. Harwood and Maruyama, 1992, pl. 5, figs. 6-9. (Plate 5, Figs. 6-7). Synonym: *Coscinodiscus praelineatus* Jousé as synonyms of *Thalassiosira leptopus* (Grun.) Hasle and Fryx in Hasle and Syversten, 1982, pl. 1, fig. 6.

Thalassiosira sancettae Akiba, 1986, p. 441, pl. 7, figs. 1-3. (Plate 5, Figs. 13-14).

Thalassiosira spinosa Schrader, 1976, p. 636, pl. 6, figs. 5-7; Gersonde and Burckle, 1990, pl. 4, figs. 3-4. (Plate 4, Fig. 7).

Thalassiosira spumellaroides Schrader, 1976, p. 636, pl. 6, figs. 1-2. (Plate 4, Fig. 10).

Thalassiosira torokina Brady, 1977, pp.122-123; Brady, 1979, pl. 4, figs. 1-5; Harwood, 1986, pl. 15, figs. 11, 13, 14; pl. 19, figs. 10, 11; pl. 25, figs. 1-3.

Thalassiothrix longissima Cleve and Grunow. Hustedt, 1958, p. 247, fig. 726.

Thalassiothrix miocenica Schrader, 1973, p. 713, pl. 23, figs. 2-5. (Plate 5, Fig. 15).

Triceratium cinnamonium Greville. Schrader, 1974, pl. 20, figs. 10-11; Van Heurck, 1880, pl. 126, fig. 1.

2.9 Plates

Plate 1

Scale bar equals 10 µm

1. *Actinocyclus ingens,* Sample 689B-6H-3, 114-115 cm.
2. *Asteromphalus kennettii*, Sample 1092A-10H-4, 79-80 cm.
3. *Coscinodiscus rhombicus*, Sample 1092A-20H-3, 20-21 cm.
4. *Actinocyclus ingens* var. *nodus* (Specimen at different focus), Sample 1092B-18H-2, 102-103 cm.
5. *Actinocyclus karstenii*, Sample 1092A-8H-3, 127-128 cm.
6. *Actinocyclus ingens* var. *ovalis*, Sample 689B-3H-5, 47-48 cm.
7. *Azpeitia tabularis*, Sample 690B-3H-7, 28-29 cm.
8. *Actinocyclus ingens* var. *ovalis*, Sample 689B-3H-5, 28-29 cm.

Plate 1

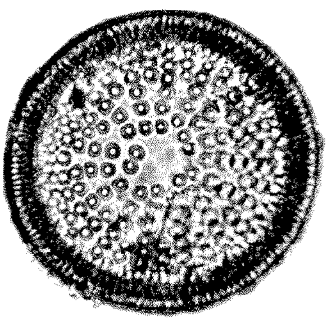

1

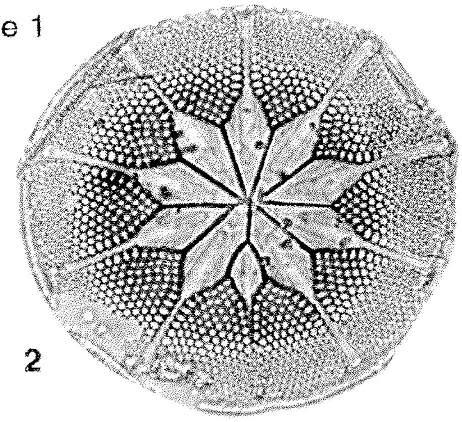

2

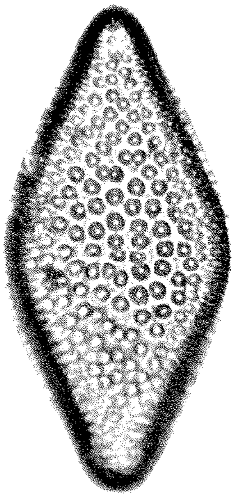

3

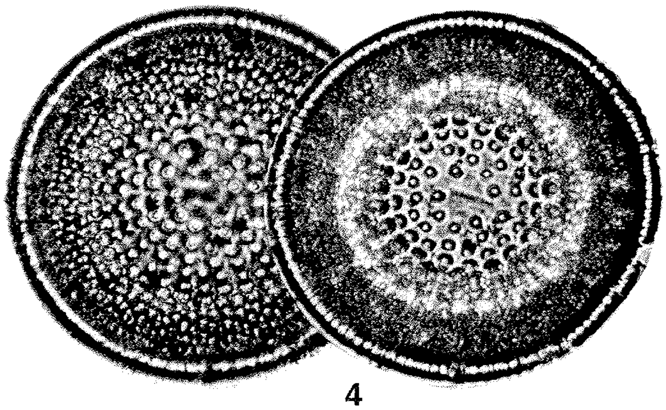

4

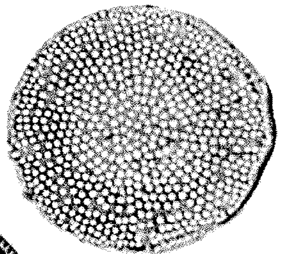

5

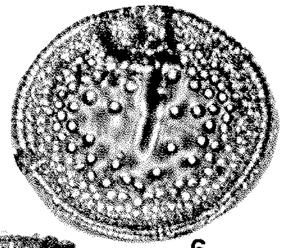

6

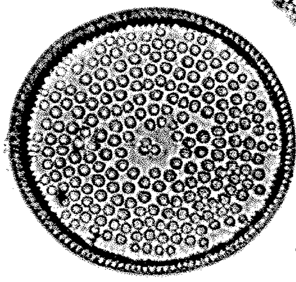

7

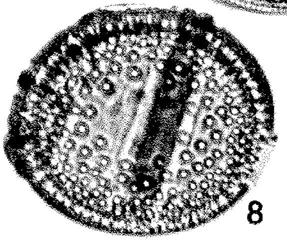

8

Plate 2

Scale bar equals 10 µm

1-6. *Denticulopsis praedimorpha*, Sample 689B-6H-1, 114-115 cm.

7. *Denticulopsis praedimorpha*, Sample 689B-6H-1, 28-29 cm.

8-11. *Denticulopsis dimorpha*, Sample 1092A-15H-6, 79-80 cm.

12. *Denticulopsis crassa*, Sample 689B-3H-3, 56-57 cm.

13. *Denticulopsis ovata*, Sample 689B-3H-5, 28-29 cm.

14. *Denticulopsis ovata*, Sample 689B-4H-5, 28-29 cm.

15. *Denticulopsis ovata*, Sample 689B-3H-3, 56-57 cm.

16,17. *Denticulopsis ovata*, Sample 689B-4H-5, 28-29 cm.

18. *Denticulopsis ovata*, Sample 1092A-15H-5, 15-16 cm.

19, 20. *Denticulopsis ovata*, Sample 689B-4H-5, 28-29 cm

21-24. *Denticulopsis simonsenii*, Sample 689B-4H-5, 28-29 cm.

25, 26. *Crucidenticula nicobarica*, Sample 1092A-20H-2, 20-21 cm.

27, 28. *Nitzschia denticuloides*, Sample 689B-6H-1, 115-116 cm.

29. *Nitzschia denticuloides*, Sample 689B-6H-4, 29-30 cm.

30, 31. *Nitzschia denticuloides*, Sample 689B-6H-31, 114-115 cm.

32. *Denticulopsis maccollumii*, Sample 689B-7H-2, 115-116 cm.

33, 34. *Denticulopsis maccollumii* (both specimen at different focus), Sample 689B-7H-4, 115-116 cm.

35, 36. *Crucidenticula kanayae* var. *kanayae*, Sample 689B-7H-4, 115-116 cm.

37, 38. *Nitzschia grossepunctata*, Sample 689B-6H-5, 54-55 cm.

39. *Nitzschia pseudokerguelensis*, Sample 689B-6H-5, 54-55 cm.

Plate 2

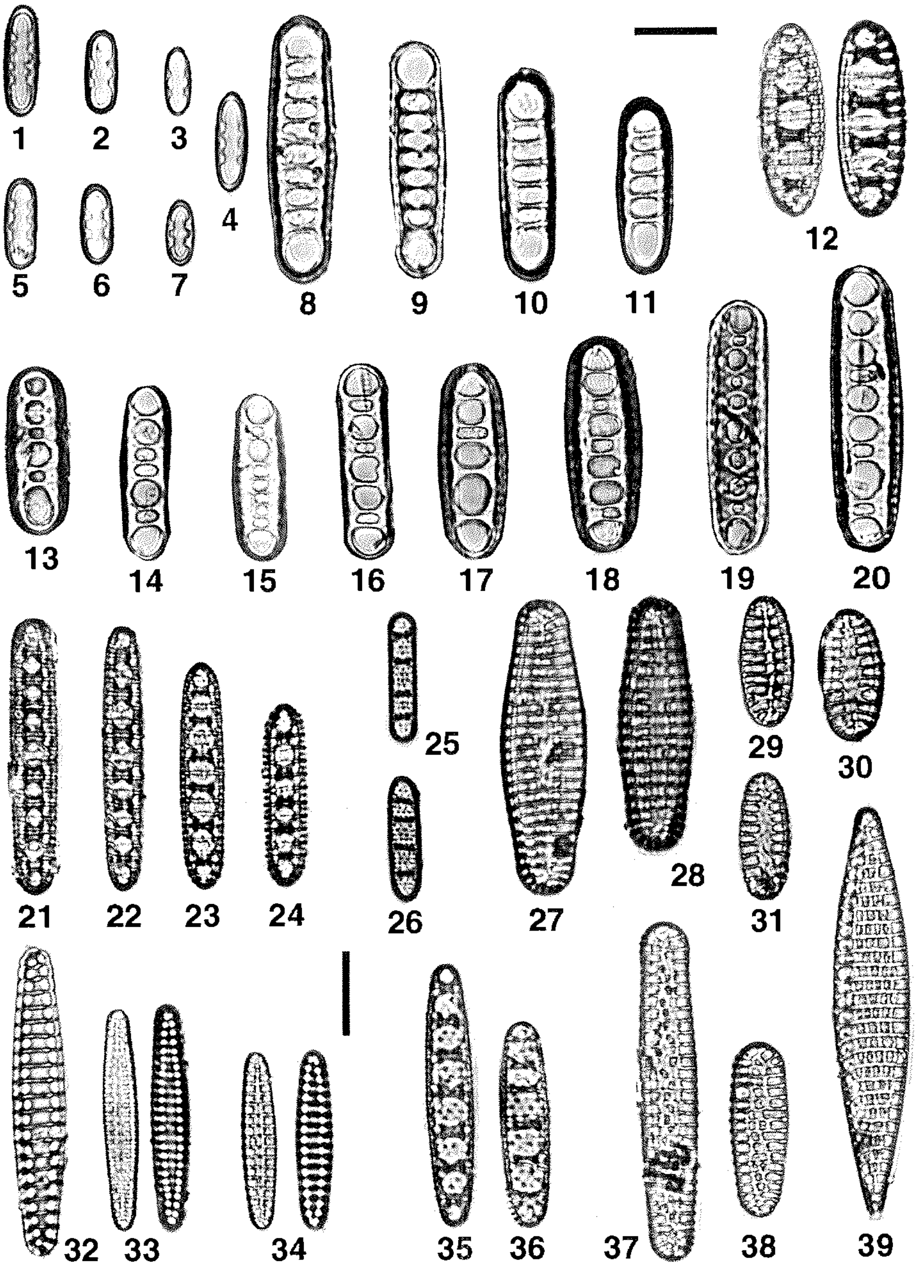
1
2
3
4
5
6
7
8
9
10
11
12
13
14
15
16
17
18
19
20
21
22
23
24
25
26
27
28
29
30
31
32
33
34
35
36
37
38
39

Plate 3

Scale bar equals 10 µm

1. *Fragilariopsis reinholdii*, Sample 1092A-7H-2, 79-80 cm.
2. *Fragilariopsis reinholdii*, Sample 1092A-7H-5, 79-80 cm.
3. *Fragilariopsis fossilis*, Sample 1092B-8H-2, 96-97 cm.
4. *Fragilariopsis fossilis*, Sample 1092A-7H-5, 79-80 cm.

5, 6. *Fragilariopsis lacrima*, Sample 1092A-6H-6, 79-80 cm.

7, 8. *Fragilariopsis clementia*, Sample 1092A-7H-3, 79-80 cm.

9. *Fragilariopsis aurica*, Sample 689B-3H-2, 114-115 cm.

10, 12. *Fragilariopsis aurica*, Sample 1092A-7H-5, 79-80 cm.

11. *Fragilariopsis aurica*, Sample 1092A-7H-2, 79-80 cm.
13. *Fragilariopsis donahuensis*, Sample 689B-6H-1, 114-115 cm.
14. *Fragilariopsis donahuensis*, Sample 689B-4H-5, 28-29 cm.
15. *Fragilariopsis arcula*, Sample 689B-3H-2, 79-80 cm.

16, 17. *Fragilariopsis arcula*, Sample 1092A-7H-3, 79-80 cm.

18. *Fragilariopsis arcula*, Sample 689B-3H-3, 50-52 cm.
19. *Fragilariopsis praecurta*, Sample 689B-3H-3, 56-57 cm.
20. *Fragilariopsis praecurta*, Sample 1092A-7H-3, 79-80 cm.
21. *Fragilariopsis praecurta*, Sample 1092D-3H-6, 20-21 cm.

22, 23. *Fragilariopsis praeinterfrigidaria*, Sample 1092A-6H-6, 79-80 cm.

24. *Fragilariopsis cylindrica*, Sample 1092A-8H-2, 76-77 cm.
25. *Fragilariopsis pusilla*, Sample 1092A-20H-2, 20-21 cm.
26. *Fragilariopsis maleinterpretaria*, Sample 689B-7H-6, 28-29 cm.
27. *Hemidiscus kastenii*, Sample 1092A-7H-7, 29-30 cm.

Plate 3

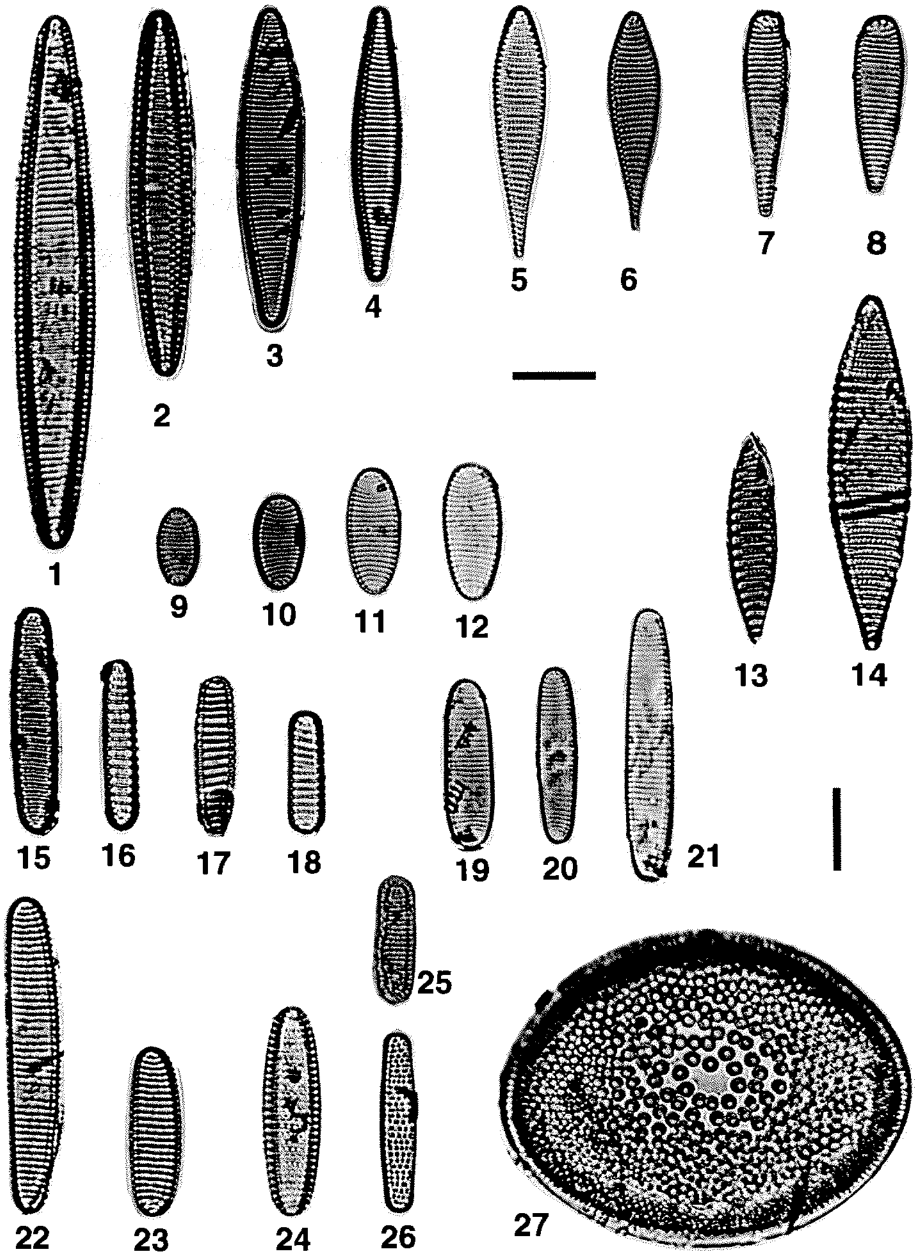

Plate 4

Scale bar equals 10 μm

1, 3, 4. *Hemidiscus triangularus*, Sample 1092A-8H-2, 79-80 cm.

2. *Hemidiscus triangularus*, Sample 1092A-8H-3, 127-128 cm.

5. *Hemidiscus cuneiformis*, Sample 1092A-6H-6, 79-80 cm.

6. *Thalassiosira fraga* (Specimen at different focus), Sample 690B-6H-5, 114-115 cm.

7. *Thalassiosira spinosa* (Specimen at different focus), Sample 689B-7H-7, 28-29 cm.

8. *Thalassiosira convexa* var. *aspinosa*, Sample 689B-3H-2, 114-115 cm

9. *Thalassiosira convexa* var. *aspinosa*, Sample 689B-3H-3, 56-57 cm

10. *Thalassiosira spumellaroides* (Specimen at different focus), Sample 690B-6H-7, 25-26 cm.

11. *Thalassiosira inura*, Sample 1092A-6H-6, 79-80 cm.

12. *Thalassiosira inura*, Sample 1092A-7H-2, 79-80 cm.

Plate 4

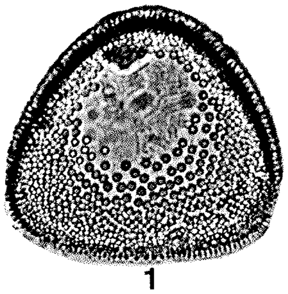
1

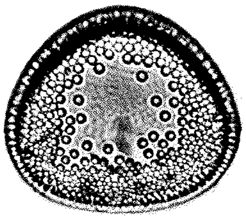
2

(for 1-4)

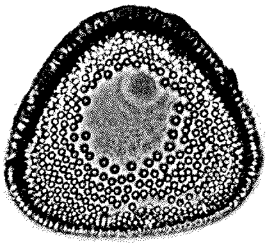
3

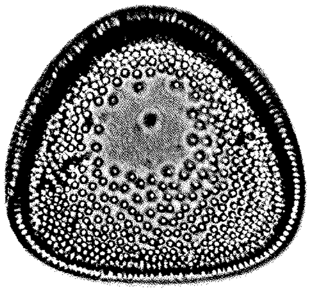
4

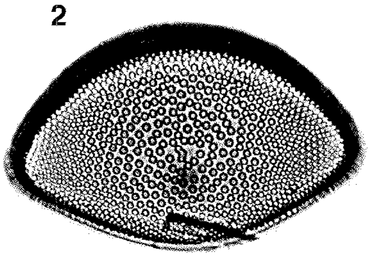
5

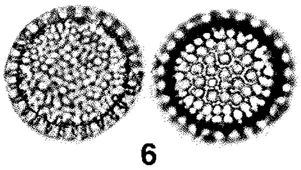
6

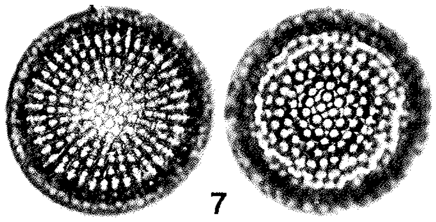
7

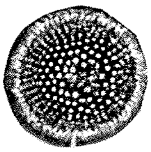
8

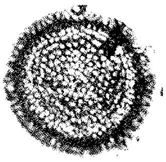
9

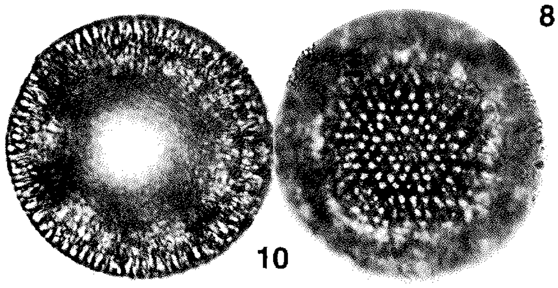
10

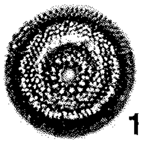
11

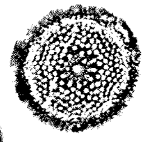
12

Plate 5

Scale bar equals 10 µm

1. *Thalassiosira oliverana* var. *sparsa*, Sample 689B-3H-3, 56-57 cm.
2. *Thalassiosira oliverana* var. *sparsa*, Sample 1092A-8H-3,127-128 cm.
3. *Diploneis bombus*, Sample 1088B-12H-4, 80-81 cm.
6. *Rouxia peragalli*, Sample 1092A-7H-5, 79-80 cm.
5. *Mediaria splendida*, Sample 1092A-7H-5, 79-80 cm.
6. *Thalassiosira praelineata*, Sample 1092A-7H-6, 52-53 cm.
7. *Thalassiosira praelineata*, Sample 1092A-7H-7, 29-30 cm.
8. *Rouxia* sp.1 Gersonde, Sample 689B-6H-5, 54-55 cm.

9, 10. *Thalassiosira oestrupii*, Sample 1092A-7H-2, 79-80 cm.

11. *Actinoptychus senarius*, Sample 689B-7H-6, 28-29 cm.
12. *Cavitatus jouseanus*, Sample 690B-6H-5, 114-115 cm.

13, 14. *Thalassiosira sancettae*, Sample 1088B-12H-4, 80-81 cm.

15. *Thalassiotrix miocenica*, Sample 1092A-7H-2, 79-80 cm.

Plate 5

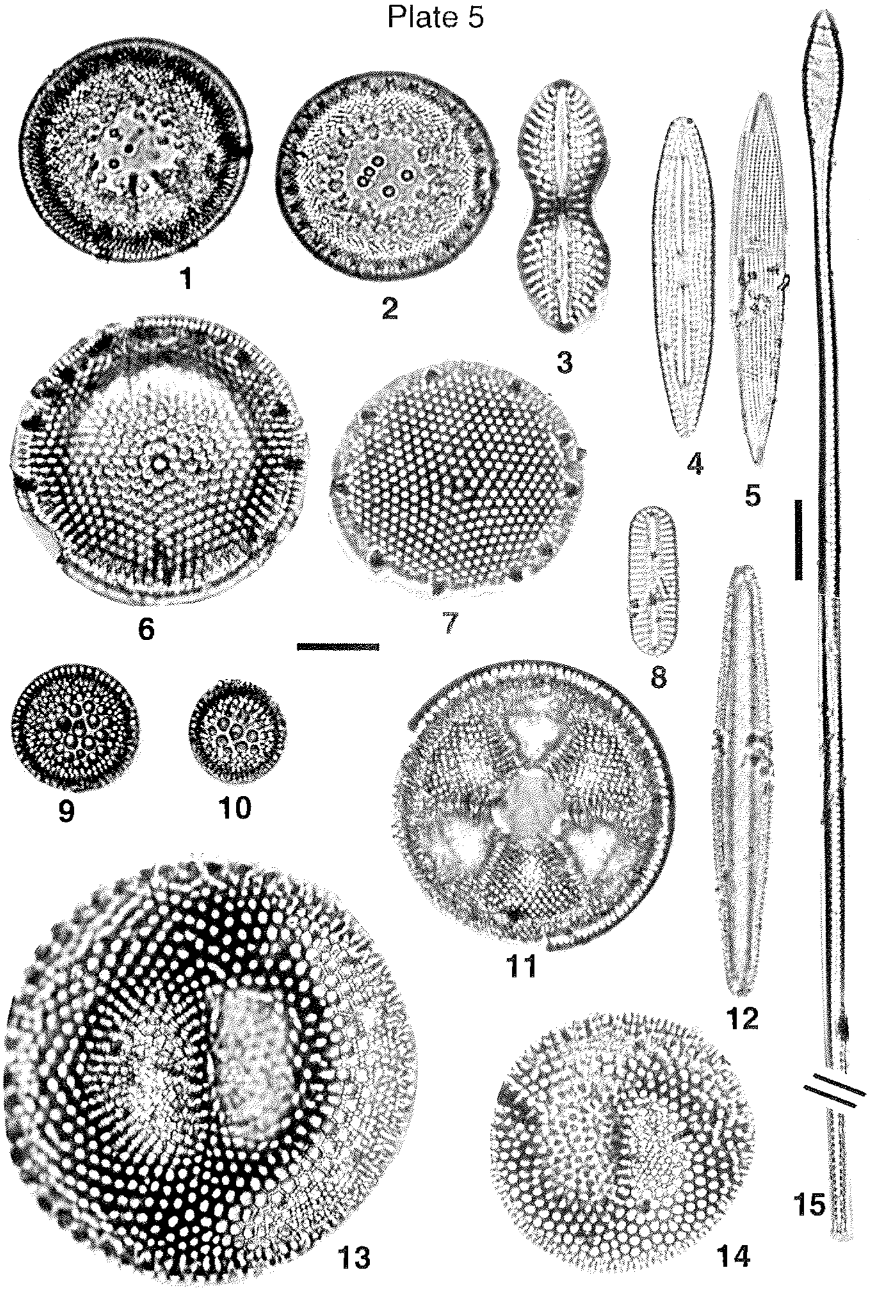

3. Miocene Climate Evolution of the Southern Ocean – Sea Surface Development as Derived from the Diatom Record (ODP Sites 689, 690, 1088 and 1092)

B. Censarek and R. Gersonde

Alfred Wegener Institute for Polar and Marine Research, Bremerhaven, Germany

(Marine Micropaleontology, submitted)

3.1 Abstract

Four ODP Sites (689, 690, 1088, 1092) located on a meridional transect across the Atlantic Sector of the Southern Ocean were studied to reveal the thermal development of the Middle and Late Miocene and the coupled variability of the Antarctic ice volume. Occurrences and abundance fluctuations of selected diatom species are used to derive evidences of thermal differences in surface water masses. Diatom classification into a warm- and a cold-water related group was used to calculate relative paleotemperatures (RPT) and estimate the development of the latitudinal thermal gradient (LTG).

Results coincide with climate evidences provided by the eustatic sea level curve. Discrepancies to the global oxygen isotope curve are ascribed to temperature-, salinity-, and vital effects blurring the signal. Relative warm- water masses and low latitudinal thermal differentiation occurred between 14.8 to ca. 13 Ma. This is followed by the stepwise establishment of a cold surface water ocean culminating with the development of cold-water assemblages in the present Subantarctic area around 10.8 Ma, a period of lowest sea level in the Miocene. A first short period of increased thermal decoupling of the Southern Ocean occurred between 10.8 to 10.4 Ma. A rapid warming in the Antarctic Circumpolar Current (ACC) caused this latitudinal differentiation. This is followed by a period of lowered thermal differences and relative warmth between 10.3 and 9.6 Ma. Starting at 9.6 Ma increasing thermal isolation of the Southern Ocean water masses might be related to the onset of major West Antarctic ice sheet (WAIS) build up. The establishment of diatom assemblages consisting of species having close affinities to modern sea-ice related taxa around 9-8.5 Ma supports the idea of a distinct cooling of Weddell Sea surface waters related to a major expansion of the Antarctic ice sheet surface.

3.2 Introduction

The Miocene is known as a period of progressive cooling and growth of the Antarctic ice sheets combined with a relative warming in the low latitudes which results in increasing latitudinal gradients (Shackleton and Kennett, 1975; Miller et al. 1991; Flower and Kennett, 1994). The growth of the Antarctic cryosphere is closely related to the opening of tectonic gateways, such as the Tasmanian Gateway and the Drake Passage, that present the main prerequisites of the development of an unrestricted ACC system, which isolated Antarctica thermally. The timing of these tectonic events however, is yet not well constraint because of the complexity of tectonic movements in both areas (Lawver et al., 1992, Cande et al., 2000). Recent drilling during ODP Leg 189 points to an opening of the Tasman Seaway close to the Eocene/Oligocene boundary (Shipboard Scientific Party, 2001) and geochemical proxies obtained from ODP Leg 177 Site 1090 in the Atlantic sector of the Southern Ocean have been interpreted to record an establishment of a deep water Drake Passage in the earliest Oligocene, around 32.8 Ma (Latimer and Fillipelli, 2002). This is in contrast to earlier estimates indicating an opening in the late Oligocene or earliest Miocene (Barker and Burrell, 1977). Despite the existence of a deep water ACC allowing thermal isolation of Antarctica, the Early and Middle Miocene represents a period of relative warmth, with an East Antarctic ice sheet that was distinctly smaller than during the colder Oligocene, as indicated by the deep-sea stable isotope record (Zachos et al., 2001) and relatively high sea level stands (Haq et al., 1987, Abreu and Anderson, 1998). Only after the Mid-Miocene climatic optimum, centered around 17-15 Ma, the isotope and sea level data point to gradual cooling and reestablishment of a major ice sheet on the Antarctic continent. The most important development in the Late Miocene was the build-up of the West-Antarctic Ice Sheet (WAIS), which started to take place in the early Late Miocene according to sedimentological and clay mineralogical data obtained from ODP Leg 113 (Kennett and Barker, 1990).

On a long-term scale both, the benthic isotope record and the eustatic sea level curve, indicate similar trends (Barrett, 1999). However, a more detailed view of both climate records reveals distinct differences that are yet not explained. In the Middle and Late Miocene distinct mismatches occur e.g. around 16, 15 and 11 Ma, when the sea level curve indicates substantial sea level lowering, while the isotope record provides no support for such instability of the Antarctic ice sheet. Wise et al. (1992) outlined that oxygen isotope data may be controversial interpreted, as a result of inaccurate estimation of components, such as temperature, salinity effects but also "vital effects" of the measured foraminifer taxa, influencing the oxygen isotope values and their significance as a tracer for ice volume changes. Using the magnesium/calcium ratio in benthic foraminifers as an independent record of deep-sea temperature, Lear et al. (2000) concluded that in average 85% of the isotope signal can be attributed during the Middle and Late Miocene to ice-volume build up.

To augment our understanding of the middle and upper Miocene Southern Ocean climate and related ice volume variability, we use the diatom record obtained from a latitudinal transect across the Atlantic sector of the Southern Ocean. Diatoms are useful proxies for the reconstruction of surface water parameters, as shown by transfer-function-based reconstructions of middle and upper Pleistocene Southern Ocean surface water temperatures (e.g. Pichon et al., 1987; Zielinski et al., 1998; Kunz-Pirrung et al., 2002; Bianchi and Gersonde, subm.) and sea-ice distribution (e.g. Crosta et al., 1998; Gersonde and Zielinski, 2000). While such studies based on modern analogs provide quantitative values of surface water parameters, paleotemperature reconstructions of pre-Pleistocene sequences must mainly rely on the distribution of extinct taxa and thus only allow the estimation of relative temperature changes. However, studies based on the abundance fluctuations and distribution of extinct diatoms have been completed successfully for the delineation of climate variability in Middle Miocene sections from the Northern and Equatorial Pacific (Koizumi, 1990; Barron, 1992b) as well as in the Pliocene of the Pacific and Southern Ocean (Barron, 1992b and 1996). The latter studies were focused to decipher the magnitude and extend of the mid-Pliocene warming event. Barron (1992b) used a modification of a diatom temperature equation originally proposed by Kanaya and Koizumi (1966), based on the simple ratio of the abundance of diatom species designated to represent warm and cold-water indicators. In our study we use the simple equation proposed by Barron (1992b) to learn more on the thermal evolution of the Southern Ocean during the middle and late Miocene and link these data with the global isotope and sea level records. The comparison of the thermal development at the different sites located on a latitudinal transect also allows the estimation of changes in latitudinal thermal gradients that provide further insights into the Miocene Southern Ocean energy balance.

3.3 Material and methods

3.3.1 Location of sites

We investigated Miocene diatom assemblages recovered at four ODP sites located on a latitudinal transect across the Atlantic Southern Ocean sector. The transect extends from Maud Rise (ca. 65°S) ODP Leg 113 Sites 689 and 690 (Shipboard Scientific Party, 1988a, b), across the northern Meteor Rise (46°S) to the Agulhas Ridge (41°S), ODP Leg 177 Sites 1092 and 1088 (Shipboard Scientific Party, 1999a, b), respectively (Fig. 3.1).

The Maud Rise Sites 690 and 689 are located nearby to each other (distance 116 km) at water depths of 2914 m and 2080 m, respectively. These sites are located close to the East Antarctic continent in the south-eastern realm of the Weddell Gyre, approx. 1000 km south of the Polar Front.

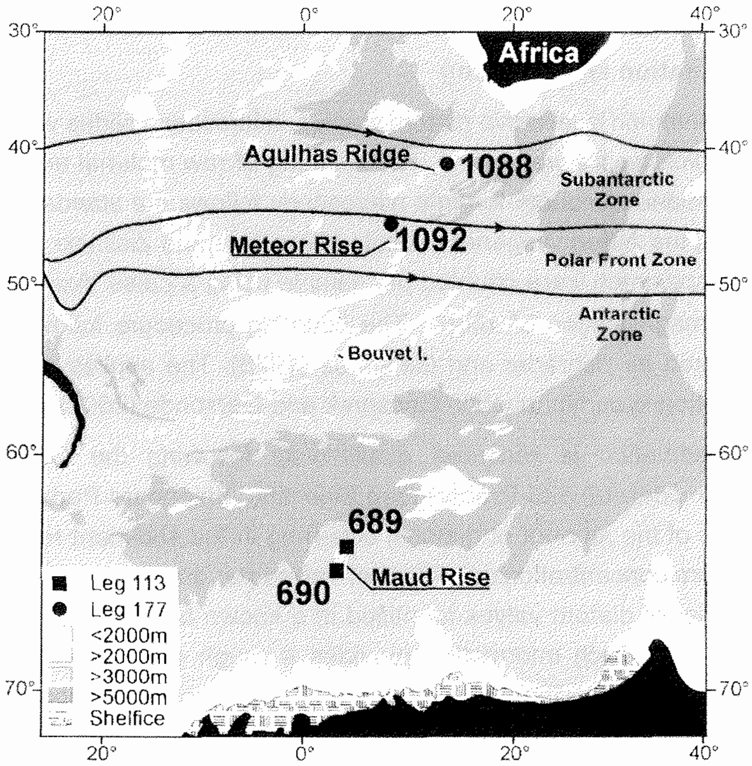

Figure 3.1: Site locations along a latitudinal transect across the Atlantic sector of the Southern Ocean are shown. Frontal zones according to Peterson and Stramma (1991).

Both sites can be spliced to form a continuous composite recording a period between 14.5 Ma and 6.5 Ma.The sediments from this composit (Site 689: 10-63 meters below sea floor (mbsf) and Site 690: 14-50 mbsf) are of pelagic origin and consist mostly of biogenic siliceous ooze (Shipboard Scientific Party, 1988 a, b). Site 1092 is located close to the Subantarctic Front (SAF). The studied section is between 60 and 209 meters composite depth (mcd) and includes a continuous composite sequence obtained from a splice of four holes to 188 mcd. The sediments consist of nannofossil ooze with variable amounts of foraminifers, diatoms and radiolarians (Shipboard Scientific Party, 1999a). The northernmost Site 1088, drilled in 2082 m water depth, is located in the northern portion of the Subantarctic Zone (SAZ) and consists in the studied section (30-220 mcd) predominantly of carbonate (mostly nannofossil) oozes (Shipboard Scientific Party, 1999b). Diatoms are a subordinate component and occur in a reliable preservation only in a few intervals.

3.3.2 Preparation and counting

For quantitative and qualitative diatom studies, microscope slides with randomly distributed microfossils were used. The cleaning of raw material and the preparation of permanent mounts for light microscopy follows the standard technique developed at the Alfred Wegener Institute (Gersonde and Zielinski, 2000). Up to 400 diatom specimen were counted per sample using a Zeiss "Axioskop" microscope at a magnification of 1000×. The counting procedure followed the concepts proposed by Schrader and Gersonde (1978). The applied diatom taxonomy information is summarised in Censarek and Gersonde (2002).

Diatom preservation is recorded qualitatively following the OPD scheme: G(good), M(moderate) and P(poor) (see Scientific Shipboard Party, 1999c). As an indication of the amount of diatoms occurring in the sediment record we calculated diatom concentrations (number of valves per gram dry sediment) based on the number of diatom valves identified in a known area of the individual microscopic slides. Such information provides a rough estimate on changes in preservation and deposition of biogenic opal and allows deciphering specific productivity regimes.

The counting results are archived in the PANGAEA information system at the Alfred Wegener Institute for Polar and Marine Research, Bremerhaven (AWI) (http://www.pangaea.de).

3.3.3 Chronology

Age models combining geomagnetic and diatom biostratigraphic record for the studied Miocene sections of Sites 689, 690, 1088 and 1092 are taken from Censarek and Gersonde (2002). Range charts showing the site-by-site stratigraphic occurrences of selected diatom species are available from a data report (Censarek and Gersonde, subm. a). The geomagnetic data obtained at Site 1088 are not interpretable (Shipboard Scientific Party, 1999b). As a consequence, the stratigraphy used at Site 1088 only relies on a combination of diatom and calcareous nannofossil biostratigraphic data (Censarek and Gersonde, 2002; Marino and Flores, 2002) limiting the accuracy of the stratigraphic correlation of Site 1088 with the three other studied sites.

Ages are tied to Geomagnetic Polarity Time Scale (GPTS) presented by Berggren et al. (1995). For direct comparison of this time scale with the previously used GPTS of Berggren et al. (1985) both time scales including their deviation are shown in Figure 3.2. A detailed description of the nomenclature of geomagnetic events is available from Cande and Kent (1992).

3.3.4 Paleotemperature estimates and diatom classification

For estimation of changes in paleotemperatures at the individual sites we apply the simple ratio established by Barron (1992b):

$$RPT = dw / (dw + dc),$$

where “dw” and “dc” are the total number of diatoms indicating warm-water and cold-water conditions, respectively. The resulting value represents a relative paleotemperature (“RPT”) estimate between the value 0 (100 % cold-water dwellers) and 1 (100% warm-water dwellers). We choose to name this value "RPT" instead of Barron's paleoclimate ratio "Tw" (Temperature warm-water) to point out the relativity of this term. The comparison of relative paleotemperatures obtained from Sites 689/690 (southern Southern Ocean) and Site 1092 (northern Southern Ocean) are used to estimate the latitudinal thermal gradient (LTG) across the Southern Ocean.

Out of the 72 diatom taxa and taxa-groups counted for this study only five are extant, which allows a delineation of the autecological demands of the taxa based on first-order observations. Of those taxa, we placed *Azpeitia tabularis*, *Hemidiscus cuneiformis*, *Thalassiosira oestrupii* and the *Thalassionema nitzschioides*-groupwithin the group of warm-water indicators (Tab. 3.1). *H. cu-*

neiformis represents a true warm-water taxon (Fryxell et al., 1986), which at present is excluded from Southern Ocean waters as revealed from surface sediment studies (Zielinski and Gersonde, 1997). *Azpeitia tabularis* belongs to a genus that generally shows a warm-water distribution (Fryxell et al., 1986). However, it represents the only exception within the genus *Azpeitia* occurring preferentially in the colder environments of the Southern Ocean. It has been reported from Southern Ocean surface sediments below surface waters, that range in temperature between 0-20°C displaying maximum abundances at temperatures above 10°C, characteristic of the Subantarctic Zone (Zielinski and Gersonde, 1997). Although, *T. oestrupii* has a cosmopolitan distribution (Fryxell and Hasle, 1980) we placed it in the warm-water group because its maximum occurrences in Southern Ocean surface sediments were recorded from the Subantarctic Zone with surface water temperatures above 12°C. The taxa combined within the *Thalassionema*-group consist of *T. nitzschioides* and the varieties *T. nitzschioides* var. *inflatum*, *T. nitzschioides* var. *lanceolatum* and *T. nitzschioides* var. *parvum*. Of those, the varieties *inflatum* and *parvum* have strong affinities to subtropical and tropical regions (Moreno-Ruiz and Licea, 1995; Hasle, 2001). *T. nitzschioides* and the *T. nitzschioides* var. *lanceolatum* are claimed to show a cosmopolitan distribution (Hasle, 2001) also being present in Southern Ocean waters. Nevertheless we also place *T. nitzschioides* and its variety *lanceolatum* within the warm-water group because their southernmost occurrence is in Subantarctic waters (Zielinski and Gersonde, 1997). Morphotypes such as the cold-water related *T. nitzschioides* fo. 1, which preferentially dwells in waters of the Polar Front and Antarctic Zone (Zielinski and Gersonde, 1997), have not been encountered in the studied sections. Another extant taxon, belonging to the genus *Thalassiothrix* has not been considered because the valves of this taxon were mostly preserved as fragments that make a light-microscopic differentiation between *T. antarctica*, a cold-water dweller and *T. longissima*, a temperate species (Hasle, 2001), impossible. However, both species are indicators for high primary productivity and upwelling conditions at frontal systems (Kemp and Baldauf, 1993; Kemp et al., 1995).

The classification of the extinct taxa, making up the majority of the middle and upper Miocene assemblages, into warm- and cold-water related species must rely upon an interpretation of their autecological demands. This interpretation is based on (1) the relationship of the occurrence pattern of taxa with well defined autecological demands (e.g. extant taxa) and extinct taxa, (2) the geographical and stratigraphical distribution, on a Southern Ocean and global scale, and (3) the generic affiliation, in case the genus can be linked to a specific thermal environment.

Classification of extinct taxa

Warm-water-indicating group (Tab. 3.1):

Although both, *Hemidiscus karstenii* and *Hemidiscus triangularis*, are species that are most probably endemic to the southern high latitudes we placed them into the warm-water group. This interpretation considers, that in general taxa belonging to the genus *Hemidiscus* are related to warmer water conditions (Hasle et al., 1995). Further evidence comes from the Pleistocene record of *H. karstenii*, where the taxon displays prominent occurrences restricted to the climatic optima of interglacials in the Subantarctic realm (Burckle, 1982) making this taxon a stratigraphic tool in the Pleistocene of the northern belt of the Southern Ocean (Gersonde and Bárcena, 1998). Little is known about the distribution of *H. triangularus*. Ciesielski (1983) reported rare to few abundances of *Cosmoidiscus insignis* var. *triangula,* the Basionym for *H. triangularus* (Harwood and Maruyama, 1992), from the Southwest Pacific. This species is found with few abundances in subantarctic sediments of the Southwest Atlantic (Ciesielski, 1986). Considering that *H. triangularus* is not yet documented at sites south of the Polar Front we classified this taxa into the warm-water indicating group. Co-occurrences of *H. triangularus* and *A. tabularis* support this classification.

Fragilariopsis reinholdii occurred from high to low latitudes, but reach highest abundances in relative warm subtropical water masses (Sancetta and Silvestri, 1986; Barron, 1992b). In our study *F. reinholdii* was only found at sites in the northern area of the Southern Ocean referring to the relative warm-water affinity of this species.

Crucidenticula nicobarica is included into the warm diatom group, because of their dominant occurrence beside some few recently occurring warm-water species (e.g. *Thalassionema nitzschioides, Thalassiothrix longissima*) in Miocene sediments of the Guadalquivir Basin (Spain) (Bustillo and Lopez-Garcia, 1997). *Crucidenticula nicobarica* was most dominant in Equatorial Pacific sediments, where it occupies more than a half of the diatom assemblage, which documented also the warm-water affinity of this taxa (Barron, 1985a).

A. ingens has a longer stratigraphic range in high latitudes compared to low latitudes (Barron, 1985b), which refers to a generally cold-water affinity. Barron and Keller (1983) did not include this species in the cold diatom group in the study of Northeast Pacific sediments, because of their common abundances in equatorial sites. However, we considered *A. ingens* as warm-water taxa, because of the dominant co-occurrence in the Southern Ocean with the warm-water indicator *Azpeitia tabularis* (Censarek and Gersonde, subm. a).

A.ingens var. *nodus* is documented beside from Southern Ocean sediments from high- and mid-latitudes of the North Pacific (Gersonde, 1990; Barron, 1985b). Also the co-occurrence with *A. tabularis* points to a relative warm-water affinity *A.i.* var. *nodus*.

A.ingens var. *ovalis* is only found at southern high latitudes. Gersonde (1990), who described this variety, mentioned that *Hemidiscus karstenii* fo.1 (Ciesielski, 1983), which is documented with common abundances from Subantarctic deposits is possibly *A.ingens* var. *ovalis*. *Hemidiscus karstenii* fo.1 occurred at a period where the assemblage is dominated by the undoubtedly warm-water species *F. reinholdii* and *H. karstenii*. We include this variety of *A. ingens* in the warm-water group also due to her higher abundances at the region of circumpolar current as at the southern Southern Ocean area (Gersonde and Burckle, 1990; Censarek and Gersonde, subm. a). This classification is provided by the co-occurrence of *A. ingens* var. *ovails* with higher abundances of warm-water taxa *A. tabularis*.

Table 3.1: Thermal classification of the selected diatom species, which are considered for relative paleotemperature estimation.

Selected diatom species	
Warm-water species	**Cold-water species**
Actinocyclus ingens	*Denticulopsis praedimorpha*
A. ingens var. *nodus*	*Denticulopsis dimorpha*
A. ingens var. *ovalis*	*Denticulopsis ovata*
Azpeitia tabularis	*Nitzschia denticuloides*
Crucidenticula nicobarica	*Fragilariopsis aurica*
Fragilariopsis reinholdii	*Fragilariopsis arcula*
Hemidiscus cuneiformis	*Fragilariopsis praecurta*
Hemidiscus karstenii	*Fragilariopsis donahuensis*
Hemidiscus triangularus	
Thalassionema spp.	
Thalassiosira oestrupii	

Derivation of the cold-water indicating group (Tab. 3.1):

Denticulopsis ovata and *Nitzschia denticuloides* are endemic species in the Southern Ocean (Yanagisawa and Akiba, 1990; Barron and Baldauf, 1995), which indicates the cold-water affinities of the species and causes the grouping as cold-taxa. Possible precursors of *D. ovata* are *D. dimorpha* and *D. preadimorpha* (Yanagisawa and Akiba, 1990). *D. dimorpha* is established in the Southern Ocean and later migrated in the northern mid- and high latitudes. There are not found in equatorial deposits (Yanagisawa and Akiba, 1990).

Highest abundances of *D. dimorpha* are found in the northern Southern Ocean area, which can be attributed to less dominance of *D. ovata* compared to the northern Southern Ocean. *D. praedimorpha* is only documented from the southern high latitudes (Yanagisawa and Akiba, 1990) and from a single North Pacific site (Barron, 1980). Highest abundances of *D. praedimorpha* are documented for the southern Southern Ocean (Censarek and Gersonde, subm. a) causing the classification as relative cold-water species.

All reported occurrences of *D. ovata*, *D. dimorpha* or *D. preadimorpha* are out of phase to abundance occurrences of distinct warm-water taxa as e.g. *A. tabularis* indicating the general cold-water affinity of this group causing also the classification as cold taxa.

Fragilariopsis aurica, F. arcula, F. praecurta and F. donahuensis are included as cold-water related, caused by their endemic occurrence and higher abundance in southern regions of the Southern Ocean. All species has an earlier first occurrence datum (FOD) in the southern Southern Ocean compared to the northern Southern Ocean indicating also their cold-water affinities (Censarek and Gersonde, 2002; Fig. 3.2). Gersonde (1991) described *F. praecurta* as possible precursor of the recent occurring *F. curta*, which is used to reconstruct the sea-ice boundary (Gersonde and Zielinski, 2000).

Excluded taxa:

Yanagisawa and Akiba (1990) remark that *D. simonsenii* is a cosmopolitan diatom documented with higher abundances and longer stratigraphical range at high, especially northern high latitudes. This species was excluded from the calculation, because of its occurrence with similar abundances in the southern and the northern area of the Southern Ocean synchronous with definite warm

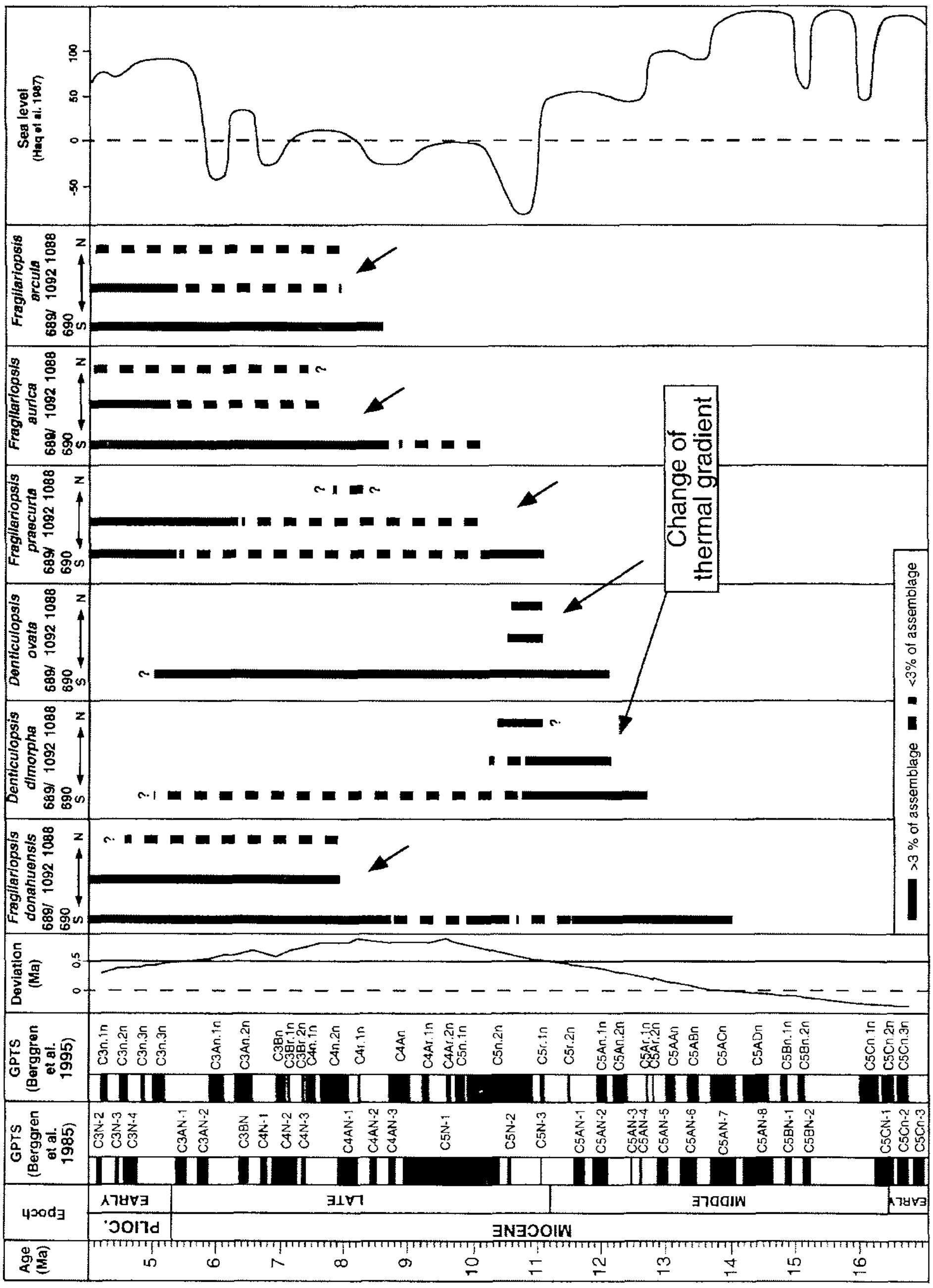

Figure 3.2: Comparisons of stratigraphic ranges of selected cold-water diatoms indicate times of a changing thermal gradient. Similar occurrence datums at Site 1092 and 1088 indicate a similar surface water mass. For reasons of comparison geomagnetic polarity time scales (GPTS) of Berggren et al. (1985, 1995) including their deviation are shown. The sea level curve of Haq et al. (1987) indicating the general climate history is also presented.

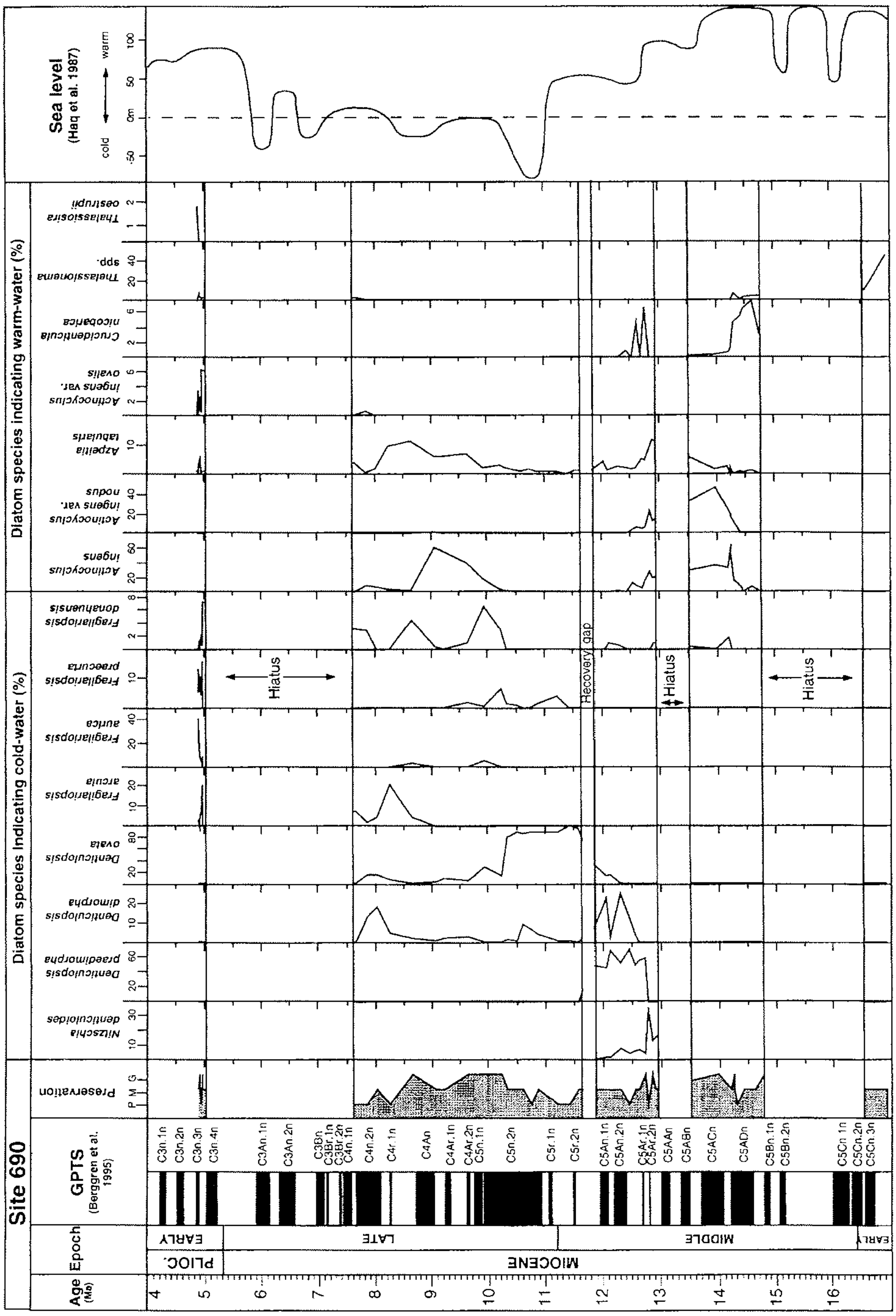

Figure 3.3: Relative abundances of warm resp. cold indicating diatoms of Site 690 as well as the diatom preservation are presented. Further, the GPTS of Berggren et al. (1995) and the sea level curve (Haq et al., 1987) are shown.

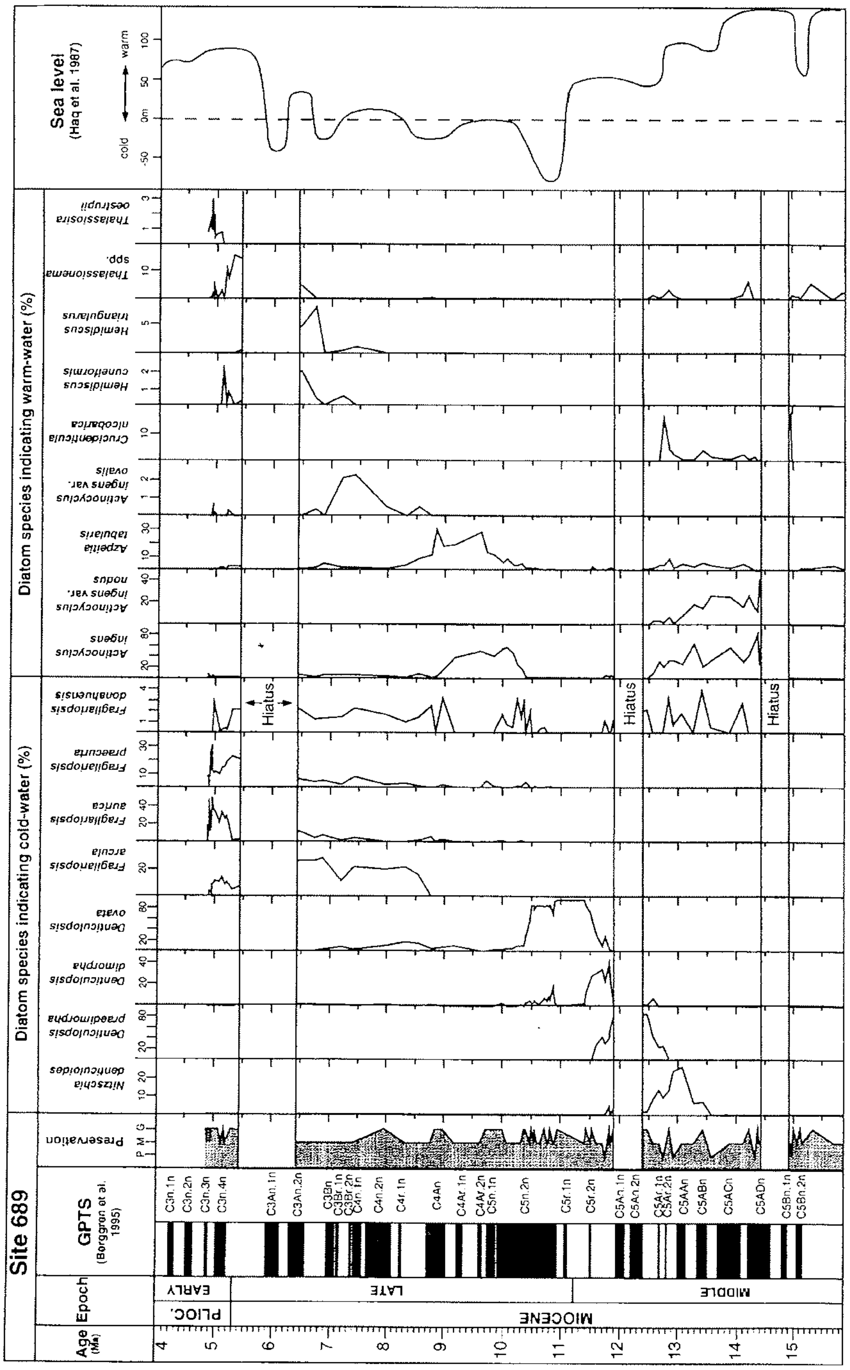

Figure 3.4: Relative abundances of warm- and cold-water indicating diatom taxa and diatom preservation at Site 689 are shown. Further, the GPTS of Berggren et al. (1995) and the sea level curve (Haq et al., 1987) are presented.

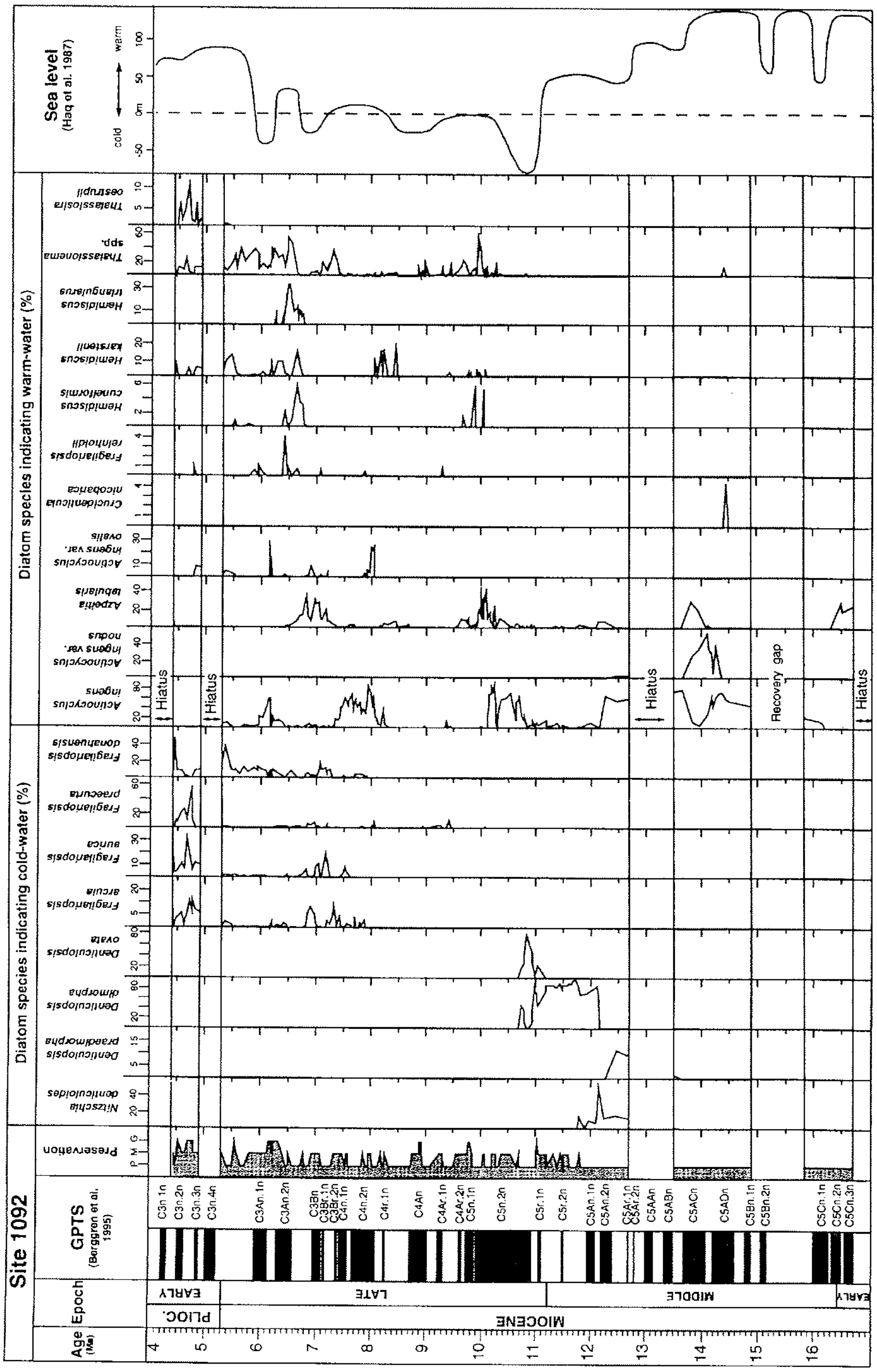

Figure 3.5: Relative abundances of warm- and cold-water indicating diatom species at Site 1092 and diatom preservation are presented. Further, the GPTS of Berggren et al. (1995) and the sea level curve (Haq et al., 1987) are shown.

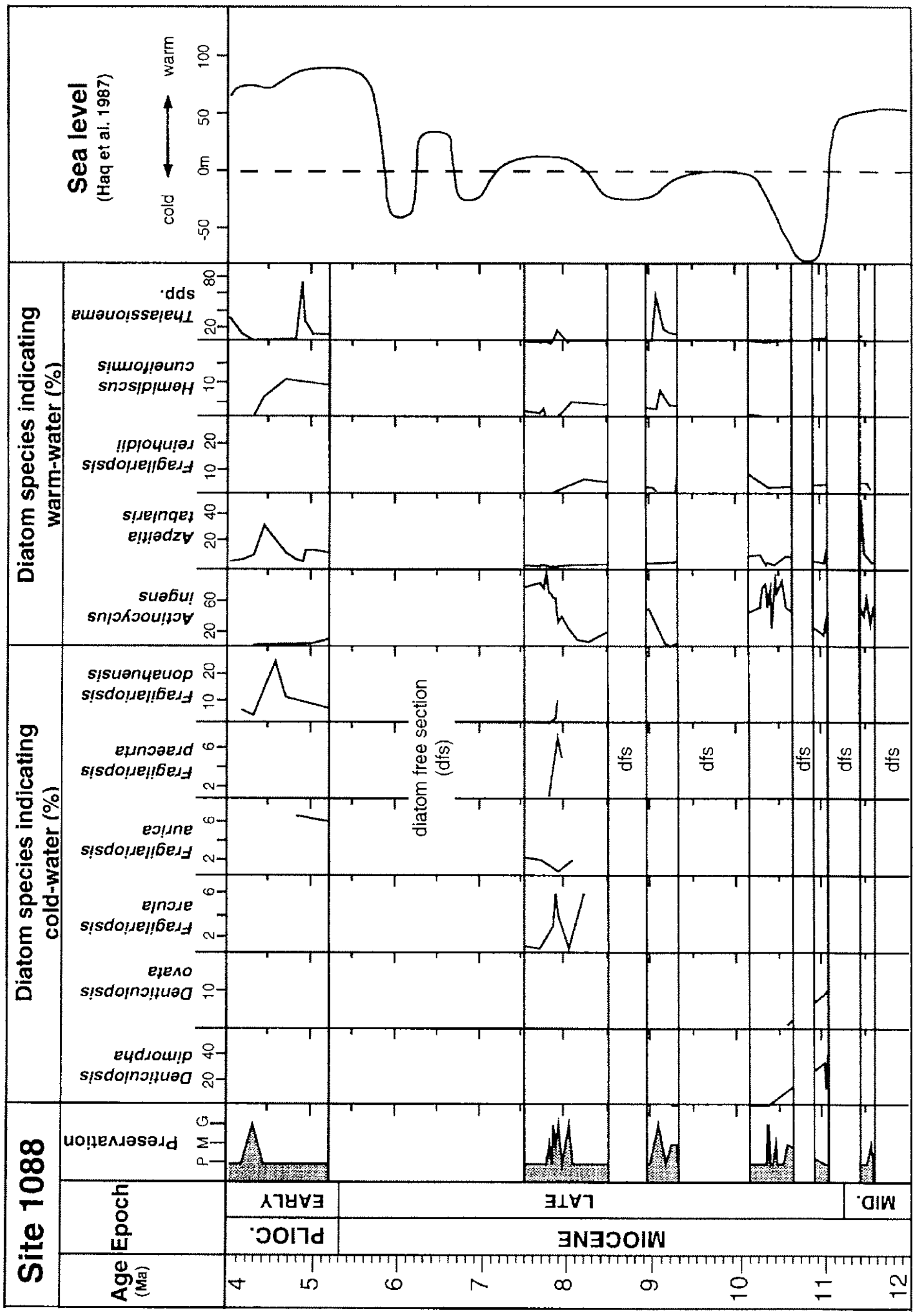

Figure 3.6: Relative abundances of warm- and cold-water indicating diatoms of Site 1088 and diatom preservation are presented. Further the eustatic sea level curve (Haq et al., 1987) is presented.

and cold species indicating the adaptation on a wide temperature range (Censarek and Gersonde, 2002). *D. crassa* and *D. hustedtii* are documented from the middle to high-latitudes, with higher abundances in the northern hemisphere. We exclude these species because of rare abundances and partly sporadically occurrences in the high southern latitudes (Yanagisawa and Akiba, 1990; Censarek and Gersonde, subm. a).

Other species from data set are excluded due to rare or trace occurrence or unidentifiable thermal demands.

3.4 Results

3.4.1 Relative paleotemperatures and the latitudinal thermal gradient

The Maud Rise Sites 690 and 689 show, as expected, similar RPT values, indicating the same thermal conditions in an more or less uniform surface water mass (Fig. 3.7). Slight differences around 10 Ma and between 9 and 8 Ma can be attributed to lower sample resolution at Site 690. Between 17 and ca. 13.5 Ma relative warm surface waters occurred throughout the Southern Ocean. Warm-water indicating *A. ingens*, *A. ingens* var. *nodus*, *C. nicobarica* and *A. tabularis* represent the dominating assemblage in this period. A cold time spread followed reaching up to ca 10.5 Ma. In this period the successively replacing cold-water species *N. denticuloides*, *D. praedimorpha*, *D. dimorpha*, *D. ovata* dominated. Site 1092 shows a comparable thermal development, whereby the cold time spread at the Middle to Late Miocene ends earlier (ca. 10.8 Ma) than at Sites 689/690 (Fig. 3.7). This is primarily indicated by an earlier dominant occurrence of warm-water species *A. ingens* at the northern Southern Ocean (Site 1092). RPTs document warm conditions at the early Late Miocene throughout the Southern Ocean (Fig. 3.7). They are turning back to cooler conditions at the southern sites between 9 and 8.5 Ma, whereas at Site 1092 warm conditions prevailed up to the Early Pliocene. This southern Southern Ocean cooling is documented by higher abundances of cold-water indicating group *F. aurica*, *F. arcula*, *F. praecurta* and *F. donahuensis* at Sites 689/690 in combination with lower abundances of the warm-water taxa *A. ingens* and the *Thalassionema*-group.

Occurrences of *Hemidiscus cuneiformis*, a recently in the southern high latitudes extinct warm-water taxon, point at 9.9 Ma in the northern Southern Ocean and around 6.6 Ma even in the southern studied area to probably warmer than present-day temperatures.

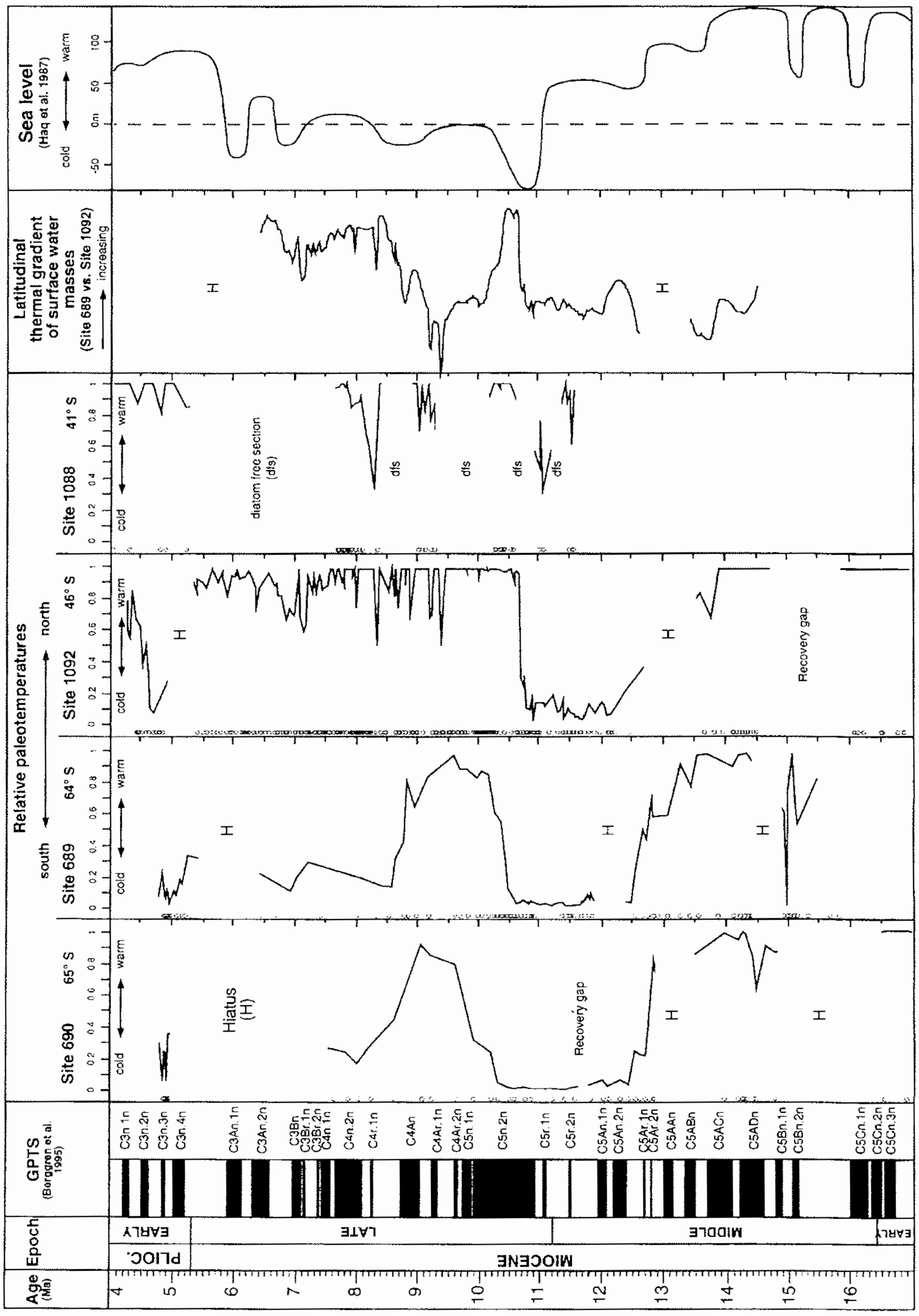

Figure 3.7: Relative paleotemperatures for Sites 689, 690, 1088 and 1092 reflect the thermal demand of diatom assemblages. The thermal gradient between northern (Site 1092) and southern (Site 689) area of the Southern Ocean are presented. Higher values indicate higher thermal differences between surface water masses. Further, the GPTS of Berggren et al. (1995) and the sea level curve (Haq et al., 1987) are shown. Small circles - sample positions. H - hiatus.

This stands in contrast to the RPTs, which refer in general to cold surface water conditions at these times. The carbonate-dominated Site 1088 shows mostly poor diatom preservation and low abundances resulting in sections without significant amounts of siliceous microfossils. At ca. 11.1 Ma and ca. 8.3 Ma colder surface water occurred indicated by *D. dimorpha*, *D. ovata, F. arcula* and *F. praecurta* in absence of a higher amount of warm-water indicating species, respectively.

All other assemblages recorded at Site 1088 refer to more or less warm conditions. Characteristic for the northern Southern Ocean area is the dominant occurrence of *A. ingens* between ca. 8 and 7 Ma (Figs. 3.5, 3.6). At the Maud Rise sites this species is an inferior component of the diatom assemblage (Figs. 3.3, 3.4). The Late Miocene thermal development of Site 1088 is as far as delineated similar to Site 1092. This can also be derived from the first occurrences (FOs) of cold-water related diatoms (Fig. 3.2).

A high latitudinal thermal gradient (LTG) between Sites 689/690 and 1092, representing the southern and the northern part of the Southern Ocean, appears around 10.5 Ma and between 8.6 to 6.4 Ma. The following younger portion around the Miocene/Pliocene boundary is cut by hiatuses. The high gradient at around 10.5 Ma is caused by a faster warming and earlier onset of warming in the northern Southern Ocean. Only one interval of long time increase in LTG occurs from 9.3 and 8.6 Ma, all other changes happened faster. The lowermost gradient (around 9.5 Ma) results from the unusual constellation of high abundances of the warm diatoms *A. ingens* and *A. tabularis* in the south (Figs. 3.3, 3.4) in combination with a poor preservation and a generally low amount of species in the north (Figs. 3.5, 3.6).

3.4.2 Diatom concentrations

At Sites 690 and 689 diatom concentration maxima occurred between 11.7 and 11 Ma in a calcareous nannofossil dominated sediment section, which is monospecificly build up by a cold-water tolerant coccolithophoridea (Wei and Wise, 1990). Furthermore, high diatom concentrations are documented at Site 689 for the period between ca. 16 and 15 Ma (Fig. 3.8). At Site 1092 low diatom concentration occurred during the middle and the lower portion of the upper Miocene up to ca. 7 Ma where values increased. Highest concentrations are reached at 6.1 and 4.8 Ma (Fig. 3.8). The carbonate dominated sediments at Site 1088 consist of portions containing only low amounts of diatom valves

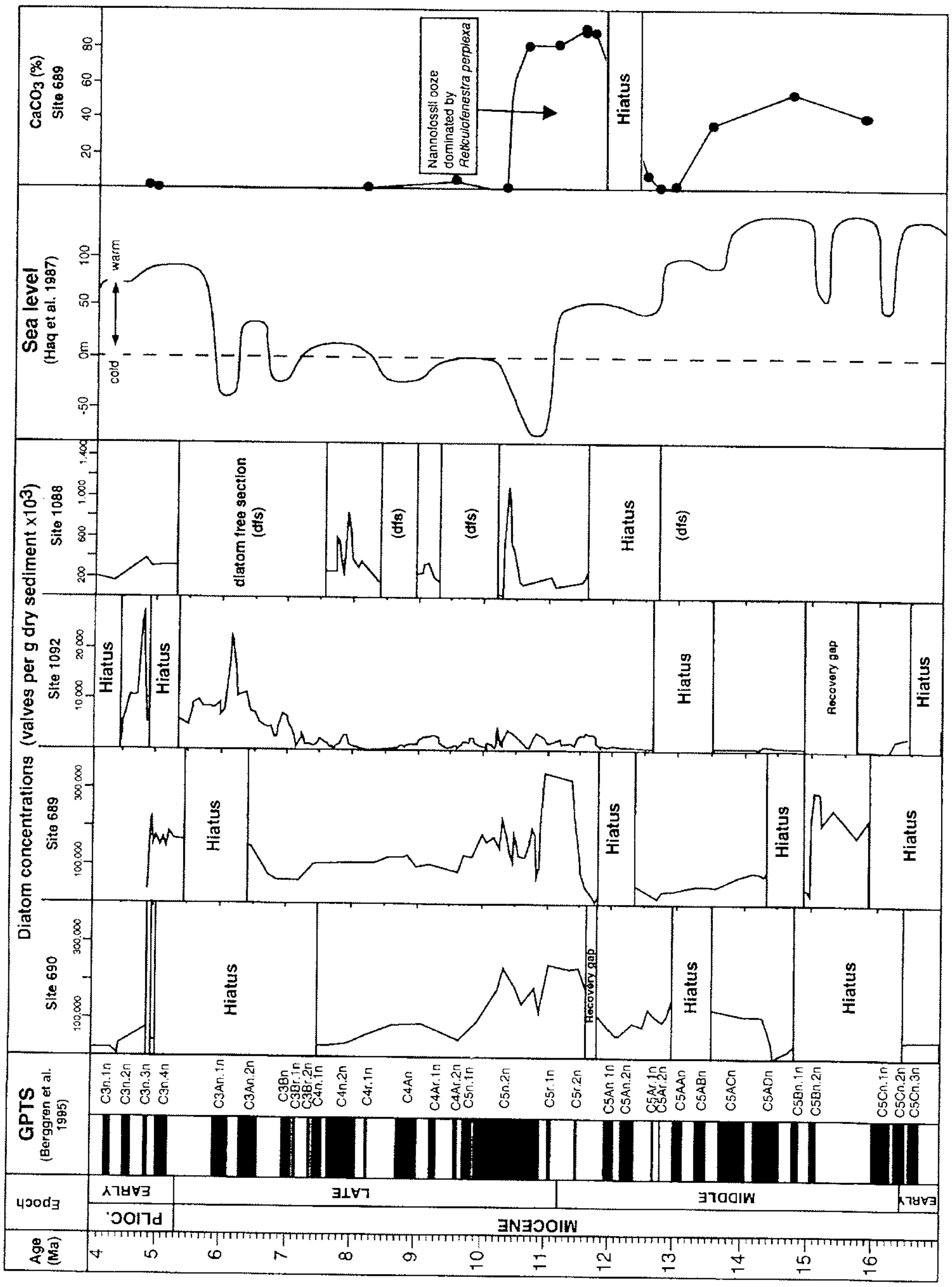

Figure 3.8: Diatom concentrations at Sites 690, 689, 1092 and 1088 are shown beside the sea level curve (Haq et al., 1987) and the $CaCO_3$ curve (Shipboard Scientific Party, 1988a).

alternating with huge diatom free sections. Increased diatom concentrations are found at 10.3 and around 8 Ma. A strong northward decrease of diatom concentrations is shown (Fig. 3.8). Detailed opal measurements for Sites 1092 and 1088 will be presented by Diekmann et al. (subm.).

3.5 Discussion and conclusions

3.5.1 Middle Miocene cooling

From the RPTs and the LTG a more detailed insight in thermal evolution can be derived considering coupled processes. We assume that the best conditions for ice volume accumulation in Antarctica are a warm northern Southern Ocean coupled with a cold southern Southern Ocean climate, which provides a high evaporation moistening the atmosphere and a cooling of the atmosphere increasing precipitation, respectively. Therefore, a high LTG refers to increased ice accumulation. These processes are comparable to the so-called "Panama paradox", which describes the heat transport to the north linked to increased evaporation and precipitation inducing the northern hemisphere glaciation (Berger and Wefer, 1996).

The major build up of the East Antarctic Ice Sheet (EAIS) started after the Middle Miocene climate optimum (Kennett, 1977; Flower and Kennett, 1995). The onset of cooling is documented by the isotope curve at ca. 14.5 Ma and at the sea level curve at around 13.5 Ma (Fig. 3.9). The RPT values refer to a slightly faster cooling starting between 13.5 and 13 Ma. This cooling might have been linked to the closure of the seaway between the Tethys and the Indian Ocean at 14.5 Ma, which led to the replacement of Tethian- and the Mediterranean Outflow Water by North Atlantic Deep Water (NADW). The termination of the Tethian Outflow Water, which was a major factor of meridional heat transport to the southern high latitudes, is proposed to cause the major growth of the EAIS (Ramsey et al., 1998). Between 13 and 12 Ma investigated sediments are characterised by hiatuses in all four cores (Fig. 3.9), which coincide with the global hiatus event NH3 by Keller and Barron (1987). The hiatus occurrences refer to increased deep-water flux, which might be attributed to the onset of southward flowing NADW at ca. 13 Ma (Ramsay et al., 1998).

The RPTs document cool surface waters up to 10.8 Ma within the Southern Ocean at times of a low LTG, which implies a lower ice volume accumulation. This interpretation coincides with the sea level curve (Haq et al., 1987), which documents a level of 50 m above recent values between 12.8 and 11.2 Ma referring to warmer global climates. This stands in contrast to the oxygen isotopes indicating a general uniform cooling between ca. 13.5 and 8 Ma (Fig. 3.9). Slight age discrepancies between the sea level data and the results from the diatom record can be ascribed to the lower resolution of the sea level curve and interpolation inaccuracies occurred at the transfer to the GPTS of Berggren et al. (1995).

3.5.2 Late Miocene thermal decoupling of the Southern Ocean from the adjacent oceans

At the Maud Rise high carbonate contents are documented between ca. 11.8 and ca. 10.6 Ma (Shipboard Scientific Party, 1988a, b). These sediments are mostly build up by the cold-water tolerant Coccolithophoridea *Reticulofenestra perplexa* (Fig. 3.8) (Wei and Wise, 1990). Subsidence of the carbonate compensation depth (CCD) supported by sea level lowering can be assumed as prerequisite for this extraordinarily carbonate preservation in this high latitudes. The high diatom concentrations in combination with increased sedimentation rates (Censarek and Gersonde, 2002) indicate high productivity at this period.

Barron and Baldauf (1995) proposed a diatom assemblage turnover event in the early Late Miocene, indicating climate changes. This coincides with a period of strong global sea level decrease pointing to an increasing ice volume in Antarctica. At this period diatoms document the establishment of a high LTG between 10.8 and 10.4 Ma (Fig. 3.9). However, no evidences on climate changes can be derived from the global oxygen isotope curve (Fig. 3.9). The high LTG is mainly deduced by an earlier dominant occurrence of the warm-water indicating *A. ingens* at Site 1092 as at Sites 689/690. Constituted by the abundant occurrence of *A. tabularis* around 10 Ma and its relation to the *A. ingens* occurrences at the different sites, this gradient can not be an artefact of inaccuracy in the age models. Furthermore, age models feature a magnetostratigraphical age point at 10.949 Ma (Base of Chron C5n.2n) and the reliable FODs of *A. kennettii*, which present at the southern Sites an age of 10.15 Ma and at the northern Southern Ocean an age of 10.3 Ma (Censarek and Gersonde, 2002). There are no evidences for a hiatus around 10.6 Ma at Site 1092 that would account for a fast change from a cold to a warm diatom assemblage.

The global sea level curve points between ca. 10.3 and 9.3 Ma to a warmer period reaching more or less recent conditions (Fig. 3.9). This coincides with RPTs documenting a warm time period throughout the Southern Ocean resulting in a decreasing LTG. Both, the sea level curve and the diatom records imply decreasing ice volume in Antarctica.

Evidences from the ice-rafted debris record and glacially triggered turbidites refer to the incipient of the WAIS build up between 10 and 8 Ma (Kennett and Barker, 1990; Hillenbrand and Ehrmann, 2001). The LTG increased strongly between 9.5 and 8.6 Ma and documented possibly the onset of the major WAIS build up in detail (Fig. 3.9). In contrast the oxygen isotope curve did not refer to any larger thermal or ice volume changes.

A long time spread characterised by a stable high LTG occurred between 8.6-6.5 Ma documenting the strong thermal decoupling of the Southern Ocean and imply the continuous existence of Antarctic cyrospheric environment.

The low RPTs at this time period in the southern area of the Southern Ocean (Sites 689/690) is deduced mainly by higher abundances of cold-water indicating diatoms *F. aurica*, *F. arcula*, *F. praecurta*, *F. donahuensis*. If we assume that *F. praecurta* is the phylogenetic precursor of the recent sea-ice indicating taxa *F. curta* as speculated by Gersonde (1991), which might also concern the morphologic similar species *F. aurica*, Late Miocene sea-ice development might be documented in their abundance pattern. However, more detailed studies on higher resolution sediment sequences and the coupling to an independent sea-ice indicating parameter are required to interpret the abundance peaks of *F. praecurta* and *F. aurica* e.g. at the northern Polar Front Zone (Site 1092).

The occurrence of *H. cuneiformis* in the Southern Ocean at 9.9 and at 6.6 Ma (Sites 689, 1092), indicating warmer than present-day temperatures, must be ascribed to distinct short ranging warming events. Such a warm period occurring around 6.6 Ma, which is just before the Mediterranean isolation started (Krijgsman et al., 1999), is documented in detail by diatom abundances at ODP Site 704 (Censarek and Gersonde, subm. c).

However, all four studied sites are characterised by the lack of sediment sections in the latest Miocene preventing the continuous estimation of thermal development. Accomplishing the reconstruction of the Southern Ocean surface water evolution and Antarctic cryospheric variability Late Miocene sections of ODP Leg 114 Sites 701 and 704 representing two of the few cores containing a complete Messinian section are studied (Censarek and Gersonde, subm. c).

The main climate-changing events in the Late Miocene might be the temporary closure of the Panama Isthmus between 8-6 Ma (Collins et al., 1996a, b)

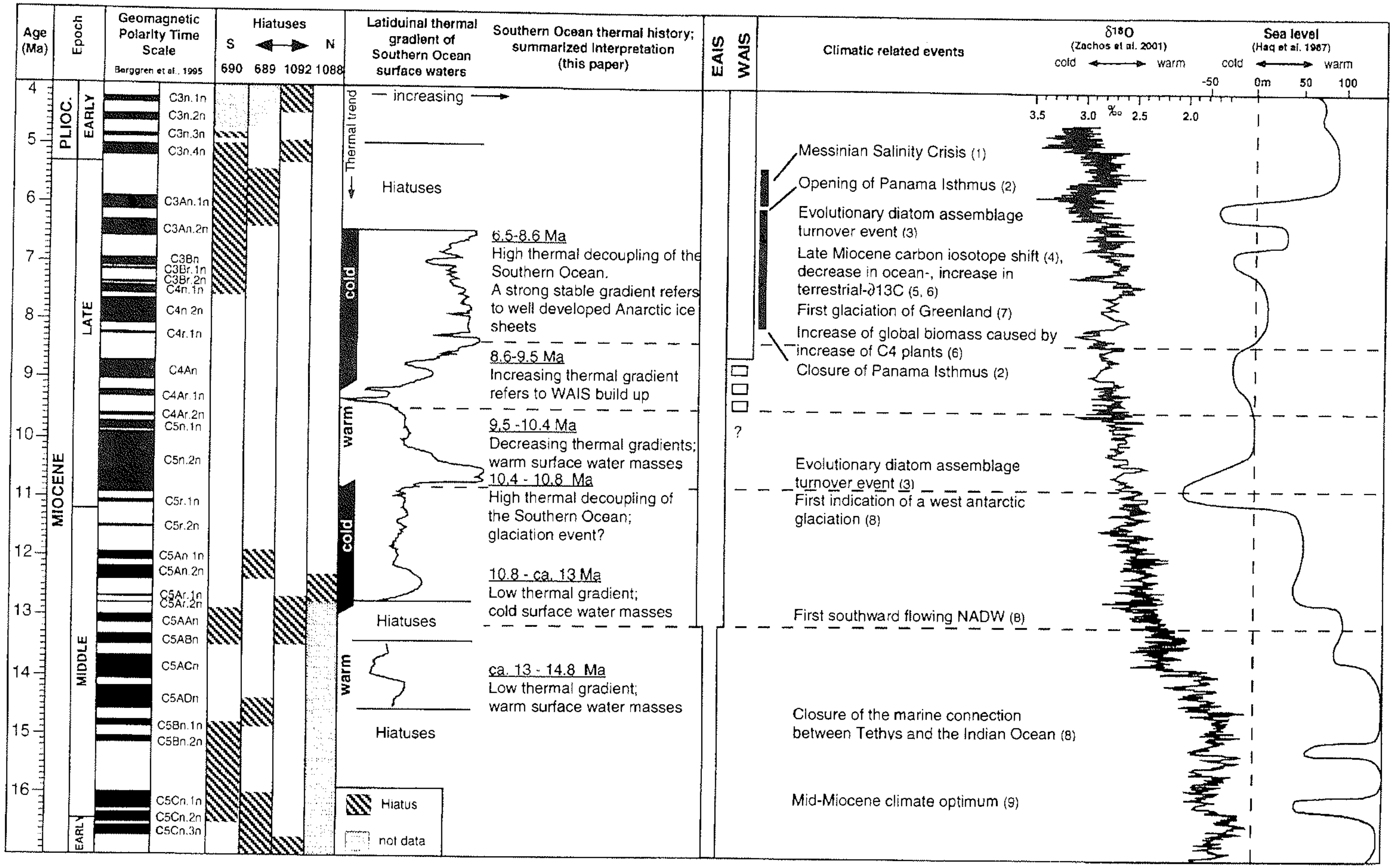
Age (Ma)
Epoch
Geomagnetic Polarity Time Scale
Berggren et al., 1995
Hiatuses
S
N
690 689 1092 1088
Latiduinal thermal gradient of Southern Ocean surface waters
Southern Ocean thermal history; summarized interpretation (this paper)
EAIS
WAIS
Climatic related events
δ18O (Zachos et al. 2001)
cold warm
3.5 3.0 ‰ 2.5 2.0
Sea level (Haq et al. 1987)
cold warm
-50 0m 50 100
PLIOC.
EARLY
MIOCENE
LATE
MIDDLE
EARLY
C3n.1n
C3n.2n
C3n.3n
C3n.4n
C3An.1n
C3An.2n
C3Bn
C3Br.1n
C3Br.2n
C4n.1n
C4n.2n
C4r.1n
C4An
C4Ar.1n
C4Ar.2n
C5n.1n
C5n.2n
C5r.1n
C5r.2n
C5An.1n
C5An.2n
C5Ar.1n
C5Ar.2n
C5AAn
C5ABn
C5ACn
C5ADn
C5Bn.1n
C5Bn.2n
C5Cn.1n
C5Cn.2n
C5Cn.3n
Thermal trend
increasing
Hiatuses
cold
warm
cold
Hiatuses
warm
Hiatuses
Hiatus
not data
6.5-8.6 Ma
High thermal decoupling of the Southern Ocean.
A strong stable gradient refers to well developed Anarctic ice sheets
8.6-9.5 Ma
Increasing thermal gradient refers to WAIS build up
9.5 -10.4 Ma
Decreasing thermal gradients; warm surface water masses
10.4 - 10.8 Ma
High thermal decoupling of the Southern Ocean; glaciation event?
10.8 - ca. 13 Ma
Low thermal gradient; cold surface water masses
ca. 13 - 14.8 Ma
Low thermal gradient; warm surface water masses
?
Messinian Salinity Crisis (1)
Opening of Panama Isthmus (2)
Evolutionary diatom assemblage turnover event (3)
Late Miocene carbon iosotope shift (4), decrease in ocean-, increase in terrestrial-∂13C (5, 6)
First glaciation of Greenland (7)
Increase of global biomass caused by increase of C4 plants (6)
Closure of Panama Isthmus (2)
Evolutionary diatom assemblage turnover event (3)
First indication of a west antarctic glaciation (8)
First southward flowing NADW (8)
Closure of the marine connection between Tethys and the Indian Ocean (8)
Mid-Miocene climate optimum (9)
4
5
6
7
8
9
10
11
12
13
14
15
16

in combination with the depressions of the North Atlantic deep-water gateways (Lavwer et al., 1990; Myhre and Thiede, 1995; Wright and Miller, 1996). This constellation might enable an Atlantic Ocean circulation pattern similar to the recent, which would result in generally increased latitudinal climate gradients and furthermore in high latitudes cryospheric build up. Larsen et al. (1994) reported the first glaciations in Greenland at around 7.3 Ma according to the GPTS of Berggren et al. (1995). Glacial till, diamictites and ice-rafted debris were found at ODP Leg 151 Sites 914-917 of southeast Greenland supporting the assumption of this early glacier occurrence.

The establishment of an Atlantic Ocean circulation system similar to present-day would occur synchronously with global biomass growth and the increase of C4 plants starting at 8 Ma (Cerling et al., 1997; Pagani et al., 1999). The possible connection between a changed ocean circulation and the global carbon flux is a topic for further studies.

This postulated strong change in ocean circulation might be documented in the diatom record by the stable high LTG.

The global climate evolution documented in the sea level curve coincides in huge portions with the thermal development of the Southern Ocean derived from the diatom record. This good agreement corroborates the assumption that a high LTG indicates ice accumulation in Antarctica. However, climate development as documented by the sea level curve or the diatom record stand in contrast to the temperature and ice volume information carried by the global oxygen isotope signal. This discrepancy must be ascribed to the different effects influencing isotopes.

Figure 3.9 (left): Different paleoclimatic indicators delineate Middle and Late Miocene climate history: The latitudinal thermal gradient curve and an overview of hiatus occurrences of the investigated sites (689, 690, 1088 and 1092) are presented. Further, the GPTS of Berggren et al. (1995) and the sea level curve (Haq et al., 1987) are included. Generally acknowledged climate related events are listed. References: (1) Krijgsman et al. 1999, (2) Collins et al., 1996a and 1996b, (3) Barron and Baldauf, 1995, (4) Hodell et al., 1994, (5) Pagani et al., 1999, (6) Cerling et al. 1997, (7) Larsen et al., 1994, (8) Ramsay et al., 1998, (9) Kennett et al., 1977. Increasing $\delta^{18}O$-values of the compiled global isotope curve of Zachos et al. (2001) reflect the overall increased cooling since the Middle Miocene optimum (ca. 15-17 Ma).

4. Late Miocene Southern Thermal Development and its Connection to Mediterranean Climate History - Diatom Evidences from ODP Sites 701 and 704

B. Censarek and R. Gersonde

Alfred Wegener Institute for Polar and Marine Research, Bremerhaven, Germany

(Submitted to Marine Geology)

4.1 Abstract

Late Miocene to Early Pliocene diatom abundance fluctuations of Ocean Drilling Program (ODP) Leg 114 Sites 701 and 704 from the Atlantic sector of the Southern Ocean are studied to describe the thermal development of the Southern Ocean and its relation to the Messinian Salinity Crisis (MSC). This study of Sites 701 and 704, which are exceptional in containing a continuous Messinian sequence, includes Late Miocene diatom biostratigraphies and revises the magnetostratigraphical interpretations. Biostratigraphical diatom occurrence datums are reconsidered revealing some diachronous occurrences. Relative paleotemperatures, which are derived from abundances of thermal conditions indicating diatoms, and individual abundance fluctuations of selected diatom taxa are used to delineate the thermal sea surface development.

Cold climatic conditions are determined for the period between 6.6 and 5.3 Ma and within seven short periods (each ca. 100 k.y.) of cold and five of warm surface water masses, which are partly interrupted by thermal balanced transition stages. The reconstructed thermal history enabled the determination of the development of the hydrographic frontal system considering additional results from ODP Leg 113 and 177 sites. A Paleo-Polar-Front was probably formed at around 8.6 Ma. At around 6.6 Ma hydrographic fronts may have reached recent latitudes and are displaced northward up to ca. 5.3 Ma.

A combination of glacio-eustatic processes and regional tectonic movements is often proposed as mechanism to induce the isolation and flooding of the Mediterranean basin and to control the deposition of evaporites during the MSC. Southern Ocean diatom occurrences and abundance fluctuations are correlated to the Mediterranean development providing evidences for glacial-eustacy processes, which are responsible for the onset of the Mediterranean isolation.

4.2 Introduction

The Middle and Late Miocene climate development is characterised by cooling, increasing latitudinal thermal gradients, ongoing ice sheet build up in Antarctica and the onset of glaciations in the northern hemisphere (Kennett, 1977; Barron et al., 1991; Larsen et al., 1994). The temporary closure of the Panama Isthmus and the lowering of the Greenland-Scotland Ridge had certainly a great influence on Late Miocene climate development (Collins et al., 1996a, b; Wright and Miller, 1996). It is speculated that an ocean circulation pattern close to the present-day situation was established (Censarek and Gersonde, subm. b). The other significant event during the Late Miocene period is the isolation and desiccation of the Mediterranean Sea, the so-called Messinian Salinity Crisis (MSC). Restricted salinity from the Mediterranean Sea water may have had a strong impact on the Atlantic circulation pattern (Haug and Tiedemann, 1998; Rahmstorf, 1998). Regional tectonic movements and sea level fluctuations, which are ascribed to Antarctic ice volume changes, are proposed as mechanisms leading to restriction and reflooding of the Mediterranean basin (Hsü et al., 1973; Benson et al., 1991; Kastens, 1992; Krijgsman et al., 1999; Hodell et al., 2001; Vidal et al., 2001). However, up to now it is under discussion, which mechanism was the dominant trigger. Evidences for Antarctic ice sheet build up caused the MSC via sea level changes can be derived from the thermal evolution of the Southern Ocean Water masses. However, Southern Ocean sediment records close to the Miocene-Pliocene boundary documenting the thermal history are usually incomplete due to hiatus occurrences. Ocean Drilling Program (OPD) Sites 701 and 704 represent two of the few Southern Ocean sediment cores containing a continuous Messinian sequence. We extracted the diatom record to estimate Southern Ocean climate development. Studies based on the abundance pattern and distributions of extinct diatoms have been completed successfully for the delineation of climate variability in Middle Miocene and Pliocene sections (Koizumi, 1990; Barron, 1986, 1992b, 1996). Censarek and Gersonde (subm. b) deduced thermal affinities of extinct Miocene Southern Ocean species, which enable the calculation of relative paleotemperatures (RPT) and allow the interpretation of diatom assemblages.

The Southern Ocean thermal evolution as derived from RPT and abundance patterns of selected diatom taxa are compared with the Mediterranean climate history revealing evidences of the glacio-eustatic influence on MSC steering. The diatom records from ODP Sites 689, 1088 and 1092, which are located latitudinal across the Atlantic sector of the Southern Ocean, are used to delineate a relative movement pattern of hydrographical paleo-fronts.

This study further includes diatom biostratigraphies of Sites 701 and 704, which improves some diatom occurrence datums and revises the magnetostratigraphic interpretation of Clement and Hailwood (1991) and Hailwood and Clement (1991b).

4.3 Material and methods

4.3.1 Core locations, sample preparation and counting

Site 701(51°59,07'S, 23°12.73'W) is locatedon the western flank of the Mid-Atlantic Ridge, around 160 km east of the Islas Orcadas Rise, located in a water depth of 4636 m (Shipboard Scientific Party, 1988c)(Fig. 4.1). This southernmost location in the Polar Front Zone is placed on a deep-sea water gateway. Site 704 sediments were drilled in a water depth of 2532 m at the Meteor Rise (46°52.75'S, 07°25.25'E), which is located in the north of the present Polar Front Zone (Shipboard Scientific Party, 1988d)(Fig. 4.1). This core location is within a mixing zone of upper North Atlantic Deep Water (NADW) and Circumpolar Deep Water (CDW). Hole 701C is selected of two cores containing Late Miocene sediments at Site 701. At Site 704 we chose Hole 704B, which is the only core drilled down to Miocene sediments. Diatom abundance pattern of selected species from ODP Leg 113 Site 689 from the north-eastern Maud Rise (68°S), Leg 177 Sites 1092 and 1088 from the northern Meteor Rise (46°S) and from the Agulhas Ridge (41°S) was also considered (Shipboard Scientific Party, 1988a; Shipboard Scientific Party, 1999a, b; Censarek and Gersonde, subm. b). Together with Site 704, which is located ca. 60 sea miles southeast of Site 1092 and allows a direct comparison of determined diatom data, a latitudinal transect across the Southern Ocean is studied. Site 701 extends the investigated area to the west (Fig. 4.1).

For a quantitative and qualitative diatom study, microscope slides with randomly distributed microfossils were used. The cleaning of the sediment samples and the preparation of permanent mounts for light microscopy follows the approved technique developed at the Alfred Wegener Institute (Gersonde and Zielinski, 2000). Up to 400 diatom valves were counted per sample following the concepts proposed by Schrader and Gersonde (1978). For counting a Zeiss "Axioskop" microscope with apochromatic optics at a magnification of 1000× was used. The applied diatom taxonomy information is summarised in Censarek and

Gersonde (2002). Range charts showing stratigraphic occurrences and abundances of selected diatom species of Holes 701C and 704B are available at the PANGAEA database (http://www.pangaea.de). Diatom concentrations are calculated as diatoms per gram dry sediment. For ease of comparison all ages are tied to the current Geomagnetic Polarity Time Scale of Berggren et al. (1995).

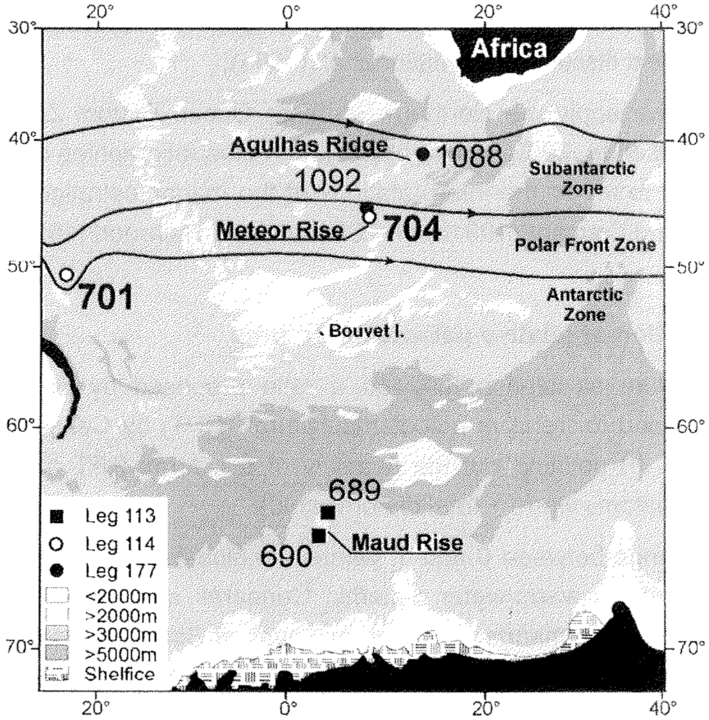

Figure 4.1: Location of ODP Sites 689, 701, 704, 1088 and 1092 in the Atlantic sector of the Southern Ocean. Frontal zones according to Peterson and Stramma (1991).

4.3.2 Chronology

Diatom biostratigraphies of the Miocene sediments recovered during Leg 114 were never published appropriately. The age control of the magnetostratigraphic interpretation at Site 701 is provided by a siliceous microfossil biostratigraphy (Ciesielski, 1991; Clement and Hailwood, 1991). For the Miocene sections of Hole 701C only shipboard diatom zone correlations are available (Shipboard Scientific Party, 1988c). The inclination record contains sections with wide sample spacing (Shipboard Scientific Party, 1988c), which results in inaccurate chron boundaries and the lack of information about complete chrons.

Diatom abundance estimates at Hole704B associated with diatom zonations of Barron (1985a) and Weaver and Gombos (1981) are published in a data report (Ciesielski, 1991). Hailwood and Clement (1991b) presented a magnetostratigraphical interpretation of Hole 704B based on biostratigraphical datums, which are compiled and discussed by Müller et al. (1991).

In this study we apply the Northern Southern Ocean Diatom Zonation (Censarek and Gersonde, 2002) to establish diatom biostratigraphies of Holes 701C and 704B and to revise the interpretations of the magnetostratigraphic records by Hailwood and Clement (1991b) and Clement and Hailwood (1991).

4.3.3 Estimation of relative paleotemperatures

Paleotemperature calculation followed a ratio proposed by Barron (1992b), which is renamed to "relative paleotemperature" (RPT) by Censarek and Gersonde (subm. b) pointing out the relativity of this term: RPT = total diatoms warm / (total diatoms warm + total diatoms cold).

RPT values range between 0 and 1, where 0 indicates entirely cold-water diatoms and 1 entirely warm-water diatoms. Censarek and Gersonde (subm. b) derived the thermal demands of extinct taxa by their Southern Ocean and global geographical and stratigraphical distribution and by the co-occurrence with extant taxa, which is classified on direct observations. Further evidence of species thermal demands is gained by the affiliation to a genus that can be linked to a specific thermal environment.

The group of warm-water indicating diatom species considered in this study consists of *Actinocyclus ingens*, *A. ingens* var. *ovalis*, *Azpeitia tabularis*, *Fragilariopsis reinholdii*, *Hemidiscus cuneiformis*, *Hemidiscus karstenii*, *Hemidiscus triangularus*, *Thalassionema* spp. and *Thalassiosira oestrupii*. The *Thalassionema*-group includes *T. nitzschioides* var. *inflatum*, *T. nitzschioides* var. *lanceolatum* and *T. nitzschioides* var. *parvum*. The group of Southern Ocean cold-water indicating diatom species is composed of *Denticulopsis dimorpha*, *D. ovata*, *Fragilariopsis aurica*, *F. arcula*, *F. praecurta* and *F. donahuensis*.

4.3.4 Derivation of hydrographic front migration

Southern Ocean surface water evolution and hydrographic front development will be roughly outlined and discussed. The average locations of these hydrographic fronts are strongly linked to the topographic features of the Southern Ocean (Moore et al., 1999). However, Late Pleistocene studies revealed front displacements of a few latitudinal degrees northward during cold/glacial and southward during warm/interglacial stages (Morley and Hays, 1979; Prell et al., 1980; Brathauer, 1996, Brathauer and Abelmann, 1999). Barron (1996) estimated the Pliocene position of the Antarctic Polar Front based on selected diatom abundance fluctuations and suggested that frontal zones in the southeastern Atlantic may have migrated southward during the Pliocene warming over approximately 6° latitude. Therefore we interpret from an estimated cold stage a relative migration of surface waters northward and from a warm period a southward relative surface water movement. Comparisons of extant taxa abundances and of diatom concentrations with present-day ranges provide further evidences of water mass migrations.

4.4 Results

4.4.1 Diatom biostratigraphy and revision of the magnetostratigraphies of Holes 701C and 704B

Hole 701C

The uppermost investigated sediment section belongs to the *T. inura* Zone as indicated by the first occurrence (FO) of *T. inura* defining the lower boundary of the *T. inura* Zone (Fig. 4.2). This first occurrence datum (FOD) is found between samples 13H-2, 50-51cm and 13H-2, 149-150 cm (113.28 mbsf) representing an age of approximately 4.9 Ma. From this evidence it can be inferred that the normal polarised chrons around 110 and 115 meter below sea floor (mbsf) are Sidufjall (C3n.3n) and Thvera (C3n.4n). The underlying sediments belong to the *Hemidiscus triangularus - Fragilariopsis aurica* Zone (Fig. 4.2). The FO of *Thalassiosira oestrupii* is at 129.27 mbsf between samples 14H-6, 49-50 cm and 15H-1, 45-46 cm, which is in the lower to middle portion of Chron C3r (5.23 - 5.89 Ma) and coincides with the FO in Hole 704B. Baldauf and Barron (1991) derived at Sites 737A and 745B an age of 5.6 Ma for the FOD of *T. oestrupii*, which is in accordance with our results. For the section following below around ca. 137 up to 130 mbsf no magnetostratigraphical data are available (Shipboard Scientific Party, 1988c).

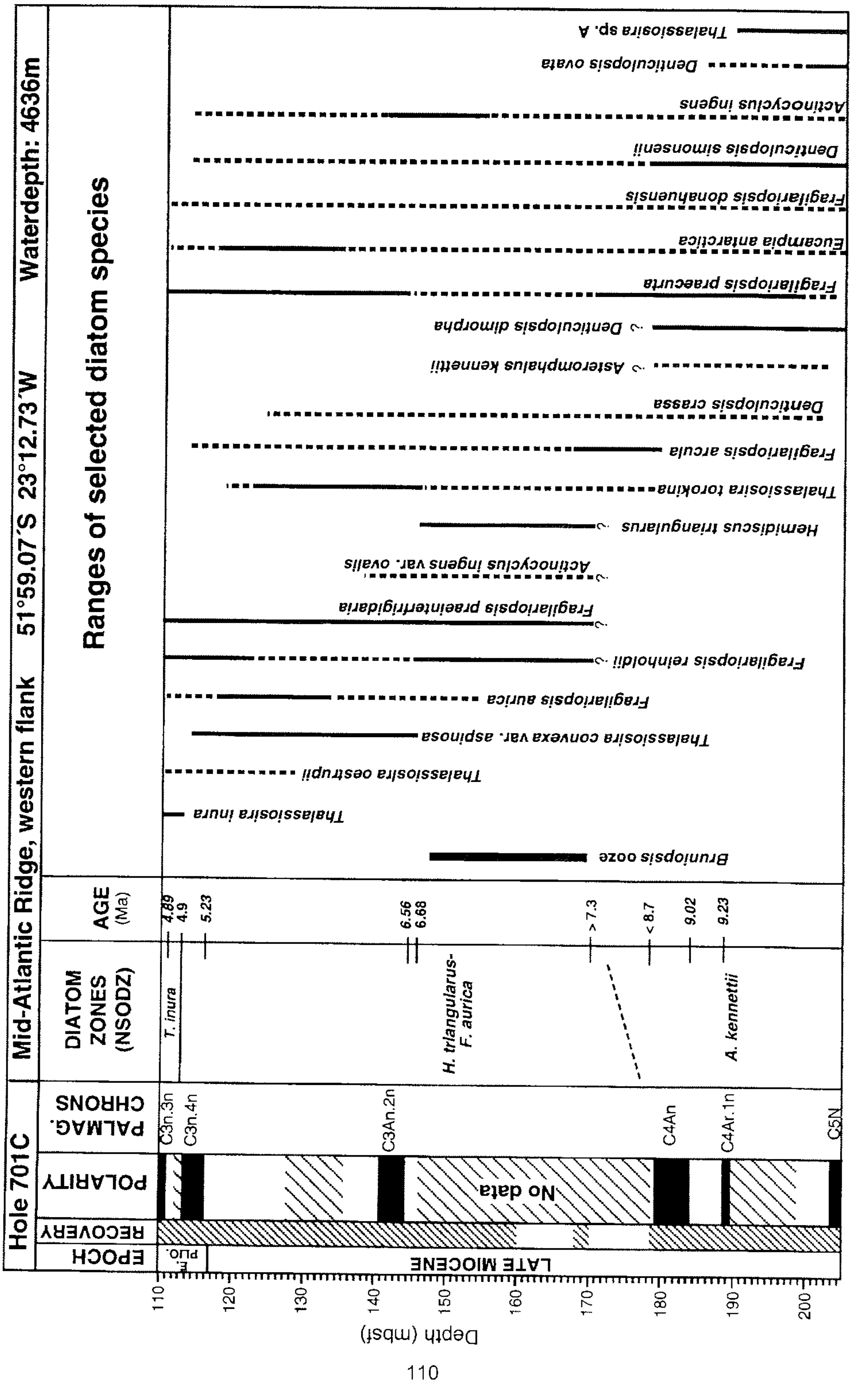
Hole 701C
Mid-Atlantic Ridge, western flank
51°59.07'S 23°12.73'W
Waterdepth: 4636m
EPOCH
RECOVERY
POLARITY
PALMAG. CHRONS
DIATOM ZONES (NSODZ)
AGE (Ma)
Ranges of selected diatom species
Plio. E
LATE MIOCENE
No data
C3n.3n
C3n.4n
C3An.2n
C4An
C4Ar.1n
C5N
T. inura
H. triangularus-F. aurica
A. kennettii
4.89
4.9
5.23
6.56
6.68
> 7.3
< 8.7
9.02
9.23
Thalassiosira sp. A
Denticulopsis ovata
Actinocyclus ingens
Denticulopsis simonsenii
Fragilariopsis donahuensis
Eucampia antarctica
Fragilariopsis praecurta
? Denticulopsis dimorpha
? Asteromphalus kennettii
Denticulopsis crassa
Fragilariopsis arcula
Thalassiosira torokina
? Hemidiscus triangularus
? Actinocyclus ingens var. ovalis
? Fragilariopsis praeinterfrigidaria
? Fragilariopsis reinholdii
Fragilariopsis aurica
Thalassiosira convexa var. aspinosa
Thalassiosira oestrupii
Thalassiosira inura
Brunopsis ooze
110
120
130
140
150
160
170
180
190
200
Depth (mbsf)

The next biostratigraphical datum point is the FO of *T. convexa* var. *aspinosa* (ca. 6.68 Ma) at 145.9 mbsf between samples 16H-5, 10-11 cm and 16H-5, 110-111 cm. This identifies the normal polarised interval around 143 mbsf as Chron C3An.2n. Accordingly it can be supposed that the missing Chron C3An.1n would be found in the magnetostratigraphical data gap above (Fig. 4.2). Between 170.1 and 145.90 mbsf a ca. 25 m thick *Bruniopsis*-ooze is located. Within this section the FO of the rare species *Fragilariopsis aurica* is found between samples 17H-4, 59-60 cm and 17H-5, 110-111 cm at 154.9 mbsf, which refers to an age somewhere in the range of 7.3 to 6.7 Ma. The *Bruniopsis*-ooze is interrupted by a recovery gap spanning from 160.20 to 168.10 mbsf. The missing time period can not be determined reliably due to the lack of nearby age control points, but, provided that sedimentation rates are linear, a gap of less than 0.1 Ma is suggests. Below the *Bruniopsis*-ooze a second recovery gap from 170.15 to 178.10 mbsf and spans the period from at least 7.3 to approximately 8.7 Ma. Sediments containing the lower portion of the *Hemidiscus triangularus* - *Fragilariopsis aurica* Zone and the complete *F. reinholdii*- and *Actinocyclus ingens* var. *ovalis* Zones are lacking due to the recovering gap.

The normal polarised intervals around 183 and 190 mbsf are interpreted as Chrons C4n and C4Ar.1n as indicated by the occurrence of *Asteromphalus kennettii* in absence of *Actinocyclus ingens* var. *ovalis*. This sediment section is in assignment to the *Asteromphalus kennettii* Zone. The co-occurrence of *A. kennettii* and *F. praecurta* reveals that underlying sediments up to at least 205 mbsf still belong to the *A. kennettii* Zone. This suggests that the long normal polarised interval at 204.01 mbsf (top) is Chron C5n (Fig. 4.2).

Age control points and the corresponding age-depth diagram are shown in Table 4.1 and in Figure 4.3. High sedimentation rates between 6.7 and 7.3 Ma can be deduced fromt the *Bruniopsis*-ooze occurrence. Remarkable in the Late Miocene section at Site 701C is the continuous occurrence of *Eucampia antarctica* reaching abundances close to the present-day range in this geographical area (Zielinski and Gersonde, 1997).

Figure 4.2 (left): Stratigraphic ranges of selected diatom species in the Late Miocene section of Hole 701C. Dotted lines indicate scattered and trace occurrences of diatom taxa. The diatom zonal assignment tied to the geomagnetic data of Clement and Hailwood (1991) is based on the Northern Southern Ocean Diatom Zonation (NSODZ)(Censarek and Gersonde, in press). Italic style ages are derived by magnetostratigraphy, normal style ages present diatom ages points.

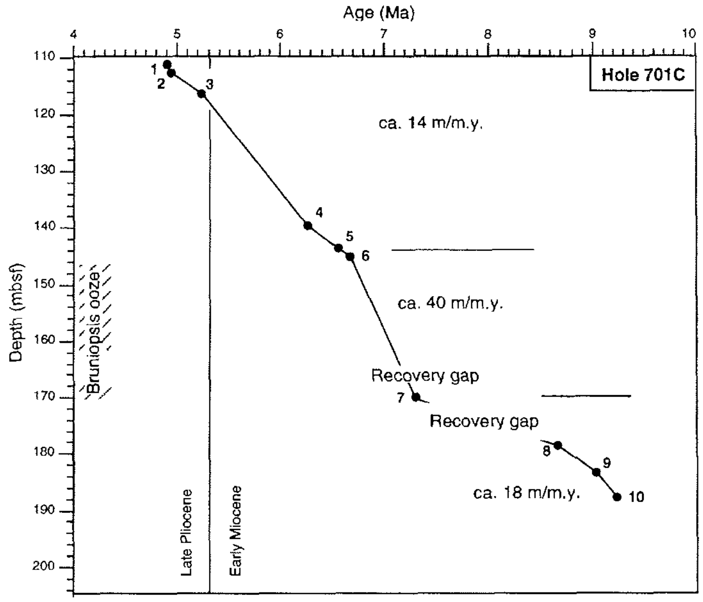

Figure 4.3: Age-depth diagram for the Late Miocene section of Hole 701C and calculated average sedimentation rates. For definition of stratigraphic datum points see Table 4.1.

Table 4.1: Definition of stratigraphic datum points in the Late Miocene section of Hole 701C used to construct the age-depth diagram in Figure 4.3.

Datum points	Depth (mbsf)	Age (Ma)	Definition
1	111.2	4.89	Base C3n.3n
2	113.3	4.9	FOD *T. inura*
3	116.1	5.23	Base C3n.4n
4	140.27	6.27	Top C3An.2n
5	144.2	6.56	Base C3An.2n
6	145.9	6.68	FOD *T.* covexa var. *aspinosa*
	160.20-168.10	Recovery gap	
7	170.14	7.3	FOD *H. triangularus*
	170.15-178.10	Recovery gap	
8	179.07	8.67	Top C4An
9	183.98	9.02	Base C4An
10	188.24	9.23	Top C4Ar.1n

Thalassionema sp. A occurred during Chron C3r (Fig. 4.2) in a short period of 300 k.y. and it might possibly be used in future to refine Late Miocene diatom zonations. This species has a bone like outline and further taxonomical and biogeographical studies are needed to evaluate its significance as stratigraphic marker. High abundances of the *Stephanopyxis* species occurred close to the Miocene/Pliocene boundary. This finding is in accordance with results from Leg 119 Site 737, which is located also close to the Polar Front within the Antarctic Zone (Baldauf and Barron, 1991).

Hole 704B

The uppermost portion of studied sediments belongs to the *T. inura* Zone. *Thalassiosira inura* occurs first between samples 24X-6, 53-54 cm and 24X-6, 129-130 cm at 222.11 mbsf, which corresponds to Chron C3r (Fig. 4.4). However, the FO of *T. inura* is generally observed within Chron C3n.3r at ca. 4.9 Ma (Censarek and Gersonde, 2002). To solve this discrepancy a short-term hiatus at around 222 mbsf omitting C3n.4n might be assumed. A comparable situation is documented at Site 1092 (Censarek and Gersonde, 2002). However, the normal polarised interval at 219 mbsf would belong consequently to Chron C3n.3n, which would lead to an unrealistic sedimentation rate of ca. 48 m/My during the Gilbert Chron (Fig. 4.4). The Gilbert Chron is well documented at the base of Hole 704A as well as at the top of Hole 704B (Hailwood and Clement, 1991b). Comparison with Site 1092 abundance fluctuations of *F. praecurta*, *F. fossilis*, *T. oestrupii* as well as comparison of the diatom sedimentation rate provide no evidences for a hiatus spanning the upper Messinian sediments. Therefore, we agree with the magnetostratigraphic interpretation of Hailwood and Clement (1991b). The FOD of *T. inura* is only well documented at the Maud Rise sediments (Censarek and Gersonde, 2002) and at Site 701 (this paper). At other sites close to the southern Polar Front boundary the FO of *T. inura* is generally found somewhere in the middle portion of the Gilbert Chron (Censarek and Gersonde, 2002). We assume that *T. inura* occurs somewhat earlier (ca. 5.2 Ma) in the northern part of the Polar Front Zone. Unfortunately no other corresponding sediment sections from this hydrographical region are available to prove this assumption. More investigations are needed to improve and clarify the diatom biostratigraphy at the Miocene/Pliocene boundary. Between samples 27X-6, 1-2 cm and 27X-6, 83-84 cm at 250.12 mbsf the FO of *Hemidiscus triangularus* (7.3 Ma) indicates the base of the *Hemidiscus triangularus - Fragilariopsis aurica* Zone (Fig. 4.4).

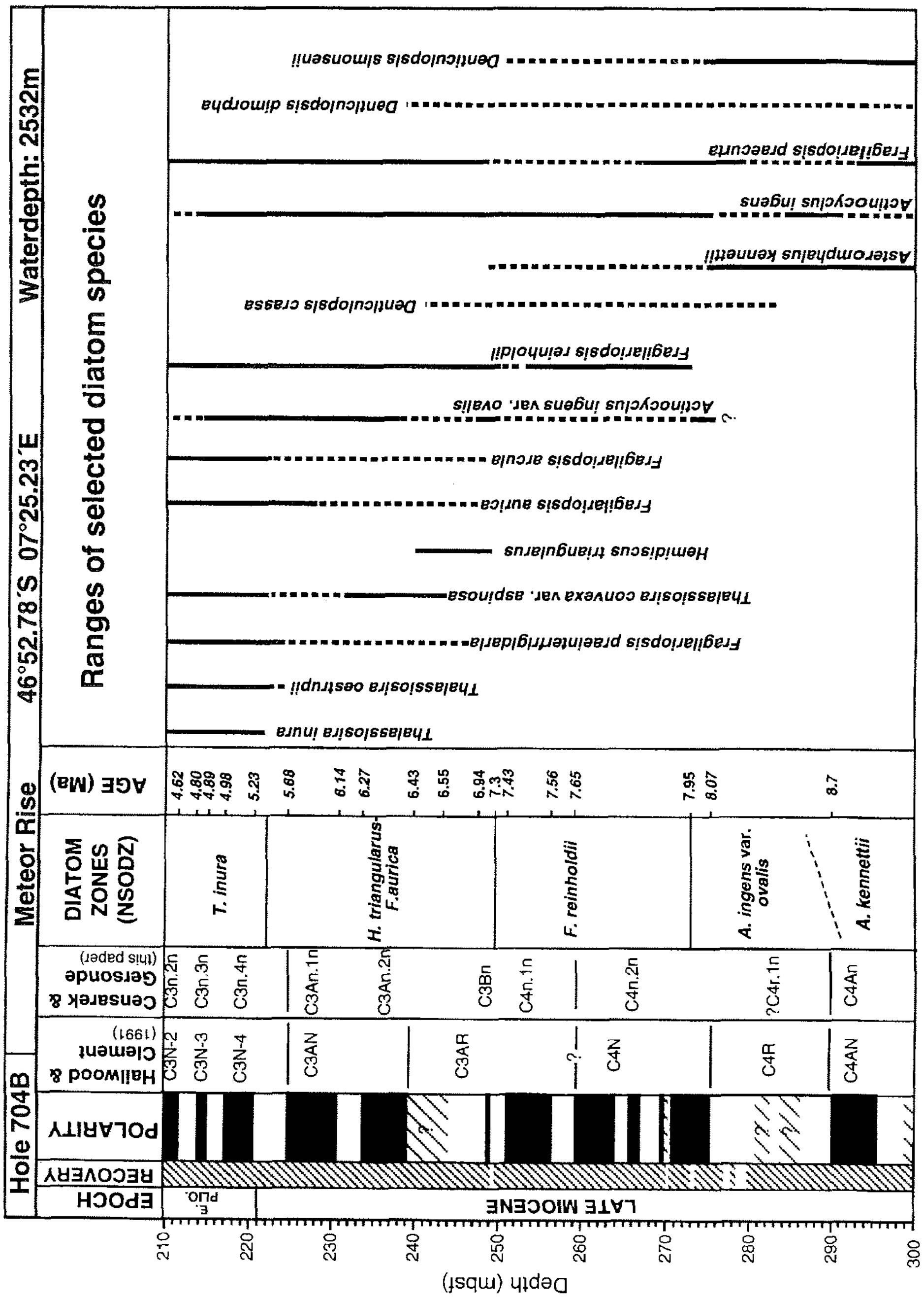

Figure 4.4: Stratigraphic ranges of selected diatom species in the Late Miocene section of Hole 704B. Dotted lines indicate scattered and trace occurrences of diatom taxa. The diatom zonal assignment based on the Northern Southern Ocean Diatom Zonation (NSODZ)(Censarek and Gersonde, 2002) is tied to the geomagnetic data of Hailwood and Clement (1991b). Italic style ages are magnetostratigraphic age points, normal style ages present diatom ages points.

This zone comprises Chrons C3Bn up to C3An.1n. As indicated by the FO´s of *F. aurica* and *H. triangularus* we identified Chron C3Bn, which differs from the interpretation of Hailwood and Clement (1991b) who interpreted this interval as a portion of Chron C3Ar (Fig. 4.4). The FO of *Thalassiosira oestrupii* (ca. 5.8 Ma), occurring in the upper portion of the *H. triangularus* - *F. aurica* Zone, is found between samples 25X-1, 93 cm and 25X-2, 18-19 cm and corresponds to Chron C3r (Fig. 4.4). This is comparable to findings in Hole 701C (this paper) and Leg 119 Site 745 (Baldauf and Barron, 1991). The FO of *F. reinholdii* is found between samples 30X-2, 71-72cm and 30X-3, 84-85cm (273.7 mbsf), marks the lower boundary of the *F. reinholdii*-Zone and suggests an age of ca. 7.95 Ma. This led us to term the normal polarised interval at around 273 mbsf as the lowermost portion of Chron C4n.2n (Fig. 4.4). Consequently, the normal polarised interval above (around 255 mbsf) is Chron C4n.1n. Low inclination values between 265 and 272 mbsf (Hailwood and Clement, 1991b, fig. 12) indicate that this portion might also belong to Chron C4n.2n. The lower boundary of the underlying *A. ingens* var. *ovalis* Zone is defined by the FOD of the this species, which cannot be determined reliably due to rare occurrences. This finding differs from Site 1092 where this boundary is clearly found (Censarek and Gersonde, 2002). However, the common occurrence of *A. kennettii* up to ca. 277 mbsf (upper portion of Chron C4r) identifies the normal polarised Chron around 293 mbsf as C4An (Fig. 4.4) according to Hailwood and Clement (1991b). Age control points and the corresponding age-depth diagram are shown in Table 4.2 and at Figure 4.5.

Stratigraphic results of both holes verify known FOD´s and reveal possible diachronous occurrences of *T. inura*. Most of the stratigraphically useful FOD´s of Hole 704B (*F. reinholdii*, *T. convexa* var. *aspinosa*, *H. triangularus* and *F. aurica*) verify the interpretation at Site 1092 (Censarek and Gersonde, 2002) and are also comparable to occurrences documented in the data report of Ciesielski (1991). All new and revised estimates of first and last occurrence datums at Sites 701 and 704 are listed in Table 4.3. Our magnetostratigraphic interpretation of Hole 701C is in agreement with those published by Clement and Hailwood (1991). We also confirm most of the magnetostratigraphic interpretations of Hole 704B by Hailwood and Clement (1991b), but suggest a slightly older age (ca. 0.3-0.5 m.y.) for the section between ca. 240 and 260 mbsf. The FOD´s of *Thalassiosira convexa* var. *aspinosa* and *Hemidiscus triangularus* revised the interpretation of Hailwood and Clement (1991b) from Chron C3Ar to Chron C3Bn and C4n.1n.

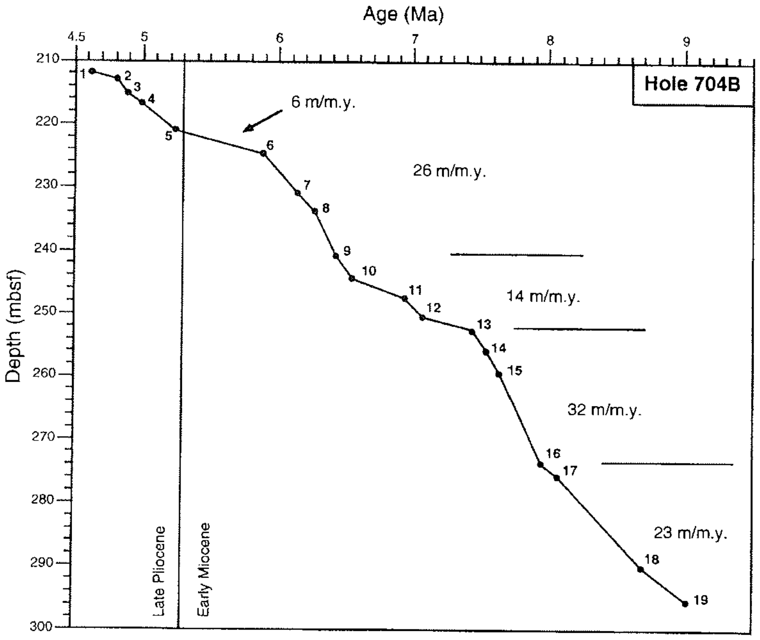

Figure 4.5: Age-depth diagram for the Late Miocene section of Hole 704B and calculated average sedimentation rates. For definition of stratigraphic datum points see Table 4.2

Table 4.2: Definition of stratigraphic datum points in the Late Miocene section of Hole 704B used to construct the age-depth diagram in Figure 4.5

atum points	Depth (mbsf)	Age (Ma)	Definition
1	212.00	4.62	Base C3n.2n
2	213.90	4.8	Top C3n.3n
3	215.30	4.89	Base C3n.3n
4	216.80	4.98	Top C3n.4n
5	220.80	5.23	Base C3n.4n
6	224.76	5.88	Top C3An.1n
7	231.04	6.14	Base C3An.1n
8	233.84	6.27	Top C3An.2n
9	240.88	6.43	LOD *H. triangularus*
10	244.52	6.55	FOD *T. convexa* var. *aspinosa*
11	247.71	6.94	FOD *F. aurica*
12	250.12	7.3	FOD *H. triangularus*
13	251.25	7.43	Top C4n1.n
14	256.75	7.56	Base C4n1.n
15	259.50	7.65	Top C4n.2n
16	273.73	7.95	FOD *F. reinholdii*
17	275.85	8.07	Base C4n.2n
18	290.07	8.7	Top C4An
19	295.60	9.02	Base C4An

Table 4.3: List of selected Late Miocene diatom events at Sites 701 and 704. The ages are interpolated by linear relationship from the age-depth plots. Additionally, diatom occurrence datums from previous studies at Sites 689, 1088 and 1088 are listed (Censarek and Gersonde, 2002). Italic style: low reliability. AZ: Antarctic Zone; SPFZ: Southern Polar Front Zone; NPFZ: Northern Polar Front Zone; SAZ: Subantarctic Zone.

Datums	**Estimated diatom ages (Ma)**					
	AZ		**SPFZ**	**NPFZ**		**SAZ**
	689B	**690B**	**701**	**704**	**1092**	**1988**
FOD *T. inura*	4.89	-	**5.00**	***5.54***	-	4.17
FOD *F. praeinterfigidaria*	5.09	-	**6.70**	**6.84**	-	-
FOD *T. oestrupii*	-	-	***5.80***	***5.84***	-	-
LOD *H. triangularus*	5.13	-	**6.60**	**6.43**	6.43	-
FOD *Thal. convexa* var. *aspinosa*	6.58	-	**6.66**	**6.57**	6.54	-
FOD *H. triangularus*	7.30	-	-	**7.29**	7.30	-
LOD *D. crassa*	*7.39*	*7.76*	***5.62***	***6.43***	7.51	-
FOD *F. reinholdii*	-	-	***7.3-8.5***	**7.96**	7.96	*8.23*
FOD *F. arcula*	8.49	8.41	***8.78***	***7.06***	*7.40*	-
FOD *A. ingens* var. *ovalis*	*8.49*	-	***7.3-8.5***	***8.10***	8.70	-
LOD *D. ovata*	*4.93*	-	**6.95**	***8.24***	10.60	*10.50*
FOD *F. aurica*	*9.50*	*10.30*	***6.91***	***6.94***	*6.94*	-

4.4.2 Diatom abundances and relative paleotemperatures

Abundance fluctuations of diatom taxa, which are used to estimate the relative paleotemperature, are presented in Figures 4.6 and 4.7. At Site 701 warm-water indicating species *Fragilariopsis reinholdii*, *Actinocyclus ingens* and *Azpeitia tabularis* characterise the assemblage between 7.3 and 6.7 Ma (Fig. 4.6). *Thalassionema nitzschiodies* and its varieties, which are also warm-water indicating diatoms, occurred at ca. 6.7 Ma and dominated the assemblage with abundances of up to more than 90%. At 5.7 Ma the warm-water species *Thalassiosira oestrupii* is also continuously present. However, higher abundances of *Fragilariopsis praecurta* document a cooling of cold surface waters between 6.7 and 5.7 Ma. Cold-water indicating *Eucampia antarctica* is frequently present at Site 701 with an abundance maximum at 5.5 Ma (Fig. 4.6). This maximum possibly correlates with a 2% abundance peak documented at Site 704, while this species is mostly absent from the rest of the Miocene core section (see datasheet).

The warm-water indicating diatom *Hemidiscus karstenii* could not be found at Site 701, whereas this species dominated the assemblage at Site 704 between ca. 9 and 8.1 Ma (Figs. 4.6, 4.7). The also warm-water indicating diatom *Actinocyclus ingens* occurred at Site 704 between 8.1 and 7.4 Ma with abundances of up to 80% and replaced *H. karstenii* as the dominant species. Higher abundances of *F. reinholdii* between 7.3 and 6.5 Ma and abundances of *Thalas-*

sionema nitzschioides up to 70% between 6.3 and 5.4 Ma suggest a warm-water influence (Fig. 4.7). *Thalassiosira oestrupii* occurred between 5.3 Ma and 4.5 Ma with abundances up to 6%. The cold-water indicating species *D. dimorpha* increased between ca. 9 and 7.3 Ma, but it is replaced by the dominant cold-water species *Fragilariopsis praecurta*, *F. arcula* and *F. aurica* at around 7 Ma (Fig. 4.7).

Relative low temperatures are estimated at Site 701 for the lower portion of the investigated Tortonian sediments (Fig. 4.8). The low amount of warm-water species combined with continuous presence of the cold-water taxa *D. dimorpha*, *F. donauhensis* and *F. praecurta* indicate cold surface water (Fig. 4.6). Early Messinian RPTs at Site 701 indicate even climatic conditions, which is documented mainly by the increased occurrence of warm-water taxa *T. nitzschioides* spp., *A. tabularis*, *A. ingens*, *A. ingens* var. *ovalis* and *F. reinholdii* (Fig. 4.6). Additionally, warm-water species *H. triangularus* occurred between ca. 7.3 and 6.5 Ma with mean abundances of 15%. A cooling event around 6.4 Ma is calculated from the abrupt extinction of *H. triangularus* in combination with an abundance peak of the cold-water taxa *F. praecurta*. Yet other cooling events are also documented around 5.8 and 5.5 Ma (Fig. 4.8). These estimates can be concluded from short-term increased abundances of cold-water species *F. aurica* and *F. praecurta* (Fig. 4.6)

Site 704 RPTs indicate generally warmer surface water conditions compared to Site 701. Distinct cooling events are documented at 8.5, 7.9, 7.6 Ma during the Tortonian stage and at 6.4 and 5.8 Ma during the Messinian. The latter coincides with cold events documented at Site 701 (Fig. 4.8). Calculation of the Tortonian cooling events (8.5, 7.9 and 7.6 Ma) resulted mainly from high abundances of *D. dimorpha* (Fig. 4.7). Starting at the uppermost Messinian, a general cooling is documented at Site 704. The occurrence of cold-water masses as indicated by RPTs is inferred from the strongly increased abundance values of the cold-water species *F. praecurta*. However, this latest Miocene/earliest Pliocene cooling is in contrast to RPT estimates from Site 701, where continuous stable temperatures are calculated (Fig. 4.8).

Late Miocene RPT curves calculated at Sites 689, 1088 and 1092 (Censarek and Gersonde, subm. b) are considered to reveal the latitudinal development of Southern Ocean water masses. Paleotemperatures at Site 689 indicate a temperature decrease between 9.5 and 8.6 Ma, which is not documented at any other site. However, the cooling started close to the Miocene/Pliocene boundary and is documented at Sites 689, 704 and 1092.

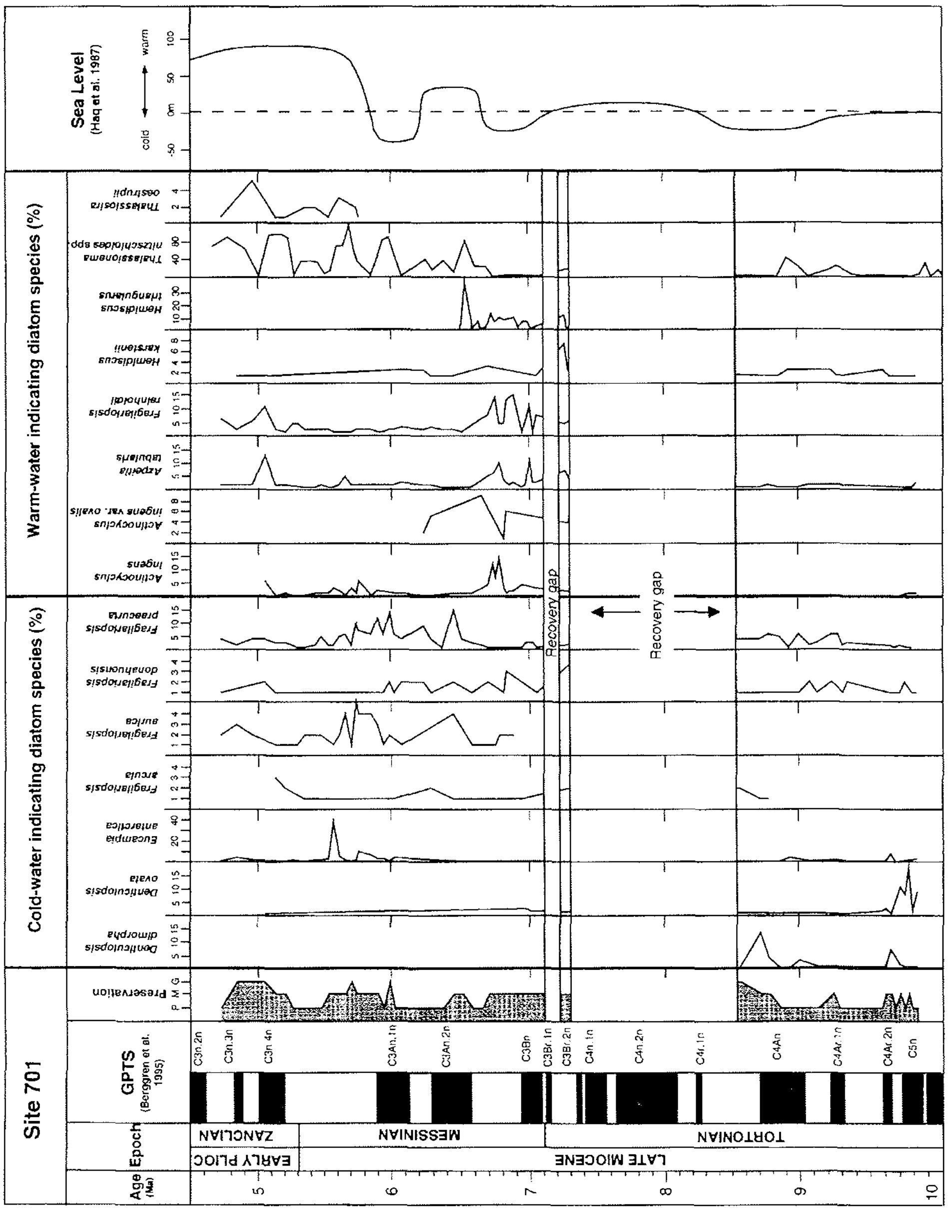

Figure 4.6: Late Miocene diatom abundance fluctuations of warm- and cold-water indicating species at Site 701 are presented. Diatom preservation (P: poor, M: moderate, G: good) refers to the degree of opal dissolution which have to be considered interpreting diatom data. The sea level curve (Haq et al., 1987) tied to the Geomagnetic Polarity Time Scale (GPTS) of Berggren et al. (1995) is presented

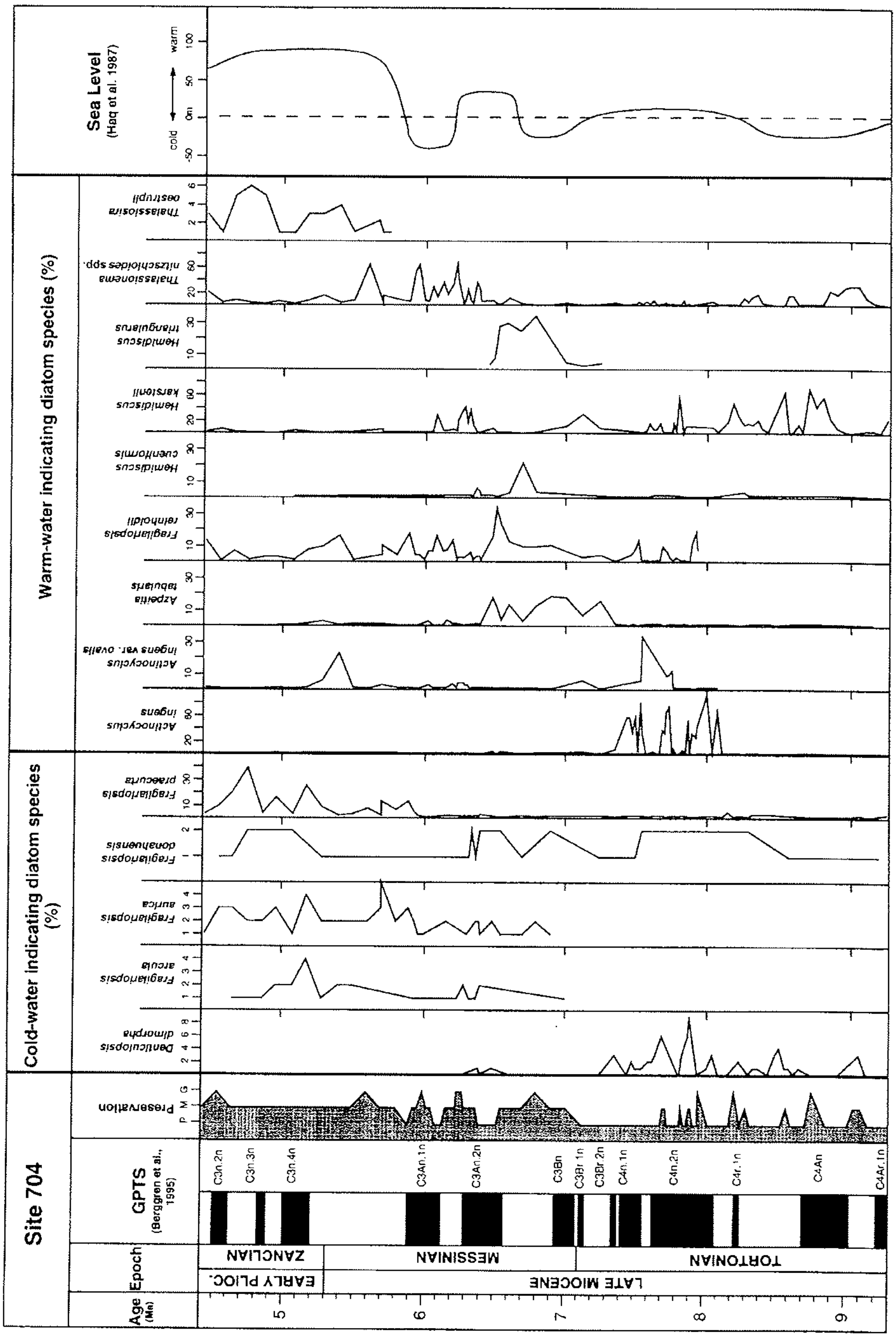

Figure 4.7: Late Miocene diatom abundance fluctuations of warm- and cold-water indicating species at Site 704 are presented. Diatom preservation (P: poor, M: moderate, G: good) indicate the degree of opal dissolution which have to be considered interpreting diatom data. The sea level curve (Haq et al., 1987) tied to the Geomagnetic Polarity Time Scale (GPTS) of Berggren et al. (1995) is presented.

RPTs estimated at nearby Sites 704 and 1092 reflect in general a comparable thermal water mass evolution (Fig. 4.8). Major events of the development of the Mediterranean Sea are compared to the climatic evolution of the Southern Ocean (Fig. 4.8). At a time when the Mediterranean basin was isolated from the Atlantic Ocean diatom concentrations at Sites 704 and 1092 reached highest values. During the period of evaporite deposition in the Mediterranean basin diatom concentrations at Sites 704 and 1092 stayed on this high level, showing minor flucuations, whereas at Site 701 a period of low values is documented (5.6 to 5.3 Ma). Paleotemperatures during this period occasionally indicate temporarily cold surface water conditions in the Southern Ocean. The onset of climate deterioration at Sites 701 and 704 can be assumed between 6.1 and 5.9 Ma, which temporally coincides with the progressive isolation of the Mediterranean basin (Fig. 4.8).

4.4.3 Thermal evidences from latitudinal abundance comparisons of selected diatom species

Abundance fluctuations of a cold-water indicating diatom (*Fragilariopsis praecurta*) three warm-water indicating species (*Hemidiscus triangularus*, *Azpeitia tabularis* and *Thalassiosira oestrupii*) and a warm-water indicating *Hemidiscus*-group consisting of *H. karstenii*, *H. cuneiformis* and *H.* sp. A (Gersonde and Burckle, 1990) reflect in detail the thermal development at Sites 701 and 704 (Fig. 4.9). Additionally abundance fluctuations of those species at Sites 689, 1088 and 1092 are considered.

A long-range warm surface water period is deduced from high abundances of *A. tabularis* and of the *Hemidiscus*-group between 7.3 and 6.6 Ma (Fig. 4.9). A cold period indicated primarily by increased abundances of *F. praecurta* (Site 701) and low abundances of *A. tabularis* and the *Hemidiscus*-group lasted until 5.6 Ma. Between 5.3 to ca. 4.5 Ma *F. praecurta* became common in the northern area of the Southern Ocean (Site 704). During the same period the warm-water species *T. oestrupii* occurred in this area. Increased abundances of *A. tabularis* at Sites 689 and 701 indicates a relative warming in the southern investigated area. Short-term cold periods are determined between 7.5 and 7.3, 8.9 and 6.8, 6.4 and 6.3, 6.2 and 6.1, 6 and 5.7, 5.1 and 5.15, 4.85 and 4.75 Ma (Fig. 4.9).

The cold-water indicating *F. praecurta* is closely related to the recent *F. curta*, probably being its phylogenetic precursor (Gersonde, 1991). *Fragilariopsis curta* is used for the reconstruction of sea-ice extension in the Southern Ocean (Gersonde and Zielinski, 2000). A similar geographical abundance distribution of both species (Zielinski and Gersonde, 1997) and the continuous succession from *F. praecurta* to *F. curta*, somewhere between 3.5 and 4.2 Ma as documented at Leg 120 Holes 747B, 748B (Harwood and Maruyama, 1992), suggest that *F. praecurta* might had also an affinity to sea-ice. Therefore an increase in seasonal sea-ice coverage might be assumed between 6.6 and 5.4 Ma, documented at Site 701 (Fig. 4.9). Between 6.4 and 5.4 Ma the sediments at Maud Rise Site 689 are not preserved. Occurrences up to 30% of *F. praecurta* in the section younger than 5.4 Ma might refer to a stronger sea-ice occurrence. However, high abundances of this species at Sites 704 and 1092 during the Early Pliocene would indicate an unusual northward expansion of sea-ice.

A comparison of Miocene abundances of the extant species *A. tabularis* and *T. oestrupii* with their present-day abundance ranges (Zielinski and Gersonde, 1997) reveals the difference to recent surface water temperatures (Fig. 4.9).

Between 7.3 and ca. 6.6 Ma abundances of *A. tabularis* indicate warmer than present surface water temperatures at all sites. During the middle to late Messinian cold period similar or lower abundances than recent are documented (Fig. 4.9). In the earliest Pliocene at Sites 689 and 701 abundances of *A. tabularis* partly exceeded the present-day range of values, indicating warmer than recent temperatures. *T. oestrupii* occurred at around 5.6 Ma with average higher abundances than present-day at Site 701 and similar values at Sites 704 and 1092. Only in some periods of the early Pliocene abundances of *T. oestrupii* exceeded the present value range.

Mediterranean climatic development is indicated by the benthic isotope record of the Salé Briqueterie drill core (Hodell et al., 1994), recording ongoing cooling and a long-term cold period between 6.6 and ca. 5.5 Ma. It is subsequently followed by a warming period up to ca. 5.25 Ma (Fig. 4.9). A similar thermal development is suggested by the diatom record for the Southern Ocean.

Figure 4.8 (right): Relative paleotemperatures at Sites 701 and 704 and at Sites 689, 1088 and 1092 (Censarek and Gersonde, subm. b) reflect the relative thermal development of the Southern Ocean surface waters. Diatom concentrations supplement thermal interpretations. Grey fields mark the recent range of diatom abundance (after Zielinski and Gersonde, 1997). For comparison with the Mediterranean Sea climate development important events of the Messinian Salinity Crises are compiled (Hodell et al., 1994 and 2001; Krijgsman et al., 1999 and 2001).

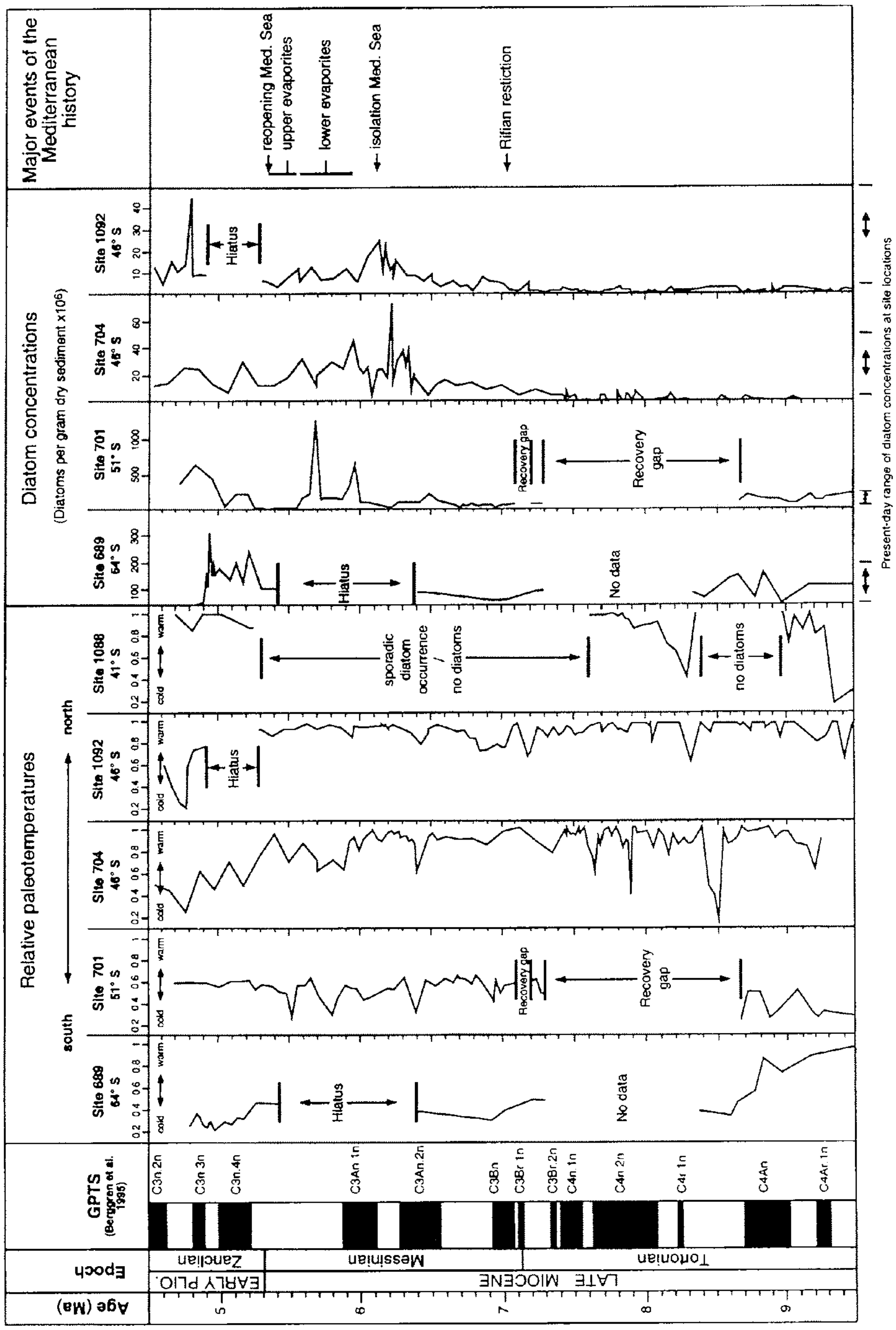
Major events of the Mediterranean history
reopening Med. Sea
upper evaporites
lower evaporites
isolation Med. Sea
Rifian restiction
Diatom concentrations
(Diatoms per gram dry sediment x10^6)
Site 1092 46° S
Site 704 46° S
Site 701 51° S
Site 689 64° S
Hiatus
Recovery gap
No data
Present-day range of diatom concentrations at site locations
Relative paleotemperatures
south
north
Site 1088 41° S
cold
warm
sporadic diatom occurrence / no diatoms
no diatoms
GPTS (Berggren et al. 1995)
C3n.2n
C3n.3n
C3n.4n
C3An.1n
C3An.2n
C3Bn
C3Br.1n
C3Br.2n
C4n.1n
C4n.2n
C4r.1n
C4An
C4Ar.1n
Epoch
Zanclian
Messinian
Tortonian
EARLY PLIO.
LATE MIOCENE
Age (Ma)
5
6
7
8
9

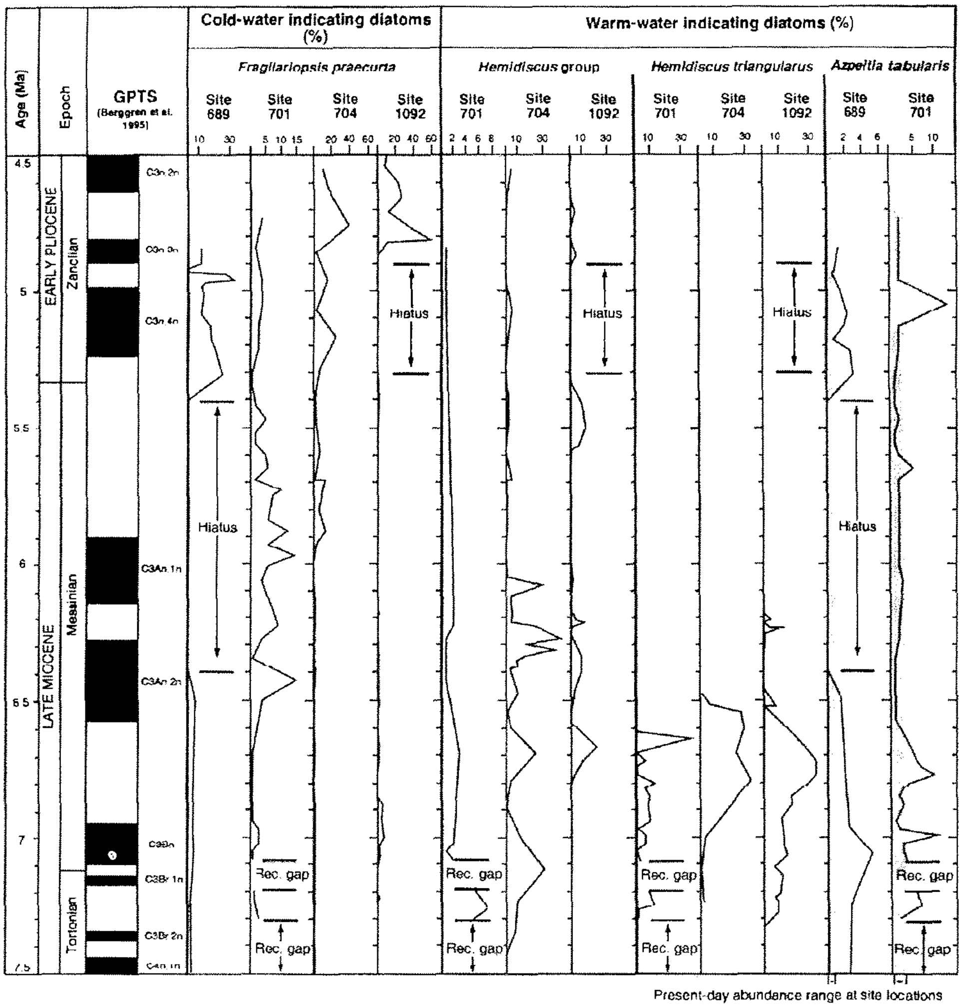

Figure 4.9 (both sides): Latitudinal comparison of abundances of selected diatom species indicating thermal conditions and deduced long-term and short-term climatic changes in the Southern Ocean. Abundance ranges of still recently occuring diatom species *A. tabularis* and *T. oestrupii* at site

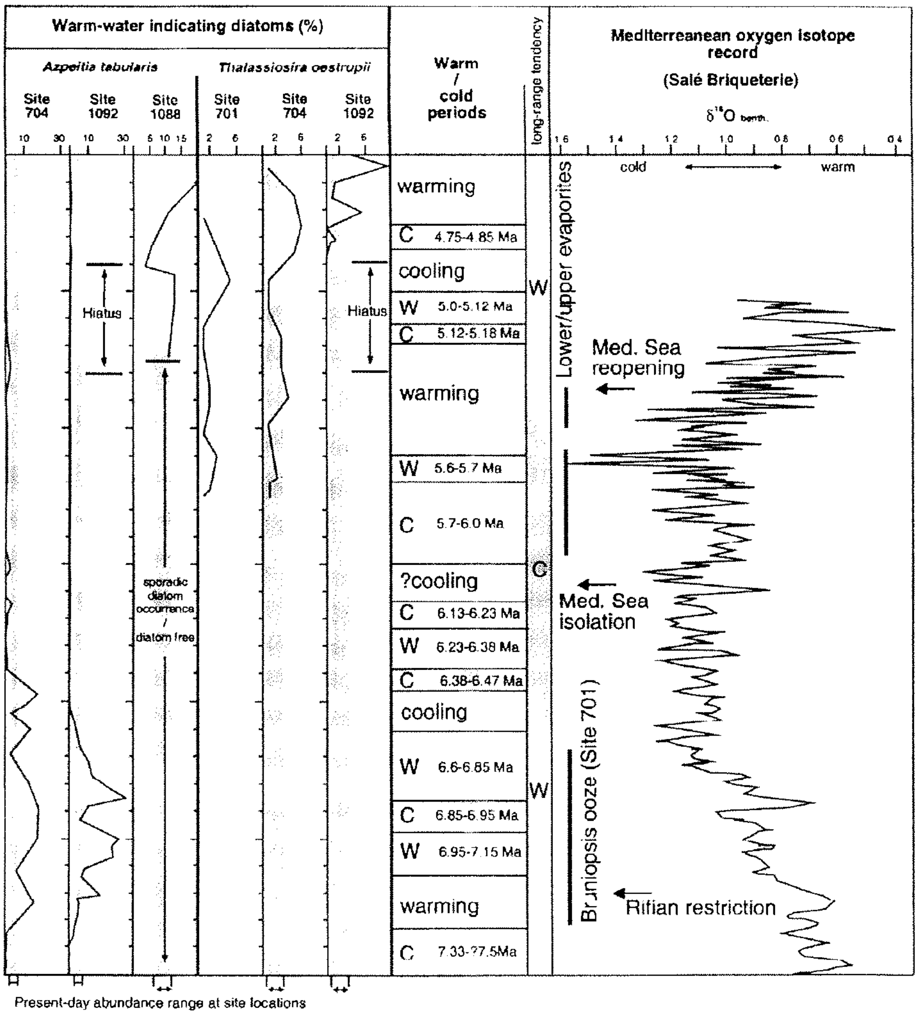

locations are marked as grey fields (after Zielinski and Gersonde, 1997). The Mediterranean oxygen isotope record from the Salé Briqueterie, northwestern Morocco (Hodell et al., 1994), shows a comparable climate development as the one deduced from diatom abundances.

Furthermore, during the isolation period of the Mediterranean Sea F. praecurta occurred for the first time at Site 704 with abundances up to 10% indicating a general cooling of Southern Ocean water masses. The end of the lower evaporite deposition (ca. 5.6 Ma) in the Mediterranean basin is succeeded temporally by the onset of relative warm Southern Ocean water masses indicated by T. oestrupii occurrences combined with decreasing abundances of F. praecurta.

4.5 Discussion and conclusions

4.5.1 Biostratigraphic remarks

Miocene diatom assemblages of southern Polar Front Zone Site 701 differ remarkably from those of the northern Polar Front Zone (Sites 704 and 1092). Therefore, different diatom assemblages within a single hydrographic zone have to be considered during further revisions of Southern Ocean diatom zonations. More than two diatom zonations will obviously be needed to improve the Latest Miocene diatom biostratigraphies. Furthermore, differences in assemblage composition within the Polar Front Zone imply that diatom linkage to hydrographical front conditions should be refined, e.g. during the application of factor analysis. It becomes obvious that hydrographic fronts are usually not strong boundaries of oceanographic parameters as they are often seen and that frontal zones represent not uniform hydrographic conditions.

Slight discrepancies in diatom assemblages found between Site 704 and close-by Site 1092 can attribute to different preservation conditions. These discrepancies occur when lightly silicified species (e.g. *F. aurica*, *F. arcula*) are involved. Sedimentation rates and diatom concentrations at Site 1092 are twice as high compared to Site 704 (Censarek and Gersonde, 2002), which indicates differences in sedimentation processes and preservation conditions.

This is the first investigation estimating a reliable FOD for *T. oestrupii* in the Atlantic sector of the Southern Ocean. It is placed at around 5.8 Ma (lower portion of Chron C3r) at both sites, which is the earliest datum compared to other partly uncertain occurrences (see discussion in Censarek and Gersonde, 2002). The absence of *T. oestrupii* below the hiatus (68.46 mcd) at Site 1092 is not yet understood (Censarek and Gersonde, 2002). The hiatus at Site 1092 comprises possibly slightly more time than calculated (4.9 to 5.3 Ma).

The ca. 25 m *Bruniopsis*-ooze at Site 701 is important for paleoclimate interpretation (Fig. 4.3). This warm-water taxa, which is mostly found in fragments, occurred cosmopolitically during the Middle and Late Miocene (Schrader, 1973, 1974 and 1976). For the same time period a diatom-ooze consisting of *Ethmodiscus rex* is documented at South Atlantic Site 520 (Hsü et al., 1984), which made the Shipboard Scientific Party (1988c) speculate about a basin wide event throughout the South Atlantic. However, an ooze made of *Bruniopsis* sp. is only reported at Site 701. Below the Bruniopsis-ooze section a ca. 3 m thick sand/gravel unit is found, which might be explained as ice-rafted debris deposits (Shipboard Scientific Party, 1988c). Therefore, a cooling event might be assumed approximately between 8.7 and 7.3 Ma. Subsequently, an extraordinarily warm surface water mass would occur between ca. 7.3 and 6.68 Ma.

4.5.2 Miocene thermal history and evidences of hydrographic frontal displacements

The combination of a cold diatom assemblage at Site 689 between at least 9.5 and 8.6 Ma and a slight warming at the northern Sites 704, 1092 and 1088 (Fig. 4.8) implies a strengthening of thermal fronts. As cold conditions at the Maud Rise (Site 689) are established, a southernly located, weakly developed Paleo-Polar Front must be supposed (Fig. 4.10.A). The RPT calculations at Sites 689 and 701support the assumption that the temperatures between 8.6 and ca. 7.3 Ma were similar to the recent ones, which in turn indicates that the Paleo-Polar Front was located close to recent position (Fig. 4.10.B). Whereas lower than present diatom concentrations between 9.5 and 7.3 Ma at Sites 704, 1092 and a warm-water indicating diatom assemblage (Fig. 4.8) indicate a Paleo-Subantarctic Front location somewhat south of the present (Fig. 4.10.C). It is followed by a generally warmer than present period (7.3 to ca. 6.5 Ma) of surface water masses (Figs. 4.6, 4.7, 4.9 and 4.10.D). The *Bruniopsis*-ooze (Site 701) and abundances of *A. tabularis,* exceeding present day values at all sites (Fig. 4.9), support the interpretation of an extraordinarily warm period possibly coupled with a southward front displacement. Decreased abundances of warm-water indicating species between 6.85 and 6.95 Ma (Fig. 4.9) refer to a prominent cooling of surface waters, interrupting the warm period of the earliest Messinian. We speculate that frontal zones migrated for ca. 100 k.y. northward (Fig. 4.10.E). This cooling might be linked to the carbon isotope shift (lower portion of Chron C3Ar), which is proposed to be a result of an increased erosion from terrigenous and shelf sediments during sea level lowering caused by Antarctic glaciation (Berger and Vincent, 1986). The cold period (6.85 to 6.95 Ma) coincides with results of Hodell et al. (1994), who suggested an increase in

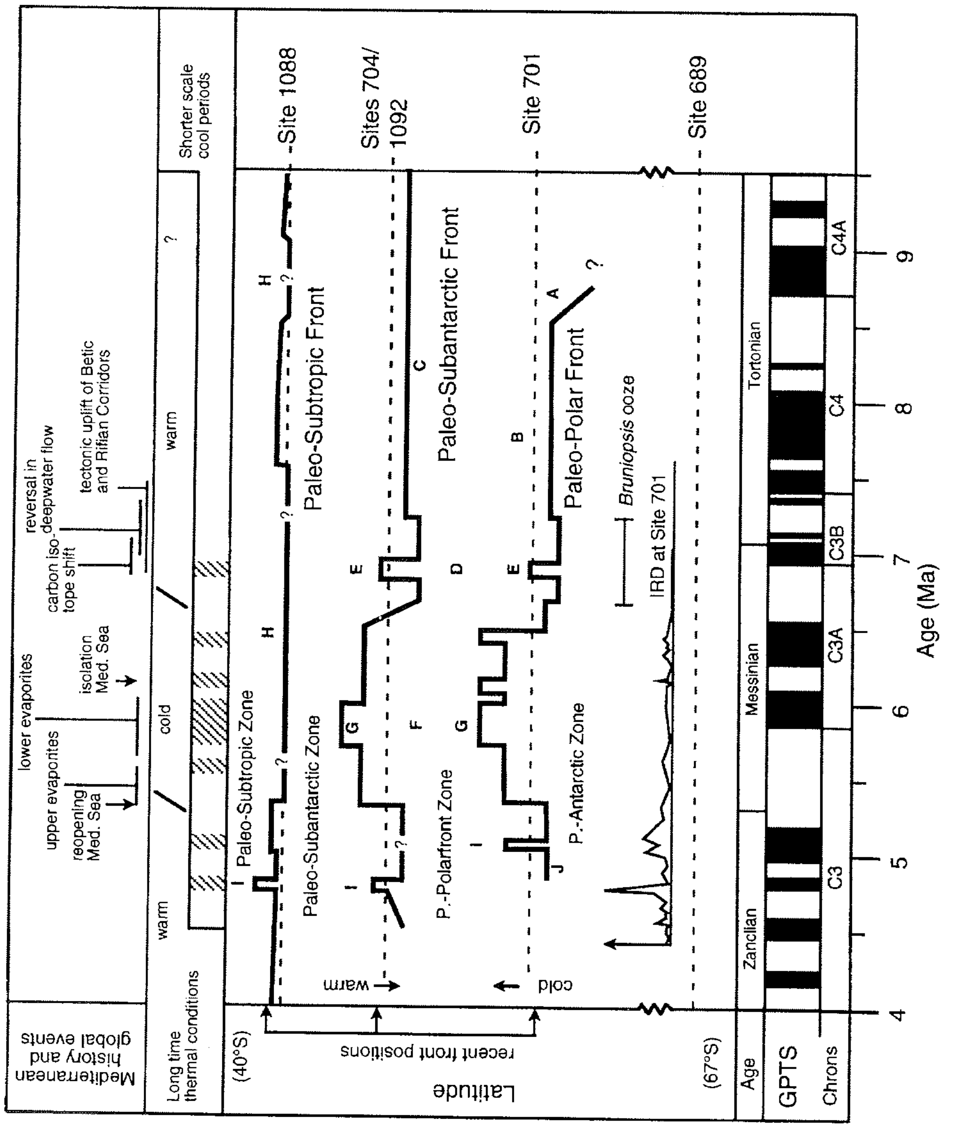

Figure 4.10: The sketch summarises estimated hydrographic front migragions relativ to site locations. Long time as well as short ranging thermal states as indicated by diatom abundance investigation are shown. Letters A to J mark the discussed interpretations. The geomagnetic polarity time scale (GTPS) is according to Berggren et al. (1995). Events of the Mediterranean history are compiled by Hodell et al. (1994 and 2001), Krijgsman et al. (1999 and 2001). The interpretation of a northward movement at Geomagnetic Chron C3Ar of hydrographic fronts up to north of the recent positions is supported by the first occrrence of IRD at Site 701 (Allen and Warnke, 1991).

continental ice volume at Site 846 (eastern Equatorial Pacific) based on oxygen isotope measurements. However, increasing oxygen isotope values during this period at North Atlantic Site 982 are interpreted to reflect a change in intermediate water temperatures and would therefore be unrelated to global ice volume (Hodell et al., 2001). A northward front system movement between ca. 6.5 and 5.3 Ma is indicated by high abundances of the cold-water species *F. praecurta* and low abundances of the warm-water species (Figs. 4.8, 4.9, 4.10.F).

Paleo-Polar Front Zone conditions might have occured on the Meteor Rise due to a northward movement of Paleo-Subantarctic Front. The interpretation of the strong northward movement beyond Site 701 location is supported by the onset of ice rafted debris (IRD) at Site 701 (Allen and Warnke, 1991; Warnke et al., 1992). First IRD occurred in the uppermost portion of Chron C3Ar corresponding to an age of ca. 6.6 Ma.

During the late Messinian cold period (6.5 to 5.3 Ma) three prominent colder intervals could be determined (Fig. 4.9), ranging from ca. 6.38 to 6.47 Ma, 6.13 to 6.23 Ma and 5.7 to 6.0 Ma, which might indicate a northward front migration (Fig. 4.10.G). Hodell et al. (2001) described 18 glacial/interglacial cycles during this period, inferred from oxygen isotope studies at Site 982 (North Atlantic). The occurrence of *T. oestupii*, decreasing *F. praecurta* abundances and RPTs (Fig. 4.8, 4.9) indicate a short-term warm interval between ca. 5.6 and 5.7 Ma, which is in good agreement with isotopic studies at Site 588 (Southwest Pacific) presented by Hodell et al. (1986). In the North Atlantic at Site 982 an interglacial event is also documented by low $\delta^{18}O$ values enclosed by two prominent glacial stages named TG 20 at 5.7 Ma and TG 12 at 5.51 Ma (Hodell et al., 2001). This was probably the warmest stage during the Messinian glaciation history. Undoubtedly Site 1088 was influenced between 9.3 and 4.4 Ma by Subantarctic Front-Zone-like conditions. The almost diatom free sections and a higher carbonate content up to 93% between 9 and 8.4 Ma and between 7.6 and ca. 5.3 Ma might reflect an influence of a warmer Subtropical Zone-like surface water mass (Shipboard Scientific Party, 1999a) (Fig. 4.10.H). However, this implies a southward frontal migration during general cold periods with northward-displaced surface waters.

Diatom abundance fluctuations suggest cooler conditions around 5.15 and 4.8 Ma (Fig. 4.8, 4.9). Further evidence for a northward displacement of water masses during these stages and particularly for the time around 4.8 Ma, came from decreasing RPTs and from high diatom concentrations (Figs. 4.8, 4.9, 4.10.I). The cold period at 4.8 Ma is also documented by a prominent ice-rafted detritus peak reported at Kerguelen Sites 745 and 746 (Ehrmann et al., 1991; Barron et al., 1991). Burckle et al. (1992) have evidence for a major glaciation in Chron C3n2r (ca. 4.7-4.8 Ma) of Hole 737A. They interpreted low percentages of opal combined with low (Ge/Si)-opal values as a glacial event at this site, which is located close to the present Polar Front. Yet, in general the Early Pliocene is characterized by decreasing diatom concentrations and occurrences of typical warm-water taxa. Higher than present-day abundances of *T. oestrupii* at Sites 701, 704 and 1092 (Fig. 4.9) refer to a strong warming and imply consequently a southward displacement of the Paleo-Polar Front Zone (Fig. 4.10.J). This warming period is also documented by the occurrence of calcareous nannofossil assemblages at Kerguelen Sites 744 and 737 (Wei and Thierstein, 1991). Bohaty and Harwood (1998) estimate a temperature difference of at least 4°C at Sites 748 and 751 for the southern Kerguelen Plateau surface waters at 4.3 and 4.5 Ma, providing an idea of differences between Early Pliocene thermal states.

4.5.3 Evidences of triggering and steering of the Messinian Salinity Crisis (MSC)

A combination of tectonic and glacio-eustatic processes are proposed to cause isolation, desiccation and reopening of the Mediterranean basin and to initiate and control the MSC (Kastens, 1992; Benson et al., 1991; Hodell et al., 1994, 2001; Krijgsman et al., 1999, 2001; Vidal et al., 2001). Continental ice volume accumulation, mainly in Antarctica, but also on the Northern Hemisphere lowered the eustatic sea level (Haq et al., 1987; Larsen et al., 1994). Our study documents for the first time the Southern Ocean thermal development during the Messinian, providing evidences for the cryospheric evolution in Antarctica. In general a synchron thermal development of the Southern Ocean and the Mediterranean Sea is documented (Figs. 4.8, 4.9, 4.10). Reconstructed RPTs at Sites 701 and 704 reflect a long-range Southern Ocean cooling from 6.3 Ma to 5.9 Ma terminating in a cold period until 5.7 Ma (Fig. 4.8). Increased abundances of *F. praecurta* at ca. 5.9 Ma at Site 704 document the northward expansion of cold-water masses (Fig. 4.9), which refers indirectly to increasing Antarctic ice volume and sea level lowering during the period of Mediterranean isolation and onset of lower evaporite deposition. This interpretation is supported by reduced abundances of warm-water indicating diatoms at this time. In contrast a rapid deglaciation and coupled sea level rise could not be deduced from the estimated thermal record for the period around the Mediterranean reopening (5.33 Ma). Therefore an explicit influence of glacio-eustatic processes can be supposed for the onset of the MSC, but not for the termination. However, the slowly proceeding warming at the Miocene/Pliocene boundary would undoubtedly rise the sea level.

This result coincides in general with the interpretation of oxygen isotope studies by Hodell et al. (1994, 2001). The increase in the benthic oxygen isotope signal in the Salé Briqueterie core (Fig. 4.9) is interpreted, at least in part, as an increase in global ice volume that lowered the sea level (Hodell et al., 1994). This conclusion is based on the 41-kyr cycle of orbital obliquity, which suggests that the oxygen isotope signal was partly controlled by changes in continental ice volume that were responding to insolation changes at high latitudes. At North Atlantic Site 982 Hodell et al. (2001) revealed 18 glacial-to-interglacial oscillations. There is evidence for a strengthened glaciation just before the onset of lower evaporite deposition in the Mediterranean. From our data reflooding of the Mediterranean basin can not be attributed to a single rapid thermal event, which suggests that tectonic changes were the main cause for the termination of the MSC (Hodell et al., 2001).

Some studies proposed regional tectonic changes as the dominant factor for the isolation of the Mediterranean basin, which contrasts the results shown in Hodell et al. (1994) and herein. Reason for this discrepancies are (i) interpretations of the 41-yr orbital obliquity isotope values as deep-sea temperature-effect (Shackleton and Crowhurst, 1997) and (ii) differences between timing of orbitally tuned isotope events and the chronology of geological features at the Mediterranean basin (Krijgsman et al., 1999; Vidal et al., 2001).

Considering the difficulties in oxygen isotope measurement interpretations, paleoecological diatom studies, as presented in this article, are a useful, independent tool to unravel the evolving discrepancies. A higher temporal resolution of Site 701 and 704 would enable a more detailed comparison of Southern Ocean thermal stages and the geological features of Mediterranean to reveal the influence of ice volume changes on the MSC.

5. Summary

Discrepancies between documented Miocene climatic developments as indicated by the benthic oxygen isotopes and the global eustatic sea level curve are the reason for the presented study. Diatom abundances are used as independent proxy to provide evidences of the Southern Ocean thermal history.

The presented detailed biostratigraphic investigation (Chapter 2) established a unique base for the paleoclimatic studies (Chapter 3, 4). Evidences for the Antarctic cryospheric development and its global climatic influence because of sea level changes, which can be deduced to Antarctic ice volume changes, are revealed (Chapter 4).

The first objective was to improve diatom biostratigraphic zonation and to establish a chronostratigraphy for middle and upper Miocene Southern Ocean sedimentary sections. The age models of six deep sea sites are either revised or established. Considering the latitudinal differences in stratigraphic diatom ranges and occurrence patterns of individual species, for the first time two diatom zonations are proposed that are applicable to the northern and southern area of the Southern Ocean. Two zonations provide a more detailed, improved stratigraphic resolution especially at the upper Middle and upper Miocene sections. The absolute counting data provide a more detailed and easier reproducible data base compared to the usually used abundance estimations.

First and last occurrence datums of diatom species are revised. Diachronous stratigraphic diatom occurrence between the southern and the northern area of the Southern Ocean could be observed. This provides first evidence for latitudinal thermal differences in the surface water masses.

To reveal the paleoclimatic development, ecological demands of the most extinct Miocene taxa are derived from the comparison of stratigraphic and geographic occurrence or from combined occurrence with extant taxa, respectively. Warm and cold water indicating diatom taxa are classified and a relative paleotemperature development is estimated and allows the assessment of the latitudinal thermal gradient development.

Calculated relative paleotemperatures and the abundance occurrences of thermally classified taxa are used to derive a detailed thermal history of the Southern Ocean:

After the Mid-Miocene climate optimum a thermal decrease is documented. At around 13 Ma Southern Ocean endemic species occurred dominantly. Up to ca. 10.8 Ma they were stepwise replaced by mostly endemic taxa. Around that time *D. ovata*, the coldest species, documents with its Southern Ocean wide dominant distribution extreme cold surface water conditions. This cold event coincides in time with a drastic sea level fall of about 75 m below the recent level (Haq et al., 1987), which indicates an increase of Antarctic ice volume accumulation. Beside a huge ice accumulation of the East Antarctic Ice Sheet the first build up of the West Antarctic Ice Sheet, up to recent dimensions, can be assumed.

A complete diatom turnover event followed and new cosmopolitan and warm water species dominated. At 8.6 Ma a group of ancestors of the recent ice algae documents a slight cooling and leads to speculations about the sea ice occurrence at this time. Furthermore, at around 6.5 Ma *H. cuneiformis* – a tropical diatom species, which does not occur recently within the Southern Ocean area – is found close to the Antarctic continent and documents extraordinarily warm short ranging periods alternating with very cold time spreads.

The temporary establishment of an ocean circulation pattern, which might be close to the present one, is proposed for a particular time period during the Late Miocene (8 – ca. 6 Ma).

The thermal development, as documented within the diatom record, coincides well with the thermal history as deduced from the sea level curve of Haq et al. (1987). Discrepancies to the oxygen isotope curve still exist.

For the first time the climatic development of the uppermost Miocene Southern Ocean is investigated on continuous sedimentary sections. This period is usually characterised by the hiatus occurrences disturbing the sediment sequences. Within this interval a dramatic ecological change occurred: the Messinian Salinity Crisis. The Mediterranean Sea was isolated from the Atlantic Ocean and the Mediterranean Sea basin desiccated. Sea level fluctuations are proposed as one possible trigger.

Cold Antarctic surface water temperatures between 6 and 5.7 Ma refer to an increasing Antarctic ice volume and a combined sea level fall. This time period coincides with the final isolation of the Mediterranean basin. Therefore the decreasing sea level can be seen as the trigger for the isolation process. The correlation between the climate changes in the southern high latitudes and the Mediterranean are documented.

Additionally, based on the different diatom occurrence pattern, the development of the hydrographic frontal system could be roughly delineated.

Assessing the results, the latitudinal separation of biostratigraphic zonations in the Southern Ocean will inspire further studies to improve the diatom stratigraphic resolution. For the first time it could be shown that diatom assemblages can be successfully used to reconstruct the Miocene climatic history in detail. Evidences for the main build up of the West Antarctic Ice Sheet are provided. The derivation of the uppermost Miocene thermal development in the Southern Ocean area, which reveals the influence of sea level fluctuations for the Messinian Salinity Crisis, should be outlined.

Isotope geochemical measurements are in progress, which may verify and improve the interpretation of our results. Based on the fact that now Miocene diatom assemblages can be used to reconstruct climate development, higher resolution studies might be focussed on selected time intervals. Possible topics might be the period around 10.8 Ma - the time spread of the West Antarctic Ice Sheet build up and the following climate turnover - or a distinct investigation of the time spread around 5.9 Ma to obtain a more detailed view of the final Mediterranean Sea isolation.

Furthermore, the potential of ancestor taxa of recent ice algae as sea ice indicators should be studied.

The presented study improves our understanding of the Miocene climate history in the Southern Ocean and gives reason for new investigations.

6. References

Abbott, W.H., 1974. Temporal and spatial distribution of Pleistocene diatoms from the south-east Indian Ocean. Nova Hedwegia Beih., 25, 291-347.

Abelmann, A., 1990. Oligocene to Middle Miocene radiolarian stratigraphy of southern high latitudes from Leg 113, Site 689 and 690, Maud Rise. In: Barker, P.F., Kennett, J.P., et al. (Eds.), Proc. ODP, Sci. Results, 113. College Station, TX (Ocean Drilling Program), pp. 675-708.

Abreu, V.S., Anderson, J.B., 1998. Glacial Eustacy during the Cenozoic: Sequence Strati-graphic Implications. AAGP Bulletin, 82 (7), 1385-1400.

Akiba, F., 1982. Late Quaternary diatom biostratigraphy of the Bellingshausen Sea, Antarctic Ocean. Rep. Tech. Res. Cen. JNOC, 16, 31-74.

Akiba, F., 1986. Middle Miocene to Quaternary diatom biostratigraphy in the Nankai Trough and Japan Trench, and modified Lower Miocene through Quaternary diatom zones for middle to high latitudes of the North Pacific. In: Kamagi, H., Karig, D.E., Coulbourn, W.T., et al. (Eds.), Init. Rep. DSDP, 87. U.S. Govt. Printing Office (Washington), pp. 393-481.

Akiba, F., Yanagisawa, Y., 1986. Taxonomy, morphostructure and phylogeny of the Neogene diatom zonal marker species in the middel-to-high latitudes of the North Pacific. In: Kamagi, H., Karig, D.E., Coulbourn W.T., et al. (Eds.), Init. Rep. DSDP, 87. U.S. Govt. Printing Office (Washington), pp. 483-554.

Akiba, F., Hiramatsu, C., Yanagishawa, Y., 1993. A Cenozoic diatom genus *Cavitatus* Williams; an emended description and two new biostratigraphically useful species, *C. lanceolatus* and *C. rectus* from Japan. Bull. Nat. Sci. Mus., Ser. C, 19 (1), 11-39.

Allen, C.P., Warnke, D.A., 1991. History of the ice rafting at Leg 114 sites, subantarctic/South Atlantic. In: Ciesielski, P.F., Kristoffersen, Y., et al. (Eds.), Proc. ODP, Sci. Results, 114. College Station, TX (Ocean Drilling Program), pp. 599-607.

Baldauf, J.G., Barron, J.A., 1980. *Actinocyclus ingens* var. *nodus*, a new stratigraphically useful diatom of the circum-North Pacific. Micropaleontology, 26, 103-110.

Baldauf, J.G., Barron, J.A., 1990. Evolution of biosiliceous sedimentation patterns - Eocene through Quaternary: Paleoceanographic response to polar cooling. In: Bleil, U., Thiede, J. (Eds.), Geological History of the Polar Oceans: Arctic versus Antarctic. NATO ASI Ser., Dordrecht (Kluwer Academic Publ.), pp. 575-607.

Baldauf, J.G., Barron, J.A., 1991. Diatom biostratigraphy: Kerguelen Plateau and Prydz Bay regions of the Southern Ocean. In: Barron, J.A., Larsen, B., et al. (Eds.), Proc. ODP, Sci. Results, 119. College Station, TX (Ocean Drilling Program), pp. 547-598.

Barker, P.F., Burrell, J., 1977. The opening of the Drake Passage. Mar. Geol., 25,15-34.

Barrett, P.J., 1999. Antarctic Climate History over the Last 100 Million Years. Terra Antarctica Rep., 3, 53-72.

Barron, J.A., 1980. Miocene to Quaternary diatom biostratigraphy of DSDP Leg 57, off northest Japan. In: Lee, M., Stout, L.N. (Eds.), Init. Rep. DSDP, 56, 57(2). U.S. Govt. Printing Office (Washington), pp. 641-685.

Barron, J.A., 1985a. Late Eocene to Holocene diatom biostratigraphy of the equatorial Pacific Ocean. In: Mayer, L.A., Theyer, F., et al. (Eds.), Init. Rep. DSDP, 85. U.S. Govt. Printing Office (Washington), pp. 413-456.

Barron, J.A., 1985b. Miocene to Holocene planctic diatoms. In: Bolli, H.M, Saunders, J.B., Perch-Nielsen, K., (Eds.). Plankton Stratigraphy, Cambridge Earth Science Series, Cambridge University Press, pp. 763- 809.

Barron, J.A., 1986. Response of Equatorial Pacific diatoms to polar cooling during the Middle Miocene. In: Ricard, M. (Ed.), Proc. of the Eight International Diatom Symposium, Paris, August 27-September 1, 1984. Koeltz Scientific Books, Koenigstein, W. Germany, pp. 591-600.

Barron, J.A., 1992a. Neogene diatom datum levels in the Equatorial and North Pacific. In: Ishizaki, K. and Saito, T. (Eds.). Centenary of Jap. Micropal. Terra Scientific Company, Tokyo, pp. 413-425.

Barron, J.A., 1992b. Pliocene paleoclimatic interpretation of DSDP Site 580 (NW Pacific) using diatoms. Marine Micropaleontology, 20, 23-44.

Barron, J.A., 1996. Diatom constraints on the position of the Antarctic Polar Front in the middle part of the Pliocene. Marine Micropaleontology, 27, 195-213.

Barron, J.A., Keller, G., 1983. Paleotemperature oscillations in the Middle and Late Miocene of the northeastern Pacific. Micropaleontology, 29 (2), 150-181.

Barron, J.A., Baldauf, J.G., 1995. Cenozoic marine diatom biostratigraphy and applications to paleoclimatology and paleoceanography. In: Blome, C.D., et al. (Eds.), Siliceous Microfossils. Paleontology Society, Short Courses in Paleontology, pp. 107-118.

Barron, J.A., Baldauf, J.G., Barrera, E., Caulet, J.-P., Huber, B.T., Keating, B.H., Lazarus, D., Sakai, H., Thierstein, H.R., Wie, W., 1991. Biochronologic and magneto-chronologic synthesis of Leg 119 sediments from the Kerguelen Plateau and Prydz Bay, Antarctica. In: Barron, J.A., Larsen, B., et al. (Eds.), Proc. ODP, Sci. Results, 119. College Station, TX (Ocean Drilling Program), pp. 813-847.

Benson, R.H., Rakic-El Bied, K., Bonaduce, G., 1991. An important current reversal (influx) in the Rifian Corridor (Morocco) at the Tortonian-Messinian boundary: the End of the Tethys Ocean. Paleoceanography, 6 (1), 164-192.

Berger, W.H., Vincent, E., 1986. Deep-sea carbonates: Reading the carbon-isotope signal. Geologische Rundschau, 75, 249-269.

Berger, W.H., Wefer, G., 1996. Expeditions into the Past: Paleoceanographic studies in the South Atlantic. In: Wefer, G., Berger, W.H., Siedler, G., Webb, D.J. (Eds.), The South Atlantic: Present and Past Circulation. Springer Verlag, Berlin, Heidelberg, pp. 363-410.

Berggren, W.A., Kent, D.V., Flynn, J.J., Van Couvering, J.A., 1985. Cenozoic geochronology. Geological Society of America Bulletin. 96 (11), 1407-1418.

Berggren, W.A., Kent, D.V., Swisher, C.C., Aubry, M.-P., 1995. A revised Cenozoic geochronology and chronostratigraphy, geochronology time scales and global correlation. Society for Sedimentary Geology, pp. 129-200.

Bianchi, C., Gersonde, R., subm.The Southern Ocean surface between Marine Isotope Stages 6 and 5d: Shape and timing of climate changes. Palaeogeogr., Palaeoclimatol., Palaeoecol.

Bohaty, S.M., Harwood, D.M., 1998. Southern Ocean Pliocene paleotemperature variation from high-resolution silicoflagellate biostratigraphy. Marine Micropaleontology, 33, 241-272.

Brady, H.T., 1977. *Thalassiosira torokina* n.sp. (diatom) and its significance in Late Cenozoic biostratigraphy. Antarct. J. U.S., 12, 122-123.

Brady, H.T., 1979. The extraction and interpretation of diatom zones. Dry Valley Drilling Project Holes 10 and 11, Taylor Valley, South Victoria Land, Antarctica. Mem. Nat. Inst. Polar Res., 13, 150-163.

Brathauer, U., 1996. Radiolarians as indicators for Quaternary climatic changes in the Southern Ocean (Atlantic sector). Reports on Polar Research, 216. Ph. D. Thesis, Alfred-Wegener-Inst. for Polar and Mar. Res., Bremerhaven, Germany.

Brathauer, U., Abelmann, A., 1999. Late Quaternary variations in sea surface temperatures and their relationship to orbital forcing recorded in the Southern Ocean (Atlantic sector). Paleoceanography, 14 (2), 135-148.

Brun, J., Tempére, J., 1889. Diatomées fossiles du Japan. Espéces Marines et Noucelles des Calcaire Argileux de Sendai et de Yedo. Société de Physique et d'Historie Naturelle de Geneve Mémories, Geneve, 30, 1-75.

Burckle, L.H., 1972. Late Cenozoic planktonic diatom zones from the eastern equatorial Pacific. Nova Hedwegia Beih., 39, 217-246.

Burckle, L.H., 1982. First appearance datum of *Hemidiscus karstenii* in late Pleistocene of the subantarctic region. Antarct. J. U.S., 17, 142-143.

Burckle, L.H., Rudolph, S., Mortlock, R.A., 1992. Evidence for an Early Pliocene cold event in the Southern Oceans. Antarct. J. U.S., 28, 110-111.

Bustillo, M.A., Lopez-Garcia, M.J., 1997. Age, distribution and comosition of Miocene diatom bearing sediments in the Guadalquivir Basin, Spain. Geobios, 30 (3), 335-350.

Cande, S.C., Kent, D.V., 1992. A new Geomagnetic Polarity Time Scale for the Late Cretaceous and Cenozoic. J. Geophys. Res., 97 (B10), 13917-13951.

Cande, S.C., Kent, D.V., 1995. Revised calibration of the geomagnetic polarity timescale for the Late Cretaceous and Cenozoic. J. Geophys. Res., 100 (B4), 6093-6095.

Cande, S.C., Stock, J.M., Müller, R.D., Ishihara, T., 2000. Cenozoic motion between east and west Antarctica. Nature, 404,145-150.

Castracane, D.A., 1886. Report on the Diatomaceae collected by HMS"Challenger" during the years 1873-1876. Rep. Sci. Results, H.M.S. Challenger, Botany, 2, 1-178.

Censarek, B., Gersonde, R., 2002. Miocene diatom biostratigraphy at ODP Sites 689, 690, 1088, 1092 (Atlantic sector of the Southern Ocean). Marine Micropaleontology, 45 (3-4), 309-359.

Censarek, B., Gersonde, R., subm. a. Relative Abundances and Ranges of Selected Diatoms from Miocene Sections at ODP Sites 689, 690, 1088 and 1092 (Atlantic sector of the Southern Ocean) – Data Report. In: Gersonde, R., Hodell, D. A., Blum, P., et al. (Eds.), Proc. ODP, Sci. Results., 177. College Station, TX (Ocean Drilling Program) and www-odp.tamu.edu/publications.

Censarek, B., Gersonde, R., subm. b. Miocene Climate Evolution of the Southern Ocean – Sea Surface Development as Derived from the Diatom Record (ODP Sites 689, 690, 1088 and 1092). Marine Micropaleontology.

Censarek, B., Gersonde, R., subm. c. Late Miocene Southern Ocean Thermal Development and its Connection to Mediterranean Climate History - Diatom Evidences from ODP Sites 701 and 704. Marine Geology.

Cerling, T.E., Harris, J.M., MacFadden, B.J., Leakey, M.G., Quade, J., Eisenmann, V., Ehleringer, J.R., 1997. Global vegetation change through the Miocene/Pliocene boundary. Nature, 389, 153-158.

Christian, T., 1887. New diatomaceous deposits. Am. Month. Micro. J., The Microscope, 7, 65-68.

Ciesielski, P.F., 1983. The Neogene and Quaternary Diatom Biostratigraphy of Subantarctic Sediments, Deep Sea Drilling Project Leg 71. In: Ludwig, W.J. and Krasheninnikov, V.A. (Eds.), Init. Repts. DSDP, 71. U.S. Govt. Printing Office (Washington), 635-656.

Ciesielski, P.F., 1986. Middle Miocene to Quaternary diatom biostratigraphy of Deep Sea Drilling Project Site 594, Chatham Rise, southwest Pacific. In: Kennett, J.P., von der Borch, C.C., et al. (Eds.), Init. Repts. DSDP, 90. Washington (U.S. Govt. Printing Office), pp. 863-885.

Ciesielski, P.F., 1991. Relative abundances and ranges of selected diatoms and silicoflagellates from Sites 699 and 704, subantarctic South Atlantic. In: Ciesielski, P.F., Kristoffersen, Y., et al. (Eds.), Proc. ODP, Sci. Results, 114. College Station, TX (Ocean Drilling Program), pp. 753-778.

Ciesielski, P.F., Kristoffersen, Y., et al., 1988. Proc. ODP Init. Repts., 114. College Station, TX (Ocean Drilling Programm).

Clement, B.M., Hailwood, E.A., 1991. Magnetostratigraphy of sediments from Sites 701 and 702. In: Ciesielski, P.F., Kristoffersen, Y., et al. (Eds.), Proc. ODP, Sci. Results, 114. College Station, TX (Ocean Drilling Program), pp. 359-366.

Cleve, P.T., Grunow, A., 1880. Beiträge zur Kenntnis der arktischen Diatomeen. K. Sven. Vetenskapsakad. Handl., 17, 1-121.

Collins, L.S., Coates, A.G., Berggren, W.A., Aubry, M.-P., Zhang, J., 1996a. The Late Miocene Panama isthmian strait. Geology, 24 (8), 687-690.

Collins, L.S., Budd, A.F., Coates, A.G, 1996b. Earliest evolution associacated with close of Tropical American Seaway. Proc. Nat. Acad. Sci. USA, 93, 6069-6072.

Crosta, X., Pichon, J.-J., Burckle, L. H. 1998. Application of modern analog technique to marine Antarctic diatoms: Reconstruction of maximum sea-ice extent at the Last Glacial Maximum. Paleoceanography, 13(3), 284-297.

De Santis, L., Prato, S., Brancolini, G., Lovo, M., Torelli, L., 1999. The Eastern Ross Sea continental shelf during the Cenozoic: Implications for the West Antarctic Ice Sheet development. Global and Planetary Change, 23, 173-196.

Diekmann, B., Fälker, M., Kuhn, G., subm. Enviromental history of the southeastern South Atlantic since the middle Miocene: Evidence from the sedimentological records of ODP Sites 1088 and 1092. Sedimentology.

Donahue, J.G., 1970. Pleistocene diatoms as climatic indicators in North Pacific sediments. In: Hays, J.D. (Ed.), Geological Investigations of the North pacific. Mem. Geol. Soc. Am., 126, pp. 121-138.

Ehrmann, W.U., 1994. Cenozoic Glacial History of Antarctica. Reports on Polar Research, 137, Alfred-Wegener-Inst. for Polar and Mar. Res., Bremerhaven, Germany.

Ehrmann, W.U., Grobe, H., Fütterer, D.K., 1991. Late Miocene to Holocene glacial history of East Antarctica as revealed by sediments from Sites 745 and 746. In: J. Barron and B. Larsen (Eds.), Proc. ODP, Sci. Results, 119. College Station, TX (Ocean Drilling Program), pp. 239-260.

Fenner, J.M., 1991. Late Pliocene-Quaternary quatitative diatom stratigraphy in the Atlantic sector of the Southern Ocean. In: Ciesielski, P.F., Kristoffersen, Y. (Eds.), Proc. ODP, Sci. Results, 114. College Station, TX (Ocean Drilling Program), pp. 97-121.

Fenner, J.M., Schrader, H.-J., Wienigk, H., 1976. Diatom phytoplankton studies in the southern Pacific Ocean, composition and correlation to the Antarctic Convergence and its paleoecological significance. In: Hollister, C.D., Craddock, C., et al (Eds.), Init. Repts. DSDP, 35. U.S. Govt. Printing Office (Washington), pp. 757-813.

Flower, B.P., Kennett, J.P., 1993. Middle Miocene ocean-climate transition: High-resolution oxygen and carbon isotopic records from Deep Sea Drilling Project Site 588A, Southwest Pacific. Paleoceanography, 8 (6), 811-843.

Flower, B.P., Kennett, J.P., 1994. The Middle Miocene climatic transition: East Antarctic ice sheet development, deep ocean circulation and global carbon cycling. Palaeogeogr., Palaeoclimatol., Palaeoecol., 108, 537-555.

Flower, B.P., Kennett, J.P., 1995. Middle Miocene deepwater paleoceanography in the southwest Pacific: Relations with East Antarctic Ice Sheet development. Paleoceanography, 10 (6), 1095-1112.

Frenguelli, J., 1949. Diatomeas fósiles de los yacimientos chilenos de Tiltil y Mejillones. Darwinia, 9 (1), 97-157.

Fryxell, G.A., Hasle, G.R., 1980. The marine diatom *Thalassiosira oestrupii*: Structure, taxonomy and distribution. Amer. J. Bot., 67(5), 804-814.

Fryxell, G.A., Sims, P.A., Watkins, T.P., 1986. *Azpeitia* (Bacillariophyceae): related genera and promorphology. Sys. Bot. Monogr., 13, 1-74.

Gersonde, R., 1980. Paläoökologische und biostratigraphische Auswertung von Diatomeenassoziationen aus dem Messinium des Caltanissetta-Beckens (Sizilien) und einiger Vergleichsprofile in SO-Spanien, NW-Algerin und auf Kreta. Ph.D. Thesis, Uni. Kiel, Germany.

Gersonde, R., 1990. Taxonomy and morphostructure of the Neogene diatoms from the Southern Ocean, ODP Leg 113. In: Barker, P.F., Kennett J.P., et al. (Eds.), Proc. ODP, Sci. Results, 113. College Station, TX (Ocean Drilling Program), pp. 791-802.

Gersonde, R., 1991. Taxonomy and morphostructure of Late Neogene diatoms from Maud Rise (Antarctic Ocean). Polarforschung, 59 (3), 141-171.

Gersonde, R., Burckle, L.H., 1990. Neogene diatom biostratigraphy of OPD Leg 113, Weddell Sea (Antarctic Ocean). In: Barker, P.F., Kennett, J.P., et al. (Eds.), Proc. ODP, Sci. Results, 113. College Station, TX (Ocean Drilling Program), pp. 761-789.

Gersonde, R., Bárcena, M.A., 1998. Revision of the upper Pliocene-Pleistocene diatom biostratigraphy for the northern belt of the Southern Ocean. Micropaleontology, 44 (1), 84-98.

Gersonde, R., Zielinski, U., 2000. The reconstruction of late Quaternary Antarctic sea-ice distribution - The use of diatoms as a proxy for sea ice. Palaeogeogr., Palaeoclimatol., Palaeoecol., 162, 263-286.

Gersonde, R., Abelmann, A., Burckle, L.H., Hamilton, N., Lazarus, D., McCartney, K., O´Brien, P., Spieß, V., Wise.S.W., 1990. Biostratigraphic synthesis of Neogene siliceous microfossils from the Antarctic Ocean, ODP Leg 113 (Weddell Sea). In: Barker, P.F., Kennett, J.P., et al. (Eds.), Proc. ODP, Sci. Results, 113. College Station, TX (Ocean Drilling Program), pp. 915-936.

Gersonde, R., Spieß, V., Flores, J.A., Hagen, R.A., Kuhn, G., 1998. The sediments of Gunnerus Ridge and Kainan Maru Seamount (Indian sector of Southern Ocean). Deep-Sea Res., I 45, 1515-1540.

Gersonde, R., Hodell, D.A., Blum, P., Shipboard Scientific Party, 1999. Proc. ODP, Init. Repts. [CD-ROM], 177: Available from: Ocean Drilling Program, Texas A&M University, College Station, TX 77845-9547, U.S.A.

Gombos, A.M., Jr. 1974. New species of fossil diatom from the Antarctic. Antarct. J. U.S., 9, 275.

Gombos, A.M., Jr., 1977. Paleogene and Neogene diatoms from the Falkland Plateau and Malvinas outer basin, Leg 36, Deep Sea Drilling Project. In: Barker, P.F., Dalziel, I.W.D., et al. (Eds.), Init. Repts. DSDP, 36. U.S. Govt. Printing Office (Washington), pp. 575-687.

Gran, H.H., 1904. Die Diatomeen der arktischen Meere. Diatomeen des Planktons. Fauna Arctica, 2, 511-554.

Greville, R.K., 1861-1866. Descriptions of new and rare diatoms. Ser.I-XX, Transactions of the Microscopical Society, London. Bibliotheca Phycologia, 6. (Reprinted 1966)

Hailwood, E.A., Clement, B.M., 1991a. Magnetostratigraphy of Sites 699 and 700, East Georgia Basin. In: Ciesielski, P.F., Kristoffersen, Y., et al. (Eds.), Proc. ODP, Sci. Results, 114. College Station, TX (Ocean Drilling Program), pp. 337-357.

Hailwood, E.A., Clement, B.M., 1991b. Magnetostratigraphy of Sites 703 and 704, Meteor Rise, southeastern South Atlantic. In: Ciesielski, P.F., Kristoffersen, Y., et al. (Eds.), Proc. ODP, Sci. Results, 114. College Station, TX (Ocean Drilling Program), pp. 367-386.

Hallegraeff, G.M., 1984. Species of the diatom genus *Thalassiosira* in Australian waters. Botanica Mar., 27, 495-513.

Hambrey, M.J., Ehrmann, W.U., Larsen, B., 1991. Cenozoic glacial record of the Prydz Bay continental shelf, East Antarctica. In: Barron, J., Larsen, B., et al. (Eds.). Proc. ODP, Sci. Results, 119. College Station, TX (Ocean Drilling Program), pp. 813-847.

Hanna, G.D., 1930. A Review of the Genus *Rouxia*. J. of Paleontology, 2 (4), 179-188.

Haq, B.U., Hardenbol, J., Vail, P.R., 1987. Chronology of fluctuating sea levels since the Triassic. Science, 235, 1156-1167.

Hargraves, P., 1968. Species composition and distribution of net plankton diatoms in the Pacific sector of the Antarctic Ocean. Ph.D. Thesis., Columbia Univ. New York, U.S.A.

Harwood, D.M., 1986. Diatoms. In: Barrett, P.J. (Ed.), Antarctic Cenozoic History from the MSSTS-1 Drillhole, McMurdo Sound. DSIR Bull. N. Z., 237, 69-107.

Harwood, D.M., Maruyama, T., 1992. Middle Eocene to Pleistocene diatom biostratigraphy of Southern Ocean sediments from the Kerguelen Plateau, Leg 120. In: Wise, S.W.Jr., Schlich, R., et al. (Eds.), Proc. ODP, Sci. Results, 120. College Station, TX (Ocean Drilling Program), pp. 682-733.

Harwood, D.M., Webb, P.-N., 1998. Glacial Transport od Diatoms in the Antarctic Sirius Group: Pliocene Refrigerator. GSA Today, 8 (4), 1 and 4-8.

Hasle, G.R., 2001. The marine, planktonic diatom family *Thalassionemataceae*: Morphology, taxonomy and distribution. Diatom Research, 16 (1), 1-82.

Hasle, G.R., Fryxell, G.A., 1977. The genus *Thalassiosira*: Some species with linear areolae array. In: Simonsen, R. (Ed.), Proc. Fourth Symp. on Recent and Fossil Marine Diatoms Oslo, Nova Hedwegia, Beih. 54,15-66.

Hasle, G.R., Syvertsen, E.E., 1982. *Coscinodiscus pseudolineatus* Pant. and *Coscinodiscus praelineatus* Jousé. In: Mann, D. (Ed.), 7th Symposium on Recent and Fossil Diatoms. Koenigstein, Philadelphia, pp. 145-155.

Hasle, G.R., Sims, P.A., 1986. The diatom genera *Stellarima* and *Symbolophora* with comments on the genus *Actinoptychus*. Br. Phycol. J., 21, 97-114.

Hasle, G.R., Sims, P.A., Syvertsen, E.E., 1988. Two recent *Stellarima* species: *S. microtrias* and *S. stellaris* (Bacillariophyceae). Botanica Mar., 31, 195-206.

Hasle, G.R., Syvertsen, E.E., Steidinger, K.A., Tangen, K., 1995. Marine Diatoms. In: Tomas, C.K. (Ed.), Identifying Marine Diatoms and Dinoflagellates. Academic Press, San Diego, New York.

Haug, G.H., Tiedemann, R., 1998. Effect of the formation of the Isthmus of Panama on the Atlantic Ocean thermohaline circulation. Nature, 393, 673-676.

Hays, J.D., Imbrie, J., Shackleton, N.J., 1976. Variations in the Earth's Orbit: pacemaker of the Ice Ages. Science, 194, 1121-1132.

Heiden, H., Kolbe, R.W., 1928. Die marinen Diatomeen der Deutschen-Südpolarexpedition 1901-1903. In: von Drygalski, E. (Ed.), Deutsche Südpolar-Expedition 1901-1903. Bd. 8, Botanik, 450-714.

Hendey, N.I., 1964. *Bacillariophyceae* (diatoms). An introductory account of the smaller algae of Bristish coastal waters. Fish. Invest., Ser. 4, Pt. 5, London (HMSO).

Hendey, N.I., 1981. Miocene diatoms from the subantarctic southwest Pacific. DSDP Leg 29, Site 278, Core 10. Bacillaria, 4, 65-124.

Hillenbrand, C.D., Ehrmann, W., 2001. Distribution of clay minerals in drift sediments on the continental rise west of the Antarctic Peninsula, ODP Leg 178, Sites 1095 and 1096. In: Barker, P.F., Camerlenghi, A., Acton, G.D., Ramsay, A.T.S. (Eds.), Proc. ODP, Sci. Results, 178, pp. 1-29 (Online). http://www-odp.tamu.edu/publications/178_SR/Volume/Chapters/Sr178_08.pdf.

Hodell, D.A., Elmstrom K.M., Kennett, J.P., 1986. Latest Miocene benthic δ18O changes, global ice volume, sea level and the "Messinian salinity crisis". Nature, 320, 411-414.

Hodell, D.A., Benson, R.H., Kent, D.V., Boersma, A., Rakic-El Bied, K., 1994. Magnetostratigraphic, biostratigraphic, and stable isotope stratigraphy of an Upper Miocene drill core from the Salé Briqueterie (northwestern Marocco): A high-resolution chronology for the Messinian stage. Paleoceanography, 9 (6), 835-855.

Hodell, D.A., Sierro, F.J., Raymo, M.E., 2001. Correlation of Late Miocene to Early Pliocene sequences between the Mediterranean and North Atlantic. Paleoceanography, 16 (2), 164-178.

Hsü, K.J., Ryan, W.B.F., Cita, M.B., 1973. Late Miocene Desiccation of the Mediterranean. Nature, 292, 240-244.

Hsü, K.J., McKenzie, J.A., Oberhaensli, H., Weissert, H., Wright, R.C., 1984. South Atlantic Cenozoic paleoceanography. In: Hsü, K.J., LaBrecque, J.L., et al. (Eds.), Init Repts. DSDP, 73. Washington (U.S. Govt. Printing Office), pp. 771-785.

Hustedt, F., 1930. Die Kieselalgen. Otto Koeltz Science Publishers, Koenigstein, Germany.

Hustedt, F., 1930-1933. Die Kieselalgen Deutschlands, Österreichs und der Schweiz mit Berücksichtigung der übrigen Länder Europas sowie der angrenzenden Gebiete. Teil 2. In: Rabenhorst, L. (Ed.), Kryptogamen-Flora von Deutschland, Österreich und der Schweiz, Akad. Verlag Leipzig, Germany.

Hustedt, F., 1958. Diatomeen aus der Antarktis und dem Südatlantik. - Dtsch. Antarkt. Exped. 1938/39, 103-191.

Jordan, R.W. , Priddle, J., 1991. Fossil member of the diatom genus *Proboscia*. Diat. Res., 6 (1), 55-61.

Jousé, A.P., 1965. Species diatomearum antarcticae novae et minus cognitae. Novitates System. Plant. non Vascularium, Akad. NAUK, Moscow, pp. 3-9.

Jousé, A.P., 1977. Atlas of microorganisms in bottom sediments of the oceans (diatoms, radiolaria, silicoflagellates and coccoliths). Akad. NAUK, Moscow.

Jousé, A.P., Koroleva, G.S., Nagaeva, G.A., 1963. Stratigraphical and paleontological investigations in the Indian section of the Southern Ocean. Okeanol. Issled., 8, 137-161.

Kanaya, T., Koizumi, I., 1966. Interpretation of diatom thanatocoenoses from the North Pacific applied to a study of core V20-130 (Studies of a deep-sea core V20-120, part IV). Sci. Rep., Tohoku Univ., 7, 89-130.

Kanaya, T., Koizumi, I., 1970. The progress in the younger Cenozoic diatom biostratigraphy in the northern circum-Pacific Region. J. Mar. Geol., 6, 47-66.

Kastens, K.A., 1992. Did glacio-eucstatic sea level drop trigger the Messinian salinity crisis? New evidence from Ocean Drilling Program Site 654 in the Tyrrhenian Sea. Paleoceanography, 7 (3), 333-356.

Keller, G., Barron, J.A., 1987. Paleodepth distribution of Neogene deep-sea hiatuses. Paleoceanography, 2 (6), 697-713.

Kemp, A.E.S., Baldauf, J.G., 1993. Vast Neogene laminated diatom mat deposits from the eastern equatorial Pacific Ocean. Nature, 362, 141-144.

Kemp, A.E.S., Baldauf, J.G., Pearce, R.B., 1995. Origins and paleoceanographic significance of laminated diatom ooze from the eastern equatorial Pacific (Leg 138). In: Pisias, N.G., Mayer, L.A., et al. (Eds.), Proc. ODP, Sci. Results 138. College Station, TX (Ocean Drilling Program), pp. 647-663.

Kennett, J.P., 1977. Cenozoic Evolution of Antarctic Glaciation, the Circum-Antarctic Ocean and their impact on global paleoceanography. Journal of Geophysical Res., 82 (27), 3843-3860.

Kennett, J.P., Barker, P.F., 1990. Latest Cretaceous to Cenozoic climate and oceanographic developments in the Weddell Sea, Antarctica: An ocean-drilling perspective. In: Barker, P.F., Kennett, J.P., et al. (Eds.), Proc. ODP, Sci. Res., 113. College Station, TX (Ocean Drilling Program), pp. 937-960.

Koizumi, I., 1985. Late Neogene paleoceanography in the western North Pacific. In: Heath, G.R., Burckle, L.H. et al. (Eds.), Init. Rep. DSDP, 86. U.S. Govt. Printing Office (Washington), pp. 429-438.

Koizumi, I., 1990. Successional changes of Middle Miocene diatom assemblages in the northwestern Pacific. Palaeogeogr., Palaeoclimatol., Palaeoecol., 77, 181-193.

Komara, S., 1976. *Sawamuraia*, *Katahiraia*, *Yoshidaia*, drei neue Diatomengattungen aus den Neogen Japans. Trans. Proc. Paleontol. Soc. Japan., N.S., 103, 379-397.

Krijgsman, W., Hilgen, F.J., Raffi, I., Sierro, F.J., Wilson, D.S., 1999. Chronology, causes and progression of the Messinian salinity crisis. Nature, 400, 652-655.

Krijgsman, W., Fortuin, A.R., Hilgen, F.J., Sierro, F.J., 2001. Astrochronology for the Messinian Sorbas basin (SE Spain) and orbital (precessional) forcing for the evaporite cyclicity. Sedimentary Geol., 140, 43-60.

Kunz-Pirrung, M., Gersonde, R., Hodell, D., 2002. Mid Bruhnes century-scale diatom sea surface temperature and sea-ice records from the Atlantic sector of the Southern Ocean (ODP Leg 177, Sites 1093, 1094 and core PS2089-2). Palaeogeogr., Palaeoclimatol., Palaeoecol., (in press).

Larsen, H.C., Saunders, A.D., Clift, A.D., Beget, J., Wei, W., Spezzaferri, S., ODP Leg 152 Scientific Party, 1994. Seven Million years of glaciation in Greenland. Science, 264, 952-955.

Latimer, J.C., Filippelli, G.M., 2002. Eocene to Miocene terrigenous inputs, paleoproductivity, and the onset of the ACC: Geochemical evidence from ODP Leg 177, Site 1090. Palaeogeogr., Palaeoclimatol., Palaeoecol., (in press).

Lawver, L.A., Müller, R.D., Srivastava, S.P., Roest, W., 1990. The opening of the Arctic Ocean. In: Bleil, U., Thiede, J. (Eds.), Geological History of the Polar Oceans: Arctic versus Antarctic. Dordrecht (Kluwer Academic Publ.), pp. 29-62.

Lawver, L.A., Gahagan, L.M., Coffin, M.F., 1992. The development of paleoseaways around Antarctica. In: Kennett, J.P., Warnke, D.A. (Eds.), The Antarctic Paleoenvironment: A Perspective on Global Change (Pt. 1). Am. Geophys. Union, Antarct. Res. Ser., 56, pp. 7-30.

Lear, C.H., Elderfield, H., Wilson, P.A., 2000. Cenozoic deep-sea temperatures and global ice volumes from Mg/Ca in benthic foraminiferal calcite. Science, 287, 269-272.

Mangin, L., 1914. Sur le polymorphism de certaines Diatomées de l'Antarctique. Compt. Rend. Hbd. Seances Acad. Sci. Paris, 159, 476-484.

Mangin, L., 1915. Phytoplankton de l'Antarctique. Deux. Exped. Antarct. Fr. (1908-1910), 2, 1-95.

Marino, M., Flores, J.A., 2002. Miocene to Pliocene calcareous nannofossil biostratigraphy for ODP Leg 177 Sites 1088 and 1090. Marine Micropaleontology, (in press).

McCartney, K., Wise, S.W., 1990. Cenozoic silicoflagellates and ebridians froms ODP Leg 113: Biostratigraphy and notes on morphologic variability. In: Barker, P.F., Kennett, J.P., et al. (Eds.), Proc. ODP, Sci. Results, 113. College Station, TX (Ocean Drilling Program), pp. 729-760.

McCollum, D.W., 1975. Diatom Stratigraphy of the Southern Ocean. In: Hayes, D.E., Frakes, L.A., et al. (Eds.), Init. Repts. DSDP, 28. U.S. Govt. Printing Office (Washington), pp. 515-571.

Medlin, L. K., Sims, P.A.,1993. The transfer of *Pseudoeunotia doliolus* to *Fragilariopsis*. Nova Hedwegia Beih., 106, 323-334.

Miller, K.G., Wright, J.D., Fairbanks, R.G, 1991. Unlocking the ice house: Oligocene-Miocene oxygen isotopes, eustacy, and margin erosion. J. Geophys. Res., 96 (B 4), 6829-6848.

Moore, J.K., Abbott, M.R., Richman, J.G., 1999. Location and dynamics of the Antarctic Polar Front from satellite sea surface temperatures. J. Geophys. Res., 102 (C2): 3059-3073.

Moreno-Ruiz, J.L., Licea, S., 1995. Observations on the valve morphology of *Thalassionema nitzschoides* (Grunow) Hustedt. In: Marino, D., Montresor, M. (Eds.), Proceedings of the Thirteenth International Diatom Symposium: Bristol (Biopress Limited), pp. 393-413.

Morley, J.J., Hays, J.D., 1979. Comparison of glacial and interglacial oceanographic conditions in the South Atlantic from variations in calcium carbonate and radiolarian distributions. Quat. Res., 12, 396-408.

Müller, D.W., Hodell, D.A., Ciesielski, P.F., 1991. Late Miocene to earliest Pliocene (9.8-4.5 Ma) paleoceanography of the subantarctic southeast Atlantic: Stable isotopic, sedimentologic, and microfossil evidence. In: Ciesielski, P.F., Kristoffersen, Y., et al. (Eds.), Proc. ODP, Sci. Results, 114. College Station, TX (Ocean Drilling Program), pp. 459-474.

Myhre, A.M., Thiede, J., 1995. North Atlantic Arctic Gateways. In: Myhre, A.M., Thiede, J., Firth, J.V., et al. (Eds.), Proc. ODP, Init. Repts. 151. College Station, TX (Ocean Drilling Program), pp. 5-26.

Orsi, H.A., Whitworth, T., Nowlin, W.D., 1995. On the meridional extent and fronts of the Antarctic Circumpolar Current. Deep Sea Res. I, 42, 641-673.

Pagani, M., Arthur, M.A., Freeman, K.H., 1999. Miocene evolution of atmospheric carbon dioxide. Paleoceanography, 14 (3), 273-292.

Peterson, R.G., Stramma, L., 1991. Upper-level circulation in the South Atlantic Ocean. Prog. Oceanogr., 26, 1-73.

Pichon, J.J., Labracherie, M., Labeyrie, L., Duprat, J. 1987. Transfer function between diatom assemblages and surface hydrology in the Southern Ocean. Palaeogeogr., Palaeoclimatol., Palaeoecol., 61, 79-95.

Prell, W.L., Hutson, W.H., Williams, D.F., BÉ, A.W.H., Geitzenauer, K., Molfino, B., 1980. Surface circulation of the Indian Ocean during the last glacial maximum, approximately 18.000 yr B.P. Quat. Res., 14, 309-336.

Pritchard, A., 1861. A History of Infusoria, Living and Fossil. Wittacker and Co., London.

Rahmstorf, S., 1998. Influence of Mediterranean outflow on climate. EOS 79, 281-282.

Ramsay, A.T.S., Baldauf, J.G., 1999. A reassessment of the Southern Ocean biochrono-logy. Geological Society Memoir, 18. The Geological Society, London.

Ramsay, A.T.S., Smart, C.W., Zachos, J.C., 1998. A model of Early to Middle Miocene deep circulation for the Atlantic and Indan Oceans. In: Cramp, A., MacLeod, C.J., Lee, S.V., Jones, E.J.W. (Eds.), Geological Evolution of Ocean Basins: Results from the Ocean Drilling Programm. Geological Society, London, Special Publications, 131, 55-70.

Round, F.R., Crawford, R.M., Mann, D.G., 1990. The Diatoms. Cambridge Univers. Press.

Sakai, H., Keating, B., 1991. Paleomagnetism of Leg 119-Holes 737A, 738C, 742A, 745B, and 746A. In: Barron, J., Larsen, B., et al. (Eds.), Proc. ODP, Sci. Results, 119. College Station, TX (Ocean Drilling Program), pp. 751-770.

Salvador, A., 1994. International Stratigraphic Guide (A Guide to Stratigraphic Classification, Terminology and Procedure), 2nd. Ed., XIX + 214. Intern. Union of Geol. Sciences and Geol. Soc. of America.

Sancetta, C., Silvestri, S., 1986. High-resolution biostratigraphy and oceanographic events in the Late Pliocene and Pleistocene North Pacific Ocean. Paleoceanography, 1 (2), 163-180.

Schmidt, A., Schmidt, M., Fricke, F., Heiden, H., Müller, O., Hustedt., F., 1874-1959 (1878). Atlas der Diatomeen-Kunde. R. Reisland, Leipzig.

Schrader, H.J., 1973. Cenozoic diatoms from the northeast Pacific, Leg 18. In: Kulm, L.D., von Huene, R., et al. (Eds.), Init. Rep. DSDP, 18. U.S. Govt. Printing Office (Washington), pp. 673-797.

Schrader, H.J., 1974. Cenozoic marine planktonic diatom stratigraphy of the tropical Indian Ocean. In: Fisher, R.L., Bruce, E.T., et al. (Eds.), Init. Repts. DSDP, 24. U.S. Govt. Printing Office (Washington), pp. 887-967.

Schrader, H.J., 1976. Cenozoic planktonic diatom biostratigraphy of the southern Pacific Ocean. In: Hollister, C.D., Craddock, C. (Eds.), Init. Repts. DSDP, 35. U.S. Govt. Printing Office (Washington), pp. 605-671.

Schrader, H.J., Fenner, J., 1976. Norwegian Sea Cenozoic diatom biostratigraphy and taxonomy. In: Talwani, M., Udintsev, G., et. al. (Eds.), Init. Repts. DSDP, 38. U.S. Govt. Printing Office (Washington), pp. 921-1099.

Schrader, H.J., Gersonde, R., 1978. Diatoms and Silicoflagellates. In: Zachariasse, W.J., et al. (Eds.), Micropaleontological counting methods and techniques - an exercise on an eight metres section of the lower Pliocene of Capo Rossello, Sicily. Utrecht Micropal. Bull., 17, 129-176.

Shackleton, N.J., Kennett, J.P, 1975. Paleotemperature history of the Cenozoic and the initiation of Antarctic glaciation: Oxygen and carbon isotope analyses in DSDP Sites 277, 279, and 281. In: Kennett, J.P., Houtz, R.E. et al. (Eds.), Init. Rep. DSDP, 29. U.S. Govt. Printing Office (Washington), pp. 743-755.

Shackleton, N.J., Crowhurst, S., 1997. Sediment fluxes based on orbitally tuned time scale 5 Ma to 14 Ma, Site 926. In: Shackleton, N.J., Curry, W.B., Richter, C., Bralower, T.J. (Eds.), Proc. ODP. Sci. Res., 154, pp. 69-82

Shipboard Scientific Party, 1988a., Site 689. In: Barker, P.F., Kennett, J.P, et al. (Eds.), Proc. ODP, Init. Repts., 113. College Station TX (Ocean Drilling Program), pp. 89-181.

Shipboard Scientific Party, 1988b. Site 690. In: Barker, P.F., Kennett, J.P, et al. (Eds.), Proc. ODP, Init. Repts., 113. College Station, TX (Ocean Drilling Program), pp. 183-291.

Shipboard Scientific Party, 1988c. Site 701. In: Ciesielski, P.F., Kristoffersen, Y., et al., (Eds.) Proc. ODP Init. Repts., 114. College Station, TX (Ocean Drilling Programm), pp. 636-482.

Shipboard Scientific Party, 1988d. Site 704. In: Ciesielski, P.F., Kristoffersen, Y., et al., (Eds.) Proc. ODP Init. Repts., 114. College Station, TX (Ocean Drilling Programm), pp. 621-796.

Shipboard Scientific Party, 1999a. Site 1088. In: Gersonde, R., Hodell, D.A., Blum, P., et al. (Eds.), Proc. ODP, Init. Repts., 177 (CD-ROM). Available from: Ocean Drilling Programm, Texas A&M University, College Station, TX 77845-9547, U.S.A.

Shipboard Scientific Party, 1999b. Site 1092. In: Gersonde, R., Hodell, D.A., Blum, P., et al. (Eds.), Proc. ODP, Init. Repts., 177 (CD-ROM). Available from: Ocean Drilling Programm, Texas A&M University, College Station TX 77845-9547, U.S.A.

Shipboard Scientific Party, 1999c. Explanatory Notes. In: Gersonde, R., Hodell, D.A., Blum, P., et al. (Eds.), Proc. ODP, Init. Repts., 177 (CD-ROM). Available from: Ocean Drilling Program, Texas A&M University, College Station, TX 77845-9547, U.S.A.

Shipboard Scientific Party, 2001. Leg 189 summary. In: Exon, N.F., Kennett, J.P., Malone, M.J., et al. (Eds.), Proc. ODP, Init. Repts., 189. College Station TX (Ocean Drilling Program), pp. 1-98.

Simonsen, R., 1972. Über die Diatomeengattung *Hemidiscus* WALLICH und andere Angehörige der sogenannten "*Hemidiscaceae*". Veröff. Inst. Meeresforschung. Bremerhaven, Germany, 13, 265-273.

Simonsen, R., 1979. The diatom system: idea on phylogeny. Bacillaria, 2, 9-71.

Smith, W.H.F., Sandwell, D.T., 1997. Global sea floor topography from satellite altimetry and ship depth soundings. Science, 277, 1956-1962.

Spieß, V., 1990. Cenozoic magnetostratigraphy of Leg 113 dill sites, Maud Rise, Weddell Sea, Antarctica. In: Barker, P.F., Kennett, J.P., et al. (Eds.), Proc. ODP, Sci. Results, 113. College Station, TX (Ocean Drilling Program), pp. 261-315.

Steininger, F.F., Piller, W.E., 1999. Empfehlungen (Richtlinien) zur Handhabung der stratigraphischen Nomenklatur. Courier Forschungsinstitut Senckenberg, 209. Senckenbergische Naturforschende Gesellschaft, Frankfurt a. Main.

Sundström, B.G., 1986. The marine diatom genus *Rhizosolenia*. A new approch to the taxonomy. Ph. D. Thesis, Lund Univ., Sweden.

Syvertsen, E.E., Hasle, G.R., 1983. The diatom genus *Eucampia*: morphology and taxonomy. Bacillaria, 6, 169-210.

Van Heurck, H., 1880-1885. Synopsis des Diatomées de Belgique: Anvers (F.J. Dieltjens).

Van Heurck, H., 1909. Expédition Antarctique Belge. Résultats du Voyage du S.Y. „Belgica" en 1897-1899, Botanique, Diatomées. Anvers (J. E. Buschmann).

Vidal, L., Bickert, T., Wefer, G., Röhl, U., 2001. Late Miocene stable isotope stratigraphy of the SE Atlantic ODP Site 1085: Relation to Messinian events. Marine Geology, 2967, 1-15.

Warnke, D.A., Allen, C.P., Müller, D.W., Hodell, D.A., Brunner, C.A., 1992. Miocene-Pliocene Antarctic Glacial evolution: A systheses of Ice-Rafted Debris, Stable isotope, and Planktonic Foraminiferal Indicator, ODP Leg 114. Antarctic Research Series, 56, 311-325.

Warnke, D.A., Marzo, B., Hodell, D.A., 1996. Major deglaciation of east Antarctica during the early Late Pliocene? Not likely from a marine perspective. Marine Micropaleontology, 27, 237-251.

Weaver, F.M., Gombos, A.M., 1981. Southern high-latitude diatom biostratigraphy. Soc. Econ. Paleontol. Mineral. Spec. Publ., 32, 445-470.

Wei, W., Thierstein, H.R., 1991. Upper Cretaceous and Cenozoic calcareous nannofossils of the Kerguelen Plateau (southern Indian Ocean) and Prydz Bay (East Antarctica). In: Barron, J. A., Larsen, B., et al. (Eds.), Proc. ODP, Sci. Results, 119. College Station, TX (Ocean Drilling Program), pp. 467-493.

Wei, W., Wise Jr., S.W., 1990. Middle Eocene to Pleistocene calcareous nannofossils recovered by Ocean Dilling Program Leg 113 in the Weddell Sea. In: Barker, P.F., Kennett, J.P., et al. (Eds.), Proc. ODP, Sci. Results, 113. College Station, TX (Ocean Drilling Programm), pp. 639-666.

Whiting, M.C., Schrader, H., 1985. *Actinocyclus ingens* Rattray: reinvestigation of a polymorphic species. Micropaleontology, 31, 68-75.

Williams, D.M., 1989. *Cavitatus* D.M. Williams, nov. gen.: a new genus of fossil diatom (Bacillariophyta) based on *Synedra jouseana* Sheshkova-Poretskaya. Rev. Palaeobotany and Palynology, 58, 357-363.

Wise, S.W., Breza, J.R., Harwood, D.M., Wei, W., Zachos, J.C., 1992. Paleogene glacial history of Antarctica in light of Leg 120 drilling results. In: Wise, S.W., Jr. SChlich, R. et al. (Eds.), Proc. ODP, Sci. Results, 120. College Station, TX (Ocean Drilling Programm), pp. 1001-1030.

Wright, J.D., Miller, K.G., 1996. Control of North Atlantic Deep Water circulation by the Greenland-Scotland Ridge. Paleoceanography, 11 (2), 157-170.

Yanagisawa, Y., Akiba, F., 1990. Taxonomy and Phylogeny of the three marine diatom genera, *Crucidenticula, Denticulopsis, Neodenticula.* Bulletin of the Geological Survey of Japan, 41 (5), 197-301.

Zachos, J., Pagani, M., Sloan, L., Thomas, E., Billups, K., 2001. Trends, rhythms, and aberrations in global climate 65 Ma to present. Science, 292, 686-693.

Zielinski, U., 1993. Quantitative estimation of palaeoenviromental parameters of the Antarctic surface water in the Late Quaternary using transfer functions with diatom. Reports on Polar Research, 126. Ph.D. Thesis, Alfred-Wegener-Inst. for Polar and Mar. Res., Bremerhaven, Germany.

Zielinski, U., Gersonde, R., 1997. Diatom distribution in Southern Ocean surface sediments (Atlantic sector): Implications for paleoenviromental reconstructions. Palaeogeogr., Palaeoclimatol., Palaeoecol., 129, 213-250.

Zielinski, U., Gersonde, R., 2002. Plio-Pleistocene diatom biostratigraphy from ODP Leg 177, Atlantic sector of the Southern Ocean. Marine Micropaleontology, (in press).

Zielinski, U., Gersonde R., Sieger, R., Fütterer, D., 1998. Quaternary surface water temperature estimations: calibration of a diatom transfer function for the Southern Ocean. Paleoceanography, 13(4), 365-383.

7. Acknowledgments

I am grateful to Prof. Dr. D. Fütterer for supporting this study. I would also like to thank Prof. Dr. H. Willems for taking on the second expert opinion.

Special thanks to Dr. R. Gersonde, who initiated this work, for supervising and for his critical and helpful comments.

I am grateful to many colleagues at the institute for their cooperation and discussion.

I wish to thank

- Dr. U. Zielinski. His PhD thesis was the decisive factor for me to work with Diatom. He gave me excellent support concerning the numerous taxonomical problems.
- Dr. C.-D. Hillenbrand for all discussions about the Miocene climate and for the good hints at literature articles.
- Anja Nimmergut for the numerous discussions and the nice time in our small office.
- Dr. M. Kunz-Pirrung, C. Bianchi and N. Kadagies for the friendly atmosphere in the research group.
- U. Bock, I. Klappstein, T. Pollak and R. Cordelair for their hints concerning diatom preparation and the fun we had in the lab.
- O. Ritzmann, Dr. J. Matthiessen, Dr. C. Hass, Dr. J. Rogenhagen, Dr. G. Eagles, Dr. T. Boebel, D. Birgel and M. Rudolph for all the „smaller“ scientific discussions.

...and to all who helped with the correction of this manuscript.

8. Appendix: Range charts of selected diatom species at ODP Sites 689, 690, 701, 704, 1088 and 1092.

For ease of comparison with previous studies, absolute counting values were converted to the ODP abundance classes. Range charts presenting relative abundances of diatom species are available at *http://www.pangaea.de*.

SSODZ = Southern Southern Ocean Diatom Zonation (see Chapt. 2.4.1)

NSODZ = Northern Southern Ocean Diatom Zonation (see Chapt. 2.4.2)

mbsf = meter below sea floor

mcd = meter composite depth

ODP abundance classes:

D (dominant)= >60 % of assemblage

A (abundant) = 30-60 % of assemblage

C (common) = 15-30% of assemblage

F (few) = 3-15 % of assemblae

R (rare) = 0.5-3% of assemblage

T (trace) = sporadically occurrence

X (present) = diatom valves cannot be counted individually

Preservation:

p = poor; only some strongly silicified, often fragmented diatoms could be observed

m = moderate; lightly silicified diatoms are still present, but with some alterations

g = good; lightly silicified forms are present, no alteration of frustules

Hole 689B range chart - Stratigraphic occurrence of selected diatom species - 1/3

Zone (SSODZ)	Hole 689B Core-section (interval in cm)	Depth (mbsf)	Preservation	Actinocyclus fasciculatus	Actinocyclus ingens	Actinocyclus ingens var. nodus	Actinocyclus ingens var. ovalis	Actinocyclus karstenii	Actinoptychus senarius	Asteromphalus hookeri	Asteromphalus inaequabilis	Asteromphalus kennettii	Asteromphalus oligocenicus	Azpeitia tabularis	Cavitatus jouseanus	Cavitatus miocenica	Chaetoceros sp.	Corethron cryophilum	Coscinodiscus lewisianus	Coscinodiscus marginatus	Coscinodiscus rhombicus	Crucidenticula kanayae	Crucidenticula nicobarica	Dacyosien antarctica	Denticulopsis crassa	Denticulopsis dimorpha	Denticulopsis maccollumii	Denticulopsis ovata
T. inura	2H-5, 27-28	11,57	G											R				T		C								
H. triangularus- F. aurica	2H-5, 55-57	11,85	G		F															A								
	2H-5, 87-89	12,17	M		F															A								
	2H-5, 114-115	12,44	G											R						F								
	2H-6, 29-30	13,09	G					R						R				T		C								R
	2H-6, 114-116	13,94	G		R		R	R												F								
	2H-7, 18-20	14,48	M		R					T										F								
	3H-1, 28-29	15,08	G		R		T							R				R		F						T		R
	3H-1, 56-58	15,36	G		R															C								R
	3H-1, 114-116	15,94	G		T									R			T			C						T		R
	3H-1, 143-145	16,23	M		T									R						F								
	3H-2, 29-30	16,59	G		T									R			T			F								R
	3H-2, 56-58	16,87	M				T							R						F								
	3H-2, 114-115	17,44	G	R	R			R		T				R						F								T
	3H-3, 58-59	18,38	M	T	F			R						R			T			F						R		R
	3H-3, 118-120	18,98	M		R		T	R				T		R				T		F						R		R
	3H-3, 148-150	19,28	M		F									F						F						R		R
F. arcula	3H-4, 56-58	19,86	M		F		R	T				R		R			T			F					F	R		F
	3H-4, 94-96	20,24	M		F		R	R				T		R						R					T	R		F
	3H-5, 28-29	21,08	G		F		T	T				T		R			R			T					R	R		F
	3H-5, 80-82	21,60	M		R							R		F												R		C
	3H-5, 114-115	21,94	M	T	F		T	T				T		F						R					R			C
A. kennettii- F. praecurta	3H-6, 28-29	22,58	M		R			T				T		F			T			F					R	R		F
	3H-6, 55-57	22,85	G		R							R		C						F					T	R		F
	3H-6, 113-114	23,43	G		F							R		C			R			F					R	T		F
	3H-6, 148-150	23,78	M		A							R		C						F								F
	4H-1, 58-58	24,86	M		A			R						C						R								R
	4H-1, 112-113	25,42	G		A							R		F						F								R
	4H-2, 28-29	26,08	G		A			R				R		F			T			R								F
	4H-2, 113-114	26,93	G		A							R		F						F					T	R		F
	4H-3, 31-32	27,30	M		A							T		F			T			F					T	R		F
	4H-3, 114-115	28,13	M		A							R		F						F					R	T		F
F. praecurta	4H-4, 29-30	29,09	M		C									F			T			F						R		F
	4H-4, 113-114	29,93	M		C									F			R			F					T	R		F
	4H-5, 28-29	30,58	G		F									R			T			F						R		F
	4H-5, 55-57	30,85	G		R									R						C						R		C
	4H-5, 148-150	31,78	M		T									R						F						F		A
	4H-6, 28-29	32,08	G		T			T		T				R						F						F		D
	4H-6, 87-89	32,67	M											R						F						F		D
	4H-6, 114-115	32,94	G		T			T						R						F						F		D
	4H-7, 32-34	33,62	M											R						R						F		D
	5H-1, 28-29	34,08	M		R			T						R			T			R						R		D
	5H-1, 118-120	34,98	G		T									R						R						F		D
	5H-2, 28-29	35,58	M		T									R						R						F		D
	5H-2, 86-88	36,16	M																	R						F		D
	5H-2, 114-115	36,44	G					T						R						R						F		D
	5H-3, 28-29	37,08	M		T			T						R						R						C		D
	5H-3, 56-58	37,36	M		T									R						T						F		D
	5H-3, 114-115	37,94	G		T			R						T						R						R		D
D. dimorpha- D. ovata	5H-3, 145-147	38,25	M		R									T						R						R		D
	5H-4, 27-28	38,57	G		R			T						T						R						F		D
	5H-4, 86-88	39,16	M											R						R						C		D
	5H-4, 114-115	39,44	G		T									R						R						C		D
	5H-5, 28-29	40,08	M		R									R			T			T						A		A
	5H-5, 114-115	40,94	M		R			T						R						R						A		F
	5H-6, 28-29	41,58	P		F									T			T			R						C		C
D. ovata- N.denticuloides	5H-6, 114-115	42,44	G		R									R						R						A		F
	5H-7, 17-19	42,97	M		F									R												C		F
	6H-1, 28-29	43,58	G		R									R			T			R						F		R
D. dimorpha	6H-1, 114-115	44,44	G		R									R			T			R						R		
	6H-2, 28-29	45,08	M		F	F								R						F						F		
	6H-2, 114-115	45,94	M	R	A	F								F			T			F						R		
	6H-3, 28-29	46,58	P		C	F								F			R			F			C			T		
D. praedimorpha	6H-3, 114-115	47,44	G		A	F								F			T	T		F			F					
	6H-4, 28-29	48,08	P		A	R								R			R			F			R					
N. denticuloides	6H-4, 114-115	48,94	M		C	F								F						R			T					
	6H-5, 28-29	49,58	M		D	C								F									T					
	6H-5, 114-115	50,44	G		C	C								F			T			R			F					
D. simonsenii- N. grossepunctata	6H-6, 28-29	51,08	P		A	C								F						F			R					
	6H-6, 114-115	51,94	M		A	C								R						R			R					
	6H-7, 28-29	52,58	M	T	A	C								F			T			F			R					
A. ingens var. nodus	7H-1, 28-29	53,18	G		A	C								F						R			R					
	7H-1, 115-116	54,05	P	R	D	C								R						R			R				F	
	7H-2, 28-30	54,68	G		D	F					T									R							R	
	7H-2, 65-67	55,05	M		C	A														R							C	
N. grossepunctata	7H-2, 115-116	55,55	M		R								R	R	R		R			F			C				A	
	7H-2, 144-146	55,84	P						R											F							D	
	7H-3, 28-29	56,18	G		R				T		T			T	R					R							D	
	7H-3, 86-88	56,76	M		T															R							D	
	7H-3, 115-116	57,05	G		T									R	F				T	R				T			D	
	7H-3, 145-147	57,35	M											R													D	
A. ingens - D. maccollumii	7H-4, 28-29	57,68	G						T					R	F		T	T	T	R		T					D	
	7H-4, 86-88	58,26	M		T								R	F						R		R					D	
	7H-4, 115-116	58,55	M		R									R	R				T	R		R					D	
C. kanayae	7H-5, 28-29	59,18	M						T		T		R		R					R		R		T				
?	7H-5, 55-57	59,45	M										T							F								
	7H-5, 86-88	59,76	P						R					R						F								
	7H-5, 115-116	60,05	M						F				R		R				T	F								
	7H-6, 28-29	60,68	G						F				R	F	F				R	F								
	7H-6, 115-116	61,55	M						T				T	F	F				T	F								
	7H-7, 28-29	62,18	M										R	F	F					R								

Hole 689B range chart - Stratigraphic occurrence of selected diatom species - 2/3

Depth (mbsf)	Denticulopsis praedimorpha	Denticulopsis simonsenii	Ethmodiscus sp.	Eucampia antarctica	Fragilaria sp.	Fragilariopsis arcula	Fragilariopsis aurica	Fragilariopsis barronii	Fragilariopsis cylindrica	Fragilariopsis claviceps	Fragilariopsis clementia	Fragilariopsis donahuensis	Fragilariopsis efferans	Fragilariopsis fossilis	Fragilariopsis maleinterpretaria	Fragilariopsis praecurta	Fragilariopsis praeinterfrigidaria	Fragilariopsis pseudokerguelensis	Fragilariopsis pusilla	Fragilariopsis reinholdii	Hemidiscus cuneiformis	Hemidiscus triangularus	Katathiraia aspera	Mediaria splendida	Navicula sp.	Neobrunia mirabilis	Nitzschia denticuloides	Nitzschia grossepunctata	Paralia sulcata	Pleurosigma directum
11,57			X			R	C	R						R		F	F													
11,85							R									F	F													
12,17						R	C							R		R	C													
12,44		T		R		F	A				R					T	F								R					
13,09						F	F							R		C	F													
13,94						R	A									A	F													
14,48						F	A									F	F													
15,08			X	R		F	A					R		R		F				T				T						T
15,36						F	A					R				F														
15,94			X			F	C					T				F	T								T					
16,23						F	A					T				F					R									
16,59			X			F	C					T		T		C						T								
16,87						F	C					T		R		C					R									
17,44					T	F	R					R		F		C						R								
18,38						C	F					R		R		F					R	F								
18,98			X		T	C	F					R		T		F					T	F								
19,28						C	F					R		R		F						R								
19,86		C				F	R					R				R					T		T							
20,24		C	X			C	F					R				F							T	T						
21,08		C	X			C	R		R			R		R		R							T			X				
21,60		A				C						R		T		F														
21,94		C				C	R					R		R		R							T	T						
22,58		A					F			R		R		T									T	T						
22,85		A								T																				
23,43		F			R		F			R		F				R							T	R						
23,78		F																												
24,86		C																												
25,42		C								R						F														
26,08		C	X							R						R														
26,93		F					R					R											T							
27,30		F					R			R		R				R														
28,13		C					R			T		T				T							T							
29,09		A					R			T		F				R														
29,93		A					R			R		R	T			R														
30,58		A					R					F				F							R							
30,85		A														F							T							
31,78		F								T		R				T														
32,08		F														T							T							
32,67		F														R							T							
32,94		F								T						R							T							
33,62		F														R														
34,08		F										T				T							T							
34,98		F										T				T							T							
35,58		R								T			T			R							T							
36,16		R														R														
36,44	T	R														R														
37,08		F	X							R						T							T							
37,36		R																												
37,94		T											T			R														
38,25		T																												
38,57		R		T						T													T							
39,16		R																												
39,44	R	R	X							R																				
40,08	C	F			T								R																	
40,94	A	R																												
41,58	A	R										R																		
42,44	A	R																									F			
42,97	D	T																												
43,58	D	T			T							R	R														F			
44,44	D	R										R	R														R			
45,08	A	F											R														F			
45,94	C	F	X							T																	F			
46,58	C	F	X																								F			
47,44	R	F	X									F	R														F			
48,08	R	C										R															C	R		
48,94		F										R												T			C	R		
49,58		R											T														F	R		
50,44		C										F	R					T					R				F	F		
51,08		F										T						R										F		
51,94		F																										F		
52,58		F		T								R																F		
53,18																		R										R	T	
54,05																														
54,68																								T						
55,05																														
55,55																								R						
55,84																												R		
56,18															T									T				F		
56,76															T									T						
57,05															T									T				R		
57,35																												R		
57,68																			R					R						
58,26																														
58,55															F															
59,18			X												D				R					T						
59,45															D				F											
59,76															D				F											
60,05			X												D				F											
60,68			X																F						R					
61,55			X												D				R											
62,18			X												A				F					R						

Hole 689B range chart - Stratigraphic occurrence of selected diatom species - 3/3

Depth (mbsf)	*Proboscia barboi*	*Raphidodiscus marylandicus*	*Rhizosolenia antenata*	*Rhizosolenia hebetata*	*Rouxia isopolica*	*Rouxia naviculoides*	*Rouxia peragallii*	*Rouxia* sp. 1	*Rouxia* sp. 2	*Rocella gelida*	*Thalassionema nitzschioides*	*Thalassionema nitzschioides* var. *parvum*	*Thalassionema nitzschioides* var. *capitulatum*	*Thalassiosira convexa* var. *aspinosa*	*Thalassiosira yabei*	*Thalassiosira inura*	*Thalassiosira fraga*	*Thalassiosira miocenica*	*Thalassiosira oestrupii*	*Thalassiosira oliverana* var. *sparsa*	*Thalassiosira praelineata*	*Thalassiosira spinosa*	*Thalassiosira torokina*	*Thalassiothrix longissima*	*Thalassiothrix miocenica*
11,57	F			F	R	F	R				R					F			R					R	
11,85	C			R	R	C					R								R						
12,17	F			R	R	C					R														
12,44	R		R	R	F	F	R				R								R					R	
13,09	F			T	R	F	R				R								R					R	
13,94	R		T	T	R	R	R				R										R		T	T	
14,48	R			R	R	T					F								T				T	T	
15,08	R		R	F	F	F	R				R								T	R			T	R	R
15,36	F		T	F	F	F	R													T				R	
15,94	F		R	F	R	F	R				T	R		R					R	T			T	R	
16,23			R	R		F	T													T			R	R	
16,59	F		T	F	T	F	R							F						T			R	R	
16,87	F			T		F	T							F						T			R	R	
17,44	F		R		R	F	R					R		F						R			R	T	
18,38	F		T	F	F	R								F						F			R	R	R
18,98	R		R	F	F	F												R		F	R		T	R	T
19,28				F		F												F		F				F	R
19,86			R	F	R	T												F		F			T	R	F
20,24			R	F	R													R		F			R	R	R
21,08			R	F	R	R														R	R		R	R	F
21,60				F																				F	
21,94	T			F	R	R																		R	
22,58	T		R	F	F	R					R										T			R	
22,85			T	R		T					T														
23,43			R	F	F	F					T													R	
23,78			R			F																		R	
24,86				R	R																				
25,42	R		R	R	T	R																		R	
26,08			F	T	R	R					R													T	
26,93	R		R	R	R																			R	
27,30	T		R	F	R																			R	
28,13			R	R	R																			R	
29,09	T		R	F	R																			R	
29,93	T		R	F	F	F																		R	
30,58			R	F	F	F																		R	
30,85			R	R	R																				
31,78			R	T																					
32,08	T		T	T	T										T						T			T	
32,67			T	T											T										
32,94	T		T	R							T				T									T	
33,62			T	R											T										
34,08	T		T	T		T									T						T			T	
34,98	R		T	T											T						R			T	
35,58	T		T	R											T						T			T	
36,16	T		T	R																					
36,44			R	R																				T	
37,08				R											R									T	
37,36																									
37,94	T		T																					T	
38,25																									
38,57	T			T																				T	
39,16																									
39,44			T	T																				R	
40,08			T	R							T														
40,94	R		R	R							T													R	
41,58	R		R	R																				R	
42,44	T			R	R																			R	
42,97	T			R																					
43,58	T		T	T									T											T	T
44,44	T		T	T	T	T					T													T	
45,08			R	F	R								R											R	R
45,94	R		R	F									R											R	R
46,58	R			R									R											F	
47,44	R			R	R	R					F													R	
48,08				R									R											F	
48,94	T			R		F		F																T	
49,58				T		R																		R	
50,44	R			F				F			T													R	
51,08				R	T			F																R	
51,94	R			T				R																T	
52,58	R			R	R			F			R													T	
53,18	R			T	F	T					R		F											T	
54,05	T										T													T	
54,68																								T	
55,05	R			R																					
55,55	R					R			F				R									F		R	
55,84	R																					R			
56,18	R			T	R						T		R											T	
56,76											T		R											T	
57,05	R			T					R		T		R									T			
57,35	R								R		T											T			
57,68	R								T				F									T			
58,26											T														
58,55		F		T					T				F									R			
59,18				T					R		T		F									R		T	
59,45				T					T				F									F			
59,76				R									F									F			
60,05				T					T				F				R					F			
60,68	R			R					F				F				F					A		R	
61,55	T			R		R			F								F					F			
62,18	R			R					R								F					C		R	

Hole 690B range chart - Stratigraphic occurrence of selected diatom species - 1/2

Zone (SSODZ)	Hole 690B Core-section (interval in cm)	Depth (mbsf)	Preservation	*Actinocyclus fasciculatus*	*Actinocyclus karstenii*	*Actinocyclus ingens*	*Actinocyclus ingens* var. *nodus*	*Actinocyclus ingens* var. *ovalis*	*Actinoptychus senarius*	*Asteromphalus kennettii*	*Asteromphalus oligocenicus*	*Azpeitia tabularis*	*Cavitatus jouseanus*	*Chaetoceros* sp.	*Corethron cryophilum*	*Coscinodiscus marginatus*	*Coscinodiscus lewisianus*	*Crucidenticula kanayae*	*Crucidenticula nicobarica*	*Dactyosolen antarcica*	*Denticulopsis crassa*	*Denticulopsis dimorpha*	*Denticulopsis maccollumii*	*Denticulopsis ovata*	*Denticulopsis praedimorpha*	*Denticulopsis simonsenii*	*Ethmodiscus* sp.	*Eucampia antarctica*	*Fragilariopsis arcula*	*Fragilariopsis aurica*	*Fragilariopsis claviceps*	*Fragilariopsis clementia*	*Fragilariopsis cylindrica*
T. inura	3H-2, 27-28	13,47	G			R						F		F	R	R														F		R	
	3H-2, 115-116	14,35	M									F				F											X	R		C			
	3H-3, 27-28	14,97	G									R			R	C											X	T	R	F			
H. triangularus- *F. aurica*	3H-3, 73-75	15,43	M									C				C													R	F			
	3H-3, 115-116	15,85	M									R				F													R	A			
	3H-4, 23-25	16,47	G			R		F				R			R	C												R		F		R	
	3H-4, 73-75	16,97	M									D				F													R	F			
	3H-4, 115-116	17,35	P					R				F				C								R		R	X	R	F	F			R
	3H-5, 27-28	17,97	G			R		T				T		T		F								R		R			C	F			
	3H-5, 73-75	18,43	P					R				D				F										R							
F. arcula	3H-5, 115-116	18,85	P									D				F													R				
	3H-6, 23-25	19,47	P		R	F		R		F		R				F					R	F		C		F			R				
	3H-6, 73-75	19,97	M			D						C				F						F		F					R				
	3H-6, 115-116	20,35	P			F		R				F				C					F	F		F		C			F				
	3H-7, 27-28	20,97	G		R	R				T		F				T					F	R		R		A			F	F	R		
A. kennettii- *F. praecurta*	4H-1, 26-27	21,66	M			A				R		F				F					T	R		F		F				T	T		
	4H-1, 49-51	21,89	M			D						F									R	R		F		F					R		
	4H-1, 115-116	22,55	G		R	A				R		F			T	F					R	R		F		C				R	R		
	4H-2, 28-29	23,18	G		T	C				R		R				F					R			C		C				F	T		
	4H-2, 115-116	24,05	G		R	F				R		F				F					R	T		F		A					T		
F. praecurta	4H-3, 26-27	24,66	M		T	R						R				F						R		D		R				T			
	4H-3, 115-116	25,55	M			T						R				R						R		D		R							
	4H-4, 27-28	26,17	M									R				R						F		D						R			
	4H-4, 115-116	27,05	P									R				T						F		D		R							
	4H-5, 26-27	27,66	M		R							R				T						F		D		R					T		
	4H-5, 115-116	28,55	P		T							R				T						R		D		R					T		
D. dimorpha- *D. ovata*	4H-6, 27-28	29,17	P									T				T						R		D									
	4H-6, 115-116	30,05	M			T						R				R								D	T	R					R		
	5H-1, 28-29	31,38	M			R						R										F		A	A	R					R		
D. ovata- *N. denticuloides*	5H-1, 116-117	32,26	M			R						F				R						C		F	A	R							
	5H-2, 28-29	32,88	M			R						R										R		C	D	T							
D. dimorpha	5H-2, 115-116	33,75	M			F						R				R						C			A	T							
	5H-3, 28-29	34,38	P			T						R				R			R			F			D								
	5H-3, 115-116	35,25	M	R		F	F					R				F						F			A	F	X				R		
D. praedimorpha	5H-4, 28-29	35,88	M			F	F					R		T		F			F						A	R							
	5H-4, 115-116	36,75	G			F	F					F				F									D	F	X						
	5H-5, 28-29	37,38	P			C	F					F				F			F						R	R	X						
N. denticuloides	5H-5, 115-116	38,25	G			C	C				T	F				R										F							
	5H-6, 28-29	38,90	M			C	F					F				F										C							
D. simonsenii- *N. grossepunctata*	5H-6, 115-116	39,77	G			A	A					R				R			T							F							
	5H-7, 28-29	40,40	M			A	C					R				F			R							F	X						
A. ingens var. *nodus*	6H-1, 27-28	41,07	G			D	C				R		R			R			R				F										
	6H-1, 50-52	41,30	M			A	C				T	R	F			F			R				F										
	6H-1, 114-115	41,94	P			C	F		R				C			F			F				C										
N. grossepunctata	6H-2, 27-28	42,57	M			F			R			R	F			F		F					A										
	6H-2, 49-51	42,79	M			F						T	C			F		F	R				A				X						
	6H-2, 114-115	43,44	M			F						R	F			F		F	F	R			A				X						
D. maccollumii	6H-3, 27-28	44,07	G								R	T	R			F		R	R				F				X						
C. kanayae	6H-3, 49-51	44,29	M								R		R			F		F															
	6H-3, 114-115	44,94	M										T			R				T													
	6H-4, 27-28	45,57	M						R		T		F			F	T										X						
	6H-4, 114-115	46,44	P								T		F			F	R	R									X						
	6H-5, 27-28	47,07	P								R		C			F		F									X						
	6H-5, 114-115	47,94	P										C			F																	
?	6H-6, 27-28	48,57	P								T		D			R											X						
	6H-6, 49-51	48,79	P								R		D			R											X						
	6H-6, 114-115	49,44	P										A			F																	
	6H-7, 27-28	50,07	P								F		A														X						

Hole 690B range chart - Stratigraphic occurrence of selected diatom species - 2/2

Depth (mbsf)	*Fragilariopsis donahuensis*	*Fragilariopsis efferans*	*Fragilariopsis maleinterpretaria*	*Fragilariopsis praecurta*	*Fragilariopsis praeinterfrigidaria*	*Fragilariopsis pusilla*	*Mediaria splendida*	*Navicula* sp.	*Neobrunia merabilis*	*Nitzschia denticuloides*	*Nitzchia groosepuncata*	*Pleurosigama directum*	*Proboscia barboi*	*Raphidodiscus marylandicus*	*Rhizosolenia hebetata*	*Rhizosolenia antenata*	*Rouxia isopolice*	*Rouxia naviculoides*	*Rouxia peragalli*	*Rouxia* sp. 1	*Rouxia* sp. 2	*Thalassionema nitzschioides*	*Thalassionema nitzschioides* var. *capitulatu*	*Thalassionema nitzschioides* var. *inflatum*	*Thalassionema nitzschioides* var. *parvum*	*Thalassiosira convexa* var. *aspinosa*	*Thalassiosira inura*	*Thalassiosira fraga*	*Thalassiosira oestupii*	*Thalassiosira oliviverana* var. *sparsa*	*Thalassiosira praelineata*	*Thalassiosira spinose*	*Thalassiosira spumellaroides*	*Thalassiosira yabei*	*Triceratium cinnamomeum*	*Thalassiothrix longissima*	*Thalassiothrix miocenica*
13,47				R	F								F		C		R	F	F			R		R			F		R							F	F
14,35				F	C								F		F	R	R	R				F					R		R							R	
14,97				F	F								C		F		R	R	F			R		R			R									R	T
15,43				R	F								R				R	R						D												R	
15,85				F	C								F		R	T		F				R		R												R	
16,47	R			F	C								F		R	R	F	R	R			F		R	R											R	R
16,97				F	C								F		R	R						R			R											R	
17,35	R			F	C								F		F	R	R	R				R			R	F				R						F	R
17,97	R			C									F		F	F	R	F	F			R		T	T	R				R						R	
18,43	R												R		R			R						T		R										R	
18,85	T												R		R									F												R	
19,47	R												T		C	R																				R	
19,97													R		F	R																				R	R
20,35															C			R																		R	
20,97	F			T			T						R		F	R	F	R	R			R														R	
21,66	T												T		F	T																				R	
21,89	R														R	R																				R	
22,55	R			R											F	R	R																			R	
23,18	F			R									R		R	F	R	R																T		R	
24,05	R			F									R		F	R	F	F																		R	
24,66				R									R		R	T		T													R			T			
25,55				R									T		R	R																				T	
26,17															R		T																	R		T	
27,05													R		R	T																				T	T
27,66				R									T		R																					T	
28,55				F											T	R																				T	
29,17																																				T	
30,05															T																					T	
31,38													R									T														T	
32,26										R			R		R	R			R			R														R	R
32,88	R									R			T		R	T			R																	T	
33,75	R									F			R		R	R			R																	R	
34,38		T								F			R		R				T																	R	
35,25		R								F			T		F	T			T			T														R	T
35,88		R								F			R		R				R			R														R	T
36,75		R								F					F				T				R													R	
37,38										A			R						R	F																F	
38,25		R								F					R					F	R															R	
38,90	R									C	F		R		R					R																R	
39,77		T									F		R		T					T	T																
40,40	R	R	R						X		F		R						R	F	R															R	
41,07			T								R		R						R													R				T	
41,30			R								R		T						F				T									R				R	
41,94			R								R		R										F									F				R	
42,57			R								R		R		T																	R				T	
42,79			T								R		R						T				R									T					
43,44			F			R					R		R	F									F													R	
44,07			D			R	R						R	T					T	T	R		F									T					
44,29			D			F													R				F									R				T	
44,94			A			R						T									R	T	A									R					
45,57			D			R		T					T	R							R		F					R				F				T	
46,44			C			F							R		T				R		R							R				A			R		
47,07			A			R		R											R				F					F				C					
47,94			F				R												C				F					C				F					
48,57			T				R	T					T															R				F	T			T	
48,79			F										R															R				F					
49,44			F										F		R													F				F	F				
50,07			F																													C	R				

Hole 701C range chart - Stratigraphic occurrence of selected diatom species - 1/2

Zone (NSODZ)	Hole 701C Core-section (interval in cm)	Depth (mbsf)	Preservation	*Actinocyclus curvatulus*	*Actinocyclus ellipticus*	*Actinocyclus ingens*	*Actinocyclus ingens* var. *ovalis*	*Actinocyclus karstenii*	*Actinoptychus undulatus*	*Asteromphalus kennettii*	*Azpeitia tabularis*	*Chaetoceros* sp.	*Coscinodiscus marginatus*	*Coscinodiscus radiatus*	*Denticulopsis crassa*	*Denticulopsis dimorpha*	*Denticulopsis ovata*	*Denticulopsis simonsenii*	*Eucampia antarctica*	*Fragilariopsis arcula*	*Fragilariopsis aurica*	*Fragilariopsis clementia*	*F. donahuensis*	*Fragilariopsis fossilis*	*Fragilariopsis praecurta*	*Fragilariopsis praeinterfrigidaria*	*Fragilariopsis reinholdii*	*Hemidiscus cuneiformis*
T. inura	13H-1, 10-11	110,90	P					R			R	R	R	R					R		R	R	R	R	F	F	F	
	13H-1, 100-101	111,80	G								R	R		R					F		R			R	R	R	R	
	13H-2, 50-51	112,80	G								R	R	R	R					R		R	R		R	F	R	F	
H. triangularus - *F. aurica*	13H-2, 149-150	113,79	G		R	F		R	F		F	F	R	F				R					R	F	F	F	F	
	13H-3, 99-100	114,79	M			T					R	R	R	R						R	R	R	R	R	F	R	R	
	13H-4, 50-51	115,80	M			R		R			R	R	R	R				R	R	R	R	R	R	R	R		R	
	13H-4, 149-150	116,79	P			T		R				R	R					R	R		R	R	R	R	R	R	F	
	13H-5, 99-100	117,79	P		R	T			R			R	R								R	R		F	R	R	F	
	13H-6, 49-50	118,79	P			T					R	R	R						R	R	R	R		R	R	R	R	
	14H-1, 49-50	120,79	P			R		R			R	R	R	R				R	R	R	R			R	R	R	R	
	14H-1, 149-150	121,79	P			R					R	R	R						R	R	R	F		R	F	R	R	
	14H-2, 100-101	122,80	M			R					R		R					R	R					R	R		R	
	14H-3, 50-51	123,80	M			R		R			R	R	R	R				F	A	R	R	R		F	R	R	R	
	14H-3, 149-150	124,79	M	R	R	R		R			R	R		R					F		R			R	F	R	R	
	14H-4, 99-100	125,79	M			T					F	R	R	R	R			R	R		F			R	F	R		
	14H-5, 50-51	126,80	G			F		R			R		R	R					R		R				R	R	R	
	14H-5, 149-150	127,79	M	R		R					R	R	F	R					R		F	R		R	F		R	
	14H-6, 49-50	128,29	M	R		F					R	F	F	R					F		F			R	F	R		
	15H-1, 45-46	130,25	M	R		T		R			R	R	C	R	R			R	F		F	R		F	F	R	R	
	15H-1, 145-146	131,25	M			R		R			R		F	R				R	R		R	R		F	F	F	R	
	15H-2, 105-106	132,35	P					R			R	R	F	R	R				F	R	R	R	R	R	F	F	R	
	15H-3, 45-46	133,25	G								R		R	R	R			R	R	R	R		R	R	F	R	R	
	15H-3, 145-146	134,25	P			R		R			R	R	F	R	R			R	F	R			R	R	F	R	R	
	15H-4, 105-106	135,35	P			R		R			R	R	C	R				R			R	R	R	R	F		F	
	16H-1, 10-11	139,40	P			T	R		R		R	R	F	R	R			R				R	R	R	F		R	
	16H-1, 109-110	140,39	P			T	F				R	R	C					R		R			R	F	F		F	
	16H-2, 59-60	141,39	P								R	R	C	R				R						F	R		R	
	16H-3, 9-10	142,39	M			R					R		C	R				R		R	F	R	R	F	F	R	R	
	16H-3, 109-110	143,39	M			R			R		R		F		R			R	R					R	F	R	R	
	16H-4, 59-60	144,39	P	R		R		R	R		R		C	R				F			R	R	R	R	R			
	16H-5, 10-11	145,40	P			F	F		R				F									R		F	R		F	
	16H-5, 110-111	146,40	M			F		R			F			F									R	F	R	F	F	
	16H-6, 60-61	147,40	M			F					F			F													F	
	16H-7, 10-11	148,40	M		R	F		F			F		R	R							R			R			F	
	17H-1, 60-61	149,40	M		R	F		F			F	R	F	R				R			R			R			F	
	17H-2, 10-11	150,40	M			R	R	R			F		R	R									R	R			F	
	17H-2, 110-111	151,40	M		R	R	F	R			R							R				R	R	F	R		F	
	17H-3, 59-60	152,39	M			R					R		R											F			F	
	17H-4, 59-60	153,89	M		R	R		F			F	R		R				F			R			F			C	
	17H-5, 110-111	155,90	M			F					R		R							R				R	R		R	
	17H-6, 75-76	157,05	M								R		F	R			R								R		F	
	17H-CC, 22-23	157,89	M		R						F			R			R										F	
	18H-1, 99-100	159,29	M								F			R										F	F		R	R
	18H-2, 40-41	160,20	M		R	R					R			F									R	R	R		F	
	19H-1, 30-31	168,10	M		F	R	F	R			F			F										R	R		F	
	19H-1, 130-131	169,10	M				F	R			F	R		R				R		R							F	R
	19H-CC, 20-21	170,14	M		R		F	R			R		R	R						R			F		F		R	
A. kennettii	20H-1, 80-81	178,10	G			T							F	R		R		R		R		R	R	R	F			
	20H-2, 30-31	179,10	M							R	R		C	R	R	F		F		R		R	R	R	F			
	20H-2, 129-130	180,09	M			T		R			R		F	R		F		R	R	R		R		F	F			
	20H-3, 81-82	181,11	P			T		R		R	R		C	R		R		F	R				R	R	F			R
	20H-4, 30-31	182,10	P					R					A	R		R		R	F				R	R	R			
	20H-4, 129-130	183,09	P			T		R		R	R		C	F		F		F				R	R	R	F			
	20H-5, 84-85	184,14	P					F		R	R		R	F		F		F	R				R	R	R			
	20H-6, 40-41	185,20	P					R		R.			C	F		R		F					R	R	F			
	21H-1, 79-80	187,59	M					R	R	F			F	R		R	R	F				R	R	R	F			
	21H-2, 37-38	188,67	P					R		R	R		C	F		R		F	R					R	F			R
	21H-2, 137-138	189,67	P							R			F	R		R		R				R	R	R	R			
	21H-3, 88-89	190,68	P					R		R			F	R		R	R	R	R				R	R	R			R
	22H-2, 24-25	198,04	P			T		R	F				R	R		R	R	R							R			
	22H-2, 121-122	199,01	M					R					F	R		R	R	F	R						R			
	22H-3, 71-72	200,01	M			T				R			R	F	R	F	R	F	F			R	R	R	R			
	22H-4, 20-21	201,00	P						C	R			R	F		F		R	R					R	R			
	22H-4, 122-123	202,02	M			T		R					R	F		R	F	F	R				R	R	R			
	22H-5, 71-72	203,01	P										R	R	R	R	F	F					R					
	22H-6, 20-21	204,00	M			R		R		R			R	F			C	F						R	R			
	22H-6, 124-125	205,04	P			R		R			R		R	R		R	R	R					R	R	R			
	22H-CC, 10-11	205,79	P			R		R			R		R	R		R	F	F	F				R					

Hole 701C range chart - Stratigraphic occurrence of selected diatom species - 2/2

Depth (mbsf)	*Hemidiscus karstenii*	*Hemidiscus triangularus*	*Mediaria splendida*	*Neobrunia mirabilis*	*Nitzschia cylindrica*	*Paralia sulcata*	*Pleurosigma directum*	*Proboscia barboi*	*Pterotheca sp.*	*Rhizosolenia miocenica*	*Rhizosolenia hebetata*	*Rhizosolenia antennata*	*Rhiz. sp.*	*Rouxia heteropolara*	*Rouxia isopolica*	*Rouxia naviculoides*	*Rouxia sp.*	*Stellarima sp.*	*Stephanopyxis sp.*	*Thalassionema nitzschioides*	*Thalassionema nitzschioides sp. A*	*Thalassionema nitzschioides var. capitulatum*	*Thalassionema nitzschioides var. inflatum*	*Thalassionema nitzschioides var. lanceolatum*	*Thalassiosira convexa var. aspinosa*	*Thalassiosira inura*	*Thalassiosira sp. A*	*Thalassiosira oestrupii*	*Thalassiosira oliverana*	*Thalassiosira oliverana var. sparsa*	*Thalassiosira praelineata*	*Thalassiosira torokina*	*Thalassiothrix longissima grp.*	*Thalassiothrix miocenica*
110,90								R			R	R	R		R	R		R	F			F		A		R		R		R	R		F	R
111,80	R											R	R		R	R		R	R					D		R			R				R	
112,80														R	R	R			F					A		R		F	F	R			F	
113,79	R		R	D	R	R					R	F	F		F	R								R						F			R	
114,79													R	R	R	R		F	R					D	R			R		R	R		R	
115,80												R		R	R		R	R	F	R				D	R			R		R			R	
116,79														R				R	F					D	R						R		R	
117,79			R			R					R	R		R	R		R	R	D	R				R	R				R	R			F	
118,79						R	R	R			R		R	R	R		R	R	A	F	C				R			R			R		R	R
120,79						R		R				R	R	R	F	F		R	C	C	F				R			R		R	F	R	F	
121,79						R		R			R	R	R	R	F	F	R	R	F	F	F				R				R	R			F	R
122,80												R		R	R			R	F	F	R				R			R				R	R	
123,80						R	R	R	R		R	F	R		R	R	R	F	F	F	R				R			R				R	F	R
124,79								R				R	R		R	R		F	R	A	R				R			R				R	R	R
125,79										R		R	R		R	R		F	R	C	C											R	R	
126,80								R				R	R			R			R	R	D												R	
127,79						R		R				R	R		F	R		R			R	A			R			R				R	F	R
128,29						R		R			R	R	R		R	F				R		C	R	R				R				F	R	
130,25						R		F			R	R	R		F	R		R	R			R		R								F	R	R
131,25			R			R		R			R	F	R		F					R		C										F	R	
132,35						R		R			R	R	R		R			R	R	R		D										R	R	R
133,25							R	R			R	R	R		F							D	R										R	
134,25						R	R	R		R	R	F	R		F			R				A	R							R		R	F	R
135,35	R		R			R	R	R		R	R	F	F		C			C				R								R		R	F	R
139,40	R							R			R	R	R		F	F	R	R				C		R	F							F	R	R
140,39	R					R		R			R	R	R		R	R						F			R						R	R	F	R
141,39						R	R	R			R	R	R		F	R						C		R	R							F	F	R
142,39	R					R		F			R	R	R		F	R				F		R		R	R						R	R	F	
143,39								R			R	R	R		F					R		A			R						R	R	R	
144,39						R		R				R	R		F	R						C			R					R		R	F	
145,40		A						R			R	R	R		R	R						C			R						R		R	R
146,40	R	R		D		F					R	F	F		R					R										F		R	F	R
147,40		F		D								F	F																	F			F	
148,40		R		D		R						F	F																	F			F	
149,40		R		D		R						C	F		F															R			R	
150,40		F		D							R	C	F		F															F		R	F	R
151,40		F		D								F	F		F					R										F			F	
152,39		F		D							F	C	C		R															R			R	
153,89		F		D		R			F		R	F	C																	F			F	
155,90		F		D		R					F	F	F																	R			F	
157,05		R		D		R					C	C			F															R			F	
157,89		F		D		F					F	C	F																	F			F	
159,29		F		D		F					F	C	R		F					R										F			F	R
160,20	R	R		D				R			R	C	R		R			R												F			C	R
168,10	F	F		D							F	F	F																	F	R		F	
169,10	R	R		D	R						F	F	R		F			F				F		F						F	R	F	F	R
170,14		R	R	D	R	R		R	R		F	R	R		F			F		F										F	R	R	F	R
178,10						R		R			A	R	R		R																R		R	F
179,10				D		R					C	R			R			F		R										R		R	R	F
180,09	R										F	R	R					R					R	A									F	F
181,11	R										C	R	R		R					C										R			F	F
182,10	R										C	R	R		R			F		R													F	F
183,09								R			A	F	R					R		F													F	R
184,14											A	R	R		R			R		F													F	R
185,20								R			C	F	R		R			R		C									R				F	R
187,59	R		R					R			A	F	R		R					F													F	R
188,67	R							R			A	F	R		R																		F	R
189,67	R							F			A	F	R							R													F	F
190,68						R		R			A	C	R				R	R		R							F						F	R
198,04						R					A	R								R							C						R	F
199,01	R							R			A	F	R							R							F						F	F
200,01	R										C	F	R					R		R							C						R	F
201,00								R			C	R	R							F							R						F	R
202,02								R			C	R	R		R					C							F						F	F
203,01											D	R			R					R							R				R		F	R
204,00								R			A	R			R					F							F						F	R
205,04											A	R	R		R					F							F						F	R
205,79	R					R		R			A	R	R		R					R							F						F	R

Hole 704B range chart - Stratigraphic occurrence of selected diatom species - 1/4

Zone (NSODZ)	Hole 704B Core section (interval in cm)	Depth (mbsf)	Preservation	*Actinocyclus curvatulus*	*Actinocyclus ellipticus*	*Actinocyclus fasciculatus*	*Actinocyclus karstenii*	*Actinocyclus ingens*	*Actinocyclus ingens* var. *ovalis*	*Actinoptychus undulatus*	*Asteromphalus kennettii*	*Azpeitia tabularis*	*Cavitatus jouseanus*	*Chaetoceros* sp.	*Coscinodiscus marginatus*	*Coscinodiscus radiatus*	*Denticulopsis crassa*	*Denticulopsis dimorpha*	*Denticulopsis ovata*	*Denticulopsis simonsenii*	*Eucampia antarctica*	*Fragilaria* sp.	*Fragilariopsis arcula*	*Fragilariopsis aurica*	*Fragilariopsis clementia*	*Fragilariopsis donahuensis*	*Fragilariopsis fossilis*	*Fragilariopsis lacrima*
T. inura	24X-1, 2-3	213,72	M			R	R		R					F										R			R	
	24X-1, 81-82	214,51	G						R		R			R	R									R		R	R	R
	24X-2, 5-6	215,25	M				R	R							R								R	F		R	F	R
	24X-2, 93-94	216,13	M				R	R							R									R		R	R	R
	24X-3, 22-23	216,92	M	R				R	R						R							R	R	R		R	R	F
	24X-3, 98-99	217,68	M					R	R			R			R							R	R	R	R		R	R
	24X-4, 29-30	218,49	M					R	R			R			F				R				R	R	R	R	R	R
	24X-4, 107-108	219,27	M				R	R	R			R			R								F	F			R	
	24X-5, 46-47	220,16	M				R	R	F			F			F								R	R		R	R	F
	24X-5, 129-130	220,99	M					R	C			R			F								R				R	
	24X-6, 53-54	221,73	M					R	R			R			F						R		R	R	R		R	R
H. triangularus - *F. aurica*	24X-6, 129-130	222,49	G						R					R	F									R	R			R
	24X-7, 56-57	223,26	M					R	F			R		R	F						R			F	R	R	F	
	25X-1, 7-8	223,27	M					R						F	C							R		F	R		R	
	25X-1, 93-94	224,13	M				F	R	R			R		R	A			R						R	R		F	
	25X-2, 18-19	224,88	P	R		R		R	R			R			A			R						R			F	
	25X-2, 98-99	225,68	M	R								R			C								R	R	R		F	
	25X-3, 32-33	226,52	M	R			R		R			R		R	F				R				R	R			R	
	25X-3, 112-113	227,32	G				R								F									R			R	
	25X-4, 42-43	228,12	M				R		F	F		R			F											R	F	
	25X-4, 120-121	228,90	M				R	R	R			R			C											R	R	
	25X-5, 50-51	229,70	P					R	R					R	F												R	
	25X-5, 129-130	230,49	P					R	R			R			F			R					R			R	F	
	25X-6, 58-59	231,28	M					R	R			F			F			R					R	R			F	
	25X-6, 138-139	232,08	M					R	F			R		R	F			R					R				R	
	25X-7, 64-65	232,84	M					R	R			R			F												F	
	26X-1, 34-35	233,04	G					R	F					R	F							R	R			R	F	
	26X-1, 108-109	233,78	G						F			R			R							R					F	
	26X-2, 28-29	234,48	M					R	R			R		R	F			R					R			R	F	
	26X-2, 108-109	235,28	M		R			R	R					R	F									R		R	F	
	26X-3, 40-41	236,10	M					R	R					R	F							R	R			R	F	
	26X-3, 119-120	236,89	M						R					R	F											R	R	
	26X-4, 53-54	237,73	M			R	R		R	R		R		R	F								R	R		R	F	
	26X-4, 133-134	238,53	P					R						R	R			R	R			R		R			F	
	26X-5, 56-57	239,26	P	R				R				R		R	R			R					R	R	R	R	R	
	27X-1, 29-30	242,49	P					F	R			C		R	R	R	R	R						R	R	R	R	
	27X-1, 110-111	243,30	P				R	R	R	R		F		R	F		R									R	F	
	27X-2, 43-44	244,13	M		R		R	F	R			F		R	R							R		R		R	F	
	27X-2, 120-121	244,90	M		R		R					F			R	R		R						R			R	
	27X-3, 50-51	245,70	M		R			R				R			R	F								R		R	R	
	27X-3, 130-131	246,50	G		R		R	R				F		R										R			R	
	27X-4, 60-61	247,30	M				R	R	R	R		C		R	R	R		R						R		R	R	
	27X-4, 142-143	248,12	M		R			R	R			C		R	R	R							R				R	
	27X-5, 69-70	248,89	P		R			F	F		R	F	R		F							R						
	27X-6, 1-2	249,71	P		R		F	R	R			C	R		F			R				R			R	R	R	
F. reinholdii	27X-6, 83-84	250,53	P		R		R	F			R	R	R		C	R		F								R	R	
	27X-7, 12-13	251,32	P				R	A				R			R			R		R		R					R	
	27X-CC, 14-15	252,08	P	R	R		R	A				R	R		F		R	R		F							R	
	28X-1, 40-41	252,10	P				F	A							F					F								
	28X-1, 120-121	252,90	P				R	A				R		R	C		R	R		R		R					R	
	28X-2, 52-53	253,72	P					A		R		R			F		R	R		R		R				R	R	
	28X-2, 132-133	254,52	P					F				R			F							R					R	
	28X-3, 60-61	255,30	P					D	F																		R	
	28X-3, 141-142	256,11	P					A	A		R				F			R				R				R	F	
	28X-4, 71-72	256,91	P				R	R		C				R	R	R						R					R	
	28X-4, 149-150	257,69	P				R	R				R		R	F		R	F		R		R						
	28X-5, 82-83	258,52	P				R	F			R	R			C			R		R		R				R		
	28X-6, 11-12	259,31	P					R			R				A	R	R	F		R							R	
	28X-6, 92-93	260,12	P				R	R		F		R										R				R		
	28X-7, 20-21	260,90	M				R	A		F		R	R		R		R	F		F							R	
	29X-1, 46-47	261,66	M					A				R			A												R	
	29X-1, 129-130	262,49	P				R	D	F	R					R													
	29X-2, 60-61	263,30	P					D	F																			
	29X-2, 137-138	264,07	P					F	F	R		R			F					R							R	
	29X-3, 73-74	264,93	P					F	R	F	F				F		R			R		F					F	
	29X-3, 149-150	265,69	P				R	R		A					R	R											R	
	29X-4, 82-83	266,52	P				R	R			R		R	R	F		R	R				R						
	29X-5, 8-9	267,28	M									R			F		R	R		F							R	
	29X-5, 88-89	268,08	P					F			R	R	R		C			F				R						
	29X-6, 24-25	268,94	P					R						R	A							R					R	
	29X-6, 102-103	269,72	M				R	A		R		R			F	R	R	F		F							R	
	29X-7, 36-37	270,56	M				R	F		F		R		R	R	R		F		F							R	
	30X-1, 62-63	271,32	P					A							A												R	
	30X-1, 138-139	272,08	P					C	R					R	A												R	
	30X-2, 71-72	272,91	G					A	R						F			R									R	
A. ingens var. *ovalis* ———?———	30X-3, 84-85	274,54	P					D	R									R									R	
	30X-4, 10-11	275,30	P					F	R	R	R		R		C	R		F		R							R	
	30X-4, 90-91	276,10	P					D	R		R		R		F			R				R					F	
	30X-5, 22-23	276,82	P					R		C		R															R	
	30X-6, 31-32	277,71	P				R	R			R				F	R	R	R		R					R		R	

Hole 704B range chart - Stratigraphic occurrence of selected diatom species - 2/4

Depth (mbsf)	*Fragilariopsis praecurta*	*Fragilariopsis praeinterfrigidaria*	*Fragilariopsis reinholdii*	*Hemidiscus cuneiformis*	*Hemidiscus karstenii*	*Hemidiscus triangularus*	*Mediaria splendida*	*Nitzschia cylindrica*	*Paralia sulcata*	*Proboscia barboi*	*Rhizosolenia hebetata*	*Rhizosolenia antennata*	*Rhizolsoenia* sp.	*Rouxia heteropolara*	*Rouxia isopolica*	*Rouxia naviculoides*	*Rouxia* sp.	*Stephanopyxis* sp.	*Stellarima* spp.	*Thalassionema nitzschioides*	*Thalassionema nitzschioides* var. *parvum*	*Thalassiosira complicata*	*Thalassiosira convexa* var. *aspinosa*	*Thalassiosira inura*	*Thalassiosira striata*	*Thalassiosira oestupii*	*Thalassiosira oliverana*	*Thalassiosira oliviverana* var. *sparsa*	*Thalassiosira praelineata*	*Thalassiosira torokina*	*Thalassiothrix longissima* grp.	*Thalassiothrix miocenica*	*Triceratium cinnamoium*
213,72	R	R	F		R					R			R			R				C		R	R	C	R	R	R				F	R	
214,51	F	F	R		F					F			R		R	F				F			F	C	R	F	R		R	R	F	R	
215,25	C	R	F		R			R	R	R		R	R			F		R		F		R	R	C	R	F	R	R			R		
216,13	A	R	R						R	R		R	R		R	F		R	R	F	R	R	F	F		F	R				R	R	
216,92	F	F	R		R					F	R		R		R	F	R		R	R	R	R	F	F		F	R	R	R		R	R	
217,68	C	F	F		R				R	F	R	R	R			F			R	F			F	R	R	R	R	R	R		F	R	
218,49	R	F	R	R	F			R	R	R	R	R	R		R	R	R	R		R	R	R	R	F		R	R	R	R		F		
219,27	C	F	F		R		R			R	R	R	R			R		R		F	F		R	F		F	R				F		
220,16	F	F	F		R					F	R	R	R		R			R		C			F	R	R	R	R		R		R		
220,99	R	F	C		F			F		F			R							F			R	R	R	F	R	R	R		R		
221,73	F	R	R		R			R		R		R	R			R	R			F			R	F	R	R	R			R	F		
222,49	F	R	R						R	R			R		F	F				D											R	R	
223,26	R	R	F		F		R	R		F	R	R	R		R	F	R			F						R			R		F	R	
223,27	F	R	F		R		R		R	R			R		F	R	R		R	F						R					R	R	
224,13	F		F		R			R		R	R	R	F		R	R				F	R					R			R		R	R	
224,88	F		C		R					R	R	R	R		R	R			R	F			R								R	R	
225,68	F	R	F					R		R	R	R	R		R	R	R		R	A											R	R	
226,52	R	R	F							R	R	R	R		R				R	D											R	R	
227,32	R	R	R							R		R	R		R		R			F											R	R	
228,12	R		F		R					R	R	F	F		R					F			R				R				F	R	
228,90	R		F		R				R	R	R	R	F		R				F	C	R								R		F	R	
229,70	R		C		C			R	R	F	R	R	F				R		R	F	R								R		F	R	
230,49	R		F		F					R	R	R	F		R	R			R	A	R		R						R		F	R	
231,28	R		F		F		R			R	R	R	R	R	F	R	R		F	C	F								F		R	R	
232,08			F		F					R	R	R	R	R	R	F			R	A	R		F						F		R		
232,84	R		R		F					R	R	R		R		F				D	R		R						R		R		
233,04	R		F		C					R	R	R	R			F				A	R		R						R		F	R	
233,78	R		R		A					R	R	R	R		R	F				R	R		R				R		R		R		
234,48	R	R	F		A					R	R		R	R	R	C				F	R		R						R		R		
235,28	R	R	F		C					R		R	R		R	F				C	R		F						F		R	R	
236,10	R		F	R	A						R	R	F		R	C				F			R						R		F	R	
236,89	R	R	R	R	F					R	R	R	R	R	R	C				F			F						F		R	R	
237,73	R		F	F	F			R	R		R		R		R	R				A	R		R						R		F	R	
238,53	R		F	F	R			F		R	R		R		R	R				C	R		F						R		F	R	
239,26	F	R	R	R	R			F		R	R	R	F	R	R	R				F			A								F	R	
242,49		F	C	R	F	R		F		R	R	R	F		R	R				F	R		R					R	R		F		
243,30	R	R	A	R	F	F		R		R			R		R	R				F			F					F			F	R	
244,13	R		C		R	C		R		R	R	R	R			R				R			F					F	R		R		
244,90	R	R	F	F	R	C		F		R	F	R	F			R			R	F	R							F	R		R		
245,70	R	R	F	C	R	C		R		R	F	F	F			R			R	R							R	R			R	R	
246,50	R	R	F	F	R	A		R		R	F	R	R		R	R			R	R								F	R		R		
247,30	R		F			C		F		R	F	R	F		R	R				R							R	C			R		
248,12			F		F	F		F	R	R	F	R	F		R	R			R	F								F		R	R		
248,89			R		C	R		F	R	R	R		F			R			R	R								F		R			
249,71	R		F		F	F		F		R	F	F	F		R	R			R	R	R							F	R	R	F	R	
250,53	R		R	R	F			R	R	R	F	F	F							F								F	F		F	R	
251,32									R	R	R	R	F							R								C	R	R	R		R
252,08	R									R		R	F		R					R								F			R		R
252,10			F					F					F															R					R
252,90			F					R	R	R	F		F							R								F			R	R	
253,72			F	R				R		R	R	R	F							R								F			R	R	
254,52	R		F				R	R	R	R	R	R	R			R				F								F			R		
255,30			R	R	R			R		R			R							R								R			R		
256,11			R		R				R				F							R								F			R		
256,91			R		F			R			F		A							F								R		R	R	F	
257,69	R		R	R	F			R	R		C	R	C			R				R								F		R	F	F	
258,52	R			R	F				R	R	F	R	C							F									R		R	F	
259,31	R				F				R		F		R		R					R								R	R		F	R	
260,12			R		C						F		A		R					R								F			F		
260,90	R		F		R				R		R	R	F		R					R								F			R		R
261,66	R		F						R	R	R	R	F							F								F			R		
262,49	R		F	R	R				R	R	R		R		R					R								F			R	R	
263,30			F		R								F							R								F			R		
264,07	R		R		R				R				F		R					R								F					
264,93	R		R	R	C						F		C							F											R	R	
265,69			F		F						C		C						R	R								F	R		R	R	
266,52	R				A				R		F	R	C		R			R		R								F	R		R	R	
267,28	R		R		A					R	C	R	C							R								R			R	F	
268,08					R						R		C		R					F								F			R		
268,94	R			R	F						F		R							R											F		
269,72	R								R	R	F	R	R		R		R			R								F	R		R		R
270,56			R				R			R	R	R	F		R					R								C	R		R		R
271,32			F								R	F	F							R								F					
272,08			C						R	R	R	R	F		R					F								R			R	R	
272,91	R		F								F	F	F		R					R								F			R	R	
274,54	R											R	R															R					
275,30	R			R	F				R		C	R	R							F								R			R	F	
276,10					F						R		F		R					R								R			R		
276,82	R				F			R			F		R		R					R								F			R	R	
277,71	F				C			R	R	R	F		R		R				R	R								F	R	R	R	R	

Hole 704B range chart - Stratigraphic occurrence of selected diatom species - 3/4

Zone (NSODZ)	Hole 704B Core section (interval in cm)	Depth (mbsf)	Preservation	*Actinocyclus curvatulus*	*Actinocyclus ellipticus*	*Actinocyclus fasciculatus*	*Actinocyclus karstenii*	*Actinocyclus ingens*	*Actinocyclus ingens* var. *ovalis*	*Actinoptychus undulatus*	*Asteromphalus kennettii*	*Azpeitia tabularis*	*Cavitatus jouseanus*	*Chaetoceros* sp.	*Coscinodiscus marginatus*	*Coscinodiscus radiatus*	*Denticulopsis crassa*	*Denticulopsis dimorpha*	*Denticulopsis ovata*	*Denticulopsis simonsenii*	*Eucampia antarctica*	*Fragilaria* sp.	*Fragilariopsis arcula*	*Fragilariopsis aurica*	*Fragilariopsis clementia*	*Fragilariopsis donahuensis*	*Fragilariopsis fossilis*	*Fragilariopsis lacrima*
A. kennettii	30X-7, 78-79	278,48	G				R				R				F		R	R		R							R	
	30X-8, 10-11	279,30	P				R	R			R	R			F		R	F		F					R		R	
	30X-8, 91-92	280,11	M					R		R	F	R			C	R	R	R	R	F								
	31X-1, 68-69	280,88	P					R		R	F			R	C		R	R		F					R	R	R	
	31X-1, 149-150	281,69	P							R	R	R			A			R		F		R					R	
	31X-2, 82-83	282,52	P							R	R				F			R		R								
	31X-3, 10-11	283,30	P								R				A							R						
	31X-3, 88-89	284,08	P		R					R	R	R		R	F		R	R	R	R								
	31X-4, 21-22	284,91	P								F	R			C		R	F		F								
	31X-4, 100-101	285,70	P					R		F					A			F		F								
	31X-5, 32-33	286,52	M					R		R	F				F		R	R		R								
	31X-5, 108-109	287,28	P					R			F		R		A		R	R		R						R		
	31X-6, 38-39	288,08	P		R			R			F				A			R		R						R	R	
	31X-6, 120-121	288,90	P					R		R		R		R	F			R		F								
	31X-CC, 3-4	289,70	P					R		F	F	R		R	C					R							R	
	32X-1, 77-78	290,47	G					R			R				F			R		R								
	32X-2, 10-11	291,30	M					R		R	F				C		R	R		F								
	32X-2, 92-93	292,12	P					R			F				C			R		R								
	32X-3, 18-19	292,88	P							R	F				C					R								
	32X-3, 99-100	293,69	P				R			R	F				C			R		R		R						
	32X-4, 32-33	294,52	P					R		R	R				C		R			R							R	
	32X-4, 113-114	295,33	M								R				A	R	R			F								
	32X-5, 41-42	296,11	M								F	R		R	A		R	F		F		R					R	
	32X-5, 120-121	296,90	P					R		F	F	R			C	R	R	R		R						R	R	
	32X-6, 48-49	297,68	P					R		R	C	R		R	F	R	R	R		F							R	
	32X-6, 128-129	298,48	P					R			C				F			R				R				R		
	32X-7, 56-57	299,26	P							F					F													

Hole 704B range chart - Stratigraphic occurrence of selected diatom species - 4/4

Depth (mbsf)	*Fragilariopsis praecurta*	*Fragilariopsis praeinterfrigidaria*	*Fragilariopsis reinholdii*	*Hemidiscus cuneiformis*	*Hemidiscus karstenii*	*Hemidiscus triangularus*	*Mediaria splendida*	*Nitzschia cylindrica*	*Paralia sulcata*	*Proboscia barboi*	*Rhizosolenia hebetata*	*Rhizosolenia antennata*	*Rhizolsolenia* sp.	*Rouxia heteropolara*	*Rouxia isopolica*	*Rouxia naviculoides*	*Rouxia* sp.	*Stephanopyxis* sp.	*Stellarima* spp.	*Thalassionema nitzschioides*	*Thalassionema nitzschioides* var. *parvum*	*Thalassiosira complicata*	*Thalassiosira convexa* var. *aspinosa*	*Thalassiosira inura*	*Thalassiosira striata*	*Thalassiosira oestrupii*	*Thalassiosira oliverana*	*Thalassiosira oliverana* var. *sparsa*	*Thalassiosira praelineata*	*Thalassiosira torokina*	*Thalassiothrix longissima* grp.	*Thalassiothrix miocenica*	*Triceratium cinnamomeum*
278,48	R				A					R	C	R	F					R		R								R		R	R	R	
279,30	R				C			R			F	R	C							R								R			R	F	
280,11				F	F					R	F	R	F		R					F						R					R	R	
280,88	R			R	F					R	R	R	C		R					F										R	F	R	
281,69	R			R	F		R			R	R		F							F											R	R	
282,52					C				R	R	R		F							C											F	R	
283,30					F						F		F							F											F		
284,08	F				R				R	R	R		C							R											F		
284,91									R	R	F	R	C							R											F	F	
285,70											R		A		R																F		
286,52					D						F		R							R								R			R		
287,28					R					R	F	R	R							C											F	R	
288,08					R						F		F							F											F		
288,90					F				R		F		C							R											R	R	
289,70					R				R		F		C		R					R											F	R	
290,47	R				D					R	R		F							R											R	R	
291,30					A						F		F			R				R								R			F	R	
292,12					A						R		F							R								R			R		
292,88				R	C						F		F							C											F		
293,69	R				F				R		C		C							C											F		
294,52	R				F					R	F		C							C											R		
295,33	R				R				R	R	R		F							C											R		
296,11	R										R		F				R			A											F	R	
296,90	R			R	F					R	F	R	F							F											F	R	
297,68	R			R	F					F	R	R	C				R			F											F	R	
298,48					R					F	R	R	A							R											F		
299,26	R			R	C		R				F		F							R											R	R	

Site 1088 range chart - Stratigraphic occurrence of selected diatom species - 1/2

Zone (NSODZ)	Core-section (interval in cm)	Depth (mcd)	Preservation	*Actinocyclus curvatulus*	*Actinocyclus ellipticus*	*Actinocyclus fasciculatus*	*Actinocyclus ingens*	*Actinocyclus ingens* var. *nodus*	*Actinocyclus ingens* var. *ovalis*	*Actinoptychus senarius*	*Asteromphalus kennettii*	*Azpeitia tabularis*	*Cavitatus jouseanus*	*Chaetoceros* sp.	*Coscinodiscus marginatus*	*Coscinodiscus rhombicus*	*Crucidenticula nicobarica*	*Denticulopsis crassa*	*Denticulopsis dimorpha*	*Denticulopsis ovata*	*Denticulopsis praedimorpha*	*Denticulopsis simonsenii*	*Ethmodiscus* sp.	*Fragilaria* sp.	*Fragilariopsis arcula*	*Fragilariopsis aurica*	*Fragilariopsis cylindrica*	*Fragilariopsis donahuensis*
	1088B-5H-1, 75-76	34,75	P									F			F													
	1088B-5H-1, 111-112	35,11	P									F																
	1088B-5H-2, 0-1	35,50	G	T			F					F			F								X					
T. inura	1088B-5H-2, 35-36	35,85	P	F								A											X					
	1088B-5H-2, 70-71	36,20	P												C													
	1088B-5H-2, 105-106	36,55	P									F											X					
	1088B-5H-2, 137-138	36,87	P									F			C								X	F		F		
	1088B-5H-3, 25-26	37,25	P									F												T				
	1088B-5H-3, 60-61	37,60	P									F			F													
	1088B-5H-3, 130-131	38,30	P																									
?	1088B-5H-4, 47-48	38,97	P	F			F					F			A								X					
	1088B-5H-5, 115-116	41,15	P																									
	1088B-5H-6, 36-37	41,86	P	F								F													F		F	
	1088B-5H-6, 70-71	42,20	P																									
---------?---------	1088B-9H-5, 120-121	79,20	P																									
	1088B-10H-1, 40-41	81,90	P				D					R			R			T				R			R			
	1088B-10H-1, 130-13	82,80	P				D			R		R			R			R				R	X			R		
	1088B-10H-2, 70-71	83,70	P				D		R	R		R			R			T				F						
	1088B-10H-3, 10-11	84,60	P				D								R													
	1088B-10H-3, 100-10	85,50	M				D	R				R			R							F						
F. reinholdii	1088B-10H-4, 40-41	86,40	P	F			D								F			R				T					R	
	1088B-10H-4, 130-13	87,30	G				D								F			T							R		F	R
	1088B-10H-5, 70-71	88,20	M				D								F									R	F			
	1088B-10H-6, 0-1	89,00	G				A					R			F										F	R	R	
	1088B-10H-6, 90-91	89,90	P				A		R						A								X					
A. ingens var. *ovalis*	1088B-10H-7, 27-28	90,77	G				C		C					R	R										R		R	
	1088B-11H-1, 31-32	91,31	P							C		R	R													R		
	1088B-11H-1, 113-114	92,13	P				F								C													
	1088B-11H-2, 46-47	92,96	P			F									C							F			F			F
	1088B-11H-2, 130-13	93,80	P				F								C													
---------?---------	1088B-11H-3, 70-71	94,70	P												F									R				
	1088B-12H-3, 47-48	104,24	P				A											C					X					
	1088B-12H-3, 140-14	104,90	M							R	F				F							R	X					R
	1088B-12H-4, 80-81	105,80	G	R						R	R				R			F				F	X					R
	1088B-12H-5, 20-21	106,70	M	R	R						C	R			A													
	1088B-12H-5, 111-112	107,61	P				F				C				F									F				
A. kennettii	1088B-12H-6, 47-48	108,47	M		R		R				C				F			R	R			F		R				
	1088B-12H-6, 140-14	109,40	M			R					F				F							F						R
	1088B-12H-7, 38-39	109,88	P		R																							
	1088B-13H-1, 90-91	110,90	P												A													C
	1088C-3H-2, 20-21	133,64	P				A				F	F											X	F				
	1088C-3H-3, 20-21	135,14	P				D															R	X					
	1088C-3H-3, 95-96	135,89	P				D																					
	1088C-3H-4, 20-21	136,64	P				D																X					
	1088C-3H-4, 93-94	137,37	G				D	F				R										F	X					
	1088C-3H-5, 20-21	138,14	G		R		A	R				T			F			T	R			F						
	1088C-3H-5, 95-96	138,89	P				D																X					R
	1088C-3H-6, 19-20	139,63	P	R			D																X					
	1088C-3H-6, 95-96	140,39	P				C																					
	1088C-4H-1, 25-26	141,69	M		T		D					R			R													
D. ovata	1088C-4H-1, 100-101	142,44	P	R			D									R						R	X					
	1088C-4H-2, 25-26	143,19	P				D																X					
	1088C-4H-3, 25-26	144,69	P				D									R				R								
	1088C-4H-4, 20-21	146,14	M				A					F			F	T				R		F		R				
	1088C-8X-4, 95-96	179,19	P				C					R			F		F		A	F				R				
	1088C-8X-5, 18-19	179,92	P				C								F				F									
	1088C-8X-5, 95-96	180,69	P				A					F							A	R			X					
	1088C-8X-6, 18-19	181,42	P				F					F			F		R		A	F		R		R				
D. dimorpha-	1088C-9X-5, 95-96	190,29	P				A					A											X					
D. simonsenii	1088C-9X-6, 20-21	191,04	P				A	F				F									F	F	X	F				
---------?---------	1088C-9X-6, 95-96	191,79	P				D															F		F				
	1088C-10X-1, 20-21	193,14	M				A	F				F			R						F	R						
	1088C-10X-1, 95-96	193,89	P				A	F				R	F		R							R		R				
D simonsenii	1088C-11X-2, 48-50	192,51	P				F	F					R									R						

Site 1088 range chart - Stratigraphic occurrence of selected diatom species - 2/2

Depth (mcd)	*Fragilariopsis fossilis*	*Fragilariopsis praecurta*	*Fragilariopsis reinholdii*	*Hemidiscus cuneiformis*	*Hemidiscus karstenii*	*Navicula sp.*	*Neobrunia marabilis*	*Nitzschia denticuloides*	*Nitzschia groosepuncata*	*Paralia sulcata*	*Proboscia barboi*	*Dilponeis bombus*	*Rhizosolenia hebetata*	*Rhizosolenia antenata*	*Rocella gelida*	*Rouxia isopolica*	*Rouxia naviculoides*	*Thalassionema nitzschioides*	*Thalassionema nitzschioides var. capitulatum*	*Thalassionema nitzschioides var. inflatum*	*Thalassionema nitzschioides var parvum*	*Thalassiosira inura*	*Thalassiosira fasciculata*	*Thalassiosira oliviverana var. sparsa*	*Thalassiosira sancetta*	*Thalassiosira torokina*	*Thalassiothrix longissima*	*Thalassiothrix miocenica*
34,75	F												C					A								A		
35,11	C		F										F					F				R				A	F	
35,50	R		F	T						R								F				R	R			A	R	
35,85				F							F		C		F											C		
36,20	C		C										C															
36,55	C		F	F																		F				A	F	
36,87	C												R								F	R					F	
37,25	F									R											D					F	R	
37,60	C												C	F				C			F							
38,30																				D								
38,97	F						X						F						F	F						F	F	
41,15												D																
41,86	A		F							F			F														F	
42,20												D																
79,20			R				X						D															
81,90	R		R	R							R		R				R									R		
82,80												R	R			R											R	
83,70				T			X						R	R												R	R	
84,60				R								R														R		
85,50	F	R	T		R						R	R	F			R	R	R						R			R	
86,40				R			X						F	R					R							R		
87,30	R		R								R		F	R		R					R						F	
88,20	R		R										R					F			F						F	R
89,00	F	F	F	R							R		R	R		R		F			F			R			F	F
89,90		F		R							R		F											F			R	
90,77											F		F			R	R	R						R			C	
91,31				F		R				R			A			F			F								F	
92,13											F		A														F	
92,96	C												C														C	
93,80											A		C														F	
94,70													D														F	
104,24													C														F	
104,90											F		A								F						C	
105,80				R							R	R	F						A						R		F	
106,70				F							R		R	R													R	
107,61				F									C						F		F						F	
108,47				F		R					F		A	F		R					F						R	
109,40											R		A	F				R			F						F	R
109,88													A			C												
110,90													C															
133,64													C															
135,14													F			R											R	
135,89													F														F	
136,64																												
137,37											R	R	F					R			R						F	
138,14				R									F								R				R		F	
138,89													C				F										R	
139,63											R																F	
140,39													C		C												C	
141,69											F		F														F	
142,44																												
143,19													F														F	
144,69													F															
146,14											R		F													R	C	
179 19													F														F	
179.92								F	F		R		F															
180,69											R																F	
181 42						R							F														F	
190,29											R																	
191,04																			F								F	
191,79													F														F	
193 14						R					C														R		F	
193,89						R					F																F	
192,51																											R	

Site 1092 range chart - Stratigraphic occurrence of selected diatom species - 1/9

Zone (NSODZ)	Core-section (interval in cm)	Depth (mcd)	Preservation	*Actinocyclus curvatulus*	*Actinocyclus ellipticus*	*Actinocyclus fasciculatus*	*Actinocyclus ingens*	*Actinocyclus ingens* var. *nodus*	*Actinocyclus ingens* var. *ovalis*	*Actinocyclus karstenii*	*Actinoptychus senarius*	*Asteromphalus hookeri*	*Asteromphalus kennettii*	*Asteromphalus inaequabilis*	*Azpeitia tabularis*	*Bogorovia praepaleacea*	*Cavitatus jouseanus*	*Cavitatus miocenica*	*Chaetoceros* sp.	*Coretron cryophilum*	*Coscinodiscus lewisianus*	*Coscinodiscus marginatus*	*Coscinodiscus rhombicus*	*Crucidenticula nicobarica*	*Denticulopsis crassa*	*Denticulopsis dimorpha*	*Denticulopsis hustedtii*	*Denticulopsis macollumii*
F. interfrigidaria	1092A-6H-5, 79-80	60,68	G	T			T		T						F				T			R						
	1092A-6H-6, 79-80	62,18	G				R					T			F							R						
T. inura	1092A-7H-1, 79-80	64,98	M				R		R						F				T			F						
	1092D-3H-4, 80-81	65,01	M												F				R			F						
	1092D-3H-4, 111-112	65,32	M	F			R															R						
	1092D-3H-4, 140-141	65,61	P												R				T			F						
	1092D-3H-5, 20-21	65,91	P																			R						
	1092D-3H-5, 50-51	66,21	M	T			R		T						T							T						
	1092A-7H-2, 79-80	66,48	G				R								T				R			T						
	1092D-3H-5, 110-111	66,81	M	T			T		R													T						
	1092D-3H-5, 140-141	67,11	M				R								R							R						
	1092D-3H-6, 20-21	67,41	G				T		T	T												R						
	1092D-3H-6, 50-51	67,71	G				R								T				T									
	1092A-7H-3, 79-80	67,96	G	T																		T						
	1092D-3H-6, 80-81	68,01	M	T			R								T							R						
	1092A-7H-3, 112-113	68,31	M	R			R		F	R					R							R						
H. triangularus - *F. aurica*	1092A-7H-3, 142-143	68,61	M				R		R													C						
	1092A-7H-4, 22-23	68,91	P				F		F										F									
	1092A-7H-4, 52-53	69,21	P						F													C						
	1092A-7H-4, 79-80	69,48	G				R		R										R			F						
	1092A-7H-4, 82-83	69,51	M				R								R							C						
	1092A-7H-4, 112-113	69,81	P																			C						
	1092A-7H-4, 139-140	70,08	P				F								R				R			A						
	1092A-7H-5, 22-23	70,41	M				F															C						
	1092A-7H-5, 52-53	70,71	M	F			R															F						
	1092A-7H-5, 79-80	70,98	M				F												F			F						
	1092A-7H-5, 82-83	71,01	M				C								T							F						
	1092A-7H-5, 111-112	71,30	M	F			C								R				T			F				T		
	1092A-7H-5, 142-143	71,61	M				A								R							F						
	1092A-7H-6, 52-53	72,21	G				A															R						
	1092A-7H-6, 79-80	72,48	G				A															F						
	1092B-8H-2, 66-67	72,51	G				R		A													F						
	1092B-8H-2, 96-97	72,81	G				C												T	T		R						
	1092B-8H-2, 126-127	73,11	M				F		C										T			F						
	1092B-8H-3, 6-7	73,41	M				C															F						
	1092A-7H-7, 30-29	73,48	G		R		C												R			F						
	1092B-8H-3, 36-37	73,71	G				F															F						
	1092B-8H-3, 96-97	74,31	G				C															F						
	1092B-8H-3, 126-127	74,61	M				F												F			F						
	1092B-8H-4, 6-7	74,91	P			F	R		R						R							R						
	1092B-8H-4, 36-37	75,21	P				R								R				R			F						
	1092A-8H-1, 79-80	75,24	M	T			F		T		R				R							F						
	1092B-8H-4, 66-67	75,51	P												R							F						
	1092B-8H-4, 126-127	76,11	P				F								F							R						
	1092B-8H-5, 6-7	76,41	P				R								F							R						
	1092A-8H-2, 79-80	76,74	M				T		T						F							F						
	1092A-8H-2, 106-107	77,01	P				R		T						C				R			R						
	1092A-8H-2, 135-136	77,30	P				F		R						A				R			R						
	1092A-8H-3, 6-7	77,51	P				F		R						F				T			T						
	1092A-8H-3, 36-37	77,81	M				F		F						F				R	R		R						
	1092A-8H-3, 66-67	78,11	M				F								C				R			R						
	1092A-8H-3, 79-80	78,24	M				R								C				R			F						
	1092A-8H-3, 96-97	78,41	M				T		R						C				R			R						
	1092A-8H-3, 126-127	78,71	P				R		R	F					F							F						
	1092A-8H-4, 6-7	79,01	P				R		R						F							F						
	1092C-9H-2, 66-67	79,61	P				R								C				R			R						
	1092A-8H-4, 79-80	79,74	P				R		R						F				R			R						
	1092C-9H-2, 96-97	79,91	P				F								F							F						
	1092C-9H-2, 126-127	80,21	P				R								F							F						
F. reinholdii	1092C-9H-3, 6-7	80.51	M	T			F			R			T		F							F						
	1092C-9H-3, 36-37	80.81	M				C								R							F						
	1092A-8H-5, 79-80	81.24	M				C								R							F			R			
	1092C-9H-3, 96-97	81.41	M	T			C			R			R		R				T			F						
	1092C-9H-3, 126-127	81.71	M				A			R					R							F						
	1092C-9H-4, 6-7	82.01	M				A				T				R							F			F		T	
	1092C-9H-4, 36-27	82.31	P				A			R			T		R				R			R			R			
	1092C-9H-4, 66-67	82.61	M				A															R						
	1092A-8H-6, 79-80	82.74	M				A		T		R		T		T				R			R			F			
	1092C-9H-4, 96-97	82.91	P				A						T		R							R			C			
	1092C-9H-5, 6-7	83.51	P				D						T		R				R			F						
	1092C-9H-5, 36-37	83.81	P				A			R	T				R				T			F			F		T	
	1092C-9H-5, 66-67	84.11	P				A								R							F			R			
	1092C-9H-5, 96-97	84.41	P				A															F			F			
	1092A-9H-1, 79-80	84.62	P				A			R			T		R				R	R		F			R			
	1092C-9H-6, 6-7	85.01	P				A			T			R		R				T			F			R			
	1092C-9H-6, 66-67	85.61	P				A			R												C						
	1092A-9H-2, 79-80	86.12	P				C			R										R		A			T			
	1092A-9H-2, 88-89	86.21	M				A		T											T		C						
	1092A-9H-3, 28-29	87.11	P				A		R		T									T		A						
	1092A-9H-3, 58-59	87.41	P				A		R				T									A						
	1092A-9H-3, 79-80	87.62	P				D															F						
A. ingens var *ovalis*	1092A-9H-3, 88-89	87.71	M				D		F											R		R						
	1092A-9H-3, 146-147	88.29	M				D		F													F					R	
	1092A-9H-4 28-29	88.61	P				A		C													F						
	1092A-9H-4, 58-59	88.91	P				A		C													F						
	1092A-9H-4, 79-80	89.12	P				C		C				T									F						
	1092A-9H-4, 88-89	89.21	P				C		F													C						
	1092A-9H-4 118-119	89.51	P				C		R													F						
	1092A-9H-4, 137-138	89.70	P				F		R		C											F						
	1092A-9H-5, 28-29	90.11	M				F						T									F						

Site 1092 range chart - Stratigraphic occurrence of selected diatom species - 2/9

Depth (mcd)	*Denticulopsis ovata*	*Denticulopsis praedimorpha*	*Denticulopsis simonsenii*	*Eucampia antarctica*	*Ethmodiscus sp.*	*Fragilaria sp.*	*Fragilariopsis arcula*	*Fragilariopsis aurica*	*Fragilariopsis barronii*	*Fragilariopsis claviceps*	*Fragilariopsis cylindrica*	*Fragilariopsis clementia*	*Fragilariopsis donahuensis*	*Fragilariopsis efferans*	*Fragilariopsis fossilis*	*Fragilariopsis interfrigidaria*	*Fragilariopsis lacrima*	*Fragilariopsis maleinterpretaria*	*Fragilariopsis miocenica*	*Fragilariopsis praecurta*	*Fragilariopsis praeinterfrigidaria*	*Fragilariopsis reinholdii*	*Hemidiscus cuneiformis*	*Hemidiscus karstenii*	*Hemidiscus triangularus*	*Mediaria splendida*	*Navicula sp.*	*Naviculopsis sp.*	*Neobrunia marabilis*	*Nitzschia denticuloides*	*Paralia sulcata*	*Pleurosigma directum*	*Proboscia barboi*	*Proboscia praebarboi*	*Raphidodiscus marylandicus*
60,68							R	F	C						T	A				T	R	F		F									R		
62,18							T	F	F						R	A	F			R		F	R	F								T	R		
64,98							F	F			T	R			R					R	F	C		F									T		
65,01					X	T	R	F						R			F			R	F	C											R		
65,32							F	C							F						F	C		F									R		
65,61					X		T	C							F		F				T	F			T		R								
65,91					X		R	F			R	R			F					R	R	A		F							R		R		
66,21							F	F							R		T			F	T	C		R									R		
66,48					X		F	F	R			R			R					F		F							X				R		
66,81							F	F				R			T		R			C	T	F											F		
67,11					X		R	F				R			R		R			C		F		R									F		
67,41							F	A				T		T	R					F	R	R		F		T							R		
67,71							F	C				T			T		R			A	F	T		T									R		
67,98							F	F				R		T	R		R			A	F	T			T								T		
68,01							F	F				R	R		R					F	R	R		R		T							F		
68,31							F	F												R	T	F		R									C		
68,61								R							R					R		C		T									F		
68,91							R	R						R						R		A		F									R		
69,21							R	R									R					F		R									F		
69,48					X		T	F			T	R			R					T		F	T	F									F		
69,51							R	R			R				R		R			R		F		R									F		
69,81											R				R		R					F				R							F		
70,08							R	R			R											F				R							F		
70,41					X			T							F					T		F	T			T							F		
70,71					X		R	R					R		F				R	T		F		R			T						F		
70.98					X		R	R			R				F							F				R							F		
71.01								R			T		R		R							F											F		
71,30					X			R			T		T		F				T	T		F		R									F		
71,61							T	R			R				F					R		F		T									F		
72,21					X		T	R			R				F					R		F											R		
72,48							T	R							F					R		F		R									R		
72,51						T									F							F		R											
72,81							R	R							F				R	R		F		F	F						T		R		
73,11						T	T				T				F							R		F									T		
73,41							R	T			R				F				T	T		R		T	F	T							T		
73,48							R	T			R				F							F		R	F								R		
73,71								T							F				R	T		F		R	R								R		
74,31							R	T							F				R	R		F		F		T			X				R		
74,61							R	R			R				F				R	R		F		F	R								F		
74,91						R	R	R			R		F		C				F	R		R	R	R	R										
75,21							R	R			R				F				R	R		R		R	F								F		
75,24					X		T	R			R		R		F				R	R		F		T	T		T						R		
75,51								T			R				F				T	R		F	R		F								R		
76,11											F		R		F					R		R	F	F	C								R		
76,41								R			C				R					R		R	F	F	A								T		
76,74								R			C											R	F	R	A				X		T		R		
77,01							T	F			C				R				T			T	T		C										
77,30			T				R	F			F				F				R	T		F			C				X				T		
77,51							F	R			F				F				T	F		F			C								T		
77.81					X		F				F	T			R					F		F		R	F	T	R		X				T		
78.11							F	R			F				R				T	F		F			F								T		
78,24					X		R	F			F	T			R				R	R		R			F								R		
78.41								F			C				R				F	R		F			C										
78,71					X		R				F		R		F				F	R		C			F										
79,01					X						F				F		F		F			F			F										
79,61								C			R				R				R			F			F								R		
79,74					X		R	F			F	R			F		T			F		F			F								R		
79.91					X		F	C			F				F							F			F								R		
80,21					X		R	R			F				F		R		R			F			F								R		
80,51					X		F				F	R			F		T		R			R					R		X		R		R		
80,81							F				R				F							T													
81,24					X		R	R			F				C																				
81,41					X		F				F				F					R		R							X		F				
81,71			R				F	R			R				F							R													
82,01			F			R	T	R							F												T				R		T		
82,31			F		X			F							F							F													
82,61			F		X		R	F							C							R													
82,74			F		X		R	F				T			F					T		T				R			X				R		
82,91			R				R	F			R				F							R													
83,51			F		X		R								T							R													
83,81			F		X		T				R				R				R			R		T					X		R				
84,11			F								R											R													
84,41			F												R							F									R		R		
84,62			F		X		F				R				F							R											R		
85,01			F		X						R				F				R			F									R		R		
85,61			T								R				F							F													
86,12					X		R				R				F					R		F									T				
86,21					X		R								F					R		F													
87,11					X		F						R		F					R		F							X		R				
87,41					X						R											R													
87,62					X						R											R													
87,71					X																														
88,29																																			
88,61																																			
88,91					X															F															
89,12					X														C																
89,21																				F				F											
89,51			F		X																			F											
89,70																																			
90,11			F		X																			F											

Site 1092 range chart - Stratigraphic occurrence of selected diatom species - 3/9

Depth (mcd)	*Rhizosolenia antenata*	*Rhizosolenia bergonii*	*Rhizosolenia hebetata*	*Rocella gelida*	*Rouxia antarctica*	*Rouxia heteropolara*	*Rouxia isopolica*	*Rouxia naviculoides*	*Rouxia peragalli*	*Stellarima* sp.	*Stephanopyxis* sp.	*Thalassionema nitzschioides*	*Thalassionema nitzschioides* var. *capitulatum*	*Thalassionema nitzschioides* var. *inflatum*	*Thalassionema nitzschioides* var. *lanceolatum*	*Thalassionema nitzschioides* var. *parvum*	*Thalassiosira complicata*	*Thalassiosira convexa* var. *aspinosa*	*Thalassiosira inura*	*Thalassiosira fraga*	*Thalassiosira spinosa*	*Thalassiosira spumellaroides*	*Thalassiosira miocenica*	*Thalassiosira oestrupii*	*Thalassiosira oliverana*	*Thalassiosira oliverana* var. *sparsa*	*Thalassiosira torokina*	*Thalassiosira praelineata*	*Thalassiothrix longissima* grp.	*Thalassiothrix miocenica*
60,68			T			T	R	R								T	R		F					T	R				F	
62,18			T		T	T	R	R					T			T	F	T	F						R		T	T	F	
64,98	R		R		T		F	F					R					T	F					R	T				F	
65,01	R		R		T	T	F	F				R				T	T	R	F					R	R		F		F	
65,32								F								R	F		R						R		F		F	R
65,61	R		R			T	F	F				F		F		T	T	R	F					R	T				F	T
65,91			R					F				R		R				R	F					R	R		R	R	F	
66,21			F			T	R	F				F		R			R		F						R			T	F	
66,48			R			R	F	F				F		R			R	T	F				R	F	F			T	F	R
66,81								F				F						R	F											
67,11			R				R	F		R		F	R		C		R	R	F					R				T	R	R
67,41			T					F	T	R		R	F		T			R	F					F				T	R	
67,71			T					F				R	R	T	T			T	F										R	R
67,98							T	F	T			R						R	F					R					R	
68,01	T							F				F	T		F			F	F					T	R			T	R	R
68,31			F					F				F				F			F									R	F	R
68,61			F					R		F		R	F	F		R													F	F
68,91	R		F									R				F														R
69,21			R							F		F	R		F	F													F	
69,48	T		F					R	F			R				A									T				F	F
69,51	R		F					R				R				F													C	F
69,81			F					F				F			C	F													F	R
70,08			R					R				F				F													F	R
70,41	R		F						F			F				C									T	T			F	R
70,71	R		R					T	F			F				A													R	T
70,98	T	T	R						F			R				C									R				R	R
71,01			R						C			F				F													F	
71,30	R		R					R	F			F				F									R				F	
71,61								T	F			F				F													R	
72,21			T						R			F				F									F				T	T
72,48	T		T						R			F				F														
72,51	R							F	F			F				F									F			R	R	T
72,81			R					F				R				C									F	R	R		R	
73,11	T							F	R			C	R			C		R										R	R	
73,41			R					F	C			C				F													R	T
73,48			R					F	R			F				F													R	
73,71	T		R					F	F			F				C													R	
74,31			R				R	F				R				C									R		F		R	T
74,61			R					F								C													R	R
74,91			R				R	R				R		F		R		C								R		R	F	R
75,21	R		R				R	R	F			C				F													R	R
75,24			R				T	T				C			T	C		F					R			T			R	T
75,51			F									A				F													R	
76,11	R		F													F												R	R	
76,41	T		C													T													R	T
76,74	T		F									R																R	R	R
77,01			F						R																				R	R
77,30			F				T																					R	R	T
77,51			F				T		F																				F	
77,81	F		F				T	T	F			F				R										F	R		F	R
78,11			F					R	F			F				R													F	R
78,24			F					R	R			T				F										T		R	F	R
78,41			R						R							T													F	R
78,71			F						R							F										F	F		F	R
79,01			R						C							C													F	R
79,61									C							F														F
79,74	T	T	F					F	T							F										R		F	T	F
79,91			F						R							F														F
80,21			C						F							C													R	
80,51			F						F							A										F			T	T
80,81			F						R							C													T	
81,24			C						R							C													F	
81,41			F						R			R				F										C			F	T
81,71			C						R							F													R	R
82,01			F						T							R										F		R	T	
82,31			F													R													R	
82,61			R						R																				R	
82,74			F				T		F			R				R										F		R	R	R
82,91			R						F			R				F													R	R
83,51			F						T							R													T	R
83,81	R		C						R			T				R										F			R	R
84,11			C						R			R																	R	
84,41			F						R																					
84,62			F									R																	R	R
85,01			F									R		T		R										F			T	
85,61			F											T		T													T	T
86,12			F						T					R		R										F			R	
86,21			C						T					T		R														
87,11			F						R					R		T										F			T	R
87,41			F													R													R	
87,62			F																										R	R
87,71			R													R													R	
88,29			R													R													R	R
88,61			F						R																				R	
88,91			F																										F	F
89,12			F													F													F	
89,21			C																										F	
89,51			A																										F	F
89,70			A																										F	F
90,11			D																										F	

Site 1092 range chart - Stratigraphic occurrence of selected diatom species - 4/9

Zone (NSODZ)	Core-section (interval in cm)	Depth (mcd)	Preservation	*Actinocyclus curvatulus*	*Actinocyclus ellipticus*	*Actinocyclus fasciculatus*	*Actinocyclus ingens*	*Actinocyclus ingens* var. *nodus*	*Actinocyclus ingens* var. *ovalis*	*Actinocyclus karstenii*	*Actinoptychus senarius*	*Asteromphalus hookeri*	*Asteromphalus kennettii*	*Asteromphalus inaequabilis*	*Azpeitia tabularis*	*Bogorovia praepaleacea*	*Cavitatus jouseanus*	*Cavitatus miocenica*	*Chaetoceros* sp.	*Coretron cryophilum*	*Coscinodiscus lewisianus*	*Coscinodiscus marginatus*	*Coscinodiscus rhombicus*	*Crucidenticula nicobarica*	*Denticulopsis crassa*	*Denticulopsis dimorpha*	*Denticulopsis hustedtii*	*Denticulopsis macollumii*
A. ingens var. *ovalis*	1092A-9H-5, 58-59	90,41	P				C			R					R							R						
	1092A-9H-5, 88-89	90,71	P				A																					
	1092B-10H-1, 60-61	91,00	M				F		F				R		F							F						
	1092B-10H-1, 140-141	91,80	P												R				F			C						
	1092B-10H-2, 70-71	92,60	P				T		R						F							F						
	1092A-9H-7, 29-30	93,12	P												F				F						F			
	1092B-10H-2, 149-150	93,39	P																			A						
	1092B-10H-4, 10-11	95,00	P				R		F						R							C			F			
	1092A-10H-1, 79-80	95,33	P		R				R				F		R				R			F			F		R	
	1092B-10H-4, 90-91	95,80	P				T		R						T							C			T		T	
A. kennettii	1092A-10H-2, 79-80	96,83	M										R		R				R			A			R			
	1092B-10H-5, 100-101	97,40	M										R		R							C			F		R	
	1092A-10H-3, 66-67	98,20	M				R															A			F			
	1092C-11H-2, 30-31	99,80	M																			C			F			
	1092A-10H-4, 79-80	99,83	G		R		R						F									C			F			
	1092A-10H-5, 79-80	101,33	G																									
	1092C-11H-3, 41-42	101,41	M										F									F						
	1092C-11H-3, 121-122	102,21	P																			C			F			
	1092A-10H-6, 79-80	102,83	P				F															F						
	1092C-11H-4, 130-131	103,80	P				R						F									A						
	1092A-10H-7, 29-30	103,83	P										F									A						
	1092C-11H-5, 60-61	104,60	P										F									F						
	1092B-11H-3, 124-125	105,63	M										C									C			R			
	1092A-11H-1, 79-80	106,78	M								R		F									F			F			
	1092B-11H-4, 134-135	107,23	P				T			T	R		C									F			R			
	1092B-11H-5, 64-65	108,03	P										R									F			F			
	1092A-11H-2, 79-80	108,28	P				F						F									F			F			
	1092B-11H-5, 144-145	108,83	P										R									R			R			
A. kennettii	1092A-11H-3, 79-80	109,78	P				F						R									F			R			
	1092A-11H-3, 144-145	110,43	P		R		T						F						T			F			F		T	
	1092A-11H-4, 74-75	111,23	P				R						R									C			C		R	
	1092C-12H-2, 118-119	112,03	M				R						R		T							F			C			
	1092C-12H-3, 48-49	112,83	M				T						F									F			C		T	
	1092C-12H-3, 128-129	113,63	M				T						T		R							F			A			
	1092C-12H-5, 68-69	116,03	M				R								F							C			F		R	
	1092A-12H-1, 79-80	116,20	M		R		R								F							F			F			
	1092C-12H-5, 148-149	116,83	M				R								F							F			F			
	1092A-12H-2, 79-80	117,70	G				R								F							F			F			
	1092A-12H-3, 79-80	119,20	G												F							F			F			
	1092A-12H-3, 82-83	119,23	G		R		T				T		T		R							A			F			
	1092A-12H-4, 79-80	120,70	M		F										T							C			F			
	1092A-12H-4, 92-93	120,83	P		F										R							A			R			
	1092A-12H-5, 79-80	122,20	P		F		T				F				R							C			R			
	1092A-12H-5, 102-103	122,43	P		R						F		R		R							A			R			
	1092A-12H-6, 32-33	123,23	P								F				F							F			F			
	1092A-12H-6, 79-80	123,70	P																			F						
	1092A-12H-7, 29-30	124,70	P										F		F							F						
	1092C-13H-4, 80-81	125,23	P												F							C			F			
	1092C-13H-5, 30-31	126,23	P				R								C							C						
	1092A-13H-1, 79-80	127,51	P				R								F							F			F			
	1092C-13H-6, 80-81	128,23	P										F		A							F			F			
	1092A-13H-3, 51-52	130,23	M												F							F			R			
	1092A-13H-3 79-80	130.51	M												F							F					R	
	1092A-13H-4, 1-2	131,23	P				R								C							F			F			
	1092A-13H-4, 79-80	132,01	P										R		A							F						
	1092A-13H-4 101-102	132,23	P		T		R								C							F			F		R	
	1092A-13H-5, 51-52	133,23	P										R		A							C			R			
	1092A-13H-6, 1-2	134,23	P				C								C							F			R			
	1092A-13H-6, 79-80	135,01	P				A						R		F							F						
D. ovata	1092C-14H-2 91-92	135,23	P				D								F							F						
	1092B-14H-2 141-142	137 23	P				D								F							R			R			
	1092B-14H-3 91-92	138.23	M				D								F							F			R			
	1092A-14H-1 79-80	138,91	M				D								F							R						
	1092B-14H-4 41-42	139.23	M				D								F							R			T			
	1092B-14H-4, 141-142	140,23	M				D								R							T						
	1092B-14H-5 91-92	141,23	M				D								F													
	1092A-14H-3, 79-80	141.91	M				A								C							R			R	T		
	1092B-14H-6, 41-42	142,23	P				F								C							C						
	1092A-14H-4 79-80	143.41	P		R						T											C					T	R
	1092A-14H-5 11-12	144.23	P				A								F							C					R	
	1092A-14H-5, 111-112	145.23	M				A								F							F					T	
	1092A-14H-6 102-103	146 64	M				D								F							F						
	1092C-15H-5, 21-22	148.91	M				D				T				R							F			R			
	1092A-15H-1 79-80	150.53	P				C								R							F			R	R		
	1092B-15H-3, 136-137	150.98	P				A								F							F				R		
	1092B-15H-4 86-87	151 98	M	T			A								F							F			R	R		
	1092A-15H-2, 79-80	152.03	P				D								F							F						
	1092A-15H-3 15-16	152,89	P				C								R							F				A		
	1092A-15H-3, 79-80	153.53	P				C								R				T			F				A		
	1092A-15H-3 115-116	153,89	P				C															F			R	C		
	1092A-15H-4 65-66	154,89	P				F															F						
	1092A-15H-4 79-80	155.03	P				R								R							F						
	1092A-15H-5 15-16	155.89	P				F															C				R		
	1092A-15H-5, 79-80	156 53	P				F								F				R			F			R	F		
	1092A-15H-5 115-116	156.89	P				F															F				A		
	1092B-16H-2 67-68	157 89	P				R																			D		
	1092A-15H-6 79-80	158.03	M				F								R							F				D		
	1092B-16H-3 17-18	158.89	G				F								R											D		
	1092B-16H-3 117-118	159 89	M				F															C				A		

Site 1092 range chart - Stratigraphic occurrence of selected diatom species - 5/9

Depth (mcd)	*Denticulopsis ovata*	*Denticulopsis praedimorpha*	*Denticulopsis simonsenii*	*Eucampia antarctica*	*Ethmodiscus* sp.	*Fragilaria* sp	*Fragilariopsis arcula*	*Fragilariopsis aurica*	*Fragilariopsis barronii*	*Fragilariopsis claviceps*	*Fragilariopsis cylindrica*	*Fragilariopsis clementia*	*Fragilariopsis donahuensis*	*Fragilariopsis efferans*	*Fragilariopsis fossilis*	*Fragilariopsis interfrigidaria*	*Fragilariopsis lacrima*	*Fragilariopsis maleinterpretaria*	*Fragilariopsis miocenica*	*Fragilariopsis praecurta*	*Fragilariopsis praeinterfrigidaria*	*Fragilariopsis reinholdii*	*Hemidiscus cuneiformis*	*Hemidiscus karstenii*	*Hemidiscus triangularus*	*Mediaria splendida*	*Navicula* sp.	*Naviculopsis* sp.	*Neobrunia marabilis*	*Nitzschia denticuloides*	*Paralia sulcata*	*Pleurosigama directum*	*Proboscia barboi*	*Proboscia praebarboi*	*Raphidodiscus marylandicus*
90,41					X																			C			R								
90,71																																			
91,00					X																			C											
91,80					X																										R				
92,60																																			
93,12																								C									F		
93,39			F		X																														
95,00			C		X																			R											
95,33			C		X																			T					X		T		T		
95,80			A																																
96,83			A		X																														
97,40			A		X																														
98,20			A																																
99,80			C																																
99,83			C																	R									X						
101.33			A																																
101,41			A																																
102,21			F																																
102,83																				R															
103,80			F																														R		
103,83			F		X																								X		R		R		
104,60			A																														F		
105,63			C		X															F													F		
106.78			C		X							R								F									X				F		
107,23			R		X								R						R	R							R				T		F		
108.03			R		X																														
108,28					X																														
108,83																																			
109,78			R		X															F				R											
110.43			C																	F				R							R		R		
111.23			A																																
112,03			C																					T									F		
112,83			F		X																								X				F		
113,63			C		X																														
116.03			C		X																														
116.20			C		X																		R												
116,83			C																														F		
117,70			F																														F		
119.20			C																					R							R		F		
119,23			F																												F		F		
120.70			F																					R					X		F		F		
120.83			F																												R		F		
122,20			F		X															T			F										F		
122.43			F																														C		
123,23			C																														F		
123.70																								F									A		
124.70																																			
125,23			F																					R					X						
126,23																								R									R		
127,51			F		X																			R			R				R		F		
128,23																																			
130.23					X																												R		
130,51			C																				F										R		
131,23					X																														
132,01																																			
132,23			C		X															R				F			T		X						
133.23					X																														
134,23					X																														
135,01			C		X																					T									
135.23																								R											
137.23																								R											
138,23			R		X															T		R									R				
138,91					X															T															
139.23			F		X															T													T		
140,23																																			
141.23					X																														
141,91			F	T	X																												T		
142.23					X																														
143,41			C																										X						
144,23																																			
145.23			F							R										R									X				R		
146.64																																	R		
148,91			R		X																			T			T								
150.53			F																														F		
150.98																																	R		
151.98			F		X																			T									F		
152,03	R		R																																
152,89	C																																		
153.53	C		R																										X				T		
153,89	A																																R		
154,89	D																																		
155.03	D																																R		
155,89	D		F																																
156,53	A		F																														R		
156.89	C		F																																
157.89	R																																		
158.03	F		R																														R		
158.89	F																																		
159,89	C		T																																

Site 1092 range chart - Stratigraphic occurrence of selected diatom species - 6/9

Depth (mcd)	*Rhizosolenia antenata*	*Rhizosolenia bergonii*	*Rhizosolenia hebetata*	*Rocella gelida*	*Rouxia antarctica*	*Rouxia heteropolare*	*Rouxia isopolica*	*Rouxia naviculoides*	*Rouxia peragalli*	*Stellarima sp.*	*Stephanopyxis sp.*	*Thalassionema nitzschioides*	*Thalassionema nitzschioides var. capitulatum*	*Thalassionema nitzschioides var. inflatum*	*Thalassionema nitzschioides var. lanceolatum*	*Thalassionema nitzschioides var. parvum*	*Thalassiosira complicata*	*Thalassiosira convexa var. aspinosa*	*Thalassiosira inura*	*Thalassiosira fraga*	*Thalassiosira spinosa*	*Thalassiosira spumellaroides*	*Thalassiosira miocenica*	*Thalassiosira oestupii*	*Thalassiosira oliverana*	*Thalassiosira oliverana var. sparsa*	*Thalassiosira torokina*	*Thalassiosira praelineata*	*Thalassiothrix longissima grp.*	*Thalassiothrix miocenica*
90,41			A						F			F				R													F	R
90,71			A									R																	R	
91,00			A						F																					F
91,80			A									R				R													R	
92,60			D						F			F																		
93,12			C									F																	F	F
93,39			C						F																				R	A
95,00			C						R			R																	R	C
95,33			C						R																				R	C
95,80			A						T																				R	F
96,83			C									R																	R	F
97,40			C						R			R																	F	
98,20			C																										R	R
99,80			C						R			R																	F	F
99,83	F	R	F				T		R			R				F													F	F
101,33			A						R			R																	F	F
101,41			C									F																	C	F
102,21			A													F													F	F
102,83			D																										F	R
103,80			A									R																	R	R
103,83			C						T			R				C													R	
104,60			C						R			R																	F	R
105,63			C						R			R				R													F	T
106,78	F	R	F						R			R																	F	F
107,23	R	T	A								R	R				F													R	R
108,03			A								R					R													R	F
108,28			D																											F
108,83			D													R													R	
109,78			A													F													F	R
110,43			C									F				F													R	R
111,23			F													R													R	R
112,03			C													F													F	
112,83			C						T			R				R													R	R
113,63			C													F													F	R
116,03			F									F				F													F	
116,20			C									F				C													F	F
116,83			C									R				C													F	R
117,70			C						R							F													F	F
119,20			F						R							F													F	F
119,23			F						T			T				F													F	F
120,70			F						T			T				F													R	C
120,83			C									R				F													R	F
122,20			F									R				F													R	R
122,43			C													F													R	R
123,23			C									F	R		F														F	R
123,70			A													F													F	
124,70			C													D														
125,23			F									R				C													R	
126,23			R									C				C													F	R
127,51			F						R			C				C													F	R
128,23			R									C				R														
130,23			F									F				R													C	A
130,51		T	F									F				R													F	C
131,23			C									F																	C	R
132,01			C									F				R													C	
132,23			C						T			F				R													F	T
133,23			C									F																	F	
134,23			C									R																	F	R
135,01			F						T			R	R			T													F	
135,23			F									R				R													F	
137,23			F													R													R	
138,23			F									R				R													R	
138,91			F													F													R	
139,23	T		F					T								F													R	
140,23			F													F													R	
141,23			R													T													F	
141,91			F													R					F								F	T
142,23			A													F													F	R
143,41			A						T							C													T	R
144,23			C						R																					F
145,23			F						R				F																T	R
146,64			C																										R	
148,91	R		F										T																R	
150,53			A									R																	F	
150,98			C																										F	
151,98			F										T																F	
152,03			F																										R	
152,89																													R	
153,53			F																										R	
153,89			F																										R	
154,89												F																		
155,03			F																										R	
155,89																													R	
156,53		R	F																										F	
156,89																													F	
157,89			R																											
158,03			R										R																R	
158,89			R																										T	
159,89			R																											

Site 1092 range chart - Stratigraphic occurrence of selected diatom species - 7/9

Zone (NSODZ)	Core-section (interval in cm)	Depth (mcd)	Preservation	*Actinocyclus curvatulus*	*Actinocyclus ellipticus*	*Actinocyclus fasciculatus*	*Actinocyclus ingens*	*Actinocyclus ingens* var. *nodus*	*Actinocyclus ingens* var. *ovalis*	*Actinocyclus karstenii*	*Actinoptychus senarius*	*Asteromphalus hookeri*	*Asteromphalus kennettii*	*Asteromphalus inaequabilis*	*Azpeitia tabularis*	*Bogorovia praepaleacea*	*Cavitatus jouseanus*	*Cavitatus miocenica*	*Chaetoceros* sp.	*Coretron cryophilum*	*Coscinodiscus lewisianus*	*Coscinodiscus marginatus*	*Coscinodiscus rhombicus*	*Crucidenticula nicobarica*	*Denticulopsis crassa*	*Denticulopsis dimorpha*	*Denticulopsis hustedtii*	*Denticulopsis macollumii*
D. dimorpha-D. simonsenii	1092B-16H-4, 67-68	160,89	M				C																			D		
	1092A-16H-1, 79-80	160,97	P				F								R							R				D		
	1092B-16H-5, 17-18	161,89	M				F								R											D		
	1092A-16H-2, 79-80	162,47	P				F								R							R				D		
	1092A-16H-2, 120-121	162,88	M				R								T							R				D		
	1092A-16H-3, 70-71	163,88	P	R			F				T				T							R				D		
	1092A-16H-3, 79-80	163,97	M				F								R							F				D		
	1092A-16H-4, 79-80	165,47	M				F								R							R				D		
	1092A-16H-4, 120-121	165,89	M				R								R							R				D		
	1092A-16H-5, 70-71	166,88	P				R								T							F				D		
	1092B-17H-1, 112-113	167,88	P	T			R								R							F				D		
	1092A-16H-6, 79-80	168,47	P				R								T											D		
	1092A-17H-1, 79-80	169,51	P				T								R							T				D		
	1092B-17H-3, 12-13	169,88	P				T								R							T				D		
	1092B-17H-3, 112-113	170,88	M	T			R								R							T				D		
	1092A-17H-2, 79-80	171,01	P												F							R				D		
	1092B-17H-4, 62-63	171,88	P				F								R											D		
	1092A-17H-3, 79-80	172,51	P				F																			D		
	1092A-17H-4, 18-19	173,40	P				F															R				D		
	1092A-17H-4, 79-80	174,01	P												F							F				D		
D. simonsenii	1092A-17H-4, 118-119	174,40	P				F								F													
	1092A-17H-5, 79-80	175,51	P				D								F							F						
	1092B-18H-2, 102-103	177,83	P	T			A	F							R		T					R						
	1092B-18H-4, 2-3	179,83	P				D																					
	1092A-18H-1, 79-80	180,64	P				F	C							C							F						
	1092B-18H-5, 2-3	181,33	P				F	A							C							A						
	1092A-18H-2, 79-80	182,14	P				C	A																				
	1092A-18H-2, 98-99	182,33	P				A	A							R							C						
	1092A-18H-2, 148-149	182,83	P				D	C																				
A. ingens var. *nodus*	1092A-18H-3, 48-49	183,33	P				A	F																				
	1092A-18H-3, 98-99	183,83	P				D	A																				
	1092A-18H-3, 148-149	184,33	P				D	C														R						
A. ingens	1092A-18H-4, 48-49	184,83	P				D															C						
	1092A-18H-4, 79-80	185,14	P				D																					
	1092A-18H-4, 138-139	185,73	P				D															C		F				
	1092A-18H-5, 48-49	186,33	P				A															A						
	1092A-19H-1, 54-55	192,38	P				C										F					A						C
	1092A-19H-1, 79-80	192,63	P				F				F						C					F						A
N.N.	1092A-19H-1, 104-105	192,88	P														F					F						D
	1092A-19H-2, 4-5	193,38	P												R		F					C						D
	1092A-19H-2, 54-55	193,88	P												F		A					A						
	1092A-19H-3, 4-5	194,88	P														A	A										
	1092A-19H-4, 104-105	197,38	P												C													
	1092A-19H-5, 4-5	197,88	P												C		C	A				A						
	1092A-20H-1, 20-21	201,54	P												C			C				A						
	1092A-20H-1, 120-121	202,54	P												F		C					A						
	1092A-20H-2, 20-21	203,04	M								F			F	R		C	R			F	A	T					
	1092A-20H-2, 70-71	203,54	P											C							F	A						
	1092A-20H-3, 20-21	204,54	M								F			F			F				F	A						
	1092A-20H-4, 20-21	206,04	P											F			F	R			R	A						
	1092A-20H-5, 20-21	207,54	P											F			C					C						
	1092A-20H-5, 70-71	208,04	P								F						C					A						
	1092A-20H-5, 120-121	208,54	P											F			F					A						
	1092A-20H-6, 20-21	209,04	P														F	F				C						
	1092A-20H-6, 70-71	209,54	P								R			F	R	R	A					F						
	1092A-20H-6, 79-80	209,63	P											F	R	R	A					F						

Site 1092 range chart - Stratigraphic occurrence of selected diatom species - 8/9

Depth (mcd)	*Denticulopsis ovata*	*Denticulopsis praedimorpha*	*Denticulopsis simonsenii*	*Eucampia antarctica*	*Ethmodiscus* sp.	*Fragilaria* sp.	*Fragilariopsis arcula*	*Fragilariopsis aurica*	*Fragilariopsis barronii*	*Fragilariopsis claviceps*	*Fragilariopsis cylindrica*	*Fragilariopsis clementia*	*Fragilariopsis donahuensis*	*Fragilariopsis efferans*	*Fragilariopsis fossilis*	*Fragilariopsis interfrigidaria*	*Fragilariopsis lacrima*	*Fragilariopsis maleinterpretaria*	*Fragilariopsis miocenica*	*Fragilariopsis praecurta*	*Fragilariopsis praeinterfrigidaria*	*Fragilariopsis reinholdii*	*Hemidiscus cuneiformis*	*Hemidiscus karstenii*	*Hemidiscus triangularus*	*Mediaria splendida*	*Navicula* sp	*Naviculopsis* sp.	*Neobrunia marabilis*	*Nitzschia denticuloides*	*Paralia sulcata*	*Pleurosigma directum*	*Proboscia barboi*	*Proboscia praebarboi*	*Raphidodiscus marylandicus*
160,89																																			
160,97			R			R																					T								
161,89			R																																
162,47					X																														
162.88			F			T																													
163.88			F			R														T															
163.97			R																																
165.47			F																																
165,89			F																										X						
166,88			F			T																													
167,88			R			R																					T						R		
168.47			T																																
169,51																																			
169,88			T			T																													
170,88			R			T																									T		F		
171,01			F																											C					
171,88																														R					
172,51																														F					
173,40			R																											F					
174,01					X																									C					
174,40			F																											A					
175,51		F	F		X																									F					
177,83		F	R		X	R																					T		X	C			R		T
179,83			C																																
180,64			F																														F		
181,33																																			
182,14			C																																
182,33			R																																
182,83			F																																
183,33																																			
183,83																																			
184,33																																			
184,83																																			
185,14																													X						
185,73																																			
186,33																																			
192,38																																	C		
192,63					X																														
192.88																																			
193.38																													X		R				F
193,88																																			
194,88																																			
197,38																		D																	
197,88																																			
201,54																																			
202,54						A																													
203,04					X													T										R			T	F		R	
203,54																		F																	
204,54																		R														F			
206,04																		F									T		X			F		R	
207,54																		C																	
208,04						F												F																	
208.54																		F																	
209.04																																			
209,54																		F									R	R				R		R	
209,63																																			

Site 1092 range chart - Stratigraphic occurrence of selected diatom species - 9/9

Depth (mcd)	*Rhizosolenia antenata*	*Rhizosolenia bergonii*	*Rhizosolenia hebetata*	*Rocella gelida*	*Rouxia antarctica*	*Rouxia heteropolara*	*Rouxia isopolica*	*Rouxia naviculoides*	*Rouxia peragalli*	*Stellarima* sp.	*Stephanopyxis* sp.	*Thalassionema nitzschioides*	*Thalassionema nitzschioides* var *capitulatum*	*Thalassionema nitzschioides* var. *inflatum*	*Thalassionema nitzschioides* var. *lanceolatum*	*Thalassionema nitzschioides* var. *parvum*	*Thalassiosira complicata*	*Thalassiosira convexa* var. *aspinosa*	*Thalassiosira inura*	*Thalassiosira fraga*	*Thalassiosira spinosa*	*Thalassiosira spumellaroides*	*Thalassiosira miocenica*	*Thalassiosira oestupii*	*Thalassiosira oliverana*	*Thalassiosira oliviverana* var. *sparsa*	*Thalassiosira torokina*	*Thalassiosira praelineata*	*Thalassiothrix longissima* grp.	*Thalassiothrix miocenica*
160,89			F																										R	
160,97			R																										R	
161,89			F																											
162,47																													R	
162,88																													T	
163,88			R									R																	T	
163,97			R																											
165,47			T																										T	
165,89			R									R	T																R	
166,88			T									T																	R	
167,88			T																										R	
168,47			T									T	T																R	
169,51			R																										T	
169,88			T									T																	T	
170,88			R																										T	
171,01			F									R																	F	
171,88			C																										R	
172,51			F																									R		
173,40			R																											
174,01																														
174,40			C																										F	
175,51			F																										F	
177,83			R	R								T	R																R	
179,83																													F	
180,64																													R	
181,33																														
182,14																														
182,33																														
182,83																														
183,33																														
183,83																														
184,33																														
184,83																													R	
185,14			A																											
185,73													F																F	
186,33																														
192,38																														
192,63			F																											
192,88																														
193,38													R																	
193,88																														
194,88																														
197,38																														
197,88																														
201,54																														
202,54			F																											
203,04			F																	T										
203,54			F																	C	F									
204,54			R						F			R								F	F									
206,04			R						T			T	R							A	R									
207,54												R	F							R	C									
208,04			F									F	F							F	F									
208,54												C	F							F	F									
209,04												F	F							F	F	F								
209,54			R									R	F							F	F									
209,63			R									R	R							C	F									

”Berichte zur Polarforschung”

Eine Titelübersicht der Hefte 1 bis 376 (1981 - 2000) erschien zuletzt im Heft 413 der nachfolgenden Reihe ”Berichte zur Polar- und Meeresforschung”. Ein Verzeichnis aller Hefte beider Reihen sowie eine Zusammenstellung der Abstracts in englischer Sprache finden sich im Internet unter der Adresse:

http://www.awi-bremerhaven.de/Resources/publications.html

Ab dem Heft-Nr. 377 erscheint die Reihe unter dem Namen: ”Berichte zur Polar- und Meeresforschung”.

Heft-Nr. 377/2000 – „Rekrutierungsmuster ausgewählter Wattfauna nach unterschiedlich strengen Wintern“ von Matthias Strasser.

Heft-Nr. 378/2001 – „Der Transport von Wärme, Wasser und Salz in den Arktischen Ozean“, von Boris Cisewski.

Heft-Nr. 379/2001 – „Analyse hydrographischer Schnitte mit Satellitenaltimetrie“, von Martin Losch.

Heft-Nr. 380/2001 – „Die Expeditionen ANTARKTIS XVI/1-2 des Forschungsschiffes POLARSTERN 1998/1999“, herausgegeben von Eberhard Fahrbach und Saad El Naggar.

Heft-Nr. 381/2001 – „UV-Schutz- und Reparaturmechanismen bei antarktischen Diatomeen und *Phaeocystis antarctica*“, von Lieselotte Riegger.

Heft-Nr. 382/2001 – ”Age determination in polar Crustacea using the autofluorescent pigment lipofuscin“, by Bodil Bluhm.

Heft-Nr. 383/2001 – „Zeitliche und räumliche Verteilung, Habitatspräferenzen und Populationsdynamik benthischer Copepoda Harpacticoida in der Potter Cove (King George Island, Antarktis)“, von Gritta Veit-Köhler.

Heft-Nr. 384/2001 – „Beiträge aus geophysikalischen Messungen in Dronning Maud Land, Antarktis, zur Auffindung eines optimalen Bohrpunktes für eine Eiskerntiefbohrung“, von Daniel Steinhage.

Heft-Nr. 385/2001 – „Actinium-227 als Tracer für Advektion und Mischung in der Tiefsee“, von Walter Geibert.

Heft-Nr. 386/2001 – „Messung von optischen Eigenschaften troposphärischer Aerosole in der Arktis“, von Rolf Schumacher.

Heft-Nr. 387/2001 – „Bestimmung des Ozonabbaus in der arktischen und subarktischen Stratosphäre”, von Astrid Schulz.

Heft-Nr. 388/2001 – ”Russian-German Cooperation SYSTEM LAPTEV SEA 2000: The Expedition LENA 2000”, edited by Volker Rachold and Mikhail N. Grigoriev.

Heft-Nr. 389/2001 – ”The Expeditions ARKTIS XVI/1 and ARKTIS XVI/2 of the Rearch Vessel ‚Polarstern’ in 2000”, edited by Gunther Krause and Ursula Schauer.

Heft-Nr. 390/2001 – ”Late Quaternary climate variations recorded in North Atlantic deep-sea benthic ostracodes”, by Claudia Didié.

Heft-Nr. 391/2001 – ”The polar and subpolar North Atlantic during the last five glacial-interglacial cycles”, by Jan P. Helmke.

Heft-Nr. 392/2001 – „Geochemische Untersuchungen an hydrothermal beeinflußten Sedimenten der Bransfield Straße (Antarktis)”, von Anke Dählmann.

Heft-Nr. 393/2001 – ”The German-Russian Project on Siberian River Run-off (SIRRO): Scientific Cruise Report of the Kara-Sea Expedition ’SIRRO 2000’ of RV ‚Boris Petrov’ and first results”, edited by Ruediger Stein and Oleg Stepanets.

Heft-Nr. 394/2001 – „Untersuchungen der Photooxidantien Wasserstoffperoxid, Methylhydroperoxid und Formaldehyd in der Troposphäre der Antarktis ”, von Katja Riedel.

Heft-Nr. 395/2001 – ”Role of benthic cnidarians in the energy transfer processes in the Southern Ocean marine ecosystem (Antarctica)”, by Covadonga Orejas Saco del Valle.

Heft-Nr. 396/2001 – ”Biogeochemistry of Dissolved Carbohydrates in thew Arctic”, by Ralph Engbrodt.

Heft-Nr. 397/2001 – ”Seasonality of marine algae and grazers of an Antarctic rocky intertidal, with emphasis on the role of the limpet *Nacilla concinna* Strebel (Gastropoda: Patellidae)”, by Dohong Kim.

Heft-Nr. 398/2001 – ”Polare Stratosphärenwolken und mesoskalige Dynamik am Polarwirbelrand”, von Marion Müller.

Heft-Nr. 399/2001 – ”North Atlantic Deep Water and Antarctic Bottom Water: Their Interaction and Influence on Modes of the Global Ocean Circulation”, by Holger Brix.

Heft-Nr. 400/2001 – ”The Expeditions ANTARKTIS XVIII/1-2 of the Research Vessel ’Polarstern’ in 2000”, edited by Victor Smetacek, Ulrich Bathmann, Saad El Naggar.

Heft-Nr. 401/2001 – ”Variabilität von CH_2O (Formaldehyd) - untersucht mit Hilfe der solaren Absorptionsspektroskopie und Modellen”, von Torsten Albrecht.

Heft-Nr. 402/2001 – ”The Expedition ANTARKTIS XVII/3 (EASIZ III) of RV ’Polarstern’ in 2000”, edited by Wolf E. Arntz and Thomas Brey.

Heft-Nr. 403/2001 – ”Mikrohabitatansprüche benthischer Foraminiferen in Sedimenten des Südatlantiks”, von Stefanie Schumacher.

Heft-Nr. 404/2002 – "Die Expedition ANTARKTIS XVII/2 des Forschungsschiffes 'Polarstern' 2000", herausgegeben von Jörn Thiede und Hans Oerter.

Heft-Nr. 405/2002 – "Feeding Ecology of the Arctic Ice-Amphipod *Gammarus wilkitzkii.* Physiological, Morphological and Ecological Studies", by Carolin E. Arndt.

Heft-Nr. 406/2002 – "Radiolarienfauna im Ochotskischen Meer - eine aktuopaläontologische Charakterisierung der Biozönose und Taphozönose", von Anja Nimmergut.

Heft-Nr. 407/2002 – "The Expedition ANTARKTIS XVIII/5b of the Research Vessel 'Polarstern' in 2001", edited by Ulrich Bathmann.

Heft-Nr. 408/2002 – "Siedlungsmuster und Wechselbeziehungen von Seepocken (Cirripedia) auf Muschelbänken (*Mytilus edulis* L.) im Wattenmeer", von Christian Buschbaum.

Heft-Nr. 409/2002 – "Zur Ökologie von Schmelzwassertümpeln auf arktischem Meereis - Charakteristika, saisonale Dynamik und Vergleich mit anderen aquatischen Lebensräumen polarer Regionen", von Marina Carstens.

Heft-Nr. 410/2002 – "Impuls- und Wärmeaustausch zwischen der Atmosphäre und dem eisbedeckten Ozean", von Thomas Garbrecht.

Heft-Nr. 411/2002 – "Messung und Charakterisierung laminarer Ozonstrukturen in der polaren Stratosphäre", von Petra Wahl.

Heft-Nr. 412/2002 – "Open Ocean Aquaculture und Offshore Windparks. Eine Machbarkeitsstudie über die multifunktionale Nutzung von Offshore-Windparks und Offshore-Marikultur im Raum Nordsee", von Bela Hieronymus Buck.

Heft-Nr. 413/2002 – "Arctic Coastal Dynamics. Report of an International Workshop. Potsdam (Germany) 26-30 November 2001", edited by Volker Rachold, Jerry Brown and Steve Solomon.

Heft-Nr. 414/2002 – "Entwicklung und Anwendung eines Laserablations-ICP-MS-Verfahrens zur Multielementanalyse von atmosphärischen Einträgen in Eisbohrkernen", von Heiko Reinhardt.

Heft-Nr. 415/2002 – "Gefrier- und Tauprozesse im sibirischen Permafrost – Untersuchungsmethoden und ökologische Bedeutung", von Wiebke Müller-Lupp.

Heft-Nr. 416/2002 – "Natürliche Klimavariationen der Arktis in einem regionalen hochauflösenden Atmosphärenmodell", von Wolfgang Dorn.

Heft-Nr. 417/2002 – "Ecological comparison of two sandy shores with different wave energy and morphodynamics in the North Sea", by Iris Menn.

Heft-Nr. 418/2002 – "Numerische Modellierung turbulenter Umströmungen von Gebäuden", von Simón Domingo López.

Heft-Nr. 419/2002 – "Scientific Cruise Report of the Kara-Sea Expedition 2001 of RV 'Academik Petrov': The German-Russian Project on Siberian River Run-off (SIRRO) and the EU Project 'ESTABLISH'", edited by Ruediger Stein and Oleg Stepanets.

Heft-Nr. 420/2002 – "Vulkanologie und Geochemie pliozäner bis rezenter Vukanite beiderseits der Bransfield-Straße / West-Antarktis", von Andreas Veit.

Heft-Nr. 421/2002 – "POLARSTERN ARKTIS XVII/2 Cruise Report: AMORE 2001 (Arctic Mid-Ocean Ridge Expedition)", by J. Thiede et al.

Heft-Nr. 422/2002 – "The Expedition 'AWI' of RV 'L'Atalante' in 2001", edited by Michael Klages, Benoit Mesnil, Thomas Soltwedel and Alain Christophe with contributions of the participants.

Heft-Nr. 423/2002 – "Über die Tiefenwasserausbreitung im Weddellmeer und in der Scotia-Sea: Numerische Untersuchungen der Transport- und Austauschprozesse in der Weddell-Scotia-Konfluenz-Zone", von Michael Schodlok.

Heft-Nr. 424/2002 – "Short- and Long-Term Environmental Changes in the Laptev Sea (Siberian Arctic) During the Holocene", von Thomas Müller-Lupp.

Heft-Nr. 425/2002 – "Characterisation of glacio-chemical and glacio-meteorological parameters of Amundsenisen, Dronning Maud Land, Antarctica", by Fidan Göktas.

Heft-Nr. 426/2002 – "Russian-German Cooperation SYSTEM LAPTEV SEA 2000: The Expedition LENA 2001", edited by Eva-Maria Pfeiffer and Mikhail N. Grigoriev.

Heft-Nr. 427/2002 – "From the Inner Shelf to the Deep Sea: Depositional Environments on the Antarctic Peninsula Margin - A Sedimentological and Seismostratigraphic Study (ODP Leg 178)", by Tobias Mörz.

Heft-Nr. 428/2002 – "Concentration and Size Distribution of Microparticles in the NGRIP Ice Core (Central Greenland) during the Last Glazial Period", by Urs Ruth.

Heft-Nr. 429/2002 – "Interpretation von FCKW-Daten im Weddellmeer", von Olaf Klatt.

Heft-Nr. 430/2002 – "Thermal History of the Middle and Late Miocene Southern Ocean - Diatom Evidence", by Bernd M. Censarek.